INFORMATION TO USERS

This dissertation was produced from a microfilm copy of the original document. While the most advanced technological means to photograph and reproduce this document have been used, the quality is heavily dependent upon the quality of the original submitted.

The following explanation of techniques is provided to help you understand markings or patterns which may appear on this reproduction.

1. The sign or "target" for pages apparently lacking from the document photographed is "Missing Page(s)". If it was possible to obtain the missing page(s) or section, they are spliced into the film along with adjacent pages. This may have necessitated cutting thru an image and duplicating adjacent pages to insure you complete continuity.

2. When an image on the film is obliterated with a large round black mark, it is an indication that the photographer suspected that the copy may have moved during exposure and thus cause a blurred image. You will find a good image of the page in the adjacent frame.

3. When a map, drawing or chart, etc., was part of the material being photographed the photographer followed a definite method in "sectioning" the material. It is customary to begin photoing at the upper left hand corner of a large sheet and to continue photoing from left to right in equal sections with a small overlap. If necessary, sectioning is continued again — beginning below the first row and continuing on until complete.

4. The majority of users indicate that the textual content is of greatest value, however, a somewhat higher quality reproduction could be made from "photographs" if essential to the understanding of the dissertation. Silver prints of "photographs" may be ordered at additional charge by writing the Order Department, giving the catalog number, title, author and specific pages you wish reproduced.

University Microfilms

300 North Zeeb Road
Ann Arbor, Michigan 48106

A Xerox Education Company

PULSE WAVE PROPAGATION ALONG FLUID-FILLED TUBES WITH HARDENED WALL SECTIONS

by

Jon Obert Jacobson

A dissertation submitted in partial fulfillment

of the requirement for the degree of

DOCTOR OF PHILOSOPHY

UNIVERSITY OF WASHINGTON

1972

Approved by Ashley F. Emery
(Chairman of Supervisory Committee)

Department Mechanical Engineering
(Departmental Faculty sponsoring Candidate)

Date June 8, 1972

UNIVERSITY OF WASHINGTON

Date: May 18, 1972

We have carefully read the dissertation entitled Pulse Wave Propagation Along Fluid-Filled Tubes With Hardened Wall Sections submitted by Jon Obert Jacobson in partial fulfillment of the requirements of the degree of Doctor of Philosophy and recommend its acceptance. In support of this recommendation we present the following joint statement of evaluation to be filed with the dissertation.

Reading Committee Report

This thesis presents the results of an experimental study which was undertaken to investigate the usefulness of the phase lock doppler ultrasound motion transducer in non-traumatically detecting the presence of and determining the extent of atherosclerotic plaques.

These plaques are intimately related to arterial disease, one of the leading causes of death today and their presence is often one of the early clues that a patient is developing an atherosclerotic condition. Consequently the early detection of the plaques is important in developing a successful treatment for this disease.

This study was devoted to determining the applicability of the transducer by comparing its performance to that of a pressure transducer mounted in a tube which simulated an artery. By propagating waves down the length of the tube, and measuring the displacement at sections where the tube was locally hardened, it was shown that the doppler transducer mounted at a significant distance away from the tube could locate a normal-hard material interface to within one arterial diameter to better than 95% confidence. Furthermore, the data secured with the doppler transducer enabled the investigator to determine the relative hardness of the plaque-like area compared to the virgin arterial wall material. It was also shown that the transducer is most sensitive when the ratio is low--that is during the early phases of plaque development when most other methods are least sensitive.

It is the opinion of the reading committee that this work which established the basic information needed to implement an early diagnostic method for atherosclerotic conditions fulfills the requirement for the doctoral dissertation and should be accepted in partial fulfillment of the requirements for the degree of Doctor of Philosophy.

DISSERTATION READING COMMITTEE:

Doctoral Dissertation

In presenting this dissertation in partial fulfillment of the requirements for the doctoral degree at the University of Washington, I agree that the Library shall make its copies freely available for inspection. I further agree that extensive copying of this dissertation is allowable only for scholarly purposes. Requests for copying or reproduction of this dissertation may be referred to University Microfilms, 300 North Zeeb Road, Ann Arbor, Michigan 48106, to whom the author has granted "the right to reproduce and sell (a) copies of the manuscript in Microform and/or (b) printed copies of the manuscript made from microform."

Signature _____

Date June 8, 1972

TABLE OF CONTENTS

LIST OF FIGURES

NOTATION

A = area

A_i = wave amplitude

a = undeformed radius

B = bulk modulus

C = wave speed

C_o = $\sqrt{Eh/2R\rho}$

Circ = circumference

Cp = capacitance

E = Elastic modulus (Young's modulus)

f = frequency, hertz

F_{10} = $\dfrac{2\,J_1(\alpha_o)}{\alpha_o J_o(\alpha_o)}$

G = shear modulus

h = tube wall thickness

i = $\sqrt{-1}$

J_o, J_1 = Bessel's functions

k_2 = attenuation constant

L = axial length

m = $\dfrac{2 + s(2\sigma - 1)}{s[F_{10} - 2\sigma]}$

p = pressure

Q = Volume flow

R = radius of tube

r = radial coordinate

$s = \dfrac{Eh}{(1 - \sigma^2) a \rho c^2}$

T_x = axial tethering force

T_r = radial tethering force

t = time

U_x = axial motion

U_r = radial motion

V_x = axial velocity

V_r = radial velocity

Z = impedance = $\dfrac{\partial p / \partial x}{\Omega}$

$RHP = \left[\dfrac{\frac{1}{N} \Sigma U_r(x,\theta)}{P(x)} \right] \left(\dfrac{c\rho\omega}{\beta} \right)$

$TMD = t(x) - t_e(x)$

$RFC = \dfrac{P_e(x) - P_o e^{\eta x}}{P_o e^{\eta x}}$

$\alpha = R\sqrt{\omega/\nu}$

$\alpha_o^2 = i^3 \alpha^2$

$\beta = \dfrac{a\omega}{c}$

ε_{ij} = strain tensor

λ = wave length

λ_i = viscoelastic parameters

μ = fluid viscosity

μ^* = Laplace transform of modulus of rigidity

ν = μ/ρ

ϕ = phase angle

ρ = density

ψ = fluid source

σ = poisson's ratio

σ_{ij} = stress tensor

θ = angular dimension

ω = $2\pi f$

ACKNOWLEDGMENTS

I would like to thank Professor A. F. Emery for providing the initial idea for this study as well as his assistance in the completion of the project. Also, I would like to sincerely thank Professor R. F. Rushmer and the Bioengineering Department for their help, and support of the project. In addition, I would like to thank all others at the University of Washington who provided facilities and assistance for me to achieve one of the most meaningful goals of my life.

CHAPTER I

INTRODUCTION

"A man is as old as his arteries" (Cabanis c. 1800)

This study has been conducted to develop a new source of information for clinically diagnosing the presence of asymptomatic arterial disease. The basic elements of the technique involve the measurement of a propagating pulse wave along the artery, and the interpretations which can be made from the data. The use of prototype instrumentation which transcutaneously measures the arterial wall motion and careful control over the experimental conditions can provide a new and valuable source of diagnostic information, previously unobtainable in an in vitro situation.

The investigation and description of the arterial pulse has been of interest to man through the ages of recorded history. Many investigators and philosophers have produced a multitude of information describing the nature and significance of the arterial pulse. At the present time with hindsight in our favor we have found some of the early researchers to be surprisingly correct in their concepts. A precise explanation of the propagation of the pulse from the heart along the arterial system was

stated in 280 B.C. by Erasistrathos when he described the pulse as appearing later in arteries that lie further from heart than in those that lie nearer the center. Erasistrathos also described the pulse as a passive phenomenon that is maintained by the action of the heart. He considered the heart, the source of immanent vital power, to be under partial influence of the brain(126). The truth of these ideas has often been neglected, even to the present time.

The application of quantified science to the analysis of the blood pressure pulse was first done by Hales in his classic experiment with a mare which had been tied to a gate. In his work in 1733, he not only obtained quantified information of the arterial and venous blood pressure but he also developed information on the output of the heart, arterial dimensions, and flow velocities besides being the first to correctly state the role of the distensibility of the arteries(53).

Leonhard Euler wrote the first analytical paper on blood flow in 1775, although it was not until 1883 that it was published posthumously. He included in his analysis the statement of the continuity equation for an incompressible fluid;

$$V\frac{\partial A}{\partial x} + A\frac{\partial v}{\partial t} + \frac{\partial A}{\partial t} = 0 \qquad 1\text{-}1$$

the equation of motion for an inviscid fluid;

$$\frac{\partial V}{\partial t} + V\frac{\partial V}{\partial x} = -\frac{1}{p}\frac{\partial P}{\partial x} \qquad 1\text{-}2$$

and a statement relating the pressure to the cross-sectional area of the tube(36);

$$A = A_o(1-e^{\frac{p}{P_o}}) \qquad 1\text{-}3$$

In 1808 Thomas Young obtained the relationship for the pulse wave velocity that is still held as the first order approximation in studies of pulse wave propagation(151). This relationship;

$$C_o = \sqrt{\frac{Eh}{2rp}} \qquad 1\text{-}4$$

is known today as the Moens-Korteweg equation(72,92). Young also suggested that the amplitude of pressure pulse should decrease as it propagates peripherally. In contrast to the normal attenuation he described the effect of a reflection, "supposing a partial reflection of the pulse to take place at every point where it meets with any resistance, which will leave a general distension of the artery."

These initial investigations which were conducted over a century and a half ago have correctly formulated the essential basis for much of the studies of pulse wave propagation that today has seen a phenomenal growth of interest and effort. The analytical techniques have been

developed to the point of near unintelligibility to those not directly concerned with the mathematical formalities of solution, while the practitioners of the clinical art of utilizing such information in the study, diagnosis and understanding of the arterial system have developed their own esoteric field of knowledge under the somewhat general title of Cardiovascular Dynamics.

This study is intended to cover the two approaches of investigating pulse wave propagation, analytical and clinical, in order to develop results which can diagnose pathologic conditions of diseased arteries. At the present time there is no adequate diagnostic method which can identify and evaluate localized changes in arterial walls until its pathology is potentially catastrophic. Arterial disease is ranked as one of the leading causes of death in the population today, being the significant factor in approximately half the recorded deaths. It has often been accepted as simply one aspect of the normal aging process; however, its occurrence in middle age, at a time when one does not expect the effects of old age to be fatal or incapacitating, has directed a considerable interest towards understanding, diagnosing and treating its symptoms. In addition to the possibility of understanding and controlling the aging process, not discounting the seriousness of the motivation to preserve life, seems to indicate that one may some time be able to reach out towards the goals of Ponce

de Leon.

This work contains information necessary for the development of a potential diagnostic procedure that can utilize the knowledge from the propagation of arterial pulse waves or other propagating waves in order to establish estimates of the mechanical properties of the arterial wall, especially the changes in these properties that are expected to occur in arterial disease. The limitations of previous studies have resulted from the use of the propagation velocity and contour of the normal pulse wave as an investigative source of information as well as limited instrumentation response. These diagnostic techniques have only been able to examine large arterial lengths in comparison to the shorter atherosclerotic plaque. Shorter segments however, can now be studied with a newly developed instrument, the phase-lock doppler ultrasound motion transducer, which can measure the motion of the wall of an artery by sending an ultrasonic beam through the surface of the skin to the artery beneath. With this instrument, the dynamic response of the wall of the artery can be examined without the need for surgical procedure to expose the surface. The information is obtained from the pulse wave, the slowest propagating axisymmetric wave, which has the largest radial motion making it most accessible for examination by an instrument such as the phase-lock doppler transducer. Other types of propagating waves have also been considered,

especially in the region where the pulse wave is being formed, where they are shown to have the largest detectable effect. These other axisymmetric waves, axial and torsional, are defined as those waves with predominantly large axial and torsional motion. This study investigated both axial and pulse waves, with the torsional waves assumed to be absent. The propagation of these waves along a fluid-filled tube or artery involves not only different velocities for each wave, but also different rates of attenuation. The combination of the velocity and attenuation for a particular wave is expressed in terms of the propagation constant. Changes in the local values of the propagation constant can be related to the changes in the mechanical properties of the material in the tube wall. Also, other quantities calculated from the radial motion of the wall and the fluid pressure are shown to be related to the local tube wall material properties. By determining normal relationships for the propagating pulse wave, these deviations which result from localized changes in the mechanical properties of the arterial wall material can be identified.

The development of a new and nontraumatic diagnostic technique for presymptomatic arterial disease involved a careful search of the literature in order to locate previous approaches to the problem. There was a paucity of information specifically concerned with the problem of utilizing pulse wave propagation for identifying short

localized segments of arteries which may or may not have exhibited symptomatic pathology. Analytic studies have recently been able to describe changes in normal pulse wave contour, only over large segments of the arterial tree.(121) Clinical studies have not identified changes in the propagation parameters that could serve as a basis for developing a new diagnostic technique. In order to approach the problem it was necessary to investigate as thoroughly as possible the alternatives which would be available.

An experimental program was undertaken to investigate in a controlled situation, the proposed technique by using models of the arterial wall. In this study, the variations in the propagation parameters for pulse wave travel along fluid-filled tubes having hardened wall sections were obtained. The role of the phase-lock transducer as a potentially useful diagnostic instrument was assessed. Configurations of the tubes and relative mechanical properties of the materials were selected to serve as a representative model of arterial disease. Studies of the dynamic material properties of the tube wall material were completed to obtain an accurate description of the material for interpreting the results from the experiment and applying them to the potential in vitro situation. The duration of the pulse wave was found to effect the results and this is discussed. In the study axisymmetric waves

were generated with a piston at one end of the tube, although pulse waves can be generated from nonaxisymmetric sources. The significant quantitative information in terms of the parameters of the tubes used in the experimental study, and the application of the results to the development of a clinically useful technique for evaluating arterial disease will be discussed as an extension of this work.

CHAPTER II

BACKGROUND

The study and explanation of the arterial pulse has been an intriguing subject over the years. Notwithstanding the philosophical or other qualitative descriptions, the analytical treatments have generated their own vast volume of literature. The extension of the knowledge of pulse wave propagation to developing a useful technique for diagnosing arterial disease has been previously investigated, but not with the instrumentation or refinement in technique utilized in this study.

EARLY WORKS

The work of Thomas Young contains the earliest statement of the correct relationship between the variables used for calculating the pulse wave velocity(151). His description of the mechanical properties of the wall of the tube was expressed in terms of the internal pressure necessary to distend the wall, and although correct, it has not been universally recognized as the earliest correct formulation of the pulse wave velocity. The early analysis of the propagation of the arterial pulse has been historically noted to have begun several decades later than when the more common expression for the

propagation velocity of the pulse wave was proposed. This relationship in the current notation is:

$$C_o = \sqrt{\frac{Eh}{2r\rho}} \qquad 2\text{-}1$$

and is commonly known as the Moens-Korteweg Equation. Moens obtained this experimentally with a leading constant that he found to equal .8, .9, and 1.036 in various situations(92). Korteweg reached the result for the expression of the propagation

$$C = \left[\frac{2r\rho}{Eh} + \frac{\rho}{B}\right]^{-\frac{1}{2}} \qquad 2\text{-}2$$

of sound waves in a fluid enclosed in an elastic tube(72). Since the bulk modulus, B, for blood is extremely large the two formulations are identical.

Even though the investigation and accurate prediction of the pulse wave velocity has constituted a source of information in the investigation of the cardiovascular system, it has been essentially neglected in one of the common models for the total circulatory system. This model, the Windkessel, considers the heart to be an analogy to the obsolescent water pumps used by fire departments at the turn of the century where the water was pumped by repeatedly compressing air in the large cylinder of the water pump(126). In this model, the flow is simply the laminar runoff due to the pressure gradient. Even today

this overly simple model has provided a heuristic basis for explaining the function of the cardiovascular system for one or more of the following reasons: 1) the time constant of the phenomena of interest is longer than the duration of a normal heartbeat, 2) the length of the body is approximately 20% of one wavelength; hence, a shallow pressure gradient along segments of the artery, and 3) the design of the cardiovascular system provides an optimum impedance matching between the proximal aorta and peripheral vessels with a minimum of exterraneous reflections(133). The Windkessel, although still commonly discussed, is not a useful basis for the more sophisticated analytical studies available today.

CURRENT FORMS OF SOLUTION: LINEARIZED MODELS

The origin of the more detailed analytic approaches to pulse propagation in fluid-filled tubes must be attributed to Witzig(142). Later studies have shown that there are several omissions in his work, but much of the general nature of the results can be interpreted as correct. His omission of the shear stress of the fluid at the inner surface of the tube wall has made the results somewhat inaccurate, but the viscous effects of the fluid itself conveys the general nature of viscosity as it is presently understood to exist. The expression proposed by Witzig for

the average axial velocity in the tube

$$V_x = \frac{\Delta P}{i\omega\rho L}\left[1 - \frac{2J_1(z)}{zJ_0(z)}\right] \qquad 2\text{-}3$$

$$z = ia\sqrt{\frac{i\omega\rho}{\mu}}$$

is the same form taken for other studies which have come more recently. Witzig's expression can be obtained as a particular solution for elastic walled tubes as was done by Womersley(144). It has been experimentally verified by Richardson and Tyler using a hot wire anemometer(117).

Assumptions:

The extension of the rigid tube models to the elastic tube models has produced the greatest amount of analytical information describing the performance of the cardiovascular system. The general assumptions which have been made with these models are: 1) axisymmetric motion, 2) a long tube with respect to wavelength, 3) long wavelength with respect to tube diameter, 4) laminar flow, 5) incompressible fluid, and 6) homogenous isotropic tube. The differences in the various solutions have been primarily in the areas of the description of the tube wall motion and the boundary conditions. The use of the Navier-Stokes equations for the description of the fluid motion is common enough to make the statement that it is the only adequate description of the fluid that has proved amenable to solution.

Fluid Model:

In order to use the Navier-Stokes equations for a representation of the fluid authors have made various simplifications. Atabeck and Lew(9), Cox(30), Jones(67) Klip(70), Morgan and Kieley(95), Taylor(132), Witzig(142), and Womersley(144) have all used the linearized Navier-Stokes equations. Morgan and Ferrante in studying the case of streaming flow considered pulsatile flow to be a small perturbation on Poiseuille flow(94). Lambert retained the nonlinear convective terms, but assumed the fluid to be inviscid(74). Barnard obtained a one-dimensional form of the Navier-Stokes equations by retaining the leading non-linear terms and integrating over the cross-sectional area (21). Streeter derived a one-dimensional form of the equations of motion including a term for viscous drag(129). Rockwell utilized a somewhat similar approach to Streeter and Barnard to obtain a one-dimensional equation of motion for the fluid(121). Fox and Saibel obtained an integral form of the equation of motion(43).

Wall Models:

The wall of the tube has been described in various ways by the different authors. Lambert(74), Barnard(21), Rockwell (121), and Streeter(129) have used the most direct relation in taking the wall to be a simple hoop. Clinically this is known as the Law of LaPlace. A greater level of sophistication

in the description of the wall is seen in the use of the membrane equations of motion. Atabeck and Lew(9), Morgan and Ferrante(94), Morgan and Kieley(95), Taylor(132), Witzig (142) and Womersley(144) have used Love's membrane theory. Jones(67) and Maxwell(83) have used Flugge's relations for the equations of motion of membrane shells, and Greenspon (47) has shown how these can be extended to thick walled cylinders. Klip(70) and Cox(38) have used the classical equations of elasticity in the derivation of the equations of motion for the wall, then used thin-walled assumptions to rework the equations for solution. Mirsky has developed the equations of motion for cylindrical shells incorporating the effects of rotary inertia and vertical shear(89,90). Klip(70), Morgan and Kieley(95), and Womersley(144) have included the effects of viscoelasticity in the wall by assuming the material to be of a Voigt nature, that is, a spring and viscous element acting in parallel. Cox extended this to include a combination of Voigt and Maxwell models to describe the time-dependent nature of the wall material, then further generalized to use a sum of Voigt and Maxwell elements to match theoretical with experimental results(30).

Boundary Conditions:

The boundary conditions that have been chosen by the various authors have been determined by the relationship chosen for the wall. Atabeck and Lew(9), Jones(67), Morgan

and Ferrante(94), Morgan and Kieley(95), Taylor(133), and Womersley(144) have used the effect of the stress of the fluid on the tube wall in the equations of motion for the wall. Cox(30), Fox and Saibel(43), and Klip(70) have used the continuity of the radial and shear stress components at the fluid-wall boundary in addition to the continuity of the velocity components. Barnard assumed continuity of the radial displacement but assumed the axial component of the wall motion to be zero(20). Maxwell(83) assumed continuity of the displacements only.

Solution Formats:

The various solution formats that have been presented have centered in a few areas. Atabeck and Lew(9), Jones(67), and Womersley(144) have solved for the pressure gradient-flow relationship in addition to the propagation constant. Klip (70), Maxwell(83), Mirsky(89,90), Morgan and Ferrante(94), Morgan and Kieley(95), and Taylor(133) have solved for the propagation constant only. Fox and Saibel(43) did not solve their expression explicitly, but left it in the form of an inversion integral. Streeter(129), and Barnard(20), did not solve their equations explicitly, but indicated the use of the method of characteristics for obtaining a solution. Rockwell has solved these equations using the method of characteristics and has obtained results in the form of propagation constants and flow-pressure relations(121).

The extensive linearized treatments that have been developed, have used the assumption that the wavelength is long with respect to the diameter of the tube, and that the tube is long with respect to the wavelength. Studies based upon these premises have not been able to include changes in the arterial system that occur over relatively short segments of the artery. One-dimensional methods, for example, like that used by Rockwell(121), have been able to consider the effects of changing the diameter, mechanical properties of the wall, and outflow through branches at distances that correspond to actual biological situations. The limitations of the models have not allowed the direct modeling of arterial disease as a perturbation on an existing solution structure. The development of a model to simulate the effects of arterial disease, or atherosclerosis, the direct effects on the artery wall must be considered.

BIOLOGICAL BACKGROUND: Arteries and Arterial Disease

In order to fairly assess the problem of modeling atherosclerosis it is necessary to understand some of the basic structural elements of the artery. The normal condition of the artery is taken to be the undiseased state with the changes related to atherosclerosis described as changes from the normal condition. It is generally agreed that an accurate over-all view of the wall can be obtained by separating it into three annular layers. From the inner

surface to the outer surface these layers or lamina are called the tunica intima, the tunica media, and the tunica adventitia. The existence of separations between these layers is well defined, but not always easy to see with an arbitrary staining technique. Arteries are structurally categorized into two types -- elastic and muscular -- and although the dividing line between the two is not always clear it provides a common basis for describing the arterial wall(55).

When analyzing the three-layered structure of the arterial wall it is noted that the two primary structural components of the artery, collagen and elastin, are distributed throughout the thickness in various amounts and structures. The inner lamina, the tunica intima, is arranged with thin, flat (squamous) epithelial cells adjacent to the lumen (the interior opening of the artery). The epithelial cells are supported by a basement membrane of primarily elastic tissue beneath which is a somewhat non-descript region containing some delicate elastic and collagen fibers in an amorphoric intercellular substance. Separating the intima from the media is the internal elastic membrane, a fairly dense and sometimes impervious layer of elastic tissue. The center lamina, the tunica media, contains the primary distinguishing features categorizing the arteries into two types, muscular and elastic. Appropriately, the muscular arteries have smooth muscle in the media and the elastic

arteries have rather dense elastic tissue in the media(55). The elastic arteries which functionally lie nearer the heart are the aorta, innominate, subclavian, common carotid, and pulmonary arteries(33). The tunica media for the elastic arteries composes the bulk of the artery wall thickness and is itself composed of lamina of elastic fibers with interspersed material to separate the lamina. For the muscular arteries the tunica media is composed of smooth muscle with varying amounts of collagen and elastin, the amounts being primarily determined by relative size of the artery. The outermost lamina of the media is the external elastic membrane, and is used as the demarcation between the media and the adventitia. The outer layer of the arterial wall is the tunica adventitia and is composed of both collagen and elastic fibers with relative amounts being determined by the type of artery. In addition to containing structural fibers, the adventitia contains many small arteries called vasa vasorum (the arteries of arteries) which supply the metabolic needs of the arterial wall. In classifying the types of arteries it is noted that the adventitia is noticeably much thinner for elastic arteries than for muscular arteries(17).

Arterial Disease:

The essential problem in the study of atherosclerosis is the evaluation of the manner in which the arterial wall

has undergone changes from what is called normal. These changes are referred to as disease states or pathological conditions that in themselves often imply very little about the actual condition of the artery. Some of the known changes which the arterial wall does experience will be given to illustrate the rather diffuse phenomena that can be experienced, as well as the severity of the condition.

Functionally there are two pathological conditions that can occur, both relating to the ability of the arterial system to supply blood for the metabolic needs of the body. The first of these, an aneurism, can be viewed as the gradual weakening, which results in a continued bulging out of the wall over a finite length, finally reaching the point where the artery bursts. The second condition, commonly put under the title atherosclerosis, is the gradual growth of material inside the artery progressively blocking off the blood supply to all parts of the body distal (downstream) to the stenosis (occlusion). In addition to atherosclerosis, per se, there is also the problem of a thrombosis that can form inside an artery, effectively shutting off the blood supply. A thrombosis is considered to be a blood clot or clot-like formation because of its composition containing degenerate blood with a fibrin matrix as a supporting structure. There are, however, some distinctive features that make the thrombus unlike the blood clot, with the primary characteristic being that a clot has a smaller percentage of red cells than

a thrombus. Fibrin, a protein that can be formed in the clotting of blood, is found both in the thrombus and in a layered fashion in the raised atherosclerotic plaque. With fibrin found in both the thrombosis and atherosclerotic plaque there is much discussion about the actual pathogenic mechanism of formation; however, in addition to this the presence of fibrin is found with a PTAH staining technique which some say is not a definite proof of the existence of fibrin(91).

The actual definition of atherosclerosis is not clearly defined in the minds of many investigators, which leads to disagreements as to the nature of atherosclerosis and its treatment: "...the biological significance of the morphological artifacts (constant or otherwise) which are observed is not established beyond reasonable doubt in the minds of many investigators, thus leading to the unfortunately wide divergence of opinion which exists with regard to alleged distinction between nonpathological or developmental 'normal aging' process and the decidedly pathological process of 'atherosclerosis' which actually bring the patient to either clinical or pathological examination".

In one of the recent attempts to more systematically classify the changes observed in the arterial walls, Mitchell and Schwartz(91) have defined four categories into which they classify atherosclerotic plaques. The immense effort which they expended is illustrative of the difficulty in

obtaining information, and indicative of the magnitude of the work yet to be done in order to more fully understand the phenomenon called atherosclerosis. They have classified atherosclerotic plaques into four distinct types. The first type of plaque which they considered is the flat plaque or intimal streak and is confined to the intimal layer only. The second and third types are the raised plaques which extend from the intima into the lumen as well as invading other lamina of the wall. The distinction between the two types is that while the second type has a coating of lipids (fats) on the surface adjacent to the lumen, the third type does not. The fourth type is a degeneration of the raised plaque to form a complicated plaque which is or could possibly be catastrophic.

The first type of plaque that is seen is the one detected at the earliest chronological age, and is called a flat plaque. A Sudan IV staining technique makes the lipid areas visible; hence, the plaques have been called flat sudanophilic plaques. When observed under the light microscope the plaque is seen to be primarily an accumulation of lipids in the intimal layer. There are other phenomena which are observed in the media and adventitia such as small fatty droplets, hyaline thickening (the presence of cartilage), and calcification (bone-like material that may be derived from cartilage), but these are believed to be ubiquitous conditions of the arterial wall and not directly related to

the presence of any sort of plaque-like formation. Their common occurrence is probably an accidental association of two unrelated processes.

The more common type of lesion that is found and commonly called atherosclerosis is the raised plaque. It is distinctly larger than the flat plaque and is apparently not part of an evolutionary process beginning with the flat plaque. The reasons supporting this view are that there have not been found any intermediate types of plaques, and that the predominant anatomical locations for each type are different. One of the charasteristic features that can be observed in a sectioned plaque under the light microscope is that there is a distinct laminated appearance in certain areas of the plaque. This comes from dense fibrous bundles that form some of the architectural structure of the plaque. This fibrous tissue encloses masses of fatty material that often is soft and pulpy, and can be squeezed out when the plaque is incised. The calcification of the plaque which often occurs can usually be found in the fibrous tissue, but has also been found in the fatty deposits. There is also calcification present in the media, and this is felt to be somewhat similar to that which occurs with the flat plaque--that is, it is an occurrence independent of the formation of the plaque itself. There is some correlation between the calcification of the internal elastic membrane and the occurrence of raised plaques, but it is not conclusive. In about 20 percent of the raised plaques

there are granular-appearing areas which are groups of many different types of cells, including multinucleate cells of the foreign body type, macrophages containing pigment or lipid, plasma cells, and many small round cells morphologically similar to lymphocytes.

The growth of the raised plaque is often assumed to be a lesion which somehow sticks to the inner surface of the artery protruding into the lumen to reduce the effective blood-carrying capacity of the artery. This overly simplified view is not correct, and overlooks the much more fundamental and diffuse phenomena which are occurring. The raised plaque not only protrudes into the lumen, but also invades the intima and media, ultimately causing the media to become much thinner. In the process of thinning out the media, the fibers of collagen and elastin become closely packed, suggesting a loss of other medial components such as smooth muscle. This becomes particularly significant in endarterectomy (the surgical removal of the plaque or other occluding material) commonly leaving the adventitia as the only remaining structural component of the arterial wall. It is also noted that the vasa vasorum develops a more extensive blood supply network creating a hypervascular artery and plaque. These additional blood vessels are prone to rupture in complicated plaques, causing the hemorrhaging into the plaque which often is found with this pathologic condition(91).

In addition to the changes that occur in the intima and media, there are changes in the adventitia that are not generally recognized as part of the atherosclerotic process. The first of these is a noticeable increase in the amount of fibrous tissue in the adventitia, making the artery very stiff and hard. This is noticeable in arterial surgery where the increased fibrous makes it difficult to make an incision in the arterial wall.

The second of the changes is an increase in vascularity of the adventitia, concomitant with the increased vascularity of the plaque. The third is the growth of groups of cells forming granular areas similar to those found in the plaque. Their extent may be confined to the adventitia only, or may go inward to join with similar areas of the plaque or outward about the artery, sometimes encircling the adjacent nerve. Their presence correlates with the growth of plaques on the luminal surface, although there is no explanation for their existence(91).

From the evidence relating the first type of plaque to the intima only, and the raised plaque to the entire wall, it appears that the one may suppose that the raised plaque is in its inception begins with the media, rather than the intima. The changing conditions which are present, and appear to be associated with advanced stages of disease, such as calcification and lipid deposits, may be found in the media when a complete raised plaque has not formed. The

plaque is assumed to form in the media with the protrusion into the lumen, and changes in the adventitia being subsequent events(91).

MECHANICAL PROPERTIES OF ARTERIES: Normal and Diseased

Associated with the histologic changes in atherosclerosis are changes in the mechanical properties of the wall. The most complete studies of the mechanical properties of the normal wall were done by Bergel on excised arterial segments(22,23). Peterson(108,111) and Patel(105) used transducers for radial displacement and internal pressure to dynamically measure the circumferential elastic properties of an exposed canine artery. The investigation of the mechanical properties of the diseased arterial wall was done by Feigel, et al.(40), in which they concluded that in the presence of mild atherosclerosis the arterial wall exhibited a general increase in the elastic modulus. This is generally accepted result and for this reason arterial disease has been referred to as "hardening of the arteries". Learoyd and Taylor in a somewhat extensive study have shown that although the thoracic arteries (inside the chest or ribcage) do demonstrate an increase in the elastic modulus, the iliac and upper femoral arteries when not heavily encrusted with atherosclerotic plaques may at times show a noticeable decrease in elastic modulus(75).

PULSE WAVE STUDIES: Effects of Age and Disease

The anticipation of detecting a change in the elastic modulus of the arterial wall that can be associated with atherosclerosis has prompted several previous investigations in the measurement of pulse wave velocity. In an early study Bramwell, Hill, and McSwiney(25) measured the difference in the arrival time of the carotid and brachial pulses and concluded that the pulse wave velocity increased from about 5 meters/second at birth to about 8.5 meters/second at 85 years of age. The studies of Woolam(147), Roach and Burton (119), Yoshimura, et al.(149), Monnier(93), Hallock(54), Haynes, et al.(60), and Nye(99) have reached the general conclusion that the pulse wave velocity increases with age. Yoshimura, et al. have used the reduction of the average pulse wave velocity in the peripheral vessels as a diagnostic indicator for assessing the success of chemotherapy in treating arterial disease(149). O'Rourke(102) neglected to measure the distance between his transducers in publishing only the transit time between anatomical sites of the aorta. But he did notice that the amplification of the arterial pulse was less in the presence of age or atherosclerosis. Since the amplification is related to the expected alteration in the amplitude and contour of the pulse wave as it propagates along the major arteries, it provides a potential diagnostic source of information.

The studies that have investigated the altered contour of the pulse wave in the presence of atherosclerosis have not been concerned with the changes propagation parameters in the presence of subsymptomatic disease, but have concentrated on studies in the presence of partially occluding plaques. Pulse contour studies have generally utilized a partially inflated cuff wrapped about the limb to determine the pulse contour. The results from these investigations have been of a qualitative nature. Hyman(63) and Edwards (34,35) found that the pulse distal to a stenosis is lower in amplitude and more rounded. These results could come from an atherosclerotic plaque as Hyman found, or from the digital compression of the artery to produce a partial occlusion as Edwards used. Lax(78) and Cooper(29), have found that the dichrotic wave is lost in the presence of an occluding or partially occluding lesion. It appears the stenosed artery can be likened to a highly damped transmission line, or to a low pass filter where the pulse has a slower rise time, a lower amplitude, and loss of definitive characteristics in the pulse contour. In order to study the effects of arterial disease in a more controlled manner Fiddian(41) fabricated model atherosclerotic plaques from sections of lucite tubes, and inserted them into the cardiovascular system, and O'Rourke (102) fabricated simulated plaques from plaster-of-paris packed about the exterior of the artery. Both these studies were somewhat too grossly executed to be of much quantitative

value, but they did qualitatively confirm that such modifications of the wall definitely can affect propagation characteristics of the pulse wave.

PRESENT STATUS OF PULSE WAVE ANALYSIS

The development of a nontraumatic diagnostic procedure for presymptomatic arterial disease involves the implementation of new methods for obtaining information as well as extending techniques from previously conducted research. McDonald(84) has measured the local pulse wave velocity by inserting two catheters into the artery. This method in requiring the insertion of pressure catheters, is traumatic, in addition to being limited in the resolution of the data. Yao(148) in utilizing the recently developed doppler ultrasound transducer has found that it is an effective instrument for assessing the effectiveness of cardiovascular surgery in improving peripheral circulation. Yoshimura, et al.(149) have found that a reduction in average pulsewave velocity following chemotherapy in treating arterial disease. Cuffs and other surface transducers are neither accurate nor specific in location for describing the presence of a small presymptomatic lesion, and to date have not produced conclusive data.

The development of a diagnostic procedure for arterial disease based upon variations in the arterial pulse wave propagation must be based upon what is known of the normal pulse. The studies which have been previously conducted have

not always utilized a sufficient amount of rigor in their technique to provide accurate quantitative answers. In this study it will be shown how a more closely controlled technique associated with more precise instrumentation can provide quantitative answers about the nature and location of lesions of the relative size with which they occur in the arterial system.

CHAPTER III

THEORETICAL CONSIDERATIONS

This chapter discusses the theoretical foundations used in the interpretations of the experimental results. The most extensive theoretical investigations of pulse wave transmission along fluid-filled elastic tubes have come in the past 15 years since the works of Womersley(144) and Morgan and his co-workers(94,95). The general form of the background for the problem has been in existence since the early 1900's with Witzig's work(142) on fluid-filled rigid tubes, but the advent of high speed electronic computers has produced solutions for flexible walled tubes using larger and more inclusive statements of the problem than had been previously possible with a reasonable effort. These solutions result from the linearization of the general equations of motion. Their formulation has included the axial and radial wall motion as well as fluid pressure and its axial and radial motion. The limitations of these solutions to infinitely long tubes and long wave lengths have motivated several investigators to further linearize the equations to produce one-dimensional solutions. The one-dimensional solutions, which have been solved by the method of characteristics or electrical analogs can account for

variations in the boundary conditions, tube wall materials, and volume flow along the axis of the tube, that were not possible with more general problem statements.

LINEARIZED EQUATIONS: Fluid Motion

The description of the fluid within the tube has been studied by assuming it to be a Newtonian fluid. Blood of course is not strictly Newtonian, but Taylor(131) in analyzing the cardiovascular system has shown that it may be assumed to follow a linear stress-shear-rate law for the larger vessels. The analytic representation of the fluid that has been used is that the Navier-Stokes equations. For the axisymmetric motion of an incompressible fluid they are:

$$\frac{\partial V_x}{\partial t} + V_r \frac{\partial V_x}{\partial r} + V_x \frac{\partial V_x}{\partial x} = \frac{1}{\rho} \frac{\partial P}{\partial x} + \frac{\mu}{\rho}\left(\frac{\partial^2 V_x}{\partial r^2} + \frac{1}{r} \frac{\partial V_x}{\partial r} + \frac{\partial^2 V_x}{\partial x^2}\right) \qquad (3\text{-}1)$$

$$\frac{\partial V_r}{\partial t} + V_r \frac{\partial V_r}{\partial r} + V_x \frac{\partial V_r}{\partial x} = \frac{1}{\rho} \frac{\partial P}{\partial r} + \frac{\mu}{\rho}\left(\frac{\partial^2 V_r}{\partial r^2} + \frac{1}{r} \frac{\partial V_r}{\partial r} + \frac{\partial^2 V_r}{\partial r^2} - \frac{V}{r^2}\right) \qquad (3\text{-}2)$$

The viscosity, μ, represents the apparent or effective viscosity for the fluid. Also used is the continuity equation for an incompressible fluid.

$$\frac{\partial V_r}{\partial r} + \frac{V_r}{r} + \frac{\partial V_x}{\partial x} = 0 \qquad (3\text{-}3)$$

As the Navier-Stokes equations are stated, they are not tractable until they are simplified and linearized. The assumptions which underlie the linearization are discussed in detail by Fry and Greenfield(44). The solution of the equations is based upon the assumptions of pressure, and velocity of:

$$\begin{aligned} P &= P(r)\ \exp\ [i\omega(t-x/c)] \\ V_r &= V_r(r)\ \exp\ [i\omega(t-x/c)] \\ V_x &= V_x(r)\ \exp\ [i\omega(t-x/c)] \end{aligned} \tag{3-4}$$

By utilizing assumptions (3-4) and the continuity relationship (3-2), equations (3-1) can be reduced to:

$$\frac{d^2V_r(r)}{dy^2} + \frac{1}{y}\frac{dV_r(r)}{dy} + i^3\alpha^2V_r(r) - \frac{V_r(r)}{y^2} = \frac{a}{\mu}\frac{dP(r)}{dy} \tag{3-5}$$

$$\frac{d^2V_x(r)}{dy^2} + \frac{1}{y}\frac{dV_x(r)}{dy} + i^3\alpha^2V_x(r) = \frac{i\mu}{C}\frac{a^2}{\mu}P(r) \tag{3-6}$$

The solution of these has been formulated as:

$$P = AJ_o(\beta\frac{r}{a})\ \exp[i\omega(t-x/c)]$$

$$V_r = [-A\frac{\beta a}{\mu\alpha^2}\ J_1(\beta\frac{r}{a}) + B\frac{\beta}{\alpha J_o(\alpha)}\ J_1[(\alpha^2+\beta^2)^{\frac{1}{2}}\ \frac{r}{a}]]\exp[i\omega(t-x/c)] \tag{3-7}$$

$$V_x = [-A\frac{\beta a}{\mu\alpha^2}\ J_o(\beta\frac{r}{a}) + B\frac{(\alpha^2+\beta^2)^{\frac{1}{2}}}{\alpha J_o(\alpha)}\ J_o[(\alpha^2+\beta^2)^{\frac{1}{2}}\ \frac{r}{a}]]\exp[i\omega(t-x/c)] \tag{3-8}$$

where:

$$\alpha^2 = i^3\ \frac{a^2\omega}{\nu} \tag{3-9}$$

$$\beta = i\ \frac{a\omega}{c} \tag{3-10}$$

Wall Motion

The development of a model chosen for the wall of the tube must be matched to the solution for the fluid at the inner surface of the tube. The tube is described with equations of motion relating the dynamic response of the tube wall to the stresses imposed upon it. The statements of the material properties of the wall material are used to relate the stresses the material to the deformations that result from those stresses.

The formulation representing the tube wall has ranged from the simple hoop stress model (clinically known as the Law of LaPlace) to the axisymmetric equations of visco-elasticity.

In describing the motion of the tube wall by incorporating the time-dependent properties of the material, the definition of the material response takes the following form:

$$\left[1 + \lambda_1 \frac{\partial}{\partial t}\right] \varepsilon_{ij} = 2\mu_o \left[1 + \lambda_2 \frac{\partial}{\partial t}\right] \varepsilon_{ij} \qquad (3\text{-}11)$$

The parameters λ_1 , the relaxation time, and λ_2 the retardation time, are assumed to be small in relation to 1.0(30,70). A complex modulus may be defined as:

$$\mu^* = \mu_o \left[\frac{1 + \lambda_2 \frac{\partial}{\partial t}}{1 + \lambda_1 \frac{\partial}{\partial t}}\right] \qquad (3\text{-}12)$$

For the Voigt material $\lambda_2 = 0$ and the above relation becomes:

$$\mu^* = \mu_o \left[1 + \lambda_2 \frac{\partial}{\partial t}\right] \tag{3-13}$$

This is incorporated into the linearized axisymmetric equations of motion:

$$\frac{\partial \sigma_{rr}}{\partial r} + \frac{1}{r} + \frac{\partial \sigma_{r\theta}}{\partial \theta} + \frac{\partial \sigma_{rx}}{\partial x} + \frac{\sigma_{rr} - \sigma_{\theta\theta}}{r} = \rho \frac{\partial^2 U_r}{\partial t^2} \tag{3-14}$$

$$\frac{\partial \sigma_{xx}}{\partial x} + \frac{1}{r} \frac{\partial \sigma_{x\theta}}{\partial \theta} + \frac{1}{r} \delta_{rx} + \frac{\partial \sigma_{rx}}{\partial r} = \rho \frac{\partial^2 U_x}{\partial t^2} \tag{3-15}$$

by utilizing the strain-displacement components in cylindrical coordinates:

$$\varepsilon_{rr} = \frac{\partial U_r}{\partial r} \tag{3-16}$$

$$\varepsilon_{\theta\theta} = \frac{U_r}{r} + \frac{1}{r} \frac{\partial U_\theta}{\partial \theta} \tag{3-17}$$

$$\varepsilon_{xx} = \frac{\partial U_x}{\partial x} \tag{3-18}$$

$$2\varepsilon_{r\theta} = \frac{1}{r} \frac{\partial U_r}{\partial \theta} + \frac{\partial U_\theta}{\partial r} - \frac{U_\theta}{r} \tag{3-19}$$

$$2\varepsilon_{rx} = \frac{\partial U_r}{\partial x} + \frac{\partial U_x}{\partial r} \tag{3-20}$$

$$2\varepsilon_{\theta x} = \frac{1}{r} \frac{\partial U_x}{\partial \theta} + \frac{\partial U_\theta}{\partial x} \tag{3-21}$$

to produce the final equations of motion:

$$\frac{\partial^2 U_r}{\partial r^2} + \frac{1}{r}\frac{\partial U_r}{\partial r} - \frac{U_r}{r} + \frac{\partial^2 U_r}{\partial x^2} = \frac{\rho}{\mu^*}\frac{\partial^2 U_r}{\partial t^2} \tag{3-22}$$

$$\frac{\partial^2 U_x}{\partial r^2} + \frac{1}{r}\frac{\partial U_x}{\partial r} + \frac{\partial^2 U_x}{\partial x^2} = \frac{\rho}{\mu^*}\frac{\partial^2 U_x}{\partial t^2} \tag{3-23}$$

The motion of the tube is assumed to be of the form:

$$U_r = U_r(r)\ \exp\ [i(\omega t - \delta x)] \tag{3-24}$$

$$U_x = U_x(r)\ \exp\ [i(\omega t - \delta x)] \tag{3-25}$$

where δ is the propagation constant in the form ω/C with C being a complex constant incorporating the effects of both the wave speed and the attenuation.

The solution of (3-22) and (3-23) provides the following statement of the tube wall motion:

$$U_r = [A_1 J_1(k_n r) + B_1 Y_1(k_n r)]\ \exp\ i(\omega t - \delta x) \tag{3-26}$$

$$U_x = [A_2 J_0(k_n r) + B_2 Y_0(k_n r)]\ \exp\ i(\omega t - \delta x) \tag{3-27}$$

The assumption of incompressibility in the continuity relationship:

$$\frac{\partial U_x}{\partial x} + \frac{1}{r}\frac{\partial (rU_r)}{\partial r} = 0 \tag{3-28}$$

produces the relationships between the constants in (3-26) and (3-27).

$$A_2 = \frac{k_n}{i\delta} A_1 \tag{3-29}$$

$$B_2 = \frac{k_n}{i\delta} B_1 \tag{3-30}$$

Obtaining the propagation constant δ is the difficult part of the solution, and the major portion of the remaining simplifications are made at this point. The solution is a result of applying the boundary conditions, and solving for the propagation constant for each frequency of interest.

Boundary Conditions

The solution of the set of equations for the fluid and the wall involves eight boundary conditions that have been expressed in various forms by the different authors. These are:

Axisymmetric motion of the fluid:

No radial velocity at the centerline:

1) $V_r = 0$ at r=0 (3-31)

The velocity profile is symmetric at the centerline:

2) $\frac{\partial V_x}{\partial r} = 0$ at r=0 (3-32)

Shear stress at the inner wall is balanced in the fluid and the tube wall:

3) $\mu[\frac{\partial V_r}{\partial x} + \frac{\partial V_x}{\partial r}] = \mu^*[\frac{\partial U_r}{\partial x} + \frac{\partial U_x}{\partial r}]$ at r=a (3-33)

The normal stress at the inner wall is the same in the fluid and the tube wall:

4) $-P + 2\mu\frac{\partial V_r}{\partial r} = 2\mu^*\frac{\partial U_r}{\partial r}$ at r=a (3-34)

The shear stress at the outer tube wall surface:

5) $\mu^*[\frac{\partial U_r}{\partial x} + \frac{\partial U_x}{\partial r}] = T_x$ at r=b (3-35)

T_x = axial tethering force

The normal stress at the outer tube wall:

6) $2\mu^*\frac{\partial Ur}{\partial r} = T_r$ at at r=b (3-36)

T_r = radial tethering force

The radial velocity is the same for both the fluid and tube at the inner tube wall:

7) $V_r = \frac{\partial U_r}{\partial t}$ at r=a (3-37)

The axial velocity is the same for both the fluid and the tube wall at the inner surface:

8) $V_x = \frac{\partial U_x}{\partial t}$ at r=a (3-38)

Solution of Linearized Equations

The solution of the linearized equations yield information about the various effects of parameters on the propagation constant $\delta = \frac{\omega}{c}$. The variation with frequency ω of the pulse wave velocity, which is essentially the group velocity of the travelling pulse wave, has been developed by Womersley(144) and is of the form:

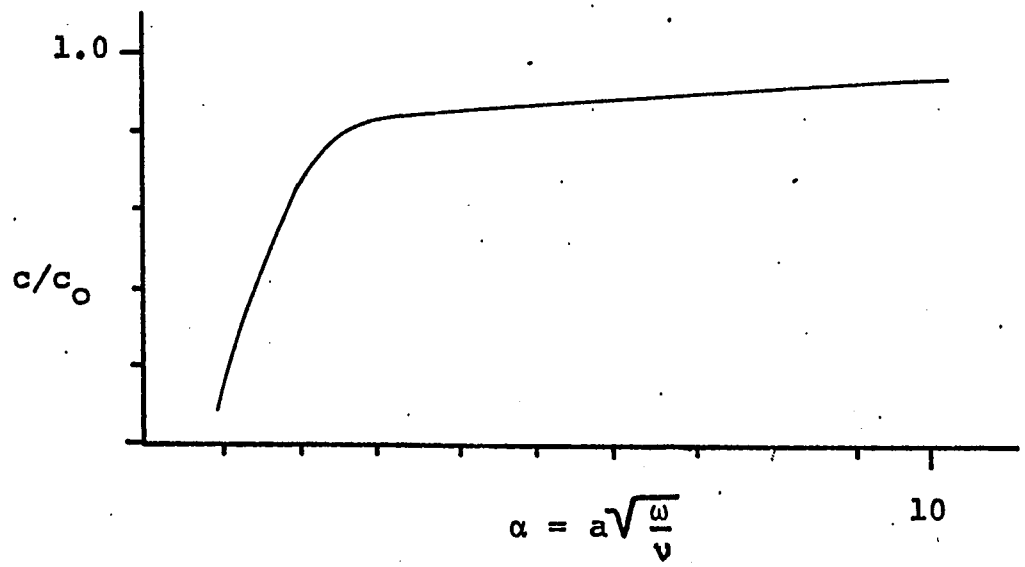

Figure 3-1
Velocity vs. Frequency for Pulse Wave

The experimental work of Anliker(67,83,139) and his co-workers has borne out the validity of this result for higher frequencies in experimental studies using canine arteries. Figure 3-1

shows the dispersion of pulse wave propagation, that is the variation in propagation velocity with frequency. The curve shows a definite break at a low frequency, here represented by the value of nondimensional quantity $\alpha = 2$. This point corresponds to a frequency of about 0.3 hertz. Above this frequency the propagation velocity changes little with frequency and can be estimated to within a few percent by C_o. The dispersion in the pulse wave propagating along a uniform tube is not sufficient to explain the observed changes in the pulse wave as it propagates along the aorta (143).

The propagation velocity also varies with the viscosity of the fluid, and has been expressed by Morgan and Kieley(95) as:

$$C = \sqrt{\frac{Eh}{2R\rho}} \left[1 - (1\text{-}5 + \frac{5^2}{4}) \frac{1}{R_o}\left(\frac{\mu}{2\rho\omega}\right)^{\frac{1}{2}}\right] \qquad (3\text{-}39)$$

The correction for water-filled tubes is relatively small. For this study the bracketed term, which can be considered as a correction factor for viscosity, is .9936.

The attenuation of the wave along the axis of the fluid-filled uniform tube follows an exponential relationship for axial length and is of the general form:

$$\frac{A}{A_o} = \exp\left(-k_2 \frac{x}{\lambda}\right) \qquad (3\text{-}40)$$

where k_2 remains constant over a large frequency range when the fluid viscosity is low. For all conditions, though, k_2

is a function of the wall thickness to diameter ratio, the viscosity of the fluid, and the mechanical properties of the wall material. The data of both Klip(71) and Cox (30) shows that the attenuation increases with increased wall thickness, as well as with increased viscosities of both the fluid and the wall material, but remains essentially constant over a wide frequency range. Anliker, Histand, and Ogden have observed experimentally that the attenuation of pulse waves in the aorta of experimental animals follows an exponential relationship at frequencies up to 200 hertz. Klip(71) has shown that only for extremely thick-walled tubes (wall thickness to internal radius ratio = 1.) and large viscosities (1. poise and larger) does k_2 begin to deviate significantly from a constant value.

The attenuation of the arterial pulse as predicted by the linearized analysis does not describe the physiological condition. The normal human arterial pulse wave shows a growth in amplitude, i.e., amplification, as it propagates along the artery.

It was previously mentioned that the dispersion of the pulse wave did not explain the observed changes as it propagated along the aorta. It was then suggested that reflections from peripheral site, presumably a branch, or or even the arterials as Remmington(116) proposed could explain the contour changes. This explanation has not been completely satisfactory. One dimensional analysis, which

formulate the pulse propagation problem in the nature of a tapered transmission line, potentially provides a more accurate explanation for the amplification of the pulse as it propagates along the aorta.

ONE-DIMENSIONAL SOLUTIONS

The integrated average impedance from the linearized analysis furnishes a link between the linearized solutions and the one-dimensional solutions. The impedance, the relation between the volume flow and the driving pressure gradient, is expressed as:

$$Z = -\frac{1}{Q}\frac{\partial P}{\partial x} \qquad (3\text{-}41)$$

A common error which was seen in early clinical literature was to study the relationship between the arterial pressure and the volume flow(123). The error was that the pressure gradient, the slope of the pressure-distance curve, is related to the volume flow, not the absolute value of the pressure at one position. This has resulted in several studies requiring significant effort and unfortunately of little value. The relation between the stroke volume of the heart and the aortic pressure was one of the more common relations that was formulated. Cox(30) has experimentally verified his calculations to show the value of using the pressure gradient rather than the magnitude of the pressure in determining the volume flow. He presented the relation

for the impedance versus the frequency as:

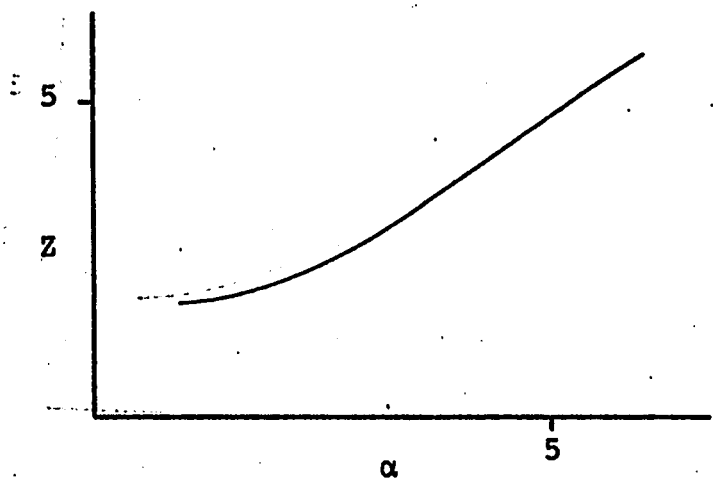

Figure 3-2
Relative Impedance versus Nondimensional Frequency

Since almost all experimental data on the cardiovascular system is gathered on a one-dimensional basis such as the pulse wave velocity, attenuation or volume flow, the one-dimensional solution provides a basis for comparison with experimental data. Also, as has been noted, the linearized analysis is normally reduced to a final form of a one-dimensional answer, and yet it does not effectively explain such commonly observed phenomena as the amplification of the pulse wave as it propagates peripherally. The one-dimensional approach, although lacking in the analytic complexity of the linearized solution has provided the means of obtaining a solution which incorporates such things as taper of the vessel, non-uniform wall properties, outflow from side

branches, and finite length sections(121).

The basis of the one-dimensional approach is obtained by taking an average velocity over the area of the tube:

$$V_{(x,t)} = \frac{1}{\pi R^2}\int_0^{2\pi}\int_0^{R} V(r,\theta,x,t)\ r\,dr\,d\theta \qquad (3\text{-}42)$$

The continuity equation can be written to include a source or outflow term, ψ , as shown in:

$$\frac{\delta A}{\delta t} + \frac{\delta (AV)}{\delta t} + \frac{1}{\rho}\psi = 0 \qquad (3\text{-}43)$$

The momentum includes a term, f , for viscous friction or other fluid force:

$$\frac{\partial V}{\partial t} + V\frac{\partial V}{\partial x} + \frac{1}{\rho}\frac{\partial P}{\partial x} = f \qquad (3\text{-}44)$$

The relationship between the pressure and the cross-sectional area of the tube is shown as:

$$A = A(p,x) \qquad (3\text{-}45)$$

Rockwell has represented the pressure dependence on the cross-sectional area as:

$$A(p,X) = A_o e^{-\beta x} \exp\left[\frac{p-p_o}{\rho c^2(p,x)}\right] \qquad (3\text{-}46$$

The variation of the area with axial distance was given by Patel(105), while the relation between the area and the internal pressure that reflects the nonlinear aspect of the wall material is a result of Histand's(62) work.

The use of the method of characteristics to solve the one-dimensional equations for pulse wave propagation in a fluid-filled tube has been effectively completed by Rockwell (121). He has shown that the amplification, and contour change are adequately explained with a one-dimensional approach. Also this method can be used to investigate the effects of nonuniform outflow, fluid viscosity, and transients resulting from the starting of a heart such as occurs in cardiac surgery after a bypass has been removed.

The one-dimensional equations, which can be solved by the method of characteristics, are also tenable with an electric analog. The electrical analog represents the momentum and the continuity equations in the following form(133):

$$-\frac{\partial E}{\partial X} = L\frac{\partial i}{\partial t} + Ri \qquad (3\text{-}47)$$

$$\frac{\partial i}{\partial x} = Cp\frac{\partial E}{\partial t} + GE \qquad (3\text{-}48)$$

The equations utilize the following analogies in the equations of motion and continuity for a fluid-filled tube:

$$\begin{aligned}
&\text{pressure} \sim \text{voltage} = E \\
&\text{flow, velocity } VA \sim \text{current} = i \\
&\text{inertance, } \rho/A \sim \text{inductance} = L \\
&\text{resistance } \frac{8\mu}{\pi r_o^2} \quad \text{resistance} = R \\
&\text{compliance } \frac{\partial A}{\partial p} \sim \text{capacitance} = C_p \\
&\text{leakage} \sim \text{conductance} = G
\end{aligned} \tag{3-49}$$

The analog provides a capability of investigating the performance of the interrelated factors as they are modeled by the analog. The accuracy of the model in representing the cardiovascular system is continually open to speculation as with all models where the results are dependent upon the initial formulations and assumptions.

The one-dimensional representation underlying these studies can be used to explain the effects of changes in impedance of the arterial system on the generation of reflections. The reflection coefficient, that is, the ratio of the reflected to the incident wave, is given by the relation(69):

$$C_{ref} = \frac{A_{ref}}{A_{inc}} = \frac{Z - Z_o}{Z + Z_o} \tag{3-50}$$

where C_{ref} is the reflection coefficient, Z is the distal impedance, and Z_o is the proximal impedance. The identification of the reflection coefficient from experimental data is dependent upon obtaining values for the magnitude of both

the reflected and the incident wave amplitudes. This is a problem when the two waves are superimposed. As an example of this, the procedure used in this study estimated the amplitude of the incident wave at the interface by knowing the amplitude of the wave in the initial portion of the tube, and the relation describing the attenuation. This is shown below:

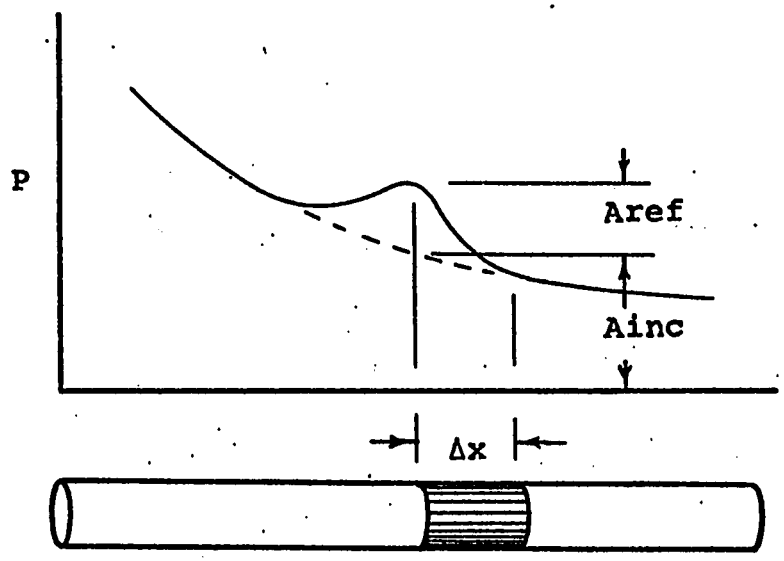

Figure 3-3 Pressure versus Axial Position

Womersley in working out the effects of adding a flow-meter with rigid walls to the exterior of the artery obtained a relation for the reflection coefficient for a finite length section with infinite elastic modulus. This relation,'

$$\frac{A_{ref}}{A_{inc}} = \frac{1}{1 + \frac{C_o}{i f_\pi \ell}} \qquad (3\text{-}51)$$

assumed continuous wave propagation with section of length ℓ (146). No experimental data is presented to verify this relation, but with the noted lack of correlation between his predicted and observed phase relationships for the elastic tube, it is anticipated that this relation is to be subject to some error in experimental verification.

FINITE DIFFERENCE SOLUTIONS

The analytic study of pulse wave propagation can potentially be performed with a finite-difference method. The availability of high speed computers provides the capability of directly integrating the equations of motion for the fluid and the surrounding tube. In this method the problem can be described, using finite-difference algorythms in place of differential equations. Wilkins has developed a workable form of these algorythms for axisymmetric deformable bodies(141). In setting up these equations it is necessary to incorporate the dilitational as well as shear deformation waves to account for the entire spectrum of effects. This poses a restriction on the stability of the solution and its role in limiting the solution will be described below. The versatility in varying material properties, lengths of tube, and forms of loading does present a potentially useful means of treating wave propagation along fluid-filled tubes.

There are several problem areas that are present in the use of finite-difference schemes to obtain wave propagation in fluid-filled tubes. Solutions by finite-difference methods are limited by storage capabilities of current computing facilities as well as requiring long computing times. One method in the evaluation of stability criteria, relates to the time necessary for a dilational (compression) wave to progress across one zone of the finite difference array describing the fluid and the surrounding tube. Zone sizes .1 inch and smaller require that each iteration of the solution per wave propagation in biological materials be performed for a real time increment of less than 1.6 microsecond. Smaller zone sizes would likely be chosen for a realistic solution and would utilize correspondingly shorter real time increments. The solution of a complete problem for a reasonably sized tube requires thousands of iterations of the problem, but most likely as many as 10^4 or 10^5 iterations. The resulting solution will use computer processing time in the order of an hour or more for fast rising pulses, and short tubes. Slowly rising pulses, such as the normally occurring arterial pulse wave, and long tubes, such as normally occurring arteries will require multiplies of the initial estimate of an hour. This necessitates an extensive amount of computing time describing a single and

unique physical system in which the physical parameters have yet to be precisely defined. Arrays of data require multiples of this expense.

The conclusions regarding solutions of pulse wave propagation with finite difference solutions are somewhat negative. Computational cost is extremely high which, with a finite budget, limits the solution method. The methods used to invoke economy into the solution will require a coarsely grided definition of the problem with a definite loss of detail. The method is appealing in that finite-length sections can be studied, material properties can be altered along the length, and arbitrary pulse shapes can be used. It appears, however, that a pragmatic solution to the problem can be initially examined on an experimental basis with the previously developed closed-form solutions to be used as a theoretical basis for evaluating the results.

CHAPTER IV

EXPERIMENTAL INVESTIGATION

An experimental study was performed to investigate the proposed method for identifying hardened sections of arterial walls. The method used requires the generation of a single short duration pulse wave in an artery, then measuring its propagation with pressure and wall-motion transducers. In the experimental study, a carefully manufactured rubber tube was used as a model of a diseased artery. The pulse generation was accomplished with a piston inside one end of the tube. In an in vivo situation the pulse wave generated by impulsively displacing either could be the exposed wall of the artery, or the skin surface above an unexposed vessel. The wave motion was recorded by measuring the fluid pressure inside the tube and the radial wall motion outside the tube. The subject of interest, the propagation in the near region of a hardened section, was investigated more thoroughly than the surrounding regions. The results are presented in this chapter, and developed in Chapter 5, in a manner directed towards an engineering viewpoint. Chapter 6 covers the extension of these results to the proposed implementation of a clinical defection method for asymptomatic atherosclerosis.

TUBES: Design and Fabrication

The tubes used in the experiment were fabricated from 20 durometer rubber with hardened sections using 30,50,70 and 90 durometer rubber. All tubes whose results presented here were fabricated in the mold shown in Figure 4-1. This mold produced identical tubes, 24 inches long with .875 inch ID and a 1.000 inch OD. The hardened sections were fabricated in the three configurations shown in Figure 4-2.

The manufacture of the tubes with nonuniform material in the wall required the development of a fabrication method. The decisions on the size of the tube, and the position and size of the nonuniform sections of the wall resulted from a combination of information from manufacturing problems, and data from prototype tubes.

Manufacturing of the experimental tubes was first attempted with a mold using a .500 mandrel for the ID of the tube. Fabrication of these prototype tubes produced a nonuniform loading of the mandrel that displaced it from its centerline position. Because of this wall thickness variations about the circumference were observed to range from .030 inch to greater than .100 inch. The .500 inch mandrel over a 24 inch length did not have sufficient rigidity to produce a uniform wall thickness tube. As an example of how much force this takes, an unsymmetric loading of 2.67 lb./inch along the mandrel would deflect it .025 inch in the center. This problem was corrected by fabricating

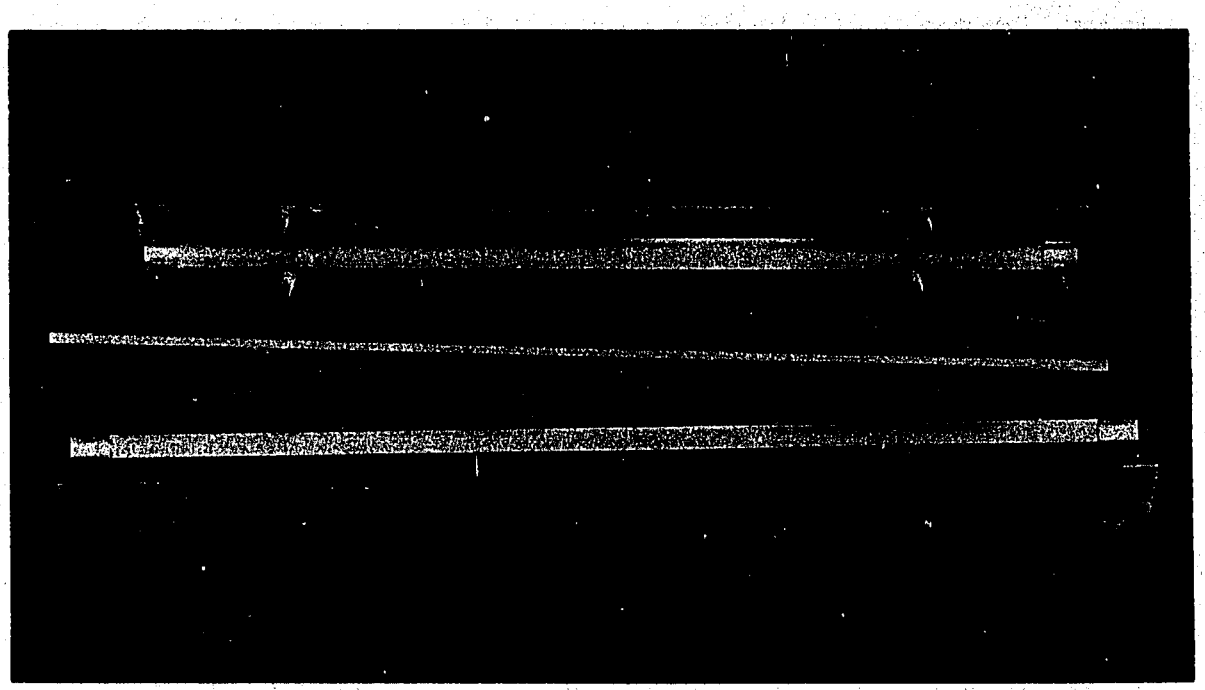

Figure 4-1

TUBE MOLD AND MANDREL

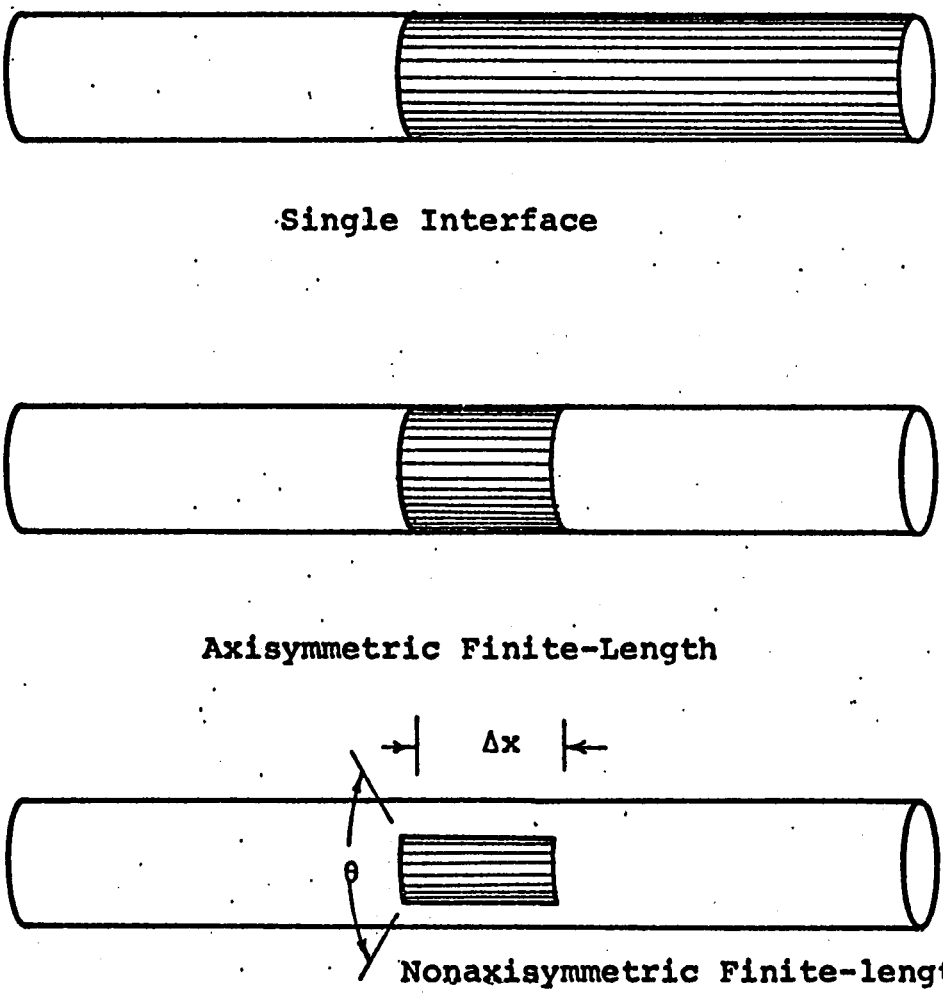

FIGURE 4-2 CONFIGURATIONS OF HARDENED SECTIONS

a new mold with a .875 inch mandrel that increased its flexural rigidity by 9.4 times; thereby reducing the observed circumferential variation in wall thickness. The incorporation of nonuniform material the wall required care in manufacturing, as well as some good fortune in the vulcanization process. The entire set of tubes was formed from a single quantity of 20 durometer rubber to eliminate variation in the samples. The tubes were fabricated by wrapping thin sheets of rubber about the mandrel, then pressing in the mold and vulcanizing with heat to form the tube. The nonuniform sections were added to the 20 durometer unvulcanized tube by carefully replacing the section with that of larger durometer rubber. The tube and mandrel were removed by prying open the external mold and lifting out the mandrel. The tube was carefully removed from the mandrel by slipping it off one end.

With the exception of the nonuniform wall thickness with smaller diameter tubes, two additional manufacturing problems were encountered with the vulcanization of the nonuniform tube walls. The first problem encountered was the flowing of the interface between 20 durometer tube and the softer rubbers (30 and 50 durometer). This flowing produced dividing lines that extended up to several diameters along the axis of the tube. The effect of this lack of axial discreteness between the different sections of

the tubes reduced the probability of locating the axial position of the interface. The effect of lack of definition will be discussed in a following section. The harder rubbers, 70 and 90 durometers, did not always produce a good bond at the interface. The two rubbers had a tendency not to join around the periphery of the interface. Manufacturing problems were overcome with care and multiple trials at fabrication. With expense and effort involved in manufacture, the tubes were selected to provide as complete an array of nonuniform tube configurations as was possible within the budget and time limitations of the study.

The placement of the hardened section was selected in order that the effects of an isolated pulse wave could be studied as it propagated past the section. It was necessary to have the section far enough from the pulse generating piston to allow the pulse wave to form completely, and for the axial wave to separate from the pulse wave. The hardened section was as close as possible to the piston so that the pulse wave would retain the generating contour throughout the section of interest. From these considerations, the leading edge of the section was nominally placed at 10" from the piston face.

The mechanical properties of the vulcanized rubber tubes was determined by the procedure described in detail in Appendix E. Table 1 gives the results of these tests.

Durometer	E_s	E_d (25 hertz)	$\|E^*\|$
20	127.1	15.6*	128.1
30	385	40.6	388
50	662	106	688
70	2080	543	2145
90	3295	1359	3590

Table 1
Dynamic mechanical properties of rubber samples used in experiment

EQUIPMENT AND EXPERIMENTAL PROCEDURE

The equipment was designed to generate a pulse wave at one end of a fluid-filled tube, and to observe its propagation as it passed a hardened section of the tube. The tube, filled with water, was mounted in a tank of water which was necessary to provide a low-loss medium for the operation of the ultrasonic motion transducer. A tube holder at one end of the water tank acted as the cylinder for the pulse-generating piston. The tube holder inside the tank contained a port into the center of the tube to allow pressurization of the fluid within the tube, and was designed to position the pressure transducer along the axis of the tube. A single pulse wave was generated by driving the piston with a modified electromagnetic shaker which was in turn driven by a waveform generator through the power amplifier of the shaker. The motion and pressure transducers were movable along the axis with the use of a three-axis

positioning carriage mounted to the top of the water tank. Data from the pressure and motion transducers was recorded with a triggered storage oscilloscope. A more complete description of the equipment and the experimental procedure is given in Appendix A.

The description of a single pulse propagating along a fluid-filled tube was obtained by using a large number of identical single waves, each time repositioning the transducer along the tube axis. Radial wall motion about the circumference was observed by rotating the tube on the tube holders. While recording radial motion, the pressure transducer was used as a monitor to maintain uniform pulse amplitudes.

TRANSDUCERS

The pressure transducer, a Konigsberg p-19, with a .196 inch diaphragm was mounted at the end of a 27 inch long, .250 inch diameter tube for positioning along the axis of the tube.

The radial position of the center of the pressure transducer diaphram was preset to vary less than .020 inch from the axis of the tube. This close control was not necessary, however, as Atabeck and Lew(9) have shown that there is essentially no radial variation in the fluid pressure for pulse waves.

The wall motion transducer, a phase-lock ultrasound device, was developed as part of this project and is described in more detail in Appendix C. Its frequency resolution and amplitude sensitivity make it particularly suited for potential clinical or experimental work. It will resolve displacements of .0003 inch and will follow frequencies up to 100 hertz. Its use required placing the tube in a water bath to provide a low loss propagation medium for the ultrasound beam. The effects of this exterior water bath on the propagation parameters of the pulse wave are discussed in Appendix B.

In general, the external water bath produces an added mass of fluid moving with the tube. For the conditions of this experiment, the effect of the added mass reduced the propagation velocity by 24.4% from that calculated for the free tube. The viscous effects of the external water bath and the compressional wave in the fluid were found to be insignificant.

THE PULSE WAVE

An initial portion of this study was devoted to the selection of the type of wave to be used. The three axisymmetric directions, radial, axial and circumferential have been used to describe the motion of propagating waves. There are three different axisymmetric waves which have major components of motion associated with each of the three

axes. These waves are coupled through Poisson's ratio and each one produces motion along all three axes. The wave associated with motion primarily in the circumferential direction is called the torsional wave and its propagation characteristics are principally determined by the shear dependent properties of the tube wall material. The wave associated with motion primarily in the axial direction is called an axial wave and its propagation characteristics are principally determined by the volume compressibility characteristics of the tube wall material. The wave associated with motion in the radial direction is called the pulse wave and its propagation characteristics are determined by elastic properties of the tube wall, the properties of the fluid, and tube dimensions. The use of the term pulse wave is to provide a direct analogy between the biologically observed pulse wave, and the axisymmetric wave present in the fluid-filled tube.

The choice of which of the waves to examine and its method of generation were considered as being important to the study. Both the axial and torsional waves were considered initially because their propagation is not dependent upon the dimensions of the tube as is that of the pulse wave. However, the limited possibility of being able to nontraumatically generate or measure either axial or torsional waves plus the unknown influence of tethering of

the arterial wall to the surrounding tissues makes them less useful than the pulse wave. The pulse wave, which propagates at the slowest velocity of the three waves can be detected with instrumentation of lower maximum frequency response than for the faster propagating axial and torsional waves. The available instrumentation; transducers for fluid pressure, and the prototype phase-lock ultrasound transducer for radial wall motion, provide their greatest response to the pulse wave because these are the two quantities that have their maximum variation with the pulse wave.

In addition to the choice of the pulse wave, it is necessary to consider using continuous waves or single pulses. The continuous wave can be used because it provides a direct correlation between theory and experiment for linearized solutions and lends its results to the use of fourier series analysis of complicated wave forms. The continuous wave can be generated experimentally with readily available equipment. However, there are some disadvantages to the use of continuous waves: the wave speed must be determined from a phase difference of two wave forms. In the absence of reflected waves accuracy better than 1% of a cycle would require sophistication not likely to be possible when applying the results to the cardiovascular system. Reflected waves are interpreted from contour changes. Long tubes are necessary to eliminate extranneous reflections. And, all waves which are generated are superimposed. As an

alternative, single pulse waves are seen to have several advantages over continuous waves: reflected waves and the different types of waves which are generated can be isolated by their different time and space relationships. The wave speed is obtainable from the arrival time of a characteristic feature of the pulse wave. Short tube lengths can be studied. And, the results from continuous wave theory provide a fundamental theoretical background for interpreting the results. The disadvantages associated with single pulses are that the frequency response of the instrumentation must be slightly higher than for continuous waves, and that arrays of time and space data require multiple transducers with a single pulse, or single transducers and multiple repeatable pulses. In evaluating the use of the single pulse versus the continuous wave, the single pulse was chosen because it can be isolated and directly observed in finite-length segments.

The pulse wave has several significant characteristics. The pulse wave which is identified with the predominant radial deformation may be called a pressure pulse because it can be identified with a pressure transducer in fluid. Its propagation is associated with the largest amount of fluid motion of the three propagating waves in the tube. The axisymmetric generation of the pulse wave also generates an axial wave. In studying only the pulse wave their

superposition can be shown to produce measurable errors in the observed data. These effects of superposition have been shown to be an increased centerline pressure and a decreased radial motion. The axial wave, which propagates at a higher velocity than the pulse wave, can be seen in Figure 4-3 to have an associated small pressure wave when separated from the pulse wave. This small pressure component of the axial wave has not been previously identified in continuous-wave experiments. In addition to the presence of an axial wave, the rise time of the pulse is related to the production of a dip or constriction at the leading portion or foot of the wave. This constriction is a result of bending in the wall in the axial direction. It was most apparent with shorter rise time pulse waves which have shorter wavelengths and hence, increased axial bending. It was not observed with pulses having rise times near the normal arterial pulse wave.

The identification of the significant features which can be used to characterize the single pulse wave and its propagation along the tube must be considered in relation to the deviations which occur at the foot of both the pressure and wall motion components. Because of the axial wave observed with the pressure transducer, and the leading constriction observed with the wall motion transducer the peak rather than the foot was chosen as the characteristic feature of the pulse wave. The peak of the wave is

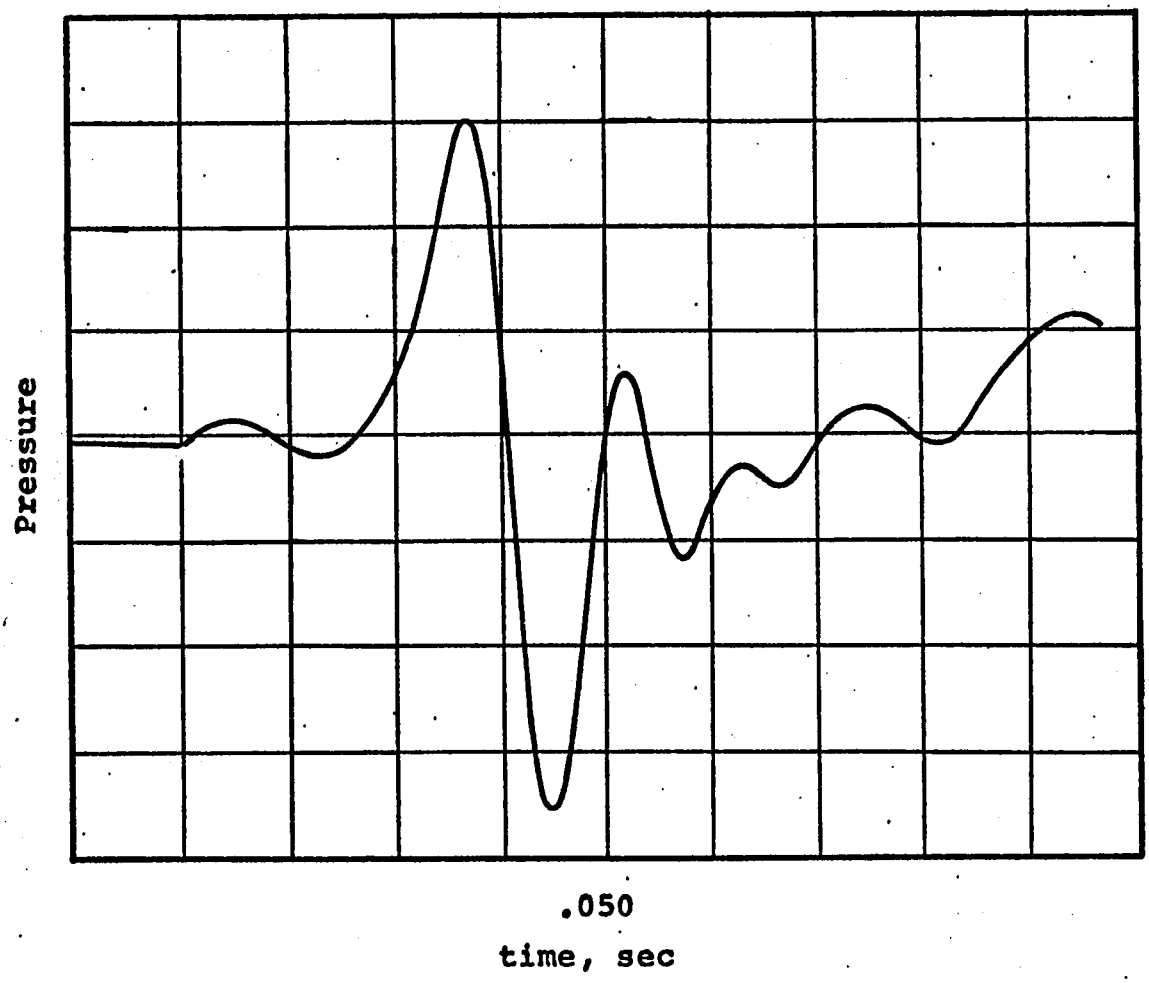

FIGURE 4-3 PRESSURE PULSE WAVE

associated with the group velocity and provides a representation of the energy present in the wave. Both Kyle(70) in a digitized analysis of the pulse wave, and Hale et al. (51) in the construction of an electronic pulse-wave identifying instrument have confirmed the use of the peak in producing statistically more significant information than other features of the wave.

The pulse wave used in the study was generated by producing a half sine wave with the piston at one end of the tube and allowing the returning motion of the fluid to create the second half of the sine wave. Only the rising portion of the pulse wave from the foot to the peak was used in studying the propagation characteristics. The trailing oscillations in time and space were not investigated. The length of the rise time of the pulse was kept as short as possible within the practicality of producing a clean pulse contour which was determined by the elimination of rebound when the armature returned to the stop. The use of maximum power from the amplifier for the electromagnetic shaker did not reduce the rise time by more than 2 milliseconds. In attempting to reduce the rise time the piston was hollowed for lightness but the armature weight of 2.6 pounds in the electromagnetic shaker dictated that further lightening procedures would be of negligible value. This configuration produced a uniform pulse with a rise time of 10 milliseconds, approximately an order of magnitude shorter than the rise

time of 10 milliseconds, approximately an order of magnitude shorter than the rise time of the normal arterial pulse wave. The total wavelength of the sine wave was approximately 6 inches long, and could be contained within the length of the tube without the presence of superimposed reflections. This is in contrast to the arterial system where the pulse wave length is approximately 5 times the length of the body and does not allow the observation of reflection-free pulses.

PROPAGATION VELOCITY: Arrival Time

The first feature noted about the propagation characteristics of a single pulse wave in a fluid-filled tube is that if the geometry of the tube is constant, and the material properties of the tube wall are constant, the wave velocity is uniform along the axis of the tube. Figure 4-4 shows the axial position versus the time of arrival for the uniform 20 durometer tube. The straight line is a linear regression of the arrival time versus the axial position and gives a wave speed of 226.6 inches/second. This can be used to calculate a standard error in the observed arrival time of less than .300 milliseconds for the experimental data by assuming the tube to be uniform. This provides a guide-line for the later experiments with tubes having hardened sections. Distance measurements were held to increments as short as .200 inches which allowed the time of arrival to be determined to a significance level greater than 0.95.

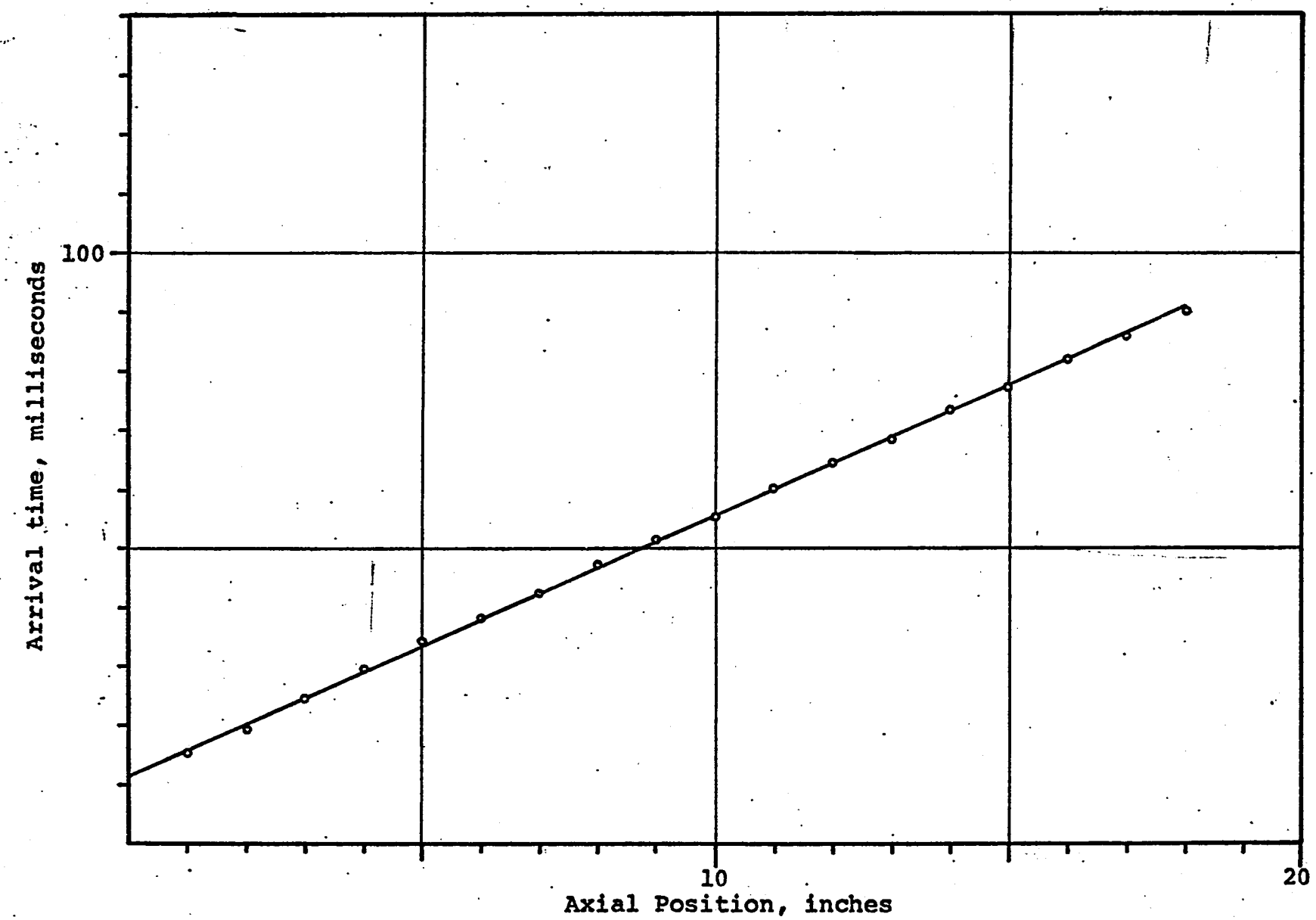

FIGURE 4-4 ARRIVAL TIME VERSUS AXIAL POSITION FOR UNIFORM TUBE

The presentation of the data representing the propagation velocity has been done in terms of arrival time of the pulse wave at each axial position rather than the local velocity. The velocity, when obtained by differentiating the experimental data over short distances, amplifies experimental errors. To reduce the error in the final result an expected value of the propagation velocity was computed from a large number of data points using the statement of uniform propagation velocity with distance. The linear regression of the values of the arrival time and axial position will provide a means of estimating the propagation velocity. This velocity obtained from the regression can be used to calculate an expected arrival time in examining the statistical validity of the data. The difference between the estimated arrival time and the experimentally observed arrival time is a useful parameter in describing the local conditions which result in an altered propagation velocity. This difference in observed arrival time compared to the expected arrival time is expressed in the parameter TMD as:

$$TMD = t(x) - t_e(x) \qquad (4\text{-}1)$$

$t(x)$ = expected arrival time

$t_e(x)$ = experimentally observed arrival time

Figure 4-5 shows the parameter TMD for the uniform tube including data from both the centerline fluid pressure and the radial wall motion. The data from the radial wall

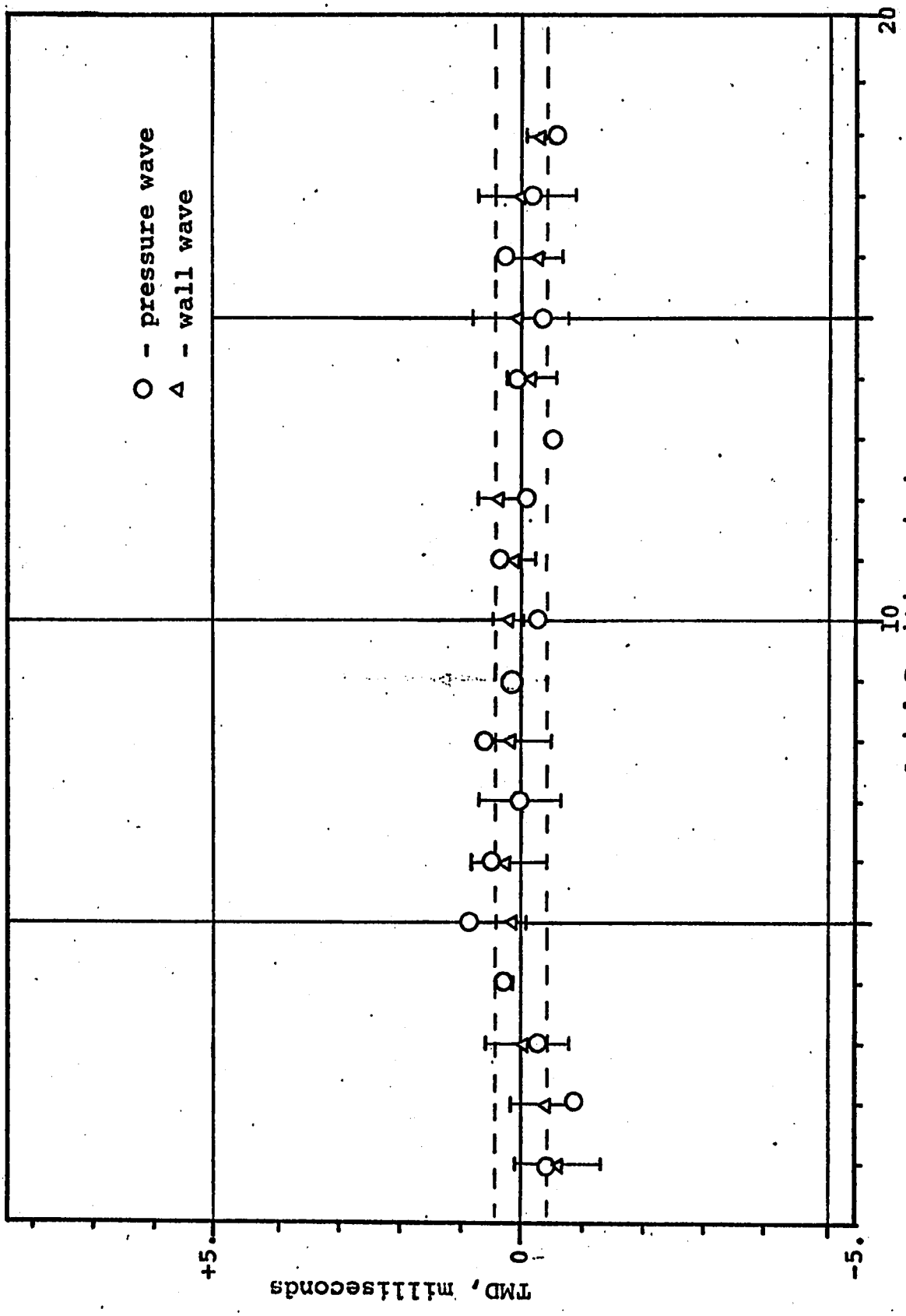

FIGURE 4-5 TMD VERSUS AXIAL POSITION FOR UNIFORM TUBE

motion is presented here in the form of average values with standard deviations obtained from measurements in the arrival time of the wave taken about the circumference of the tube. The values for the wall motion have been plotted as mean values with one standard deviation indicated at each position. The value of one standard deviation is shown by the dashed line for the pressure wave. The data from the pressure wave has a standard error of .3 milliseconds from the expected value. The wall wave shows somewhat more scatter having a standard deviation at each axial location of slightly less than .5 millisecond. Both the pressure wave and the axial wave provide an accurate estimate of the pulse wave, the wall motion having somewhat more variation than the pressure wave.

Attenuation

In addition to the propagation velocity of a pulse wave, it is necessary to know the nature of the attenuation with distance. For the uniform tube the pressure pulse is shown to obey the exponential relation:

$$P(x) = P_0 e^{\eta x} \qquad (4\text{-}2)$$

where η is a negative real number. Figure 4-6 shows the pulse wave amplitude versus the axial position. The calculated exponential decay is shown with the curve. Knowledge of the form of the attenuation is necessary for obtaining quantitative results from changes in the pulse wave contour and

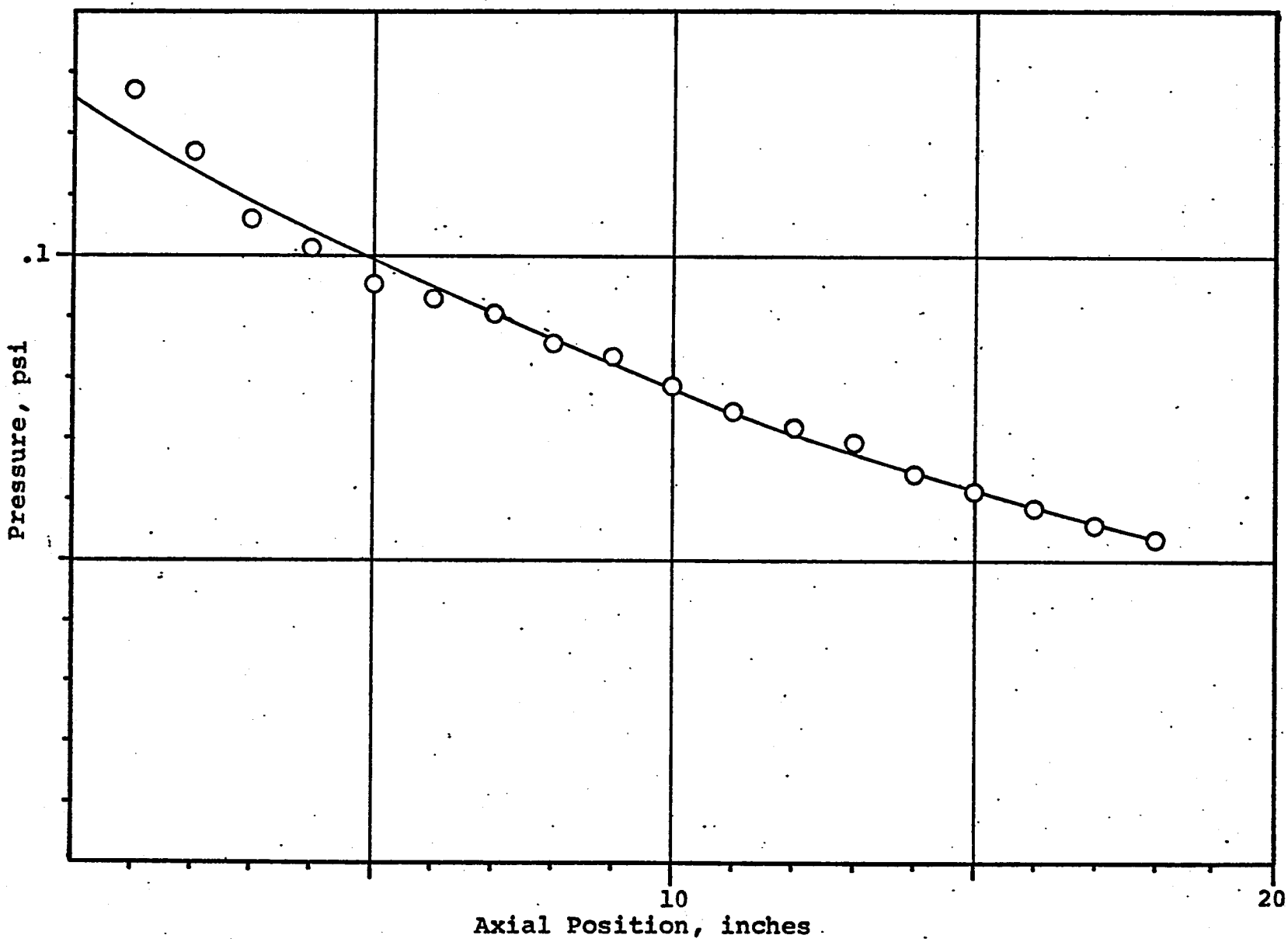

FIGURE 4-6 PRESSURE VERSUS AXIAL POSITION FOR UNIFORM TUBE

amplitude. When the reflected wave is superimposed upon the incident wave the use of the normal attenuation provides a means of estimating the amplitude of the incident wave. By separating the incident from the reflected wave, the reflection coefficient can be obtained. The fluid pressure has been used for calculating the attenuation of the pulse wave. Radial wall motion, which is related to the fluid pressure, can also potentially provide data for use in the calculating of the attenuation but as will be shown later, the wall motion is more variable and not as accurate as the pressure for calculating attenuation. The centerline pressure, is a combined effect of the average motion of the wall and is more suitable for calculating parameters relating to the attenuation. Radial wall motion is subject to variations about the circumference that contribute larger uncertainty in the result than is present with the fluid pressure.

The data from centerline pressure can be used to compute a parameter RFC, which is calculated from the experimental data and the attenuation relationship. The exponential attenuation is linearized by taking the logarithm of equation (4-2).

$$\ln P(x) = \ln P_o + \eta x \qquad (4-3)$$

The unknown constants, P_o and η , may be determined by a regression analysis of the transformed experimental data. This method was used to obtain the exponential curve in

Figure 4-6. The parameter RFC is then calculated according to the relation:

$$RFC = \frac{P_e(x) - P_o e^{\eta x}}{P_o e^{\eta x}} \qquad (4\text{-}4)$$

$P_e(x)$ = experimentally observed pressure

Figure 4-7 shows the values of RFC versus axial position for the uniform tube. In tubes with hardened sections the reflection coefficient is the maximization of RFC at the leading edge of the section. Two regions of the uniform tube can be identified from the values of RFC in Figure 4-7; the region near the piston face, and the remainder of the tube distal to this region.

In the region near the piston the axial and pulse waves are superimposed. This near-piston region extends from the piston to the point where the axial wave has separated from the pulse wave. This can be determined by calculating the respective velocities of the axial and the pulse waves. In this region the axial and pulse waves are generated simultaneously, and the centerline pressure is observed to be elevated above that which is expected for a pulse wave propagating along a uniform tube. This increase is seen by the values of RFC being approximately .05 one-inch from the piston, and decreasing with distance from the piston as the two waves become separated.

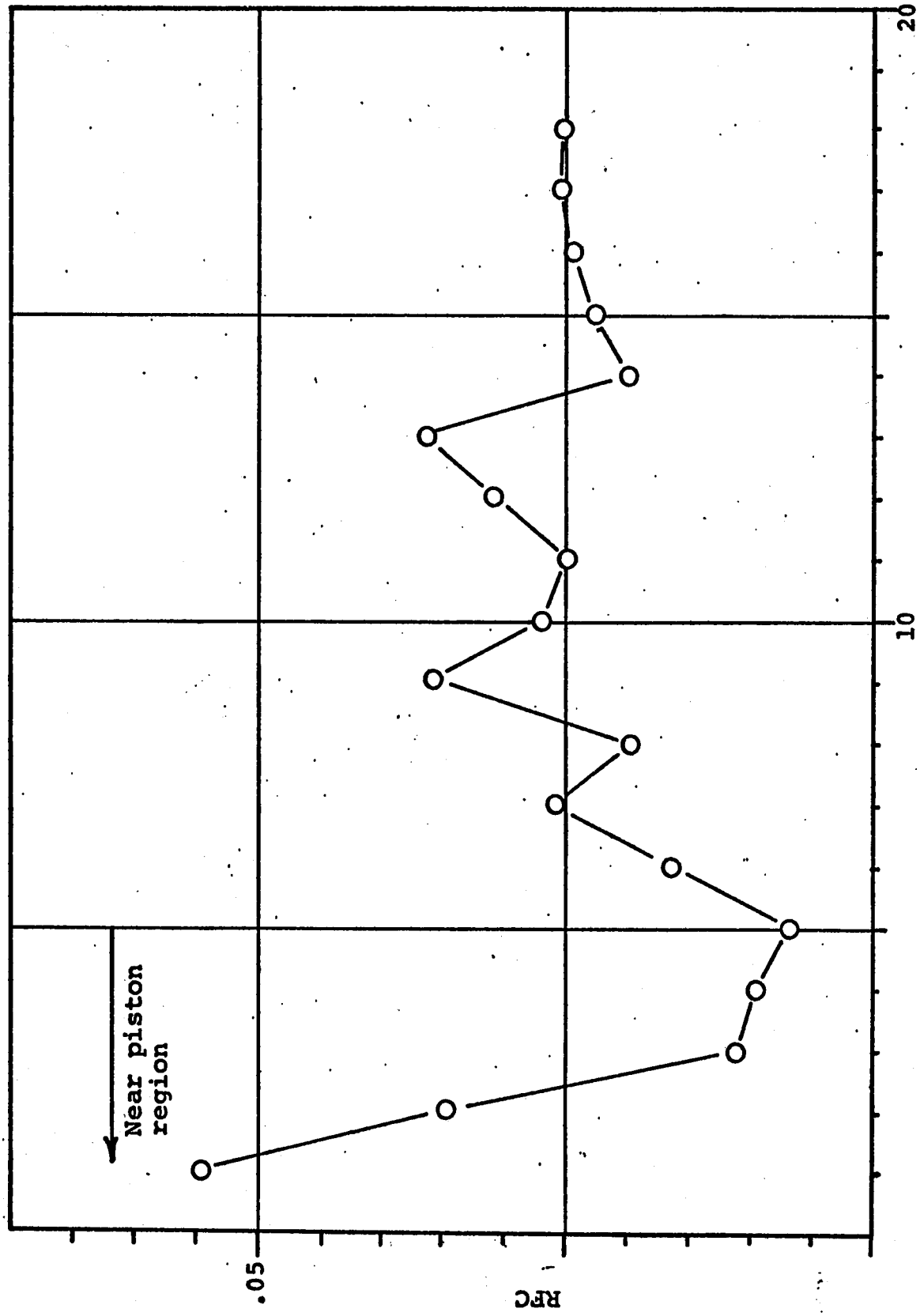

FIGURE 4-7 RFC VERSUS AXIAL POSITION FOR UNIFORM TUBE

The use of an axisymmetric model for the tube wall forms the basis for attempting to use the radial wall motion to calculate the parameter RFC. That this could be done would be the potentially valuable result of calculating the reflection coefficient from radial wall motion with at least the same accuracy as using the centerline pressure. Two factors, however, preclude the use of radial wall motion for directly relating the centerline pressure to the radial wall motion, and its use in calculating the reflection coefficient. First, the geometric values, the mechanical properties, and the pulse frequency are necessary to accurately relate the centerline pressure to the radial wall motion. Second, the experimentally observed variability in the radial wall motion about the circumference is sufficiently large so that the calculated values from radial wall motion are not as statistically significant as the values from the centerline pressures.

RADIAL WALL MOTION: Normalized and Nondimensional

In order to obtain a relationship between the centerline fluid pressure and the radial wall motion, a nondimensional quantity RHP was formed. It will be seen that the variability in the radial motion is accounted for by using the mean value of the radial motion in assuming axisymmetric deformation. The analytic relations for the radial wall velocity and the centerline pressure as derived

by Atabeck and Lew(9) form the basis for this quantity. The expression for the radial velocity is:

$$V_r = \frac{A\beta}{c\rho}\, i\left[\frac{r}{a} + \frac{mJ_1\alpha_o(r/a)}{\alpha_o J_o(\alpha_o)}\right] \exp[i\omega(t-x/c)] \qquad (4\text{-}5)$$

The expression for the pressure is:

$$P = A \exp[i\omega(t-x/c)] \qquad (4\text{-}6)$$

The rate of change of pressure is:

$$\frac{\partial P}{\partial t} = i\omega A \exp[i\omega(t-x/c)] \qquad (4\text{-}7)$$

The ratio of the radial velocity to the rate of change of pressure at r=a is:

$$\frac{V_r}{\partial p/\partial t} = \frac{\beta}{c\rho\omega}\left[1 + m\frac{J_1(\alpha_o)}{\alpha_o J_o(\alpha_o)}\right] \qquad (4\text{-}8)$$

The nondimensional parameter RHP is taken to be:

$$RHP = \left(\frac{V_r}{\partial p/\partial t}\right)\left(\frac{c\rho\omega}{\beta}\right)\left[1 + m\frac{J_1(\alpha_o)}{\alpha_o J_o(\alpha_o)}\right] \qquad (4\text{-}9)$$

The radial velocity is replaced by the average of the radial displacements about the circumference of the tube, and the rate of change of pressure is replaced by the amplitude of the pressure pulse. The parameter RHP is calculated from:

$$RHP(x) = \left[\frac{\frac{1}{N}\sum U_r(x,\theta)_{max}}{P(x)_{max}}\right]\left(\frac{c\rho\omega}{\beta}\right) \qquad (4\text{-}10)$$

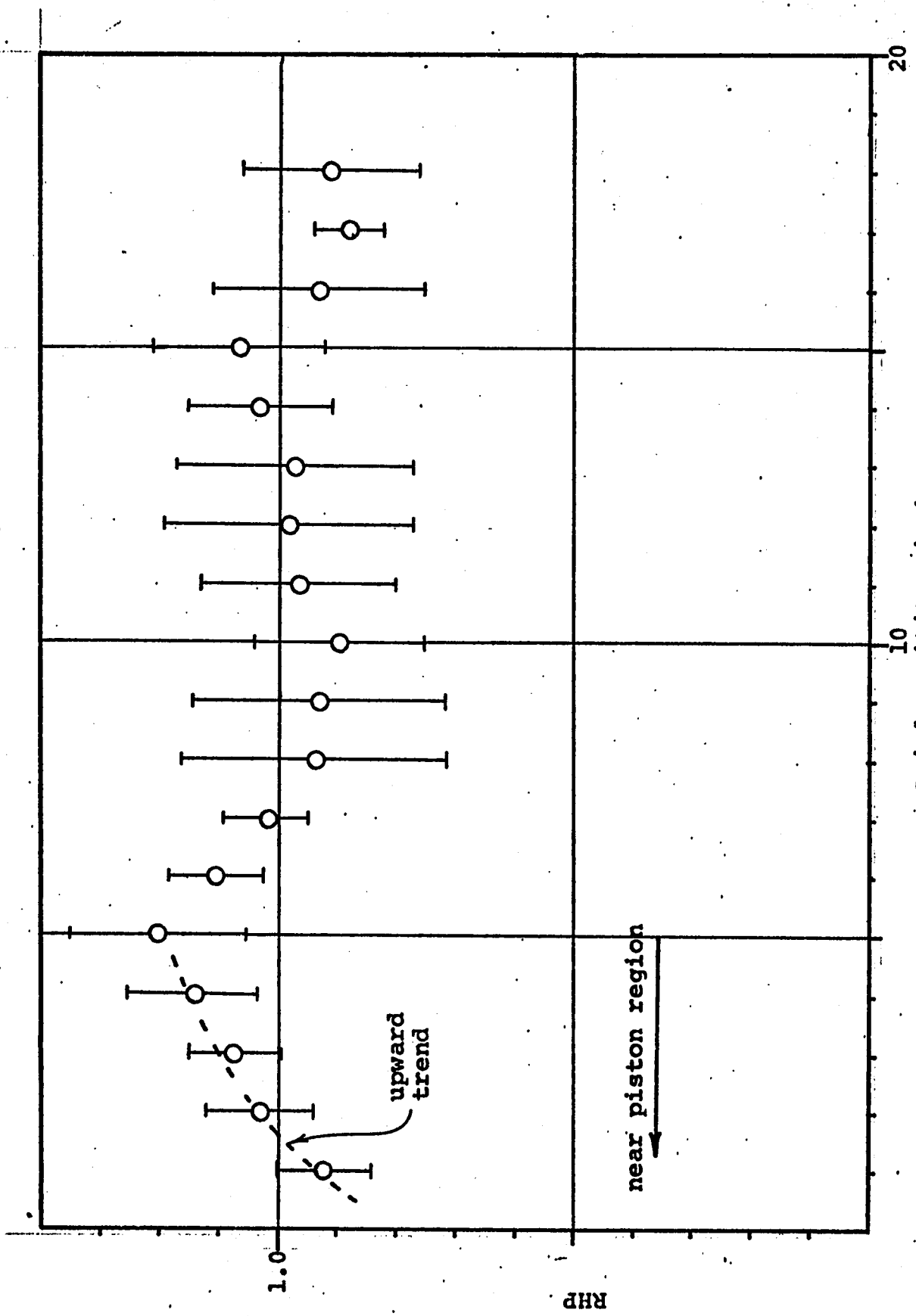

FIGURE 4-8 RHP VERSUS AXIAL POSITION FOR UNIFORM TUBE

The evaluation of the term

$$m \frac{J_1(\alpha_o)}{\alpha_o J_o(\alpha_o)}$$

under the conditions of the experiment yields:

$$m \frac{J_1(\alpha_o)}{\alpha_o J_o(\alpha_o)} = -.0247 + i\ .0258$$

This was taken to be small in relation to 1.0 and was neglected in the evaluation of the parameter RHP. Figure 4-8 shows the variation of the parameter RHP with axial position for the uniform 20 durometer tube. The standard deviation of RHP is plotted about the average value and is evaluated as:

$$\sigma(RHP(x)) = \frac{\sigma(U_r(x))}{P(x)} \left(\frac{c\rho\omega}{\beta}\right) \qquad (4\text{-}11)$$

RHP is calculated to have an expected value of 1.0 for the uniform tube.

The region near the piston was observed to have a value of RHP of approximately .85. In the section extending from the piston to where the axial and pulse waves were separated RHP showed a rising trend to the expected value near 1.0.

GENERATION REGION: Superimposed Pulse and Axial Waves

The generation of a single pulse wave in a uniform tube is accomplished with the simultaneous generation of an axial wave. The axial wave propagates approximately three

times faster than pulse wave and the two waves become adequately separated after about 5 inches of travel. This generation region has been identified by measurements of axial and pulse waves as well as deviations in the expected values of the quantities RFC and RHP. The coupling between the axial and the pulse waves is a result of Poisson's ratio for the material properties of the tube wall. The separation of the two waves has provided a greater accuracy in the calculated values of RFC and RHP in explaining the significance in deviations of pressure and wall motion in the generation region.

The effective separation of the axial and the pulse waves is achieved 5 inches from the piston face. Figure 4-3 shows the arrival times of the coupled axial wave and the pulse wave 6 inches from the piston to illustrate their separation in arrival time at this distance. The axial wave in Figure 4-3 was identified by positioning a second motion transducer to record the axial motion of a target attached to the tube wall. The attenuation of the axial wave is large enough that it does not produce significant effect in the pulse wave recordings after the waves have initially separated. This is confirmed by studies of Anliker and Moritz(7) where they experimentally observed the attenuation of axial waves in exposed canine arteries. When values of their attenuation constants are applied to the parameters of the tube used in this study, they predict that the axial

wave will decay to produce a coupled centerline pressure of less than 1% of the original amplitude in propagating the length of the tube and back to the hardened section. The data of this experiment has confirmed this in showing that the axial wave is not observable upon reflecting from the terminal end. The propagation velocity was experimentally determined to be 885 inches/second for the .875 inch ID 20 durometer tube. Anliker and Moritz(7) observed that the axial wave speed for the carotid artery of a dog is 910 inches/second and Van Citters(137) stated that the axial wave travels about 30 meters/second (1180 inches/second) in a fluid-filled rubber tube. Van Citters also observed the coupling between the axial and the pulse waves(137).

RELATIONSHIP BETWEEN WALL WAVE AND PRESSURE WAVE

One of the interesting points concerning the relation between the pressure wave and radial wall motion is at the foot or leading portion of the wave. Figure 4-9 shows the comparison between pulse waves from centerline fluid pressure and the radial wall motion. The gain of the oscilloscope has been adjusted to produce pulses of nearly equal amplitude for comparison of similarity of wave contour. At the foot of the wave the centerline pressure is increasing as associated with the axial wave, while at a later time difference of 3 milliseconds, the radius is seen to be constricting. Neither the timing of the axial wave and hence its axial position, nor the inherent background noise of the phase-lock

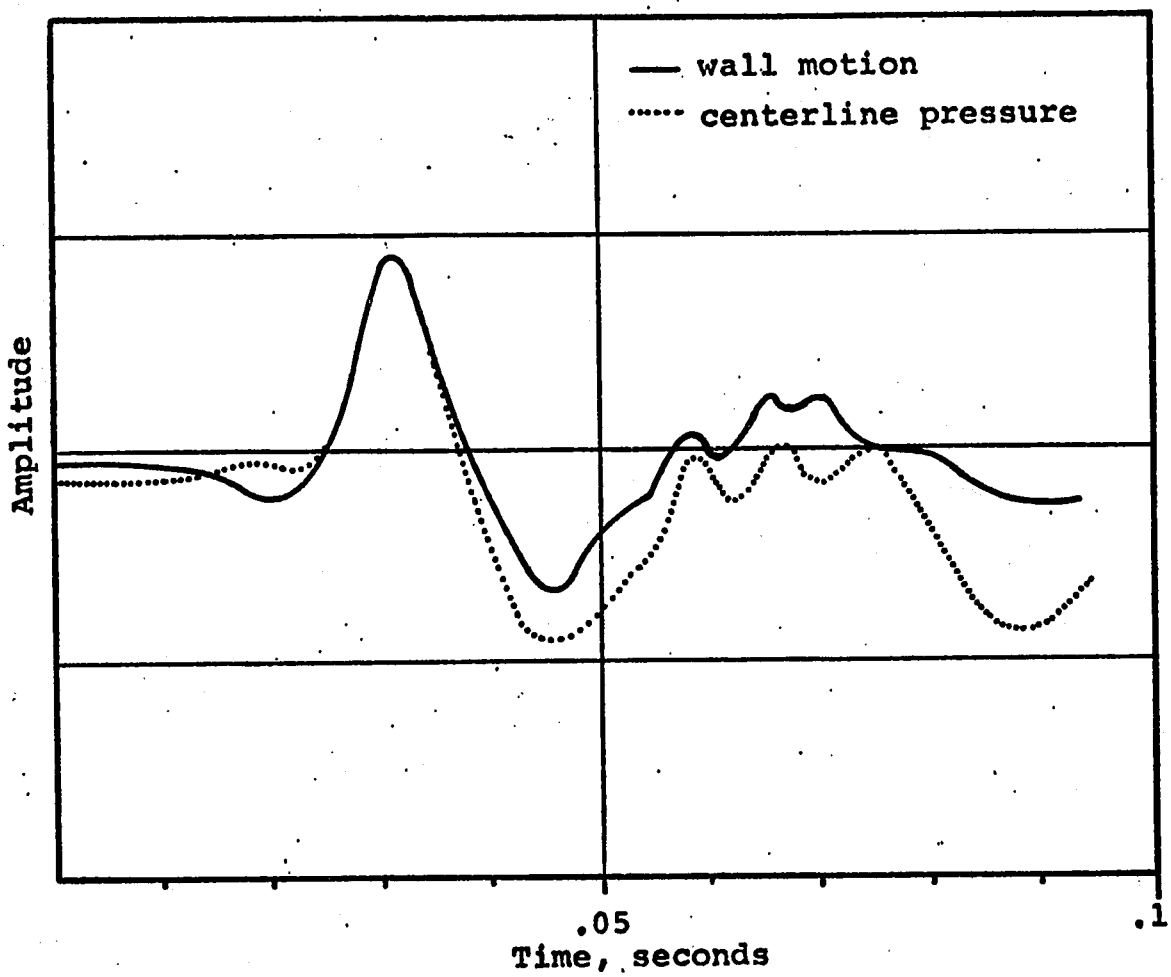

FIGURE 4-9 COMPARISON OF PULSE WAVE CONTOUR FROM CENTERLINE PRESSURE AND WALL MOTION

transducer effectively explain the occurrence of the slight contraction preceding outward radial bulge of the pulse wave.

The supporting evidence for explaining the existence of a constriction ahead of the pulse wave comes from the shell theory developed by Hermann and Mirsky(61). Their approach to the extension of the shell theory is to use an analogous approach for cylindrical shells that Mindlin(88) used for flat plates by incorporating rotary inertial and vertical shear. Professor A. F. Emery has developed the necessary Lagragian code to solve the relations developed by Hermann and Mirsky(61). For a test case a step change in pressure was propagated along an empty tube at the characteristic velocity, C_o . Figure 4-10 shows a plot of the radial position at one instant in time. The wall is seen to exhibit a negative radial motion immediately ahead of the pressure wave which produces a corresponding positive radial motion. The tube wall develops bending stresses in the axial direction which do not allow the wall to directly follow the pressure wave contour, but develops a contour where the bending stresses produce deformation that extends beyond the limits of the pressure pulse. The verification that the axial bending accounts for the constriction is not as strong as if a more complete analysis had been followed, but the results are within the range of the experimental results whereas the explanation of either the coupled axial wave, or the equipment noise does not. This evidence would lead one to consider

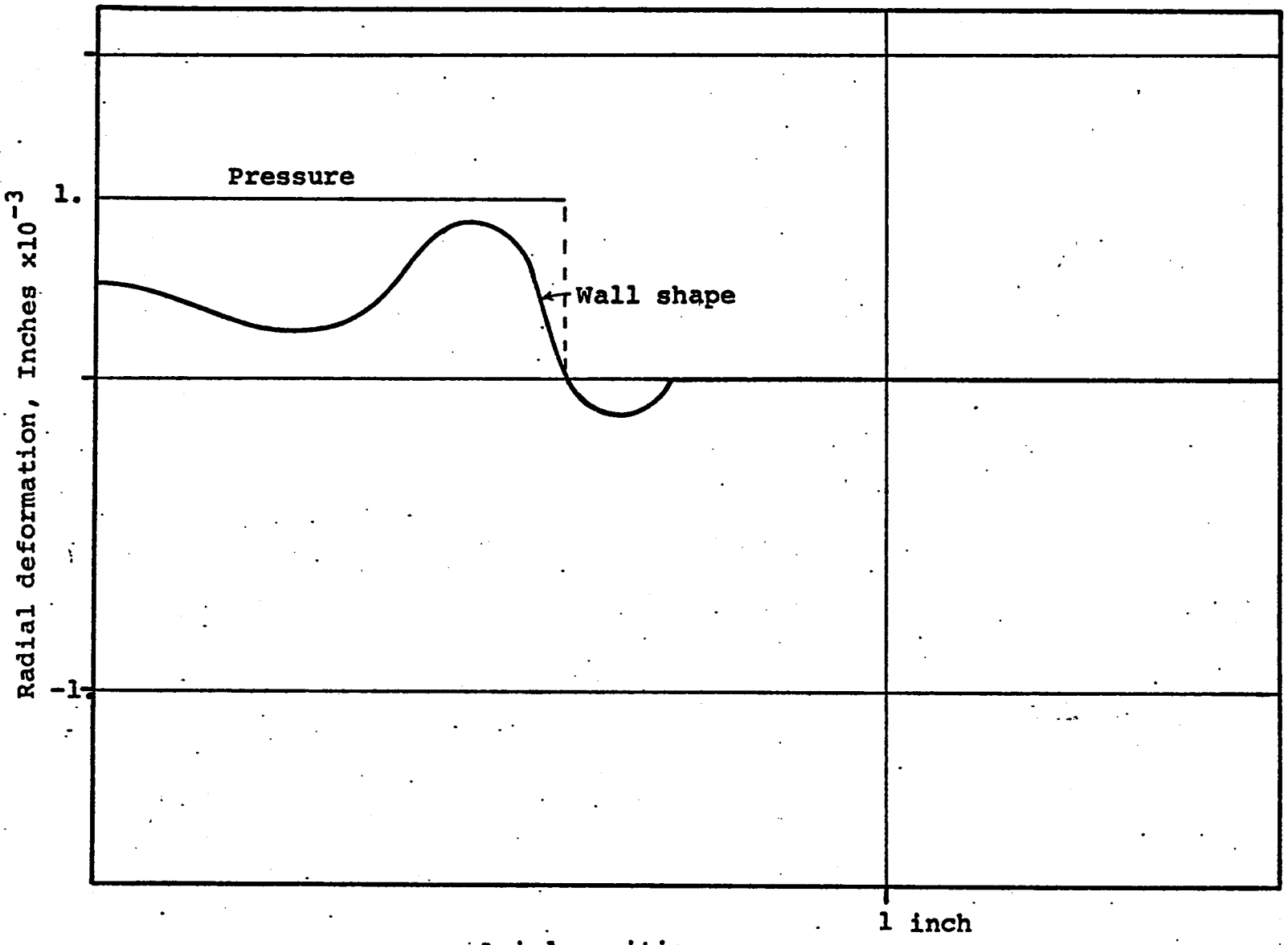

FIGURE 4-10 RADIAL DISPLACEMENT OF FREE TUBE FOR PROPAGATING PULSE

the development of analytic representations of the vessel wall incorporating rotary inertia and vertical shear in cases where the frequency of consideration is above 25 hertz. Mirsky(89) has solved a portion of this problem with linearized representations of the vessel wall for frequencies up to 10 hertz. It appears from these observations that the effects of rotary inertia and vertical shear are significant at higher frequencies and should be included into wall models where these effects could be significant. Mirsky(83) did not present information on the attenuation coefficient, which it appears would provide an interesting study.

NONUNIFORM TUBES: Hardened Wall Sections

The specific subject area of this study was the propagation of a pulse wave past a hardened section of a fluid-filled tube. The configuration shown in Figure 4-2 was specifically selected to be studied in addition to the uniform tube. As was noted previously, all tubes were fabricated from the same tube mold making all tubes 24 inches long with a uniform .875 inch ID and 1.000 inch OD. The tubes were nominally fabricated from 20 durometer rubber with hardened sections from 30,50,70 and 90 durometer rubbers. In the first section the proximal interface will be discussed; then, the next section will discuss proximal and distal interfaces in producing a finite length axisymmetric segment. The final section will cover finite length nonaxisymmetric segments.

Single Interface

The joining of two tubes with walls having different mechanical properties was used to study the proximal interface of an axisymmetric section. Figures 4-11, 4-12, and 4-13 show the comparison of the respective quantities TMD, RFC, and RHP along the axis for 20-90 and 20-50 tubes. The positions of the interfaces are shown in each figure, being 10.5 inches for the 20-90 tube and 11.0 inches for the 20-50 tube.

Figure 4-11 shows the comparison of TMD versus axial position for a 20-90 and a 20-50 tube. The higher velocity of the pulse wave in the hardened section is shown by the increasingly negative values of TMD in the hardened section. The steeper slope of 20-90 curve compared to the 20-50 curve in the hardened region shows the higher propagation velocity with tube walls of higher elastic modulus. Both curves show a slight peaking of TMD one diameter proximal to the interface. The 20-90 curve is greater than 2 milliseconds while the 20-50 curve is .85 milliseconds. Both peaks are statistically significant with both the 20-90 curve and the 20-50 curve at the 99% level. This peaking shows a slight deceleration, with the establishment of an increased pressure gradient to propagate the wave along the hardened section.

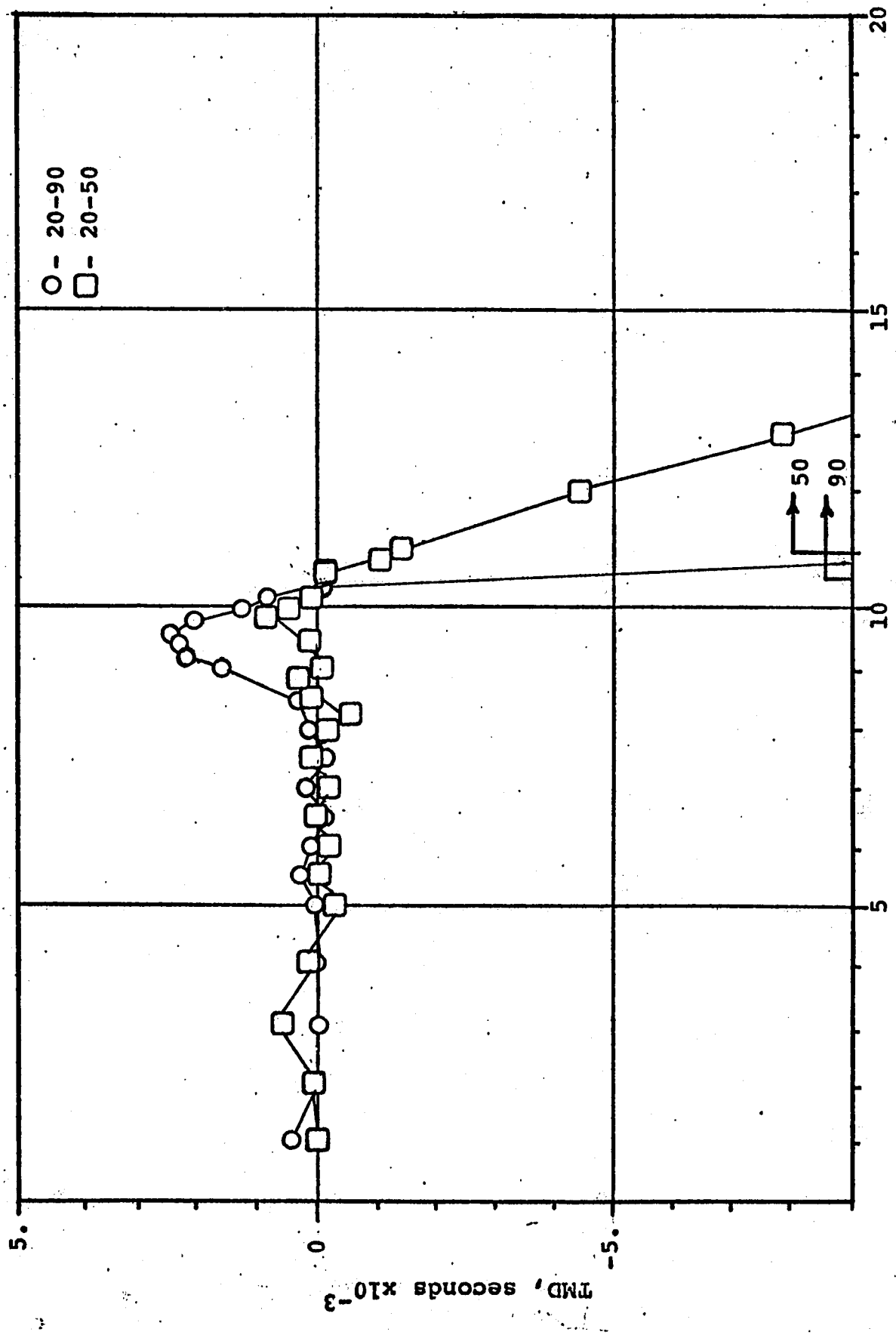

FIGURE 4-11 TMD VERSUS AXIAL POSITION FOR SINGLE INTERFACE HARDENING

Figure 4-12 shows RFC versus axial position for the 20-90 tube and the 20-50 tube. The increased proximal impedance of the 90 durometer tube produced an increased value of RFC over the 50 durometer tube.

Figure 4-13 shows RHP versus axial position for the 20-90 tube and the 20-50 tube. Both tubes show a significant decrease in RFC in the hardened region. The change from the expected value of 1.0 occurs over a one diameter axial length for both tubes. For each tube, the change in RHP occurs proximal to the interface of the hardened region.

Axisymmetric finite-length section:

A hardened section approximately two diameters in length was chosen as the model for a finite-length section. Figures 4-14, 4-15 and 4-16 show the comparison of a 90 durometer and a 70 durometer section using the variables TMD, RFC, and RHP.

Figure 4-14 shows the quantity TMD for the 90 and 70 durometer sections. Both show characteristically similar curves with a decrease in TMD across the hardened section. The change in TMD for the 70 durometer section is 7.3 milliseconds and for the 90 durometer section it is 8.4 milliseconds. After the distal interface of the 70 durometer hardened section there is a decrease in TMD of slightly greater than 1 millisecond. This would imply a slightly higher propagation velocity in this region which most likely results from a slight change in the mechanical properties of that

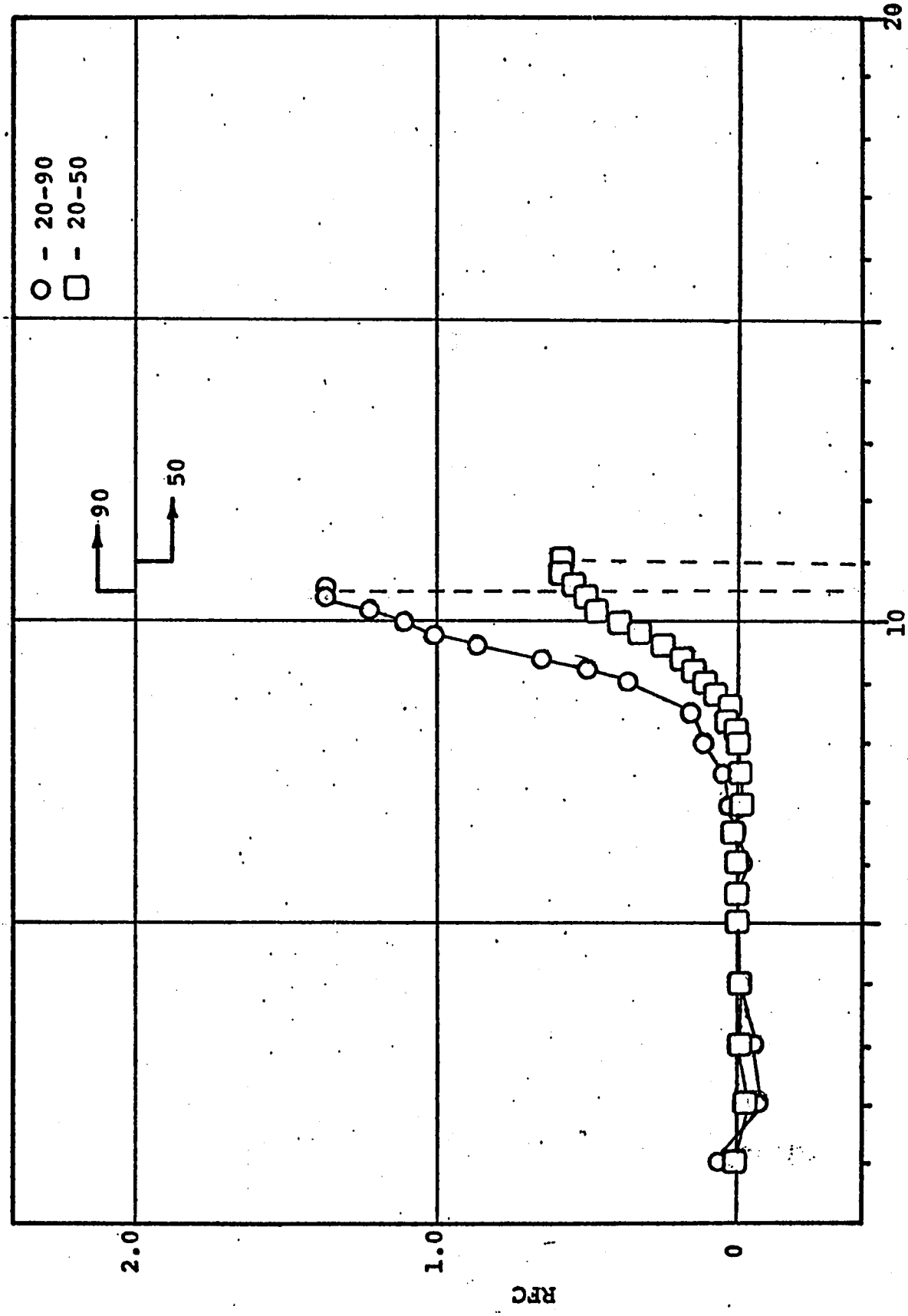

FIGURE 4-12 RFC VERSUS AXIAL POSITION FOR SINGLE INTERFACE HARDENING

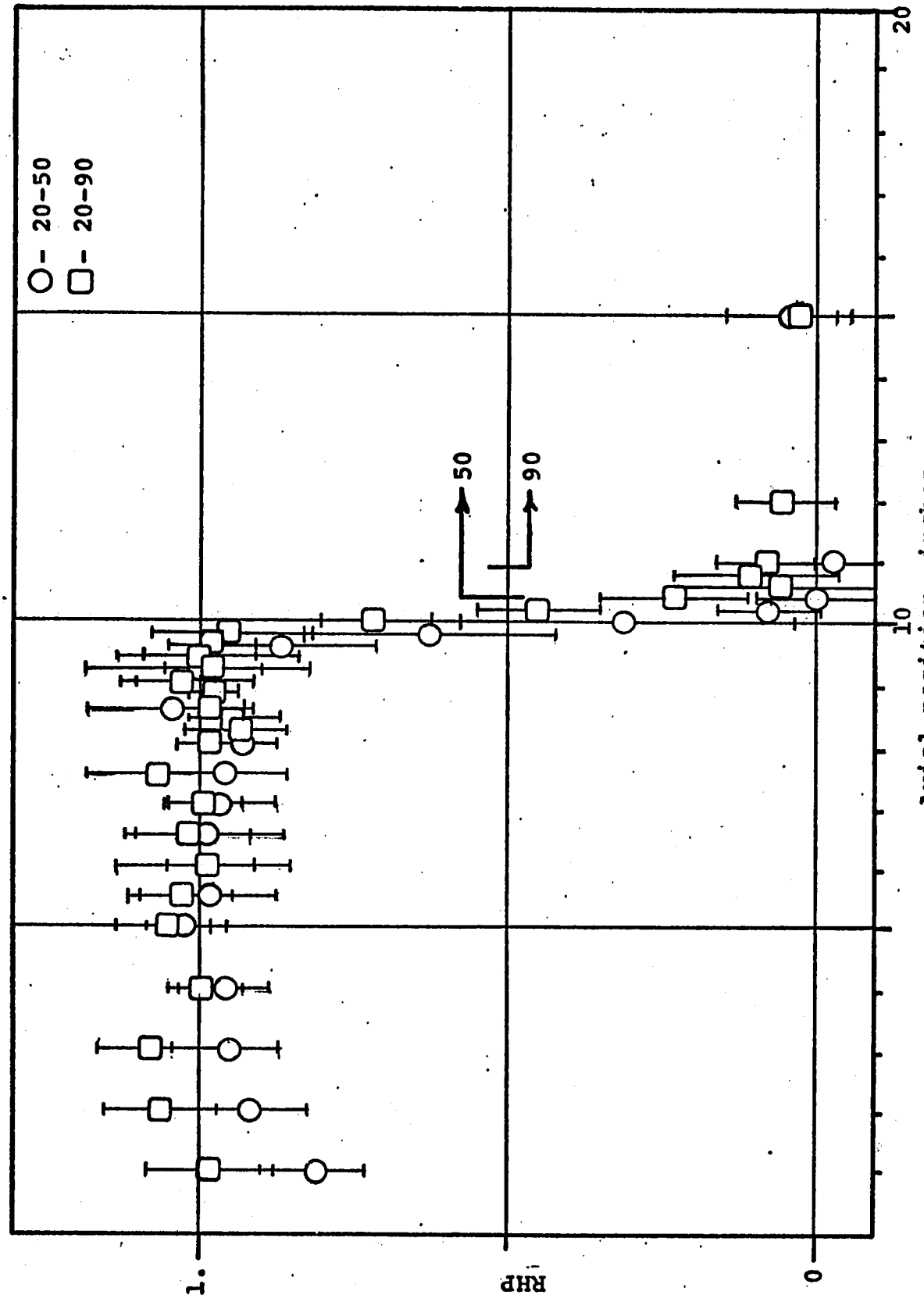

FIGURE 4-13 RHP VERSUS AXIAL POSITION FOR A SINGLE INTERFACE HARDENING

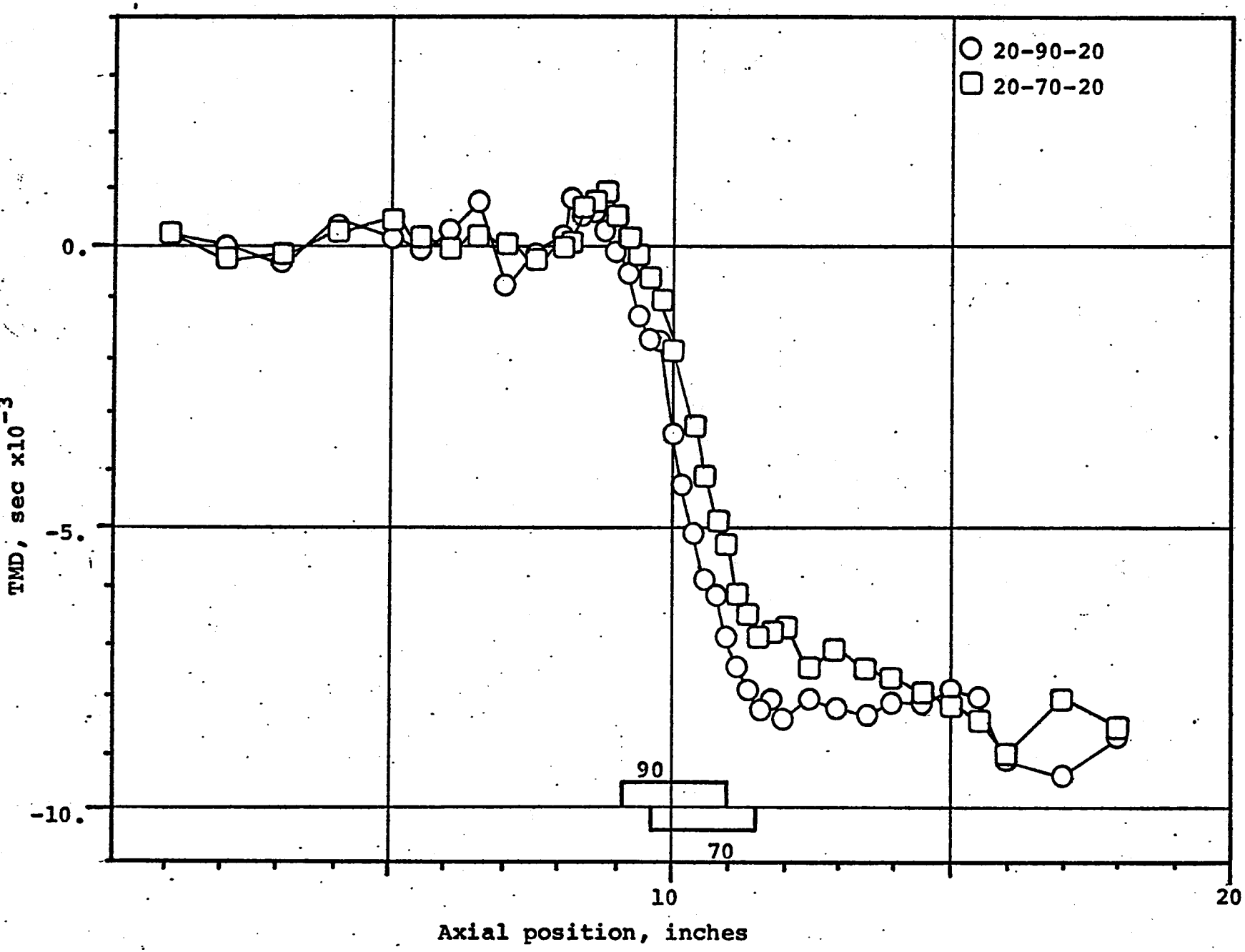

FIGURE 4-14 TMD VERSUS AXIAL POSITION FOR AN AXISYMMETRIC HARDENED SECTION

portion of the rubber tube. Extreme care in fabricating the tubes eliminated the major source of these anamolous effects. The tubes with lower durometer hardened sections, which tended to flow along the axis were excluded because of the difficulty of defining the interface and in producing tubes with propagation velocities changing over distances several diameters in length.

Figure 4-15 shows RFC versus the axial position for the 20-90-20 tube and the 20-70-20 tube.

The 90 durometer section produces a slightly larger reflection coefficient than the 70 durometer section, but the two are nearly identical.

Figure 4-16 shows RHP versus the axial position for the 20-90-20 and the 20-70-20 tubes. The axial position of the proximal and distal interfaces can be identified to within 1. diameter with greater than 99% certainty. The more rigid 90 durometer section showed negligible motion, and the 70 durometer section produced some motion although in the mean it was negligible.

Nonaxisymmetric finite-length section

The nonaxisymmetric hardened section was the model proposed to have the closest similarity to an atherosclerotic plaque. The single-interface tube and the axisymmetric sections established the form of the results. The array of the mechanical properties of the hardened sections is given

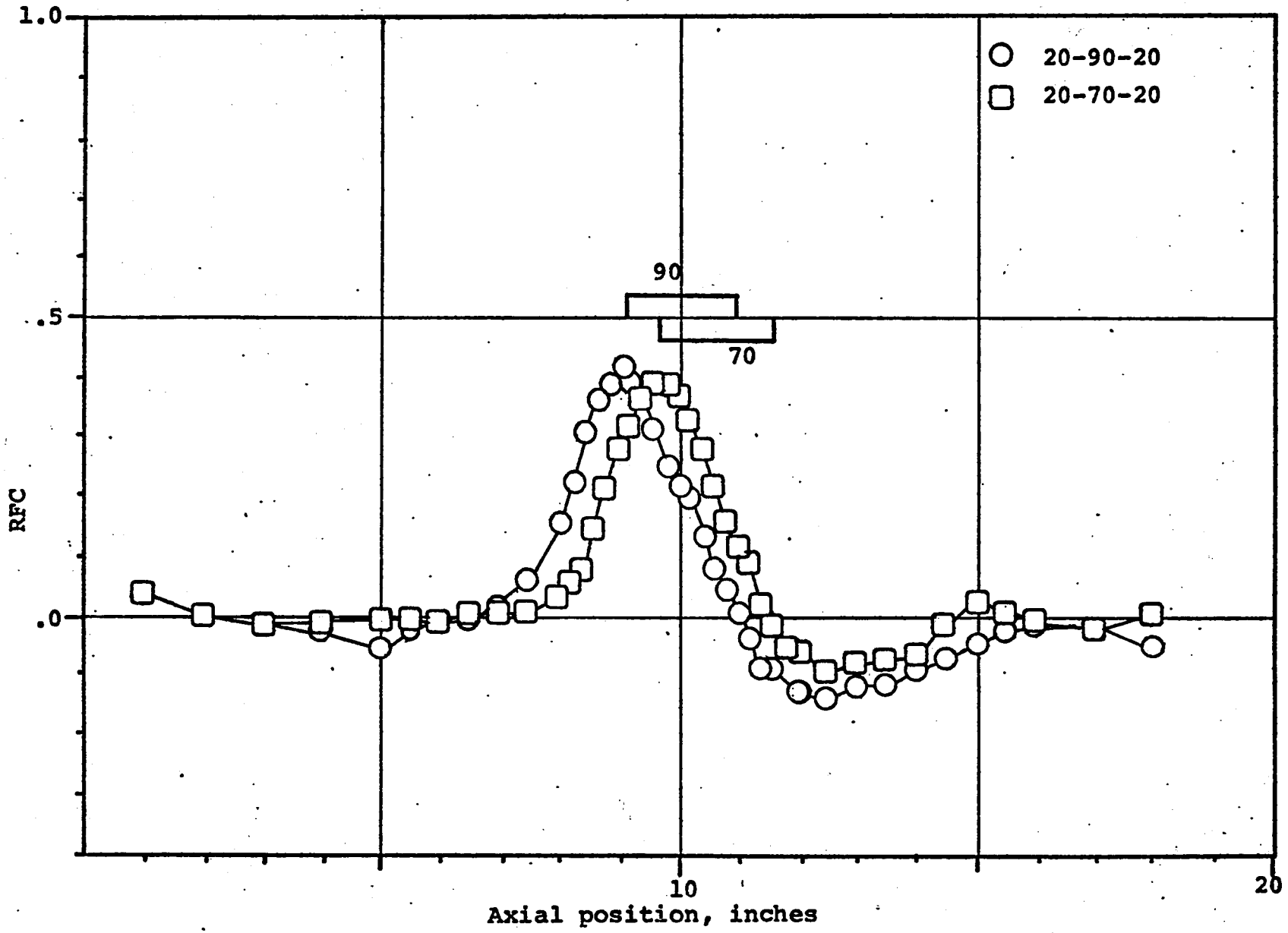

FIGURE 4-15 RFC VERSUS AXIAL POSITION FOR AN AXISYMMETRIC HARDENED SECTION

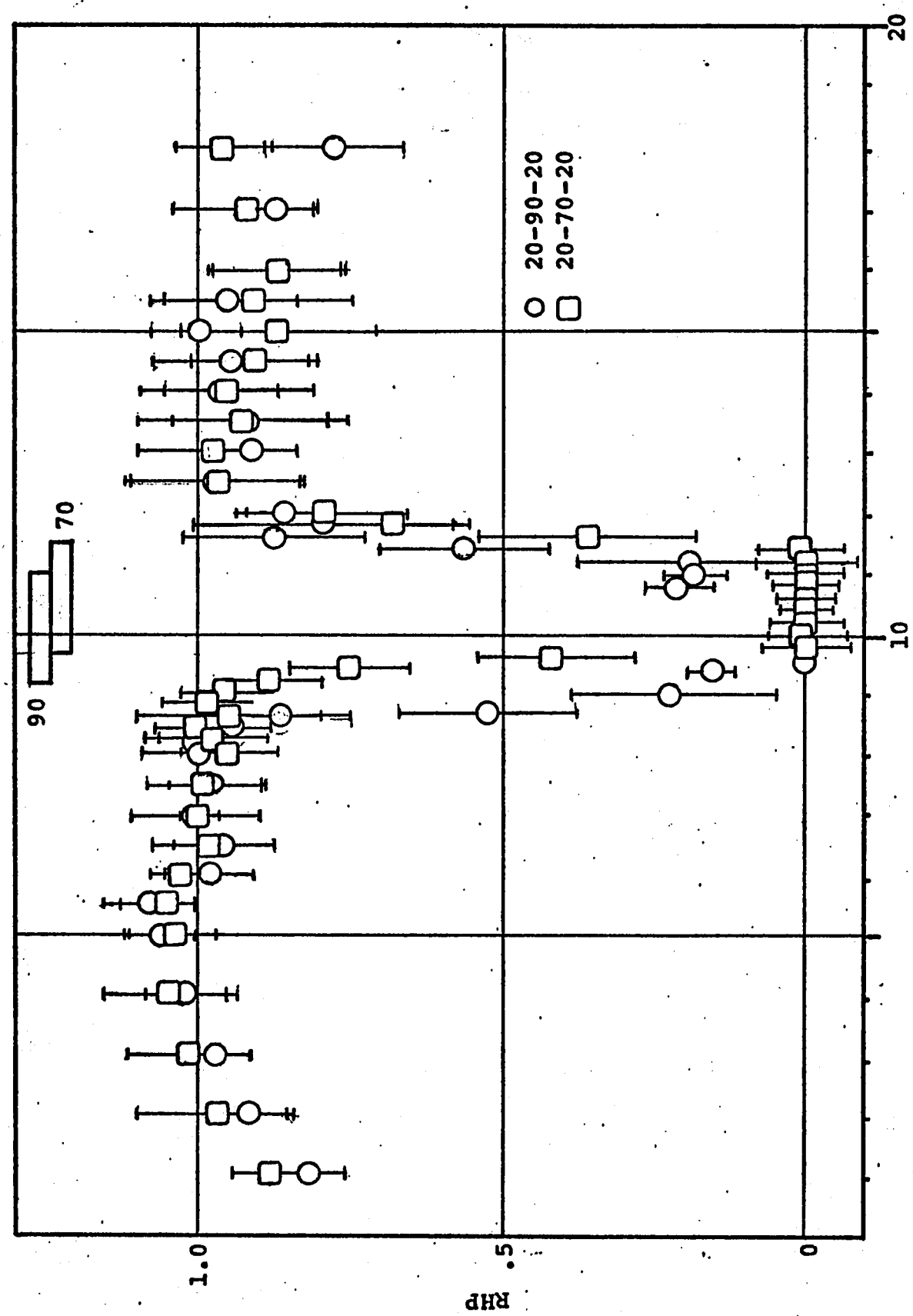

FIGURE 4-16 RHP VERSUS AXIAL POSITION FOR AXISYMMETRIC HARDENED SECTION. DATA INDICATES MEAN VALUE WITH ONE STANDARD DEVIATION.

and the sectors of hardening covered the range of proposed samples and the results are given for all samples in Appendix F. The 20-30-20-120° section and the 20-90-20-120° sections were selected for comparison and discussion in this chapter.

Figure 4-17 shows TMD versus axial position for the nonaxisymmetric hardened sections. The 20-30-20-120° section produces a change in TMD of 2 milliseconds while the 20-90-20-120° section is greater than 3 milliseconds. The 20-90-20-120° tube shows a gradual shift in TMD to -4.5 milliseconds after the section. This variation in 1 millisecond along the length of the tube is a 1% error in total time, showing how changes that occur with the propagation controlling parameters can affect the interpretation of the results. Being aware of this type of error is necessary for interpreting the results and making judgments regarding them. The small changes in arrival time which are caused by small changes in local mechanical properties of the wall require that the method of estimating the arrival time be accurate to less than a fraction of a millisecond.

The parameter RFC is shown in Figure 4-18. The reflection coefficient for the 20-30-20-120° tube is estimated to be .05 and for the 20-90-20-120° tube to be .12. The development of a detection technique incorporating the calculation of a reflection coefficient would be limited to large changes in the elastic moduli because reflection

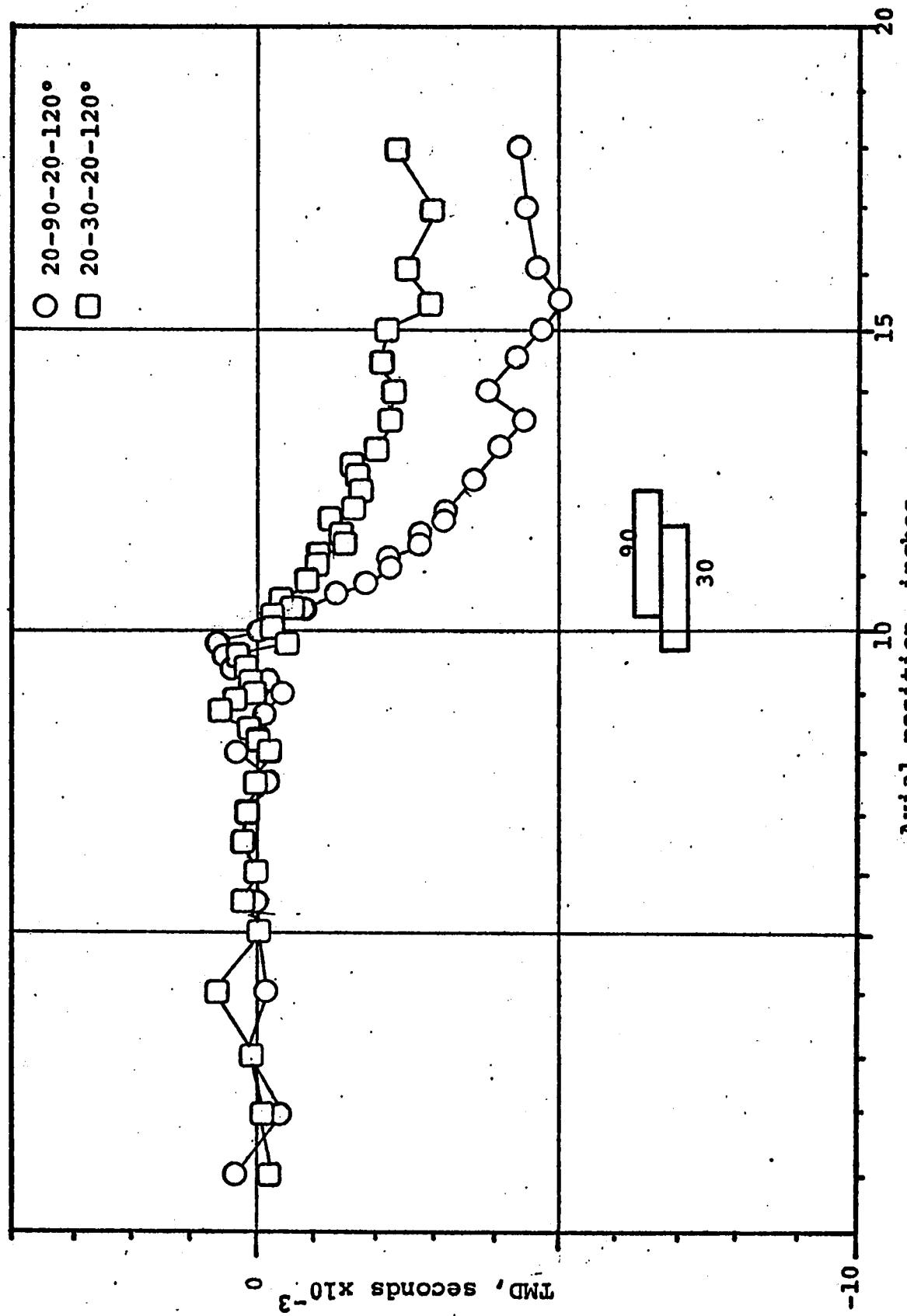

FIGURE 4-17 TMD VERSUS AXIAL POSITION FOR NONAXISYMMETRIC FINITE-LENGTH HARDENED SECTIONS

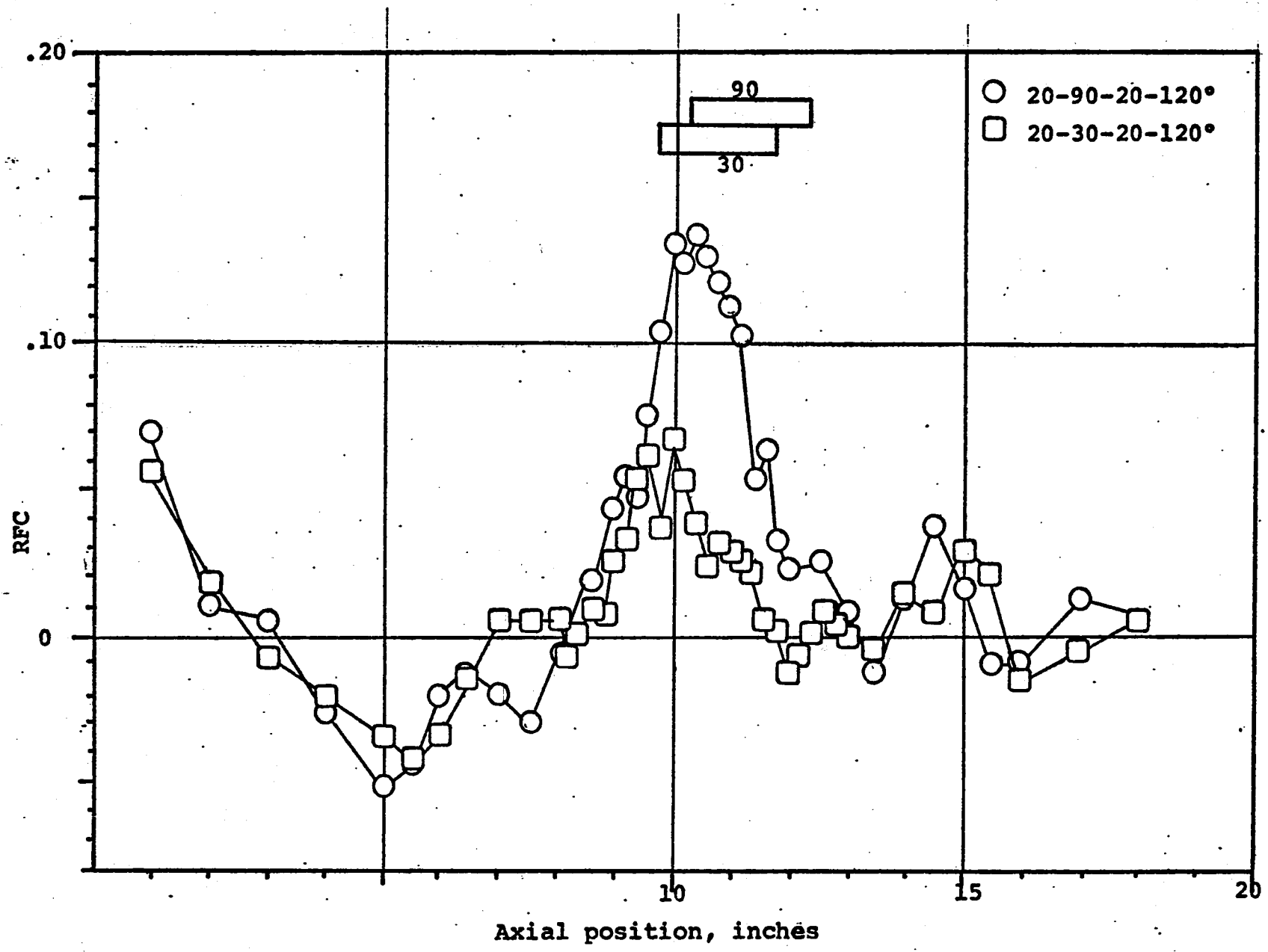

FIGURE 4-18 RFC VERSUS AXIAL POSITION FOR NONAXISYMMETRIC FINITE-LENGTH HARDENED SECTIONS

coefficients below .06 or .07 would not be statistically significant in the presence of observed variations in pulse amplitude. The 20-30-20-120° tube has a reflection coefficient that is definitely detectible with experimental tubes, but in making a priori judgments from recorded data, one must have a larger reflection coefficient such as is shown with the 20-90-20-120° tube.

Figure 4-19 showing RHP versus axial position illustrates the accuracy with which radial wall motion can identify the proximal and distal interfaces of the hardened section. The two sections were slightly greater than one-half inch apart in spacing as plotted showing that this difference was indicated. There was some increase in nonaxisymmetric motion of the wall from the nonaxisymmetric plaques as indicates by the large standard errors in the motion distal to the section. A correlation of this observed increased motion relative to the plaque location was not observed. The discussion of these results is covered in Chapter 5 and the extension to a proposed diagnostic technique for presymptomatic plaques is covered in Chapter 6.

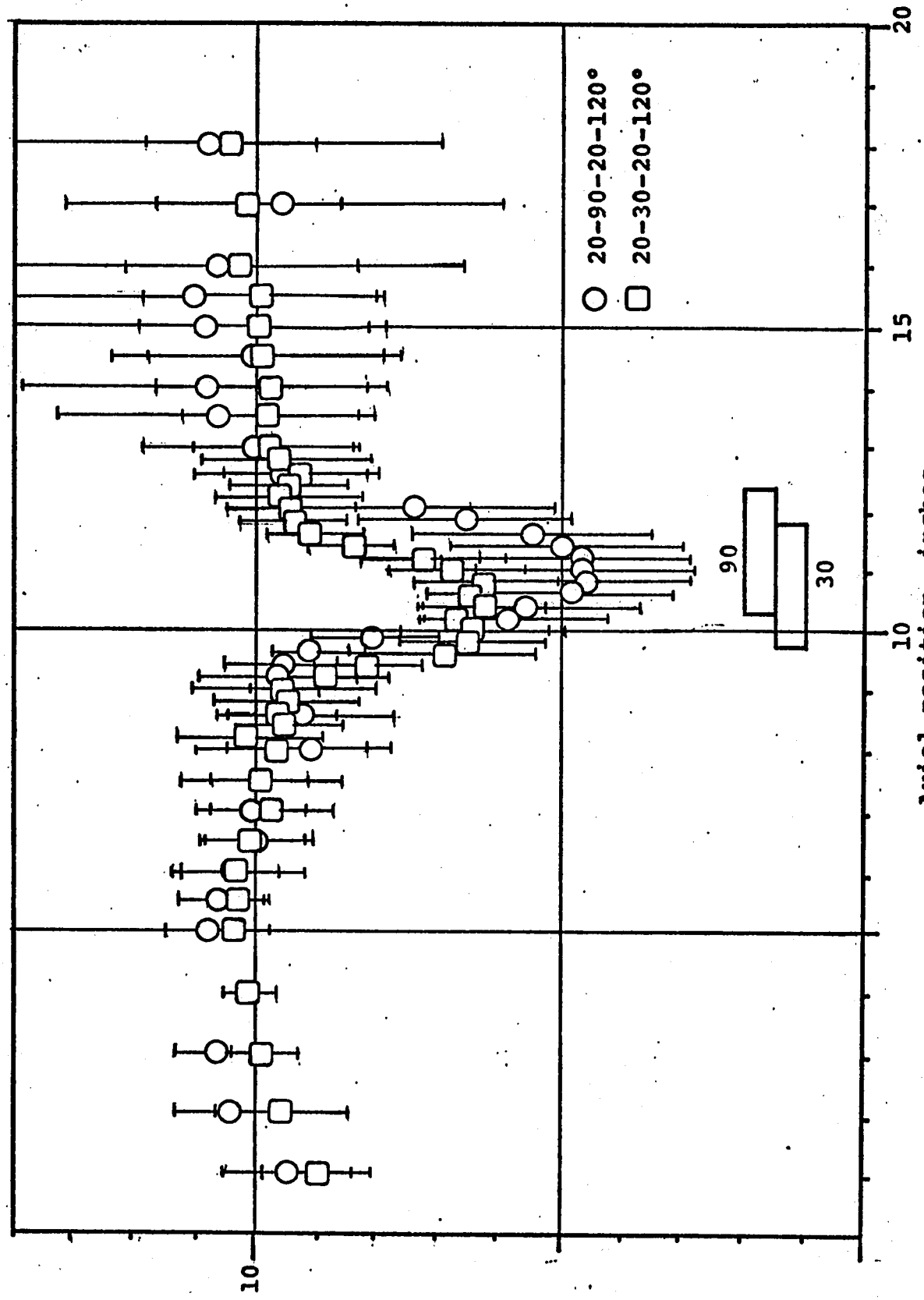

FIGURE 4-19 RHP VERSUS AXIAL POSITION FOR NONAXISYMMETRIC FINITE-LENGTH HARDENED SECTIONS. DATA INDICATES MEAN VALUES AND ONE STANDARD DEVIATION.

CHAPTER V

EXPERIMENTAL RESULTS

The results of this study can be evaluated from a standpoint of an engineer examining pulse-wave propagation along a fluid-filled tube or of a physician attempting to extend these results to the future development of a diagnostic technique for arterial disease. It is assumed that an engineer in examining pulse wave propagation is able to measure the necessary quantities; wall motion, fluid pressure, mechanical properties of the wall material, and the dimensions of the tube and the hardened section. However, because of the limited data which will probably be available to the physician and the different final use of the data, it is felt that the clinical aspects of the results may best be treated in a separate chapter.

The experimental study has produced two basic types of results. The first was associated with the assembly of the equipment, the manufacture of the experimental rubber tubes, and the conduction of the experiment. The second refers to the data which were obtained from pulse wave propagation along tubes with hardened wall sections. Chapter 4 discussed these first two points, and this chapter will cover the integration of these results from an

engineering viewpoint. Chapter 6 will consider the results in terms of their extension to the future clinical application for the detection of hardened section of arterial walls.

PROPAGATION VELOCITY

The manifestation of the propagation velocity is that the pulse wave moves in time along the axis of the tube. The recorded data from this is not velocity directly, but the paired values of axial location and arrival time. The velocity may be determined from either forming a difference relation or fitting a curve of velocity as a function of position to the data. With uniform tubes, which have a constant propagation velocity along their length, one can determine the velocity of the wave with a linear regression of arrival time and axial position. The particular aspect of the velocity that was of interest in hardened tubes was that the velocity changed abruptly at the axial location where the mechanical properties of the wall were altered. This abrupt change was of interest in localizing the hardened section, and because of the limitations on the accuracy of the data the use of a difference relation in determining pulse wave velocity was eliminated. The errors associated with using the difference relationship;

$$V_{1,2} = \frac{X_2 - X_1}{t_2 - t_1} \qquad (5\text{-}1)$$

$V_{1,2}$ = velocity from 1 to 2

X_1 = position of ith section

t_i = time of arrival at x_i

were large enough that statistically more significant information was determined from the linear regression technique. The result of the regression as defined by the linear equation relating the arrival time to the axial position, x:

$$t_a = t_o + \zeta x \qquad (5\text{-}2)$$

t_a = arrival time

t_o = initial time

ζ = reciprocal of velocity

This equation may be used to compute the expected arrival time both over region of the regression and at points past the last experimental data point used in the regression. A standard error, which is analogous to a standard deviation, is computed over the region of the linear regression to determine the statistical relevance of the data. This is done by using the calculated arrival time as the expected value. With uniform tubes the technique yielded standard errors in arrival times of less than .3 millisecond from

the expected times. When the linear equation is used to estimate the arrival time past the last experimental data point of the regression, the statistical significance of variations in arrival time can be determined. The quantity TMD is used for this estimate. TMD is calculated at each axial position:

$$TMD(x) = t_e(x) - t_a(x) \qquad (5\text{-}3)$$

$t_e(x)$ = experimental arrival time at x

$t_a(x)$ = calculated arrival time at x

The expected value of TMD is zero for the uniform tube. The hardened section, with a higher propagation velocity will have an arrival time that is less than the uniform tube, and TMD will become negative in this region. Figure 4-14, for a 20-90-20 tube, shows that along the uniform portion of the tube TMD is near zero; in the hardened section TMD deviates linearly with distance implying a constant but different velocity from the uniform portion of the tube; and in the distal portion with uniform properties, TMD is parallel to the expected value of zero, but offset depending on the time shift through the hardened section. No significant effect on pulse wave velocity with superimposed axial and pulse wave velocities was observed in the region near the piston.

The relationship between the propagation velocity and the average elastic modulus of the hardened section can be represented through the elastic modulus ratio, EMR, which is defined:

$$EMR = \frac{E_o}{2\pi} \int_0^{2\pi} \frac{d\theta}{E(\theta)} \qquad (5\text{-}4)$$

The increased propagation velocity as derived in Appendix D is:

$$C = \frac{C_o}{\sqrt{EMR}} \qquad (5\text{-}5)$$

The averaging of the elastic modulus about the circumference is represented by EMR over a range of 0. to 1.0 for hardened sections with EMR decreasing with the increase in the average elastic modulus of the wall.

For the experimental tubes that were investigated, Figure 5-1 shows the value of TMD versus the Elastic Modulus Ratio. The curve which is shown has been calculated with the following relationship:

$$TMD = \frac{\Delta x}{C} - \frac{\Delta x}{C_o} \qquad (5\text{-}6)$$

The data shown includes both axisymmetric as well as non-axisymmetric sections. This shows the increased value in the magnitude of TMD with a decreased elastic modulus ratio. The limit of the curve at EMR = 0. is $\Delta x/C_o$. The experimentally observed values of TMD can be used to estimate the

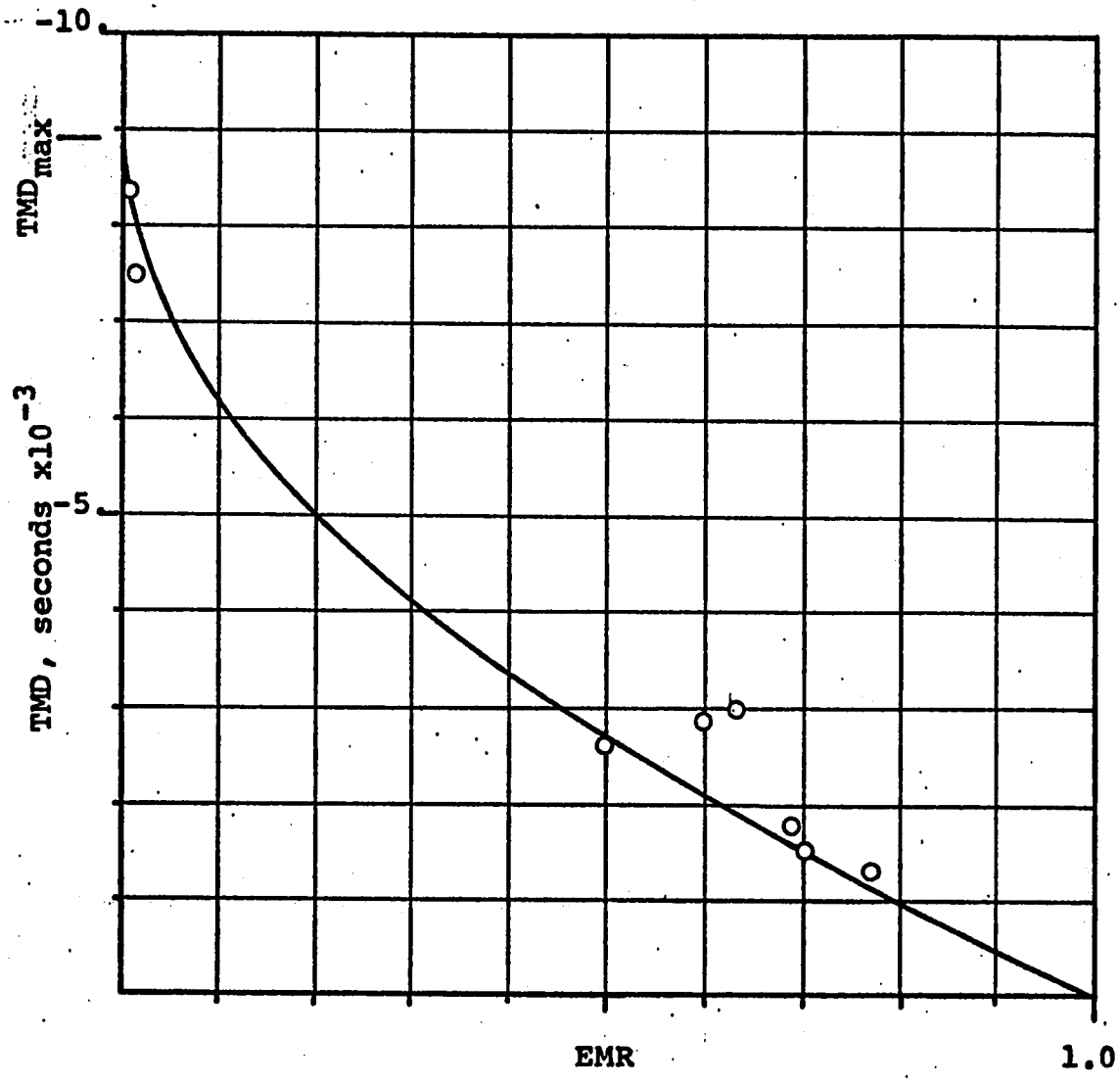

FIGURE 5-1 TMD VERSUS EMR FOR 2" HARDENED SECTION IN A TUBE WITH c_o = 225 in/sec

TMD max = $\Delta x/c_o$

elastic modulus ratio for the hardened section within the limits of the accuracy of the data, here being to within one millisecond of the expected values.

The representation of the propagation velocity with TMD has been shown in Chapter 4 using both radial wall motion and centerline fluid pressure. The wall motion and fluid pressure can furnish information which is sufficiently accurate to estimate shifts in TMD of greater than 1 millisecond. The variation in the wave about the circumference of the tube as obtained from wall motion data contributes to increasing the standard error in calculating TMD. Estimates of the standard error in TMD for wall motion showed that its expected value is less than twice the standard error from the pressure pulse (approximately .5 milliseconds for the wall motion). Hence, wall motion can be used with nearly the same degree of accuracy as the pressure pulse in estimating the location of the pulse wave.

The characteristic shape of TMD shows that the change in the velocity at the interfaces of the hardened section generally takes place over a distance of about one-half diameter in axial length when the ratio of hardened to soft section is not large. The deviation from this pattern as shown in Figure 4-11 was observed with the tube showing the largest change in impedance, the half-section 20-90 tube. In this tube, the pressure pulse showed a positive shift of 2 milliseconds in the quantity TMD before the interface

indicating a slight deceleration of the wave. This deceleration was confirmed in the values from the wall wave, but of a slightly smaller value showing a mean shift in TMD of only 1 millisecond. The 20-70 tube also exhibited this deceleration in the pressure wave, but for the wall wave, the statistical significance of the data was not conclusive. This deceleration, which would be expected to be less in finite length sections, was only observed in the 20-90-20-180° tube. With expected values in this positive shift of TMD of less than 1 millisecond for finite sections, its appearance in the 20-90-20-180° tube would, in the absence of other data, have been neglected as an experimental artifact.

REFLECTION COEFFICIENT: Pressure Wave

The viewing of wave propagation along a fluid-filled tube as analogous to a transmission line results in the concept of a reflection coefficient. When the incident wave encounters a section of different impedance, a portion of the wave is reflected. The ratio of the amplitude of the reflected wave to the incident wave is the reflection coefficient.

$$C_{ref} = \frac{A_4}{A_1} \qquad (5\text{-}7)$$

A_4 = reflected wave

A_1 = incident wave

For the ideal case where the waves are measured several wavelengths from the interface, and the propagation medium is

nonattenuating, the incident and reflected waves can be measured directly. In the experimental situation, the data was recorded in the near field where the waves were superimposed as well as propagating along a tube having significant attenuation. In order to determine the reflection coefficient, the value of the incident wave had to be obtained at the leading edge of the hardened section where the experimentally observed pressure was the sum of both the incident and the reflected pressures.

The estimate of the amplitude of the incident wave of the pressure pulse was made with the use of the attenuation relation for the tube. As was described in Chapter 4, the attenuation of the pulse wave for a uniform tube is determined with an exponential relationship,

$$p = P_o e^{\eta x} \qquad (5\text{-}8)$$

where the constants P_o and η, for the particular tube are obtained from a linear regression of the transformed attenuation relation. The difference between the experimentally observed pressure and the calculated incident pressure was the deviation from the expected amplitude. When this difference was used to form a ratio with the incident wave, it provided a means of estimating the effects of the superimposed axial and pulse waves as well as estimating the reflection coefficient of the hardened section. The quantity

RFC was defined as the ratio:

$$RFC(x) = \frac{P_e(x) - P_o e^{\eta x}}{P_o e^{\eta x}} \qquad (5\text{-}9)$$

$P_e(x)$ = experimentally observed pressure

In this relationship the expected value of RFC for a uniform tube is 0.

There are two regions of interest that have non-zero expected values of RFC. In the first, near the piston where the axial and pulse waves are superimposed, the pressure is observed to be about 5% above the expected value at a distance of one diameter from the piston face and approaches the expected value of 0. at 5 diameters from the piston where the waves are separated. The second, in the vicinity of the hardened section, the quantity RFC is observed to increase to a maximum at the leading interface of the hardened section, and then decreases throughout the length of the section. The maximum value of RFC at the leading interface is the estimate of the reflection coefficient. Figure 4-15 shows a graph of RFC versus axial position for axisymmetric hardened sections illustrating the region near the piston, and the maximizing of RFC to the value of the reflection coefficient at the proximal interface.

The elastic modulus ratio (EMR) of the hardened section can be used as an estimate of the reflection coefficient with

the effective axisymmetric model described in Appendix D. The effect of the elastic modulus on the reflection coefficient originates from the impedance relations of the transmission line analogy. The reflection coefficient can be calculated from these impedances.

$$C_{ref} = \frac{Z - Z_o}{Z + Z_o} \qquad (5\text{-}10)$$

Z_o = proximal impedance

Z = distal impedance

Figure 5-2 shows the measured and predicted reflection coefficient plotted against the elastic modulus ratio for the hardened section. The predicted values were obtained from the derivation in Appendix D. The lower curve was calculated using the fabricated length of the hardened section and the upper curve was calculated after increasing the length by one diameter to account for the effective added length of the hardened section which influences the motion of the tube material near the hardened section.

The errors in calculating the reflection coefficient from experimental data result primarily from two sources; the error in obtaining experimental data, and the error in estimating the amplitude of the incident wave. The relationship expressing this is obtained by taking a variational form of Equation 5-7.

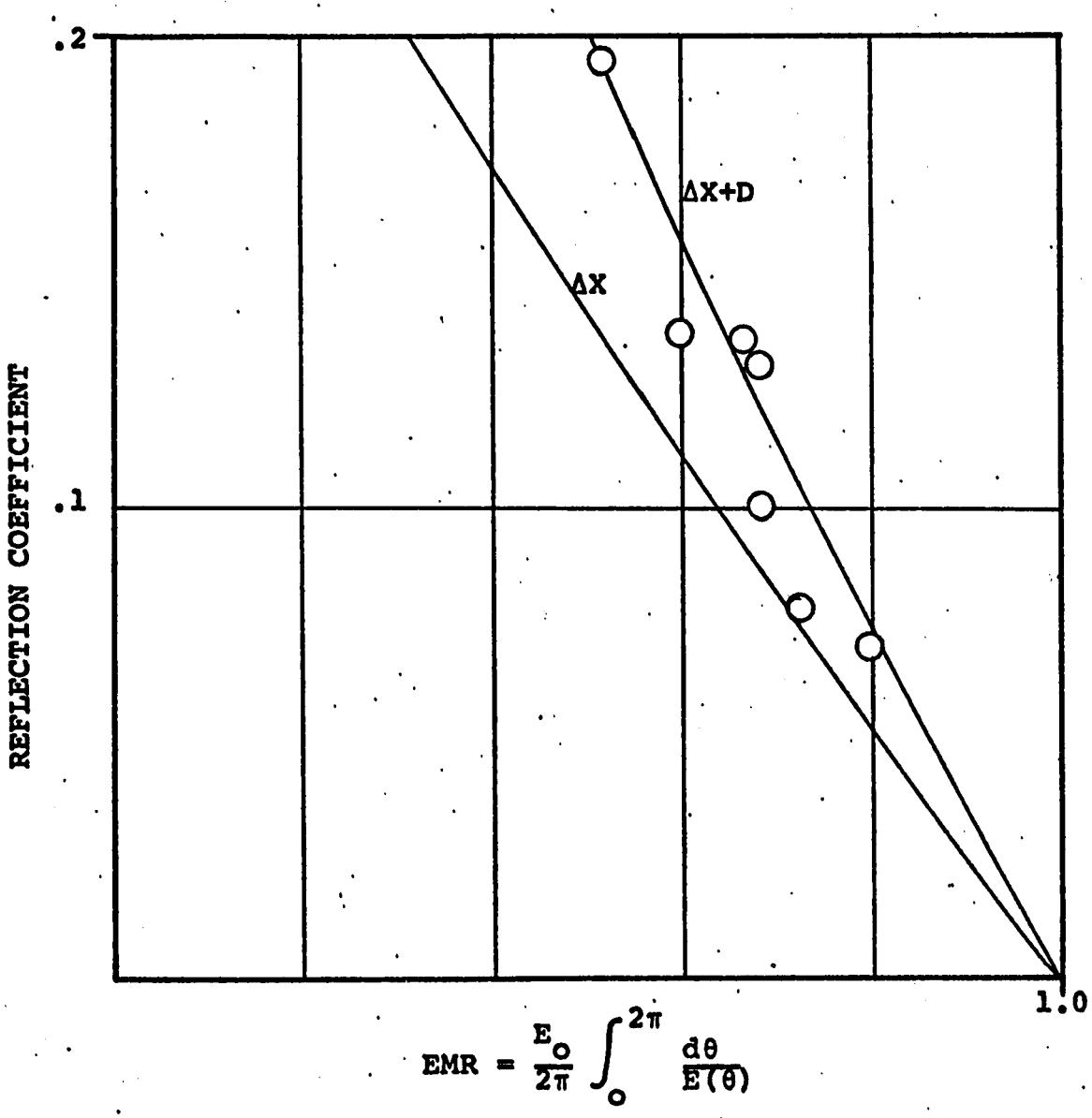

FIGURE 5-2 REFLECTION COEFFICIENT VERSUS EMR FOR NONAXISYMMETRIC FINITE-LENGTH HARDENED SECTION

$$\delta C_{ref} = \frac{\delta A_e}{A_1} - (1 + C_{ref}) \frac{\delta A_1}{A_1} \qquad (5\text{-}11)$$

A_e = experimental data

A_1 = calculated incident amplitude

From Equation 5-11 we can anticipate that the use of wall motion with its standard deviation in the displacement of 15% would not provide a suitable source of data for estimating reflection coefficients of .10 or less. The pressure pulse however, which is an integrated or averaged result of the wall motion about the circumference produces data with a lower inherent fluctuation, provides a better estimate of the reflection coefficient.

RADIAL DISPLACEMENT

The use of the radial motion of the wall potentially provides as much information as that obtainable from centerline pressure transducers as well as being a more quantitative source of information about the axial extent of the hardening and the local values of the elastic modulus ratio. In Chapter 4 figures of TMD versus axial position were presented with both centerline pressure data and radial wall motion data showing that both were effective in calculating TMD along the axis of the tube.

Radial wall motion would be a potential source of information for calculating RFC, and hence, estimating the reflection coefficient, but it is limited by the large scatter in the measured radial wall motion. The data from wall motion has shown that a uniform tube deforms as expected in the mean, that is, the average displacement is that which is predicted. However, the standard deviation in the range of .15 of the mean precludes its successful use in estimating of small reflection coefficients.

The radial wall motion provides its most significant information in two ways. First, the axial extent of the hardened section can be identified by noting the limits of the change in the magnitude of the pulse wave. Second, the average radial displacement at the hardened section can be utilized to estimate the value of the Elastic Modulus Ratio if the centerline pressure is known. The use of a non-dimensional quantity RHP, which relates the radial wall motion to the centerline pressure through the use of geometric and performance variables forms the basis for evaluating the usefulness of radial wall motion. The non-dimensional quantity RHP is defined as:

$$RHP(x) = \frac{\frac{1}{N}\sum U_r(x,\theta)}{p(x)} \left(\frac{c\rho\omega}{\beta}\right) \qquad (5\text{-}12)$$

By forming a nondimensional parameter using the displacement and the experimentally observed pressure, the effects of attenuation and reflection have been normalized showing the relative accuracy of using wall motion to correlate with fluid pressure. RHP has the expected value near 1.0 in the normalized form. This can be seen in Figure 4-16 for an axisymmetric tube. The use of RHP in estimating the mechanical properties of the tube at a hardened section is shown in Figure 5-3 where the minimum value of RHP in the region of the hardened section is plotted versus the Elastic Modulus Ratio. The dotted line shows the linear relationships which would be expected from an axisymmetric model of the tube wall. There was some consideration given to the effects of non-axisymmetric hardening on the wall motion. The data from radial wall motion has been represented in terms of average displacements taken from observations about the circumference of the tube. This was done with the nonaxisymmetric tubes as well as the axisymmetric ones. The supporting reason for this is that the pressure pulse producing the deformation is symmetric as it shows no radial variation. In keeping with this symmetric loading it was found that the wall motion could be effectively treated as if the hardened sections were all axisymmetric. The observed data from radial wall motion showed that although the average motion could be used in explaining the results, there were cases where the motion itself was not axisymmetric. The nonaxisymmetric

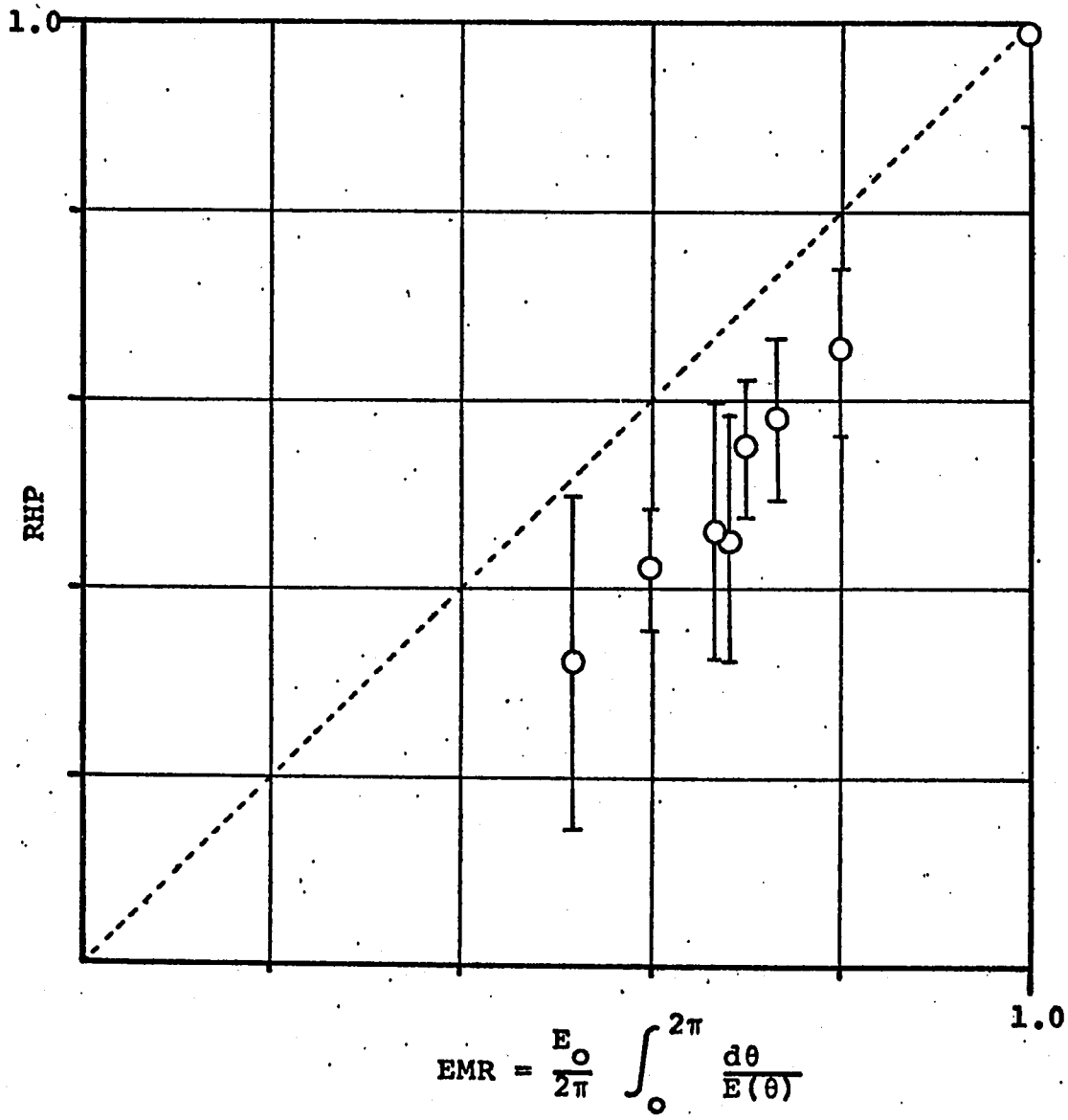

FIGURE 5-3 RHP VERSUS EMR FOR NONAXISYMMETRIC FINITE-LENGTH HARDENED SECTION

motion occurs when the sector of the hardened section is as large as 180° and the elastic modulus is greater than an order of magnitude that of the uniform section. For the 20-90-20-180° section the deformation was of the form:

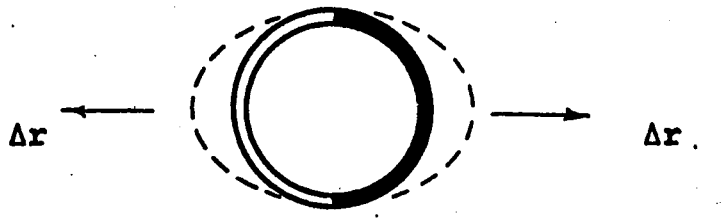

Figure 5-4

Radial motion for a 180° hardened section

It was observed that although the motion may be nonaxisymmetric, acceptable information for interpreting the presence of a hardened section can be obtained from a single trace at one angular position. Hence, there are times when the motion is nonaxisymmetric, but one need not record information about the entire circumference to have adequate data for making relative interpretation regarding the change in mechanical properties.

RHP may also be used to accurately locate the axial position of the proximal and distal edges of the hardened sections. Figure 4-16 as a typical example shows that RHP, indicates the presence of a hardened section by its deviation

from the expected value near 1,0. The change in RHP occurs in all cases over a distance of one diameter proximal and distal to the hardened section. Normalizing the radial displacement with the observed centerline pressure shows the consistent relation between the pressure and the wall motion. This is evident in the elimination of the attenuation and reflection effects. The statistically significant changes are identifiable in regions where the elastic properties of the wall are altered. The effect of the hardened section on the radial wall motion appears to extend only one diameter from the termination of the hardened section. This distance may very likely be altered for different pulse lengths and elastic properties of the wall. In arguing from a purely heuristic standpoint it appears that the effect of the hardened section as shown in the change of RHP from its expected value of 1.0 to that of the hardened section will be longer than 1 diameter with longer pulses and increased elastic modulus of the soft material.

A feature that has been removed from the representation of the radial displacement with RHP is related to the reflection coefficient and can be determined from the quantity RFC. Since the radial wall motion follows the pressure pulse it will increase in amplitude corresponding to the increased amplitude from the partial reflection of the wave.

When examining the unreduced radial wall motion data the position of the leading edge is somewhat accentuated because the reflected wave increases the rate of change in amplitude with distance. This is useful in the clinical application where the data from wall motion very likely will not be presented in terms of RHP, but examined in a more unreduced form.

In summary the results can be viewed in relation to an experimental analysis of wave propagation along fluid-filled tubes, or towards the development of a diagnostic procedure for examining arterial disease. The experimental investigation has covered topics relating to assembly of the experimental apparatus, the fabrication of the subject tubes, and the procedure used to conduct a controlled experiment, as well as the analysis of the results in relation to current theoretical level of knowledge of pulse wave propagation along fluid-filled tubes. The extension of these results to clinical application can utilize much of the information from the experimental investigation, and the literature review to serve as a foundation for describing the possibility of developing a diagnostic technique. The following chapter will cover the relevant areas of concern in relation to the development of instrumentation and experimental techniques for the investigation of the presence of arterial disease by using pulse wave propagation.

CHAPTER VI

CLINICAL IMPLICATIONS

The central theme of this study has been directed towards the development of an alternative source of information to be used in the clinical diagnosis of atherosclerosis. The possibility of accomplishing this task has been precipitated by the development of the phase-lock ultrasound transducer, an instrument that is capable of measuring the motion of the wall of an artery beneath the surface of the skin. The development of a system of interpreting the data recorded from radial wall motion has been based upon the analytic and experimental results from pulse wave propagation in fluid-filled tubes. Reduction of this information into a workable clinical scheme for the detection and identification of localized hardening of the arterial wall constitutes the basis of this chapter.

INFORMATION SOURCE: The Pulse Wave

The information describing the mechanical properties of the arterial wall material can be derived by examining the propagation of a pulse wave along the axis of the artery. For example, the normal arterial pulse wave has been used in previous investigations for the measurement of pulse wave velocity by O'Rourke(102) and reflection coefficients along the axis of the artery by Remington(114,115,116). Analytic

studies by Womersley(143,144,145,146) and others, have examined the propagation of the normal pulse by the use of Fourier series decomposition and the investigation of the effects of changes in frequency on the propagation parameters.

With the exception of Anliker(7,62,139) and his co-workers, and Landowne(77) investigations of pulse wave propagation have utilized the normal arterial pulse wave as the basis of their studies. Anliker(7) used short trains of sine waves with frequencies up to 200 hertz and Landowne(77) used single short-duration waves for the study of pulse wave propagation. The use of short duration waves does not present the problem of superimposed reflections from peripheral structures that is present with the long wavelength of the normal pulse wave.

The pulse wave which was used in the experimental study and proposed for clinical studies is similar to the normal arterial pulse wave, although of shorter duration and smaller amplitude. This wave is axisymmetric and is associated with the largest radial motion, the greatest fluid displacement, and the slowest propagation velocity of the other types of axisymmetric waves which can propagate along fluid-filled tubes. These other waves, for illustration and comparison, are the axial and the torsional waves. The axial wave is, by definition, that wave which possesses the largest axial motion, and the torsional wave is that wave with the largest circumferential motion. The

characteristics of wave propagation and the variables which predominately control each of the different waves, imply something of the information content that is available when these variables are changed. The torsional wave results from a twist about the axis of the artery, and is controlled mainly by the properties of the artery wall in shear. The axial wave produces a lengthwise pull on the artery and its propagation is controlled by properties of the wall material to withstand a volume compression (bulk modulus). Both the torsional and the axial waves invite consideration for use in a detection scheme because their propagation is primarily controlled by the mechanical properties of the wall material. Axial and torsional wave propagation in an artery present a problem in that they are affected by tethering, the attachment of the outer surface of the wall of the artery to the surrounding tissue, and its effect on propagation is not fully understood at the present time. The unknown effects of tethering combined with the potential difficulty of generating and measuring in a repeatable and nontraumatic manner, either a uniform axial or torsional wave, have excluded them from further consideration. The pulse wave in contrast can be generated and measured in a nontraumatic transcutaneous manner.

The choice of using the pulse wave also results in an investigation into the form of the wave, be it a continuous wave or a single pulse. The continuous wave is useful because

it provides the opportunity of investigating the direct correlation between linearized solutions and experimental observations. Fourier series analysis may be directly applied to the experimental data. Furthermore, continuous waves are more easily generated than single pulses. But, there are some distinct disadvantages to the use of continuous waves. The wave speed must be determined by the phase difference of two wave forms rather than arrival time differences at different locations, and reflected waves must be eliminated from altered wave forms to provide accurate analysis. In the construction of the phase-lock motion transducer, it was observed, though not to be held as a universal limit, that phase comparison with an accuracy of less than 1% of the period is not a practical goal. To obtain accuracies in the arrival time of the pulse wave of less than 1 millisecond, this dictates that the continuous wave must be studied at frequencies above 10 hertz. The extranneous reflected waves, which are present because of the relatively short arterial length in comparison to normal pulse wavelengths are superimposed on the incident wave form and are potentially a major factor affecting the accuracy of the analysis.

The use of a single pulse wave has advantages in some areas over the continuous wave: Reflected pulse waves, or other waves can be separated by their different locations in time and space. The wave speed is obtainable from the time

of arrival of a characteristic feature of the pulse wave. Short arterial lengths can be examined without the confusion of extranneous reflections. And, the results from continuous wave theory provides a fundamental theoretical background for interpreting the pulse wave results. Wells(139) has obtained limited data from experimental animals to support this conclusion, which was shown in Chapters 4 and 5 to be a valid assumption. There are some disadvantages to using single pulse waves, though. The frequency response of the instrumentation must be somewhat higher than for continuous waves. Arrays of data in time and space require multiple transducers with a single pulse or multiple repeatable pulses with a single transducer. The repeatibility of single pulses in relation to amplitude, duration, and contour is more difficult than for continuous waves. Considering the relative merits of continuous versus single pulses, the single pulse has been chosen because, though tedious, the isolated pulse wave can be directly studied in a short arterial segment.

In selecting the pulse wave, it is to be emphasized that short duration pulses be used. This must be done to minimize extranneous reflections from the peripheral vasculature, to reduce the error in determining the arrival time of the pulse, and to a slight extent, amplify the magnitude of the reflection coefficient at the interface of a hardened section. The normal arterial pulse wave is approximately five times the length of the body, and when

measuring the magnitude of the pulse wave one must note that the effects of attenuation and reflections from peripheral vasculature appear superimposed upon one another. Short duration pulses which will be examined in the vicinity of a hardened section have superimposed the incident wave and the reflected wave, but from the hardened section only, and not from peripheral vasculature. This reflection from hardened sections is accountable and later in this chapter will be discussed in its relation to determining the reflection coefficient. The position of the wave can be determined to within a percentage of its wavelength. Hence, a short-duration wave can be located with proportionally greater absolute accuracy than a longer wave where the necessary instrumentation frequency response is increased by being inversely proprtional to the wavelength. It is anticipated that the accuracy required for clinical analysis will require that the arrival time of the pulse wave be known with a 95% confidence to less than .5 milliseconds. This would require achieving an accuracy of .05% of the duration of the normal arterial pulse wave, an unlikely possibility for clinical instrumentation. By using a pulse wave with a 10 millisecond rise time, a technique accurate to within 5% of the rise time can be derived. The shorter pulse wave, as shown by the derivation in Appendix D, also increases the magnitude of the reflected wave at the hardened

section. Although no substantial data is available to support this result, Womersley confirms its general nature in a theoretical analysis of rigid flowmeter sections about arterial segments(146).

The usefulness of the pulse wave in obtaining clinical information originates from techniques which can accurately measure its characteristics. The sphygmomanometric method which provides a clinical estimate of maximum and minimum pressures in the arterial pulse wave is neither accurate nor specific enough to act as a measurement technique. The usual clinical catheter uses a pressure transducer external to the body to record arterial blood pressure by connecting the transducer and the artery with a long fluid-filled tube. A catheter of this form is limited in frequency response and will not accurately measure short duration pulse waves. The required high-frequency response dictates the use of a catheter-tip transducer to eliminate the long connecting tube between the artery and the transducer. The other acceptable method of observing the pulse wave is to directly measure arterial wall motion. The experimental study described in Chapters 4 and 5 has shown the comparison of the use of arterial wall motion and fluid pressure for studying the propagation of the pulse wave. The use of both fluid pressure and wall motion will be discussed in the remainder of the chapter in their relationship to the detection and identification of hardened sections of the

arterial wall.

It must be noted that there is a difference in wave contour for the fluid pressure and the radial wall motion. This difference, noted in the experimental study, was at the foot or initial portion of the pulse wave. The pressure is seen to increase slightly ahead of the pressure pulse as a result of the more rapid propagation of the axial wave preceding the arrival of the pulse wave. The coupling between the axial and pulse waves produces an observable small pressure wave. In contrast to the pressure, the wall motion shows a small dip ahead of the pulse wave to account for flexural bending in the wall from the radial expansion of the pulse wave. This is shown in an exaggerated form in Figure 6-1.

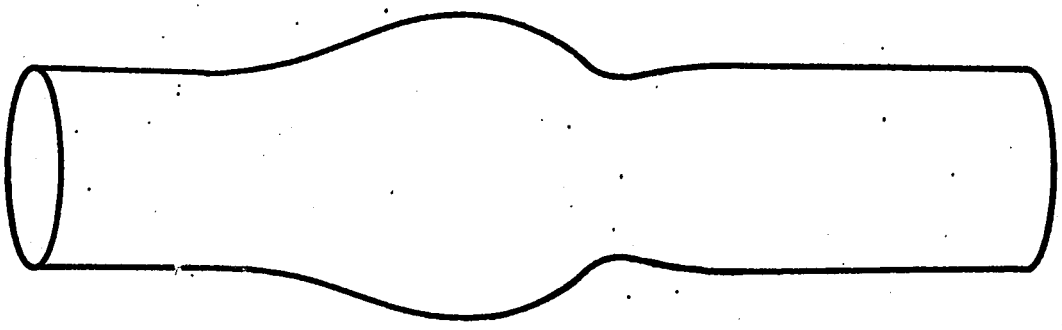

Figure 6-1
Exaggerated shape of wall deformation for a Pulse Wave

This constriction was not observed for long pulse rise times near that of the normal arterial pulse, but must be considered for pulse waves with faster rise times and shorter pulse lengths. Throughout the rise and over the initial peak of the wave, the contour from the fluid pressure, and the radial wall motion were observed to have identical contours. The changes observed at the hardened section, and surrounding regions, in the pressure pulse, and wall motion do not follow identical patterns. What these are, how they differ from one another, and what information can be obtained from them, will be discussed later in the chapter.

INSTRUMENTATION: Performance Limitations

The duration of pulse wave places some requirements on the response of the instrumentation to the received signal from the transducer. The frequency response of the instrumentation must provide less than 3dB attenuation at the frequency:

$$f = \frac{.45}{t_r} \qquad (6\text{-}1)$$

where t_r is the rise time of the pulse. When the signal passes through a series of instruments, the final rise time of the pulse becomes:

$$T_r = \sum t_r \qquad (6\text{-}2)$$

The final result is that the acceptable minimum rise time is the sum of the minimum rise time of each instrument in series (Lewis & Wells,80).

All existing instrumentation for measuring the pulse wave does not meet the requirements for accurate reproduction of short duration pulse waves. The phase-lock motion transducer and the catheter-tip pressure transducer, however, can accurately measure pulse waves with rise times less than 10 milliseconds. Clinical catheters with the pressure transducer external to the body normally have just sufficient capability to measure a normal arterial pulse wave. With a natural frequency in the range of 6 hertz, the clinical catheter can accurately follow a pulse with a rise time longer than .075 second, which is only approximately 20% fasterthan a normal arterial pulse. Investigations of non-normal pulse waves are severely limited when only clinical catheters are available. The use of an inflated cuff about the limb to measure the pulse appears to be at least limited in its frequency response as that of the clinical catheter. The cuff has been shown by Carter to produce pulse contours with rise times in the range of .140 sec., but comparison with accurate pressure measurements were not made and it is doubtful if shorter rise times can be recorded. It appears that much higher frequency response with a cuff will not be attainable because of 1) the need to transfer a definite

mass of blood into the limb to compress the cuff, and 2) the compressibility of the gas volume within the cuff. In addition, the large size of the cuff measures the pulse averaged over an axial distance somewhere in the region of the width of the cuff, possibly up to several inches. The mercury strain gage also is somewhat limited in that direct arterial measurement can only be done with exposed arterial segments. Its use in a limb plethysmograph similar to the cuff is subject to large volume displacements of blood, eliminating its use for short duration low-amplitude pulse waves. From this discussion it is concluded that either a wall motion transducer similar to the phase-lock ultrasound unit, or a catheter-tip pressure transducer possess the necessary frequency response to detect short duration pulse waves.

GENERATION

The clinical generation of a pulse wave is not a straightforward procedure. The pulse wave is axisymmetric, but it is unlikely that it can be generated solely as an axisymmetric wave. It is proposed that a brief impulse on the skin surface, in the manner used successfully by Landowne(77) can produce a propagating pulse wave in the artery. This procedure will generate a pulse wave but also because of the nonaxisymmetric deformation by compacting the skin surface it will generate axisymmetric axial wave as

well as other nonaxisymmetric waves. The axial wave, which propagates faster and attenuates faster than the pulse wave, will very likely not be detectable with a pressure transducer or radial motion transducer after more than one wavelength of the pulse wave. The nonaxisymmetric waves attenuate faster than the axial wave and will not be detected by pulse wave monitoring instrumentation after the axial wave has attenuated. Anliker(7) has confirmed this by successfully gathering meaningful data from experimental animals with a transducer placed one wavelength or more from the wave generation source. It is concluded that it is possible to generate a pulse wave from a nonaxisymmetric deformation of the wall of the artery, and the experimental observations will be accurate if the transducers are separated far enough from the pulse generation source so that axial and non-axisymmetric waves have been sufficiently attenuated in order that they not affect the propagation of the pulse wave.

PULSE WAVE PROPAGATION: Normal Artery vs. Uniform Tube

The analytic description of pulse wave propagation has commonly been based upon using a long, straight, and uniform fluid-filled tube as a model of the artery. There are several problems that arise in the comparison of the performance of uniform tubes with arteries because arteries are neither uniform nor are they long and straight. The early theoretical studies when compared to experimental observations

revealed enough inconsistencies that analytic investigations were of little clinical value. The two measured values that related to this study are wave speed and attenuation. The wave speed for a uniform tube is constant along its length. In contrast to this McDonald(84) has shown that in an artery the wave speed can change from 5 meters per second in the arch of the aorta to greater than 15 meters per second in the peripheral vessels. Histand(62) in studying short arterial segments has utilized uniform pulse wave velocities to determine the transmission characteristics of pulse waves short segments (3-5 cm.) of the aorta. The pulse wave in a uniform tube attenuates according to an exponential decay. In the arterial system of canine arteries, Wells(143) has utilized an exponential decay for retrograde propagation of impulse and continuous waves over segments from 2 to 6 cm. in length. Rockwell(121), in acknowledging the amplification present in the normally propagating pulse wave, has developed a model that accounts for changing diameter, wall thickness, and mechanical properties along the arterial tree. His model has reproduced the amplification of the pulse wave that has been observed by Womersley(144) and Remmington(116) for nondiseased arterial segments. At the present time a precise description has not been formulated for attenuation of pulse wave propagation in the aorta. In reviewing the available information it appears that the modeling of short lengths of an artery have been accomplished utilizing a

uniform tube, yet longer segments have shown the arterial system to be nonuniform along its length. The conclusion that can be drawn from this apparently conflicting data is that the arterial system is normally non-uniform along its length, but the changes occur slowly enough to permit short segments to be studied as uniform tubes.

PROPAGATION VELOCITY: Arrival Time vs. Distance

The search along an artery for a hardened section can be done by examining the local propagation velocity. It has been shown in the preceding work that the local propagation velocity of the pulse wave increases in the region with a hardened wall section. The velocity is commonly used in describing the propagation of the pulse wave, but it is not the best way to display the data for interpretation when the distance between data points is decreased. The computation of the local propagation velocity produces statistically less significant results than working directly with the axial location and the arrival time of the pulse wave.

In Chapters 4 and 5 it was shown that the experimentally observed arrival times of the pulse wave can be used to locate local changes in the propagation velocity. If the velocity were accurately known, the experimental observations could be compared with the known velocity to determine the error in observation method. In the experimental study with uniform tubes the mathematical form of

the velocity was known, and the unknown constants in the mathematical relationship were determined as a statistically best estimate. In the artery the mathematical description of the expected velocity is not known, but may be approximated. Rockwell has used the relationship:

$$C = C_o(1 + .02x) \qquad (6\text{-}3)$$

x = distance, cm.

C_o = propagation velocity at $x = 0$

As noted previously, and formulated above, the expected variation in the propagation velocity with distance is a slowly changing proeprty. In contrast to this, the change in velocity at a local hardened section will be greater than the normal variation.

As an analogy to the experimental study, the use of the arrival time and axial location of the pulse wave could be used to locate hardened sections. The data would be obtained in the following form:

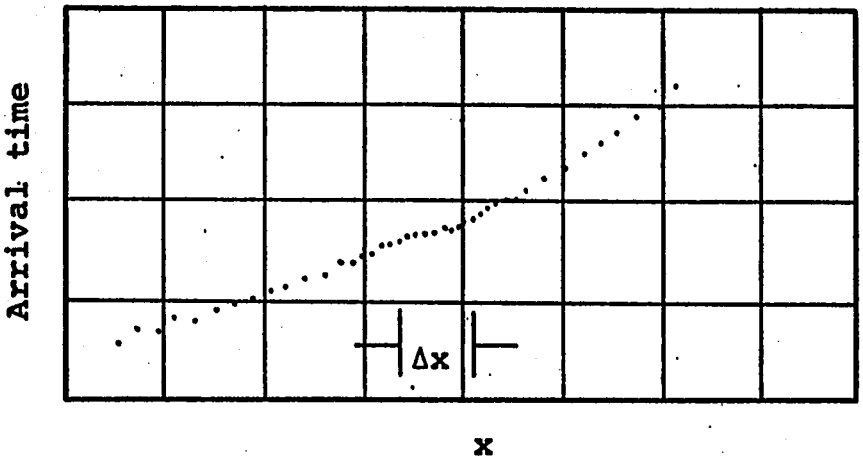

Figure 6 - 2
Arrival time versus axial position, Δx indicates hardened section

where x indicates the hardened section. The plot of the error from the expected arrival time is the quantity called TMD.

$$TMD = t_e - (t_o + \frac{x}{C(x)}) \qquad (6\text{-}4)$$

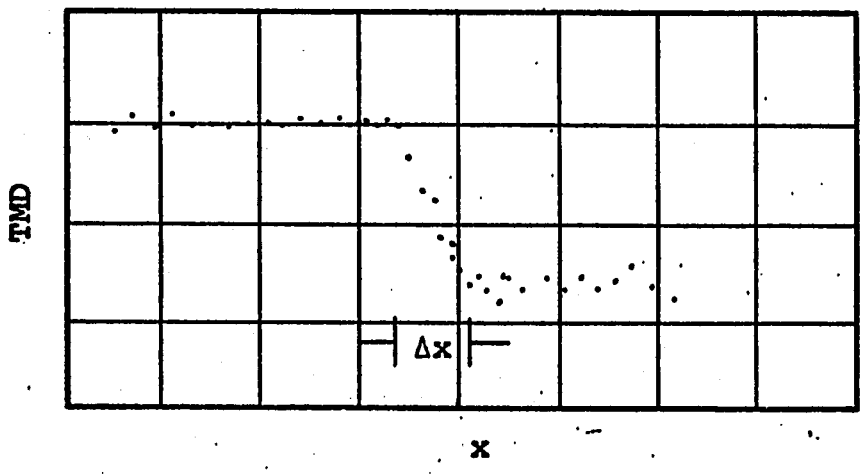

Figure 6-3
TMD versus axial position, Δx indicates hardened section

The development of an accurate interpretative method depends upon the accuracy with which c(x) in the normal state can be described. Statistical analysis can be utilized to determine the significance of the data by utilizing the calculated arrival time as the expected value. Deviations from a zero value of TMD can be evaluated in terms of the accuracy of the data and the estimate of the variation in propagation velocity with distance.

The experimental study has shown that both wall motion and fluid pressure can be used to determine the arrival time of the pulse wave. It has been noted that pressure must be monitored with a catheter capable of responding at higher frequencies than clinical catheters; hence, the use of a catheter-tip transducer is necessary. The radial wall motion can provide a similar form of information about the arrival time as does the pressure transducer, with two exceptions: First, the variability of the pulse wave along the axis and about the circumference impart slightly more scatter than is observed in pressure data. Second, hardened sections may decrease the amplitude of the wave in the wall to the point where it is unobservable in the region of interest.

WALL MOTION: Axial Location

The variation in amplitude of pulse wave along the artery can be used to estimate the axial length as well as the relative change in elastic modulus of the hardened section. This requires that measurements be taken with axial spacings much shorter than the expected length of the hardened section. The magnitude of the pulse wave will include effects of amplification from normally changing arterial dimensions and wall material properties as well as the effect reducing the amplitude in the region of the hardened section and the reflection at the proximal interface. The raw data would have the general form:

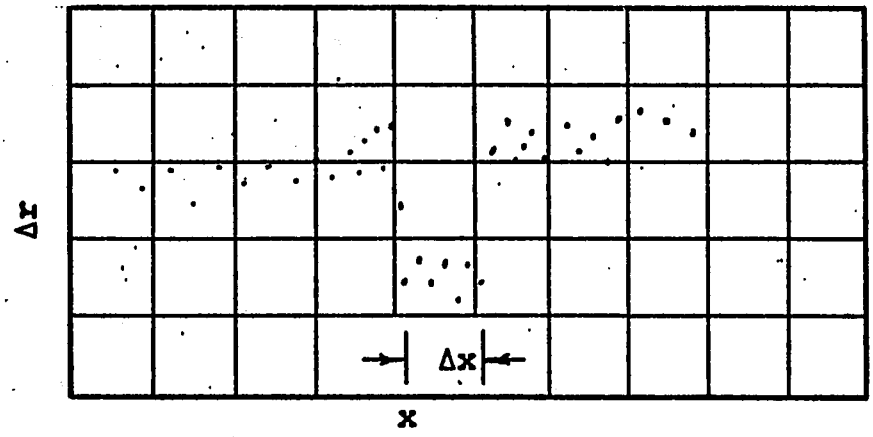

Figure 6-4
Radial wave amplitude versus axial position,
Δx indicates hardened section

The major decrease, that indicated in the region of Δx in Figure 6-4, will occur at the hardened section. The overall rising of the data is presented to describe the slight amplification anticipated in the arterial system. Proximal to the hardened section there will be a slight increase resulting from a reflected wave from the hardened section. The reflected wave will be discussed in the following section. The presence of a reflected wave slightly enhances the appearance of the leading edge by increasing the amplitude of the wave at the proximal interface. For this reason the distal interface may not be as definitive as the proximal interface.

In the experimental study it was shown that the effects of the reflected wave, and the attenuation can be normalized with the use of a nondimensional quantity that incorporates the fluid pressure, geometry, mechanical properties, and frequency. It is unlikely that all this information will be available to the physician for use in analyzing the data. We will very likely want to use the unreduced data from the wall motion to derive his conclusions. Even considering this, the use of radial wall motion in locating the axial location and extent of the plaque is a goal that holds a high likelihood of success. Large changes in the amplitude of the wall wave at the axial interfaces of the plaque can identify its location and size. The accuracy of using wall motion is sufficient to be able to identify the interfaces

with less than one diameter error.

ELASTIC MODULUS: Arrival Time and Wall Motion

The elastic modulus of the plaque can be estimated with data from arrival time of the pulse wave or the amplitude of the wall motion. We can anticipate the magnitude of change in the elastic modulus of the plaque from the data of O'Rourke(102) and Yoshimura(149). They each note average increases in pulse wave velocities of 1.5 to 2.0 in the presence of arterial disease. In terms of average increase in the elastic modulus this would imply average increases in the elastic modulus of 2.25 to 4.0. But average increase are not a fair estimate of the increased elastic modulus, because a plaque is assumed to affect only a sector of the circumference. From the results of the experimental study it can be shown that a 150% increase in the wave speed would require an essentially rigid tube extending over 200° of the circumference. From extensions of this argument it can be shown that using average wave speed information over long distances for small sector plaques having material properties near that of the normal artery will require extremely fine definitions of changes in the velocity. We conclude from this both that the change in the elastic modulus is significant in the presence of arterial disease, and that it can cover major sectors of the artery. In noting the size of arterial plaques Mitchell and Schwartz(91) have observed

small plaques of 1 cm^2 in area and moderate plaques of 6-8 cm^2. The normal sector of an arterial plaque was observed to be in the range of one half the circumference, or less. Roberts has confirmed this in studies of the coronary arteries(120).

The experimental portion of this study can provide estimates of the elastic properties of the presymptomatic plaque. A polynomial expression was used to fit the data from Figure 5-3. Because clinical data on radial wall motion will not be normalized to remove the presence of the reflected wave, the expression was adjusted to account for this effect. Figure 6-5 shows the graphical result plotting the wall wave ratio:

$$\frac{\Delta r_p}{\Delta r_o}$$

Δr_p = wall wave amplitude at center of plaque

Δr_o = estimated wave amplitude in absence of plaque

versus the ratio of the elastic moduli

$$E_p / E_o$$

E_p = elastic modulus of plaque

E_o = elastic modulus of undiseased artery

for the circumferential sectors of 90°, 120°, and 180°.

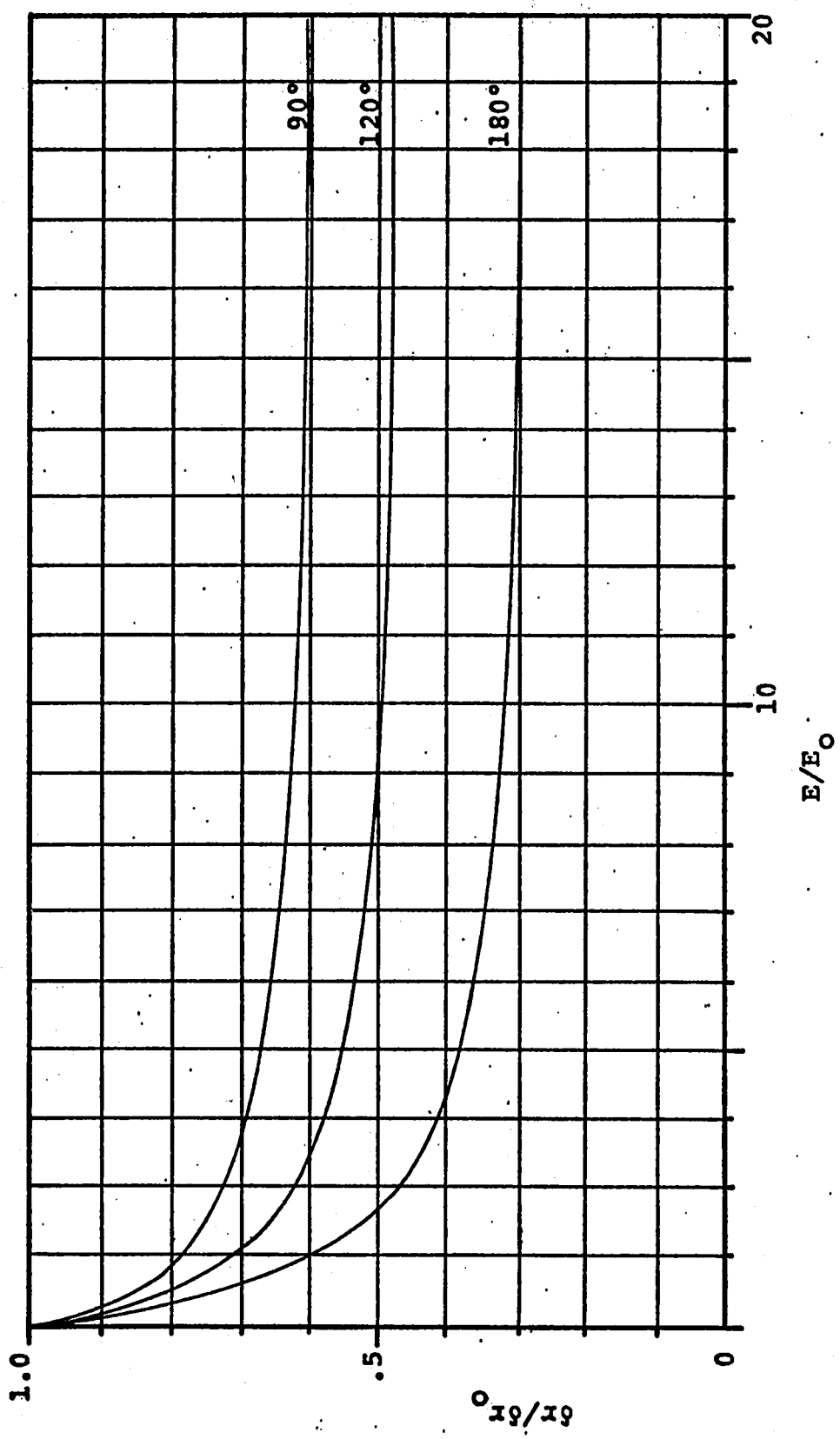

FIGURE 6-5 PULSE WAVE WALL MOTION RATIO VERSUS ELASTIC MODULUS RATIO FOR A NON-AXISYMMETRIC HARDENED SECTOR

The significance of Figure 6-5 is that it shows that the observed information $\Delta r_p/\Delta r_o$ can be used to determine the circumferential extent of a plaque if the ratio of the elastic moduli ratio is assumed, or if the ratio of the elastic moduli is assumed, the sector can be determined. The general view of this result is that it is possible to locate hardened sections with high statistical significance even when the relative changes are as low as 2.0 of the undiseased elastic moduli. This is a significant improvement over the method of using average increased wave velocity. The comparison would be: an increase in the elastic modulus to twice the undiseased modulus for a 180° plaque could be identified using wall motion with greater than 95% confidence. The elastic modulus change in the hardened section can be determined from the arrival time of the pulse wave. Figure 6-6 shows the ratio of the time shift variable TMD and the maximum time $\Delta x/C_o$ versus the ratio of the elastic moduli in the plaque and the unaltered tube E/E_o for different sectors of hardening from 90° to 180°. The characteristic shape is similar to the wall motion, showing the greatest relative change in TMD with elastic modulus changes less than 5 times that of the unaffected wall. To make an estimation of the relative elastic modulus of the hardened section, one must obtain TMD, Δx, and C_o from experimental observations and data reduction. By assuming the sector size of the plaque, the relative elastic modulus can be

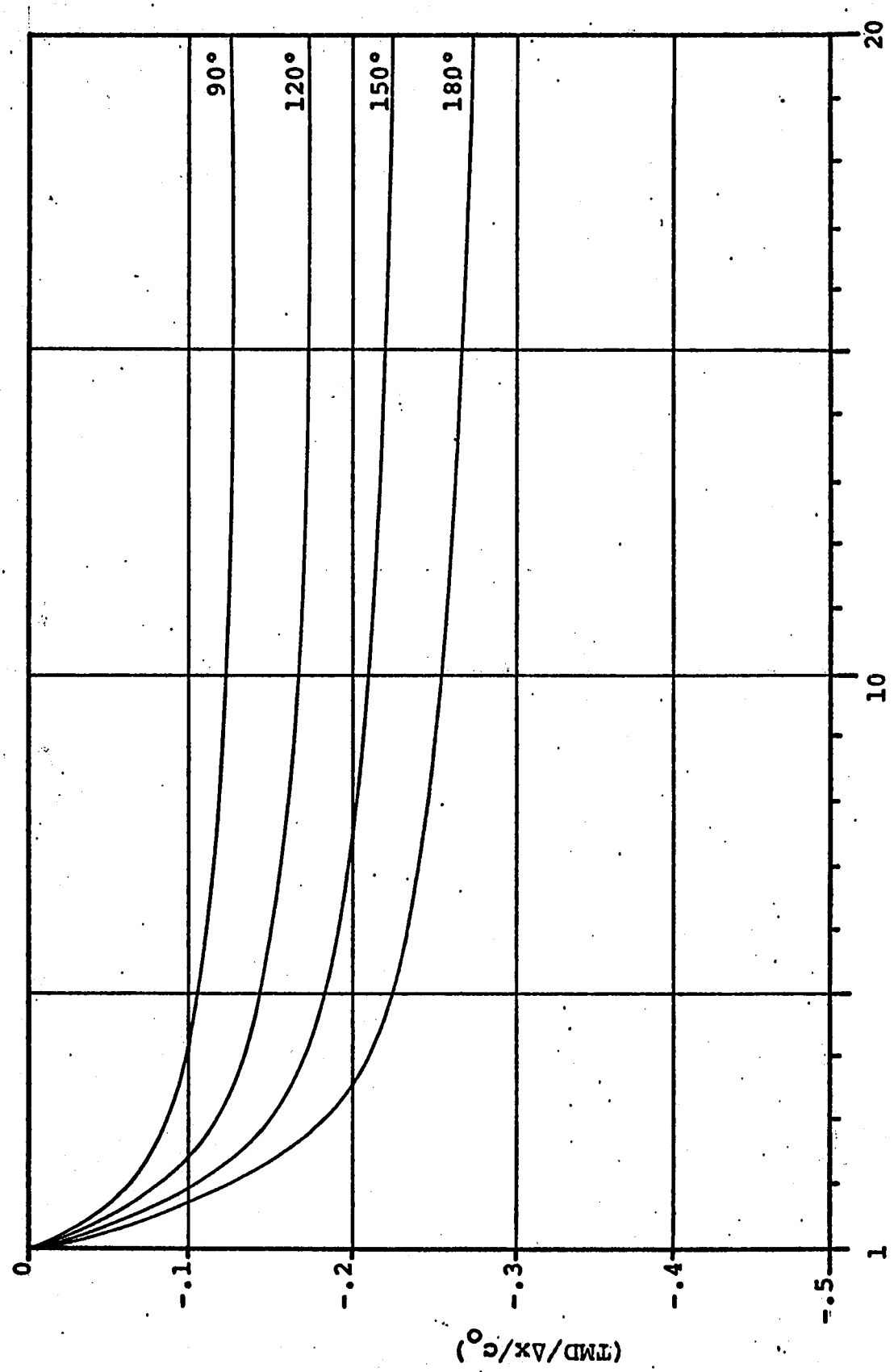

FIGURE 6-6 NONDIMENSIONAL TIME-SHIFT, TMD/($\Delta x/c_o$), VERSUS ELASTIC MODULUS IN PLAQUE FOR DIFFERENT SECTORS

determined. The required accuracy for the conditions of the observation can also be obtained from Figure 6-6. In the case of a 10 cm long plaque in an artery with a nominal propagation velocity of 10 μ/s, $\Delta x/C_o$ = .010 second. The arrival time of the pulse wave must be obtained accurate to less than 1 millisecond to utilize arrival time for evaluating the relative elastic modulus.

After examining both the wall motion and arrival time it was seen that the sector must be assumed to evaluate the relative elastic modulus change. But, it was found that both Figure 6-5 and Figure 6-6 were asymtotic at larger elastic modulus changes. This allows the data to be used to evaluate the sector size for the more rigid sections. This particularly is significant in more advanced disease when one would want to know the total extent of the hardening rather than the relative change.

Consideration must also be given to the circumferential position of the plaque relative to the motion transducer. First, it should be noted that the artery deforms symmetrically so that even if the plaque is opposite the transducer, the data will be indicative of the mechanical properties of the plaque. In the case where the plaque is extremely stiff, and extends to cover half the artery the motion shown below can be expected.

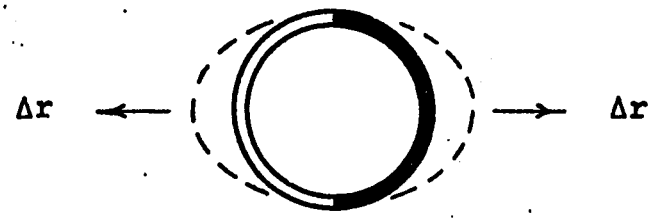

Figure 6-7
Radial motion for a 180° hardened section

Included in this is the lack of ability of the method to determine the circumferential position. The more significant conclusion, however, is that it makes little or no difference where the data is recorded about the circumference of the artery, because the axial position of the plaque will be evident at all angular locations.

REFLECTION COEFFICIENT: Pressure Wave

The reflection coefficient deserves mention in that it can be derived from the data, and can potentially be used for estimating the relative magnitude of a hardened section in the artery wall. It has received attention by such noted investigators as Remmington(115,116) and Womersley(146) in explaining normal changes in the arterial pulse wave. Waves reflected from peripheral vasculature were proposed as the reason for amplification of pulse waves along the aorta and major peripheral vessels when the dispersion had not

provided an adequate answer. Taylor(133) and Rockwell(121) have shown, however, that the source of the amplification arises from the anatomical changes in cardiovascular system making it unlike a uniform infinitely long tube.

It was shown in the experimental study that a reflected wave is generated when the pulse wave encounters a portion of a tube that has a hardened section. In utilizing the transmission line analogy of Taylor(133) or that from the derivation in Appendix D, the reflection coefficient can be calculated as:

$$C_{ref} = \frac{Z-Z_o}{Z+Z_o} \qquad (6\text{-}5)$$

Z_o = proximal impedance

Z = distal impedance

The impedances depend upon the mechanical properties of the arterial wall and as a result, the calculated reflection coefficient can be used to estimate the magnitude of the hardened section.

The reflection coefficient used for making estimates about the wall properties can be obtained from pulse wave amplitude data. The reflection coefficient is defined as:

$$C_{ref} = \frac{A_4}{A_1} \qquad (6\text{-}6)$$

A_4 = reflected wave

A_1 = incident wave

The recorded data is obtained in terms of superimposed incident and reflected waves, that is, $A_1 + A_4$. In a probable example the pulse wave amplitude along the axis of the artery would be of the form:

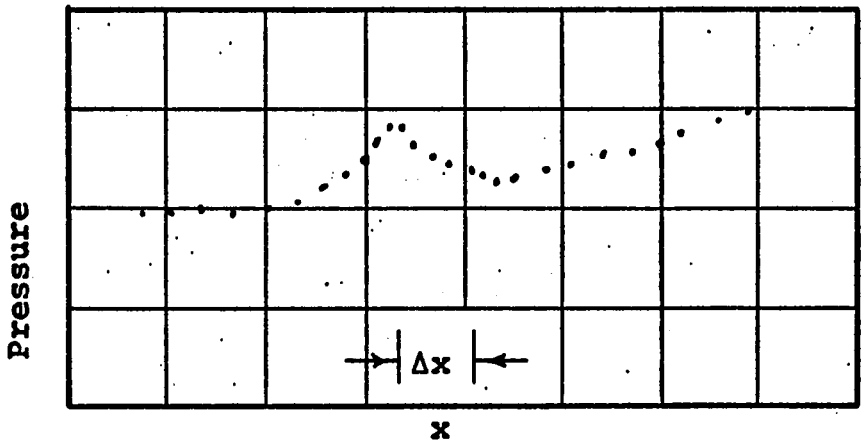

Figure 6-8
Pressure versus Axial Position

Here Δx indicates the position of the hardened section.

Because of the superimposed incident and reflected waves it is necessary to establish an estimate of the amplitude of the incident wave at the proximal interface. This may be done by using data that is removed from the presence of the reflected wave, then extrapolated with the use of the attenuation relation to where the reflected

wave is a maximum. This procedure generates data that can be expressed in terms of its statistical significance. Because of 1) the small magnitude of the reflection coefficient, possibly about .10, 2) the unknown attenuation relationship for the normal artery and 3) the lack of a priori knowledge of the location of the hardened section, the usefulness of the calculated reflection coefficient will be less than propagation velocity or wall motion. A variational equation can be derived from the definition of the reflection coefficient to evaluate the effects of errors in experimental data and calculation methods. This is:

$$\delta C_{ref} = \frac{\delta A_e}{A_1} - (1 + C_{ref}) \frac{\delta A_1}{A_1} \qquad (6\text{-}7)$$

The first term on the right hand side is the relative experimental error. From the experimental study it was found that the standard error in the equipmental data was always less than .03 of the incident wave. In the clinical situation where experimental conditions can not be closely controlled, as a conservative estimate, this will be doubled. The error in estimating the amplitude of the incident wave amplitude can be extrapolated from Wells'(139) data to yield a relative standard error of approximately .08. Equation 6-7 estimates a standard error in the reflection coefficient to

be no less than .148. It could be said that with certainty one would not investigate situations with reflection coefficients below .30. Short hardened wall sections do not produce reflection coefficients of this magnitude; hence, will not serve as reliable an indicator as arrival time or wall motion. The presence of raised plaques, or thromboses that invade the lumen can provide reflection coefficients larger than for hardened walls alone and this may result in a useful interpretation of data producing large reflection coefficients.

CONCLUSIONS AND RECOMMENDATIONS

This study undertook the task of identifying the observable changes associated with the propagation of a pulse wave along a tube with hardened wall sections. It was demonstrated that it was possible to obtain information about the size and location of hardened sections as well as the relative change in the elastic modulus using both the fluid pressure and the wall displacement wave. The use of short-duration pulse waves was shown to be a necessity for implementing the methods used in this study for reducing and interpreting the primary sources of data; the arrival and the amplitude of the wall and pressure wave.

From an array of the arrival time of the pulse wave along the axis, 1) the expected value of the wave speed, 2) the axial position of the proximal and distal boundaries of the hardened section, and 3) the combination of sector size and increased elastic modulus can be evaluated. Both the pressure wave and the wall wave provide acceptable arrival time data, although the greater variability in the wall displacement introduces a larger uncertainty into the results than is present with the pressure wave.

The amplitude of the wall wave could also be used, independently of the arrival time, to estimate the axial

position of the boundaries and the combination of sector size and increased elastic modulus of the hardened section. Using the amplitude of the wall wave, the axial position of the boundaries can be located to within 1 diameter of their actual location with greater than 90% certainty. Measurements obtained along one meridianal plane were shown to be statistically accurate for both axisymmetric and non-axisymmetric hardened sections in straight tubes.

Either the arrival time of the pressure or the wall wave or the amplitude or the wall motion can be used to estimate the combination of sector size and elastic modulus of the hardened section. When the ratio of the elastic modulus of the hardened section to the original elastic modulus is low, below about 5, the sector size must be assumed when estimating the ratio of the elastic moduli. When the ratio of the elastic moduli is large, the magnitude of the ratio cannot be determined, but the data may be used to estimate the size of the hardened sector.

The use of the pressure wave for calculating a useful reflection coefficient describing hardened, non-invading wall sections does not appear to be a fertile area for study. In a controlled laboratory situation useful results can be obtained with uniform tubes, but in a clinical situation the expected errors due to uncertainty in arterial architecture, control of the wave amplitude,

and attenuation factors are large enough to make the final results statistically uncertain.

The results of this study can be implemented by studying pulse wave propagation with either a pressure sensing catheter, or a wall motion transducer. At the present time the most readily accessible data is available from the pressure wave. However, before data can be obtained, it is necessary to fabricate equipment capable of producing pulse waves having a repeatable, or known amplitude with rise times in the order of 10 milliseconds. Arrival time data will require that standard errors in the expected arrival time be less than 5×10^{-4} seconds. This will necessitate an arterial scan of sufficient length proximal to the hardened section to verify this accuracy, say over a distance greater than 8 cm. at .5 cm. increments. Amplitude data, as has been discussed, may not be valuable in estimating hardened sections in the arterial wall, but in the case of luminal invasion, the reduced cross section can produce an increased reflection coefficient that may have significant clinical importance. It must be noted that the catheter frequency response and accuracy must be adequate for the low amplitude, short-duration waves being used.

The utilization of radial wall motion in addition to the fabriation of a pulse wave generator, will require

the development of an adequate skin-surface mounting transducer. From the results of the laboratory study, a usable instrument that readily tracks radial wall motion may be developed from the prototype phase-lock transducer. The utilization of radial wall motion will require an axial scan at least as great as for using arrival time data plus an additional distance to allow the axial and radial waves to separate. This additional distance with the finite size of the wave generator (approximately 1 cm.) may preclude the use of this method for all but the longest arteries. Consequently additional effort is required to develop a useful short-scan amplitude technique for clinical use.

REFERENCES

1. Akers, W.W., A.C.L. Barnard, H.M. Bourland, W.A. Hunt, W.P. Timlake, and E. Varley. Numerical Hydrodynamic Calculations of Catheter Characteristics. Biophysical H., 6:725-733, 1966.

2. Alexander, R.S. Transformation of the Arterial Pulse Between tne Aortic Arch and the Femoral Artery. Am. J. Physiol. 158:294, 1949.

3. Alexander, R.S. Factors determining the control of pressure pulses recorded from the aorta. Federation Proc. 11:738, 1952.

4. Alexander, R.S. The genesis of the aortic standing wave. Circ. Res. 1:145, 1953.

5. Alfrey, T., Jr. Mechanical Problem of High Polymers. Interscience Pub. N.Y., 1948.

6. Allen, P.W., P.B. Lindley and A.R. Payne. Use of Rubber in Engineering. McLaren and Sons, Ltd., London, 1967.

7. Anliker, M., W.E. Moritz, and E. Ogden. Transmission characteristics of axial waves in blood vessels. Stanford University Biomechanics Lab. SUDAAR 343, April, 1968.

8. Aperia, A. Hemodynamical studies. Skandinavisches Archiv. fur physiologie, 83(16), 1940.

9. Atabeck, H.B., and H.S. Lew. Wave propagation through a viscous incompressible fluid contained in an initially stressed elastic tube. Biophysical J. 6:481-503, 1966.

10. Attinger, E.O. Pulsatile Blood Flow. McGraw Hill Co., Inc., New York, 1964.

11. Attinger, E.O. The physics of pulsatile blood flow with particular reference to small vessels. Invest. Ophthal. 4:973-987, 1965.

12. Attinger, E.O. Pressure transmission in pulmonary arteries related to frequency and geometry. Circ. Research. 12:623-641, 1963.

13. Attinger, E.O. and A. Anne. Simulation of the cardiovascular system. Ann. NY Acad. Sci., 128:810-829, 1966.

14. Attinger, E.O., H. Sugawara, and D.A. McDonald. Use of Fourier Series for the Analysis of Biological Systems. Biophysical J. 6:291-304, 1966.

15. Attinger, E.O., H. Sugawara, A. Navarro, A. Ricetto, and R. Martin. Pressure-flow relations in dog arteries, Circ. Res. 19:230-246, 1966.

16. Attinger, E.O., H. Sugawara, and A. Navarro. Pulsatile flow patterns in distensible tubes. Circ. Research, 18:447-456, 1966.

17. Bailey, P.E. Smith, and W.M. Coperhaver. Bailey's Textbook of Histology. The Williams & Wilkins Co., 1953.

18. Baker, D.F., J.M. Redi, and V.E. Simmons. Transcutaneous detection of arterial wall motion using phase lock doppler. Proc. 7th Intern. Conf. on Med. and Biol. Engr., Stockholm, 1967.

19. Barker, W.F. Surgical treatment of Peripheral Vascular Disease. McGraw-Hill, 1962.

20. Barnard, A.C.L., W.A. Hunt, W.P. Timlake, and E. Varley. A theory of flow in compliant tubes, Biophysical J., 6:717-724, 1966.

21. Barnard, A.C.L., W.A. Hunt, W.P. Timlake, and E. Varley. Peaking of the pressure pulse in fluid-filled tubes of spatially varying compliance. Biophysical J., 6:735-746, 1966.

22. Bergel, D.H. The static elastic properties of the arterial wall. J. Physiol. 156:445-457, 1961.

23. Bergel, D.H. The dynamic elastic properties of the arterial wall. J. Physiol. 156:458-469, 1961.

24. Bland, D.R. The Theory of Linear Viscoelasticity. The McMillan Co., New York, 1960.

25. Bramwell, J.C., A.V. Hill, and B.A. McSwiney. The velocity of the pulse wave in man in relation to age as measured by the hot wire sphygmogram. Proc. Royal Soc. 93(B):298, 1922.

26. Branson, H. The flow of a viscous fluid in an elastic tube: A model for the femoral artery. Bull. Math. Biophys. 7:181-188, 1945.

27. Carter, S.A. Indirect systolic pressures and pulse waves in arterial occlusive disease of the lower extremities. Circ. 37:624-637, 1968.

28. Connor, J.A. Clinical evaluation of arterial occlusive disease, in: Barker, W.F., Surgical Treatment of Peripheral Vascular Disease. McGraw-Hill Pub. Co., New York, 1962.

29. Cooper, D. Detection of early atherosclerosis by external recording. J. Am. Med. Soc. 199:449-454,1967.

30. Cox, R.H. Wave propagation through a newtonian fluid contained within a thick-walled viscoelastic tube: A model for arterial blood flow. Ph.D. Dissertation, University of Pennsylvania, 1967.

31. Cox, R.H. Comparison of linearized wave propagation models for arterial blood flow analysis. J. Biomechanics, 2:251-265, 1969.

32. Cox, R.H. Blood flow and pressure propagation in the canine femoral artery. J. Biomechanics, 3:131-149, 1970.

33. Crouch, J.E., Functional Human Anatomy, Lea and Febiger, Philadelphia, 1965.

34. Edwards, E.A., and L. Ottinger. Pulse registration in the study of peripheral arterial disease. New England J. Med., 259:101-107, 1958.

35. Edwards, E.A., L. Ottinger, and U. Ruberti. Pulse registration as a means of evaluating peripheral vascular patency and vasomotor activity. Am. J. Cardiology, 4:572-579, 1959.

36. Euler, L. Principa pro motu sangins per arterios determinado Opera posthuma mathematica et physica anno 1844 detecta, ediderant P.H. Fuss et N. Fuss Petropol: Apud Eggers et socios, 2:814-823, 1862.

37. Evans, R.L. Pulsatile flow through tapered distensible vessels, reflection and the hosie phenomenon. Nature 108:290, 1960.

38. Evans, E.L., K.F. Hosie, R.H. Kookier, J. Perry, and R.J.Stish. Reflection in model and arterial waves. HAP 15(2):258-260, 1960.

39. Evans, R.L. A unifying approach to blood flow theory. J. Theoretical Biol. 3:392-411, 1962.

40. Feigel, E.O., L.H. Peterson, and A.W. Jones. Mechanical and chemical properties of arteries in experimental hypertension. J. Clin. Invest. 43:1640, 1963.

41. Fiddian, R.V., D. Byar, and E.A. Edwards. Factors affecting flow through a stenosed vessel. Arch. Surg. 88:83-90, 1964.

42. Fox, E.A., and E. Saibel. Attempts in the mathematical analysis of blood flow. Trans. of the Soc. of Rehology. 7:25-31, 1963.

43. Fox. E., and E. Saibel. A formulation of the problem of flow through tubes. Proc. 4th Intern. Cong. Rheol., A. Copely, ed. New York, Interscience Pub. 1965.

44. Fry, and Greenfield. The mathematical approach to hemodynamics with particular reference to wamersby's theory, in: E.O. Attinger, Pulsatile Blood Flow. McGraw-Hill, 1964.

45. Gabe, I.T. The measurement of oscillatory blood flow and impedance in the human external iliac artery. Clin. Sci. 29:45-88, 1965.

46. Gow, B.S., and M.G. Taylor. Measurements of visco-elastic properties of arteries in living dogs. Circ. Res. 23:111-112, 1968.

47. Greenspon, J.E. Axially symmetric vibrations of a thick cylindrical shell in an acoustic medium. J. Acous. Soc. of Am. 32(8):1-17-1025, 1960.

48. Greenspon, J.E. Vibrations of thick and thin cylindrical shells surrounded by Water. Office of Naval Research, Project NR 385-412. Technical Report No. 4, September 1960.

49. Greenspon, J.E. Vibrations of thick and thin cylindrical shells surrounded by Water. J. Scous. Soc. of Am. 33(10):1321-1328, 1961.

50. Greer, J.C., H.C. McGill, and J.P. Strong. The fine structure of human atherosclerotic lesion. Am. J. Pathol., 38:263, 1961.

51. Guard, H.R. and Y.M. Behude. Changes due to aging in the abdominal aorta. Indian J. Med. Res. 41:267, 1953.

52. Hale, J.F., D.A. McDonald, M.G. Taylor, and J.R. Womersley. The counter chronometer method for recording pulse-wave velocity, Proc. Physiological Soc. 27P-28P, May 21, 1955.

53. Hales, S. Statistical Essays. Vol. II. Haemastatick. Innays and Manby, London, 1783, Reprinted by Hafner Publishing Co., New York, 1964.

54. Hallock, P. Arterial elasticity in man in relation to age evaluated by the pulse wave velocity method. Arch. Int. Med., 54:770, 1934.

55. Ham, A.W. Histology. J.B. Lippincott Co., Philadelphia, 1957.

56. Hamilton, W.F. The patterns of the arterial pulse. Am. J. Physiology, 141:235, 1944.

57. Hamilton, W.F., and W.J. Brown. Positive wave reflection on an elastic model from a wider segment with higher resistance. Am. J. Physiol., 197-730, 1959.

58. Hamilton, W.F., and P. Dow. An experimental study of standing waves in the pulse propagated through the aorta. Am. J. Physiol., 125:48, 1939.

59. Hamilton, W.F., J.W. Remington, and P. Dow. The determination of the propagation velocity of the arterial pulse wave. Am. J. Physiology, 144:521, 1945.

60. Haynes, F.W., L.B. Ellis, and S. Weiss. Pulse wave velocity and arterial elasticity in arterial hypertension, atherosclerosis and related conditions. Am. Heart J., 11:385, 1936.

61. Herrmann, G., and Mirsky, I. "Three-dimensional and Shell-theory Analysis of Axially Symmetric Motions of Cylinders," Journal of Applied Mechanics, Dec. 1956, pp. 563-568.

62. Histand, M.B., "An Experimental Study of the Transmission Characteristics of Pressure Waves in the Aorta," Ph.D. Dissertation, Stanford University, 1969.

63. Hyman, C., and T. Winsor. What can be found in arterial pulse waves. Am. Heart J., 61:424, 1961.

64. Jacobs, R.B. On the propagation of a disturbance through a viscous liquid flowing in a distensible tube of appreciable mass. Bull. Math. Biophys., 15:395-409, 1953.

65. Jones, A.W., E.O. Feigl, and L.H. Peterson. Water and electrolyte content of arteries in dogs. Federation Proc., 20:117, 1961.

66. Jones, A.W., E.O. Feigel and L.H. Peterson. Water and electrolyte content of normal and hypertensive arteries in dogs. Circ. Res., 15:386, 1964.

67. Jones, E., I. Chang, and M. Anliker. Effects of viscosity and external constraints on wave transmission in blood vessels. Stanford University Biomechanics Laboratory, SUDAAR, No. 344, May, 1968.

68. Junger, M.C. The physical interpretation of the expression for an outgoing wave in cylindrical coordinates. J. Acoust. Soc. Am., 25(1), Jan. 1953.

69. Karreman, G. Some contributions to the mathematical biology of blood circulation. Reflections of pressure waves in the arterial system. Bull. Math. Biophys., 14:327-350, 1952.

70. Klip, W. Velocity and Dampting of the Pulse Wave. Martinus Nijhoff, The Hague, 1962.

71. Klip, W., P. VanLoon, and D.A. Klip. Formulas for phase velocity and dampting of longitudinal waves in thick-walled viscoelastic tubes. J. Appl. Physics, 38:3745-3755, August, 1967.

72. Kortweg, D.J. Uber die fortpflanzungsgeschwindig kert des Schalles in elastichen rohren. Annalen der physik und chemie, Ser. 3, Vol. 5, pp. 525-542, 1878.

73. Kyle, M.C., J.D. Klingeman, and E.D. Fries. Computer identification of brachial arterial pulse waves. Computer and Biomedical Research, 2:151-159, 1968.

74. Lambert, J., "On the Nonlinearities of Fluid Flow in Nonrigid Tubes," J. Frank. Instit., V. 266, p. 83, 1958.

75. Lamb, H. On the velocity of sound in a tube as affected by the elasticity of the walls. Manchester memoirs, XLII, 1898.

76. Landowne, M. A method using induced waves to study pressure propagation in human arteries. Circ. Res. 5:594, 1957.

77. Landowne, M. Pulse wave velocity as an index of arterial elastic characteristics, p. 168 in: Tissue Elasticity, Am. J. Physiol. Soc., Wash. D.C., 1957.

78. Lax, H., A.W. Feinberg, and B.M. Cohen. The normal pulse and its modification in the presence of human atherosclerosis. J. Chron. Disease, 3(6):618-631, June, 1956.

79. Learoyd, B.M., and M.G. Taylor. Alterations with age in the viscoelastic properties of human arterial walls. Circ. Res., 18:278-292, 1966.

80. Lewis, I.A.D., and F.H. Wells, Millimicrosecond Pulse Techniques, Permagon Press, New York, 1959.

81. Malindzak, G.S., Jr., "Reflections of Pressure Pulses in the Aorta," Medical Research Engineering, V. 6, pp. 25-31, 1967.

82. Malindzak, G.S., Jr., and R.W. Stacy, "Dynamics of Reflection of Pressure Pulses in the Aorta," Annals N.Y. Acad. Sciences, 128:921-938, 1966.

83. Maxwell, A., and M. Anliker. Dispersion and dissipation of waves in blood vessels. Stanford University Biomechanics Lab. SUDAAR No. 312, May, 1967.

84. McDonald, D.A. Regional pulse wave velocity in the arterial tree. JAP 24:73-78, 1968.

85. McPherson, A.T., and A. Klemin. Engineering Uses of Rubber. Reinhold Publishing Corp., New York, 1956.

86. Meisner, J.E. and J.W. Remington. Pulse control changes in carotid and foreleg arterial system. Am. J. Physiol. 202(2):527-535, 1962.

87. Milch, R.A. Matrix properties of the aging arterial wall. in: Monographs in the Surgical Sciences. The Williams & Wilkins Co., 1965.

88. Mindlin, R.D. "Influence of Rotary Inertia and Shear on Flexural Motions of Isotropic Elastic Plates," Journal of Applied Mechanics, Trans. ASME, 73:31-38, 1951.

89. Mirsky, I. Pulse velocities in an orthotropic elastic tube. Bull. Math. Biophysics. 29:311-318, 1967.

90. Mirsky, I. Wave propagation in a viscous fluid contained in an orthotropic elastic tube. Biophysical J. 7:165-186, 1967.

91. Mitchell, J.R.A., and C.J. Schwartz. Arterial Disease. F.A. Davis Co., Philadelphia, 1965.

92. Moens, A.I. Die Pulskurve. Brill, Leiden, 1878.

93. Monnier, M. Geront. Clin. 9:81-86, 1967.

94. Morgan, G.W. and W.R. Ferrante. Wave propagation in elastic tubes filled with streaming liquid. J. Acoustical Soc. of Am. 27(4):715-725, 1955.

95. Morgan, G.W., and J.P. Kieley. Wave Propagation in a viscous liquid contained in a flexible tube. J. Acous. Soc. of Am., 26:324-328, 1954.

96. Muller, A. Uber die fortpflanzungsgeschwindigkeit von Druckwellen in clenkaren Rohren bie rahender und stromender Flussigkeit. Helv Physiol. Acta., 8:228-241, 1950.

97. Muller, A. Uber der abhangigkeit der fortpflanzungsgeschwindigkeit und der dampfung der druckwellen in dehnbarren Rohren von deren Wellen lange. Halv. Physiol. Acta., 9:162, 1951.

98. Nordergranf, A. Hemodynamics. In: Biological Engineering, H.P. Schwan, ed., McGraw-Hill, 1969.

99. Nye, E.R. The effect of blood pressure alteration on the pulse wave velocity. Brit. Heart J., 26:261, 1964.

100. Olsen, J.H. Waves in fluid-filled elastic tubes. Ph.D. Dissertation, Mass. Inst. Tech., 1966.

101. O'Rourke, M.F. Steady and pulsatile energy losses in the systemic circulation under normal conditions and in simulated arterial disease. Cardiovasc. Res., 1:313-326, 1967.

102. O'Rourke, M.F., J.V. Blazek, C.L. Morreels, and L.J. Korretz. Pressure wave transmission along the human aorta; changes with age and in arterial degenerabive disease. Circ. Res., 23:567-579, 1968.

103. Parker, F. An electron microscope study of coronary arteries. Am. J. Anat., 103:247, 1958.

104. Parker, F. An electron microscope study of experimental atherosclerosis. Am. J. Pathol. 36:17, 1960.

105. Patel, D.J., F.M. DeFrectas, J.C. Greenfield, and D.L. Fry. Relationship of radius to pressure along the aorta in living dogs. JAP, 18:1111-1117, 1963.

106. Patel, D.J., and D.L. Fry. Longitudinal tethering of arteries in dogs. Circ. Res., 19:1011-1021, 1966.

107. Payne, A.R., and J.R. Scott. Engineering Design with Rubber. McLaren and Sons Ltd., London, 1960.

108. Peterson, L.H. Properties and behavior of the living vascular wall. Physiol. Rev., 42(5):309, 1962.

109. Peterson, L.H. Current trends in cardiovascular physiology. Physiologist, 6:115-120, 1963.

110. Peterson, L.H. Systems behavior, feed-back loops, and high blood pressure research. Circ. Res., 12:585, 1963.

111. Peterson, L.H., R.E. Jensen, and J. Parnell. Mechanical properties of arteries in vivo. Circ. Res., 8:622-639, 1960.

112. Pollack, G.H., R.V. Reddy, and A. Nordergraf. Input impedence, wave travel, and reflections in the human arterial tree: studies using an electrical analog. IEEE trans. on Biomedical Engr. BME-15(3):151-164, 1968.

113. Porje, I.G. Studies of the arterial pulse wave, particularly in the aorta. Acta Physiologica Scandinavia, 13(42):1-68.

114. Remington, J.W., and E.H. Wood. Formation of peripheral pulse contour in man. JAP, 9:433-442, 1956.

115. Remington, J.W. Unexplained features of the left ventricular pressure pulse. Am. J. Physiol. 199(2):328-330, 1960.

116. Remington, J.W. Contour changes of the aortic pulse during propagation. Am. J. Physiol. 199(2):331-334, 1960.

117. Richardson, E., and E. Tyler. The transverse velocity gradient near the mouths of pipes in which an alternating or continuous flow of air is established. Proc. Phys. Soc. V. 42:1, 1929.

118. Ried, J.M., D.W. Baker, and V.E. Simmons. Phase detection of doppler signals for measurement of biological displacements. Proc. 7th Intern. Conf. on Med. and Biol. Engr. Stockholm, 1967.

119. Roach, M.R., and A.C. Burton. The effect of age on the elasticity of human iliac arteries. Can. J. Biochem. Physiol. 7:557, 1959.

120. Roberts, W.C. Coronary Arteries in Fatal Acute Myocardial Infarction, Circulation, 45:224, Jan. 1972.

121. Rockwell, R.L. Nonlinear analysis of pressure and shock waves in blood vessels. Ph.D. Dissertation. Stanford Univ. 1967.

122. Roy, C.S. The elastic properties of the arterial wall. J. Physiol (London) 3:125, 1880.

123. Rudiger, G. Review of current mathematical methods for the analysis of blood flow. Biomedical fluid mechanics symposium. ASME, pp. 1-33, 1966.

124. Ryan, J.M., R.W. Stacy, and R.N. Watman. Role of Abdominal aortic branches on pulse wave contour genesis. Circ. Res., 4:676, 1956.

125. Sexton, J.A. Elastic properties of the rabbit aorta in relation to age. Arch. Pathol. 34:262, 1942.

126. Skalak, R. Wave propagation in blood flow. in: Biomechanics, Y.C. Fung ed., ASME, 1966.

127. Spencer, M.P. and A.B. Denison. Pulsatile blood flow in the vascular system. Handbook of Physiology Sect. 2, Vol. 2, ch. 25, p. 849.

128. Steele, J.M. The interpretation of arterial elasticity from measurements of pulse wave velocities, Part 1, Effects of Pressure. Am. Heart J. 14:452, 1937.

129. Streeter, V.L., W.F. Keitzer, and D.F. Bohr. Pulsatile pressure and flow through distensible vessels. Circ. Res. 13:3-20, 1963.

130. Taylor, M.G. An experimental determination of the propagation of fluid oscillation in a tube with a viscoelastic wall; together with an analysis of the characteristics required in an electrical analogue. Physics in Med. and Biol. 4:63, 1959.

131. Taylor, M.G. The influence of the anamolous viscosity of blood upon its oscillatory flow. Phys. in Med. & Biol. 3:273, 1959.

132. Taylor, M.G. Wave travel in arteries and the design of the cardiovascular system in: Pulsatile Blood Flow, E.O. Attinger, ed. pp. 343-372, McGraw-Hill, 1964.

133. Taylor, M.G. Wave travel in a non-uniform transmission line in relation to pulses in arteries. Phys. Med. Biol. 10(4):539-550, 1965.

134. Thurston, G.B. Periodic flow through circular tubes. J. Acous. Soc. Am. 24(6):653, 1952.

135. Tichner, E.G., and A.H. Sacks. A theory for the static elastic behavior of blood vessels. Biorheology. 4:151-168, 1967.

136. Treloav, L.R.G. The Physics of Rubber Elasticity. Oxford at the Clarendon Press, London, 1958.

137. Van Citters, R.L. Longitudinal Waves in the walls of fluid-filled elastic tubes. Circ. Res. 8:1145-1148, 1960.

138. Van Dyke, P. Stresses in a cylindrical shell with a rigid inclusion. AIAAJ 5(1):125-137, 1967.

139. Wells, M.K. On the Determination of the Elastic Properties of Blood Vessels From their Wave Transmission Characteristics. Ph.D. Dissertation, Stanford University, 1969.

140. Wiener, F., E. Morking, R. Skalak, and A.P. Fishman. Wave propagation in the pulmonary circulation. Circ. Res. 19:834, 1966.

141. Wilkins, M.L. Calculation of Elastic-Plastic Flow, in: Methods of Computational Physics, 3:211-263, Academic Press, 1964.

142. Witzig, K. Uber erzwung ene Wellenbewegungen Zuher, inkonpressibler Flussigkeuten in elastichen Rohen. Inaugural Dissertation Universitat Bern, K.J. Wyss, Bern, 1914.

143. Womersley, J.R. Method for the calculation of velocity rate of flow and viscous drag in arteries when the pressure gradient is known. J. Physiol. 127:553, 1955.

144. Womersley, J.R. Oscillatory motion of a viscous liquid in a thin-walled elastic tube. I: The linear approximation for long waves. Phil. Mag. Ser. 7, 45:199, 1955.

145. Womersley, J.R. An elastic tube theory of pulse transmission and oscillatory flow in mammilian arteries. WADC Tech. Report TR 56-614, Jan. 1957.

146. Womersley, J.R. Oscillatory flow in arteries II: the reflection of a pulse wave at junctions and rigid inserts in the arterial system. Phys. Med. & Biol. 2:313-323, 1958.

147. Woolam, G.L., P.L. Schnur, C. Valbona, and H.E. Hoff. The pulse wave velocity as an early indicator of atherosclerosis in diabetic subjects. Circ. 25:533, 1962.

148. Yao, S.T., J.T. Hobbs, and W.T. Irvine. Pulse examination by an ultrasonic method. British Med. J. 4:555-557, 1968.

149. Yoshimura, S., J. Sugai, H. Hashimoto, T. Okamura, N. Yamigishi, M. Hasegawa, T. Hayashi, F. Ostuka, E. Ishikawa, H. Yamashita, and M. Kozaki. An estimation of atherosclerosis by the measurement of pulse-wave velocity and an analysis of the clinical effect of therapeutic agents on atherosclerosis. COR VASA, 10:173-182, 1968.

150. Young, D.F., and C.C. Shih. Some experiments on the effect of isolated protuberances on flow through tubes. Experimental mechanics pp. 225-229, 1969.

151. Young, T. On the functions of the heart and arteries, Philosophical tans. of Roy. Soc. Lond. 99:1-31, 1809.

APPENDIX A

EXPERIMENTAL APPARATUS AND PROCEDURE

General Description

The experimental apparatus was constructed to produce a pulse wave at one end of a fluid-filled tube and to examine its propagation along the axis of the tube. The general arrangement of the equipment selected is shown in Figure A-1. The tubes were mounted along the long axis of the water-filled tank, and the pulses were generated at one end with a piston driven by an electromagnetic shaker. The shaker was powered by an amplifier which followed the signal from a pulse generator. The centerline pressure transducer, and radial motion transducer were positioned with a carriage mounted on top of the tank. Information from the transducers was recorded on a dual-trace memory oscilloscope.

Tank and Attached Equipment

The tubes were mounted horizontally along the major axis of a water-filled tank 2 feet square and 8 feet long. Figure A-2 shows the tube holder and the piston used to generate the pulse waves. The collar holding the tube provided a fixed end condition with no rotation at the edge of the tube holder. The piston for generating the waves was inside tube holder at one end of the tank. The tube

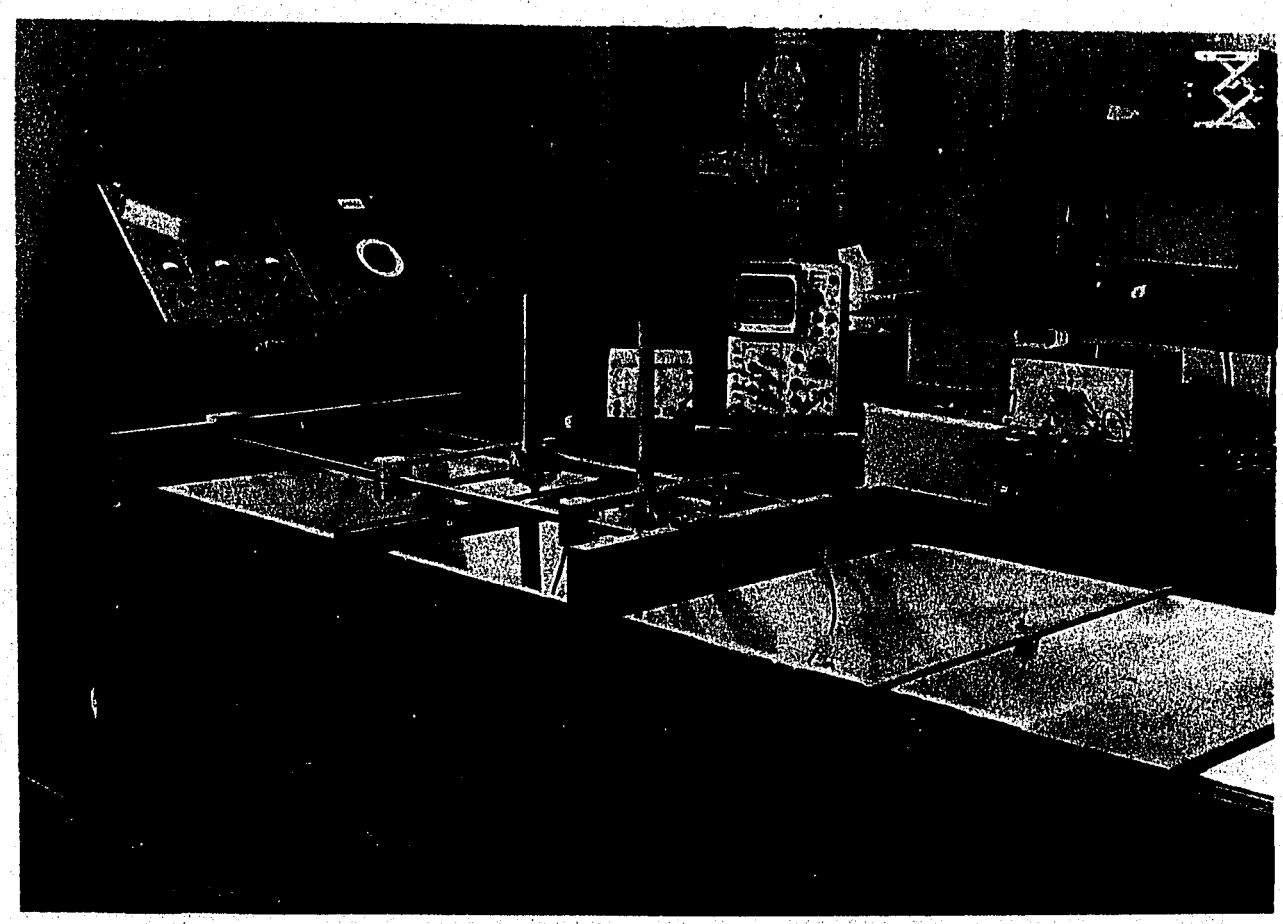

Figure A-1

EXPERIMENTAL APPARATUS

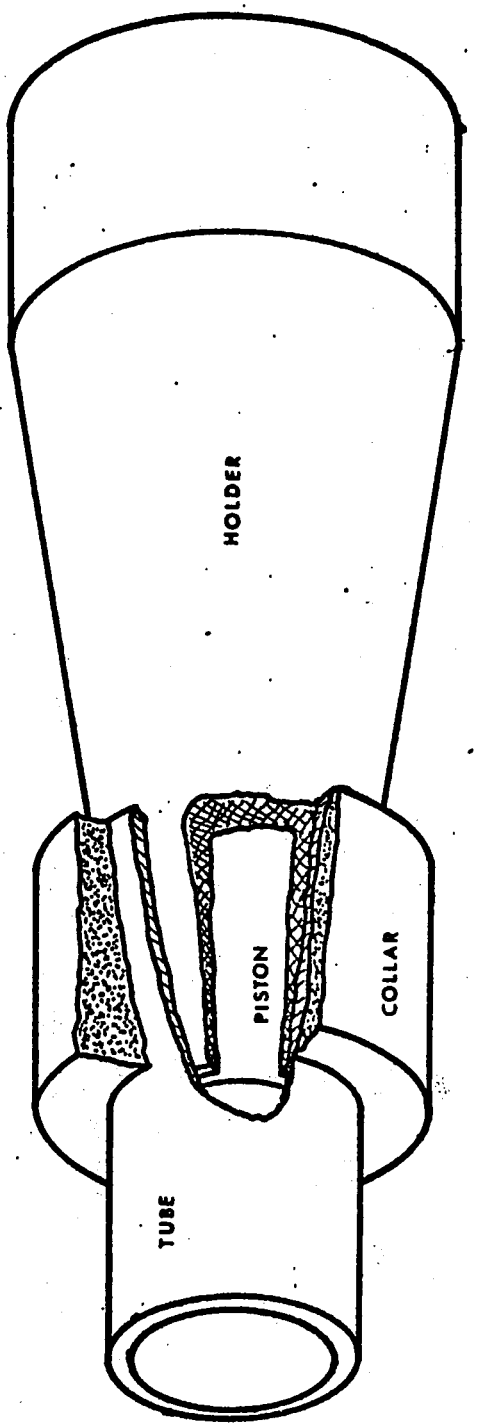

FIGURE A-2 TUBE HOLDER AND PISTON

holder at the terminal end of the tube was movable along the axis of the tank and provided a positioning mount for the .250 inch tube holding the pressure transducer. The mount holding the pressure transducer also contained a port which allowed the tube to be pressurized above the ambient fluid in the tank. The tank was filled with water to provide a low-loss medium to propagate the ultrasound beam from the motion transducer.

A three-axis positioning carriage mounted on top of the tank was used to locate the motion transducer and the center-line pressure transducer. Machinist's rules with minimum gradations of .010 inch were used for indicating the position.

Piston and Pulse Generating Equipment

The piston for generating the pulse waves moved axially inside the tube holder mounted at the end of the tank. An MB C-11 electromagnetic shaker was attached to the piston with a universal coupling used to allow for some misalignment in the motion of piston and shaker as shown in Figure A-3. The piston seal inside the tube holder was accomplished with three raised rings that served as piston rings. Motion of the piston was determined statically with a micrometer and observed dynamically with an LVDT. The slug for the LVDT was attached to the shaker mounting plate and the coil was attached to a bracket on the cover of the degaussing coil of the shaker as shown in Figure A-3. The shaker motion was

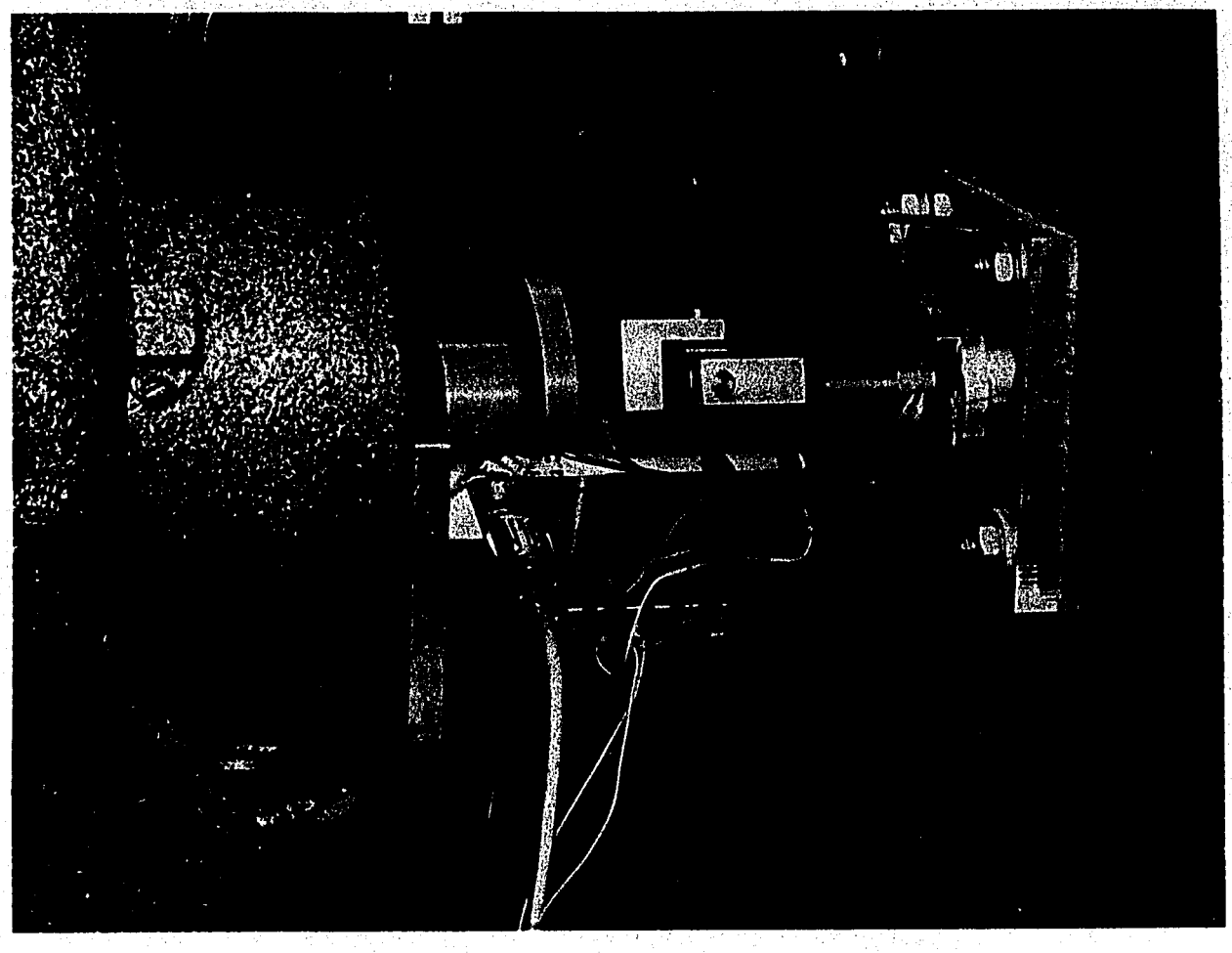

Figure A-3

COUPLING OF ELECTROMAGNETIC SHAKER TO PISTON

constrained to move only forward from the reference position in describing a half sine pulse. This was accomplished by mounting a nylon stop against the armature to prevent it from moving back into the negative region.

The shaker was driven by its accompanying equipment, an MB 2750 amplifier. The B and K signal generator which was integral with the amplifier was by-passed and a Wavetek 112 signal generator was used to produce single half sine wave pulses to drive the amplifier.

Transducers

An LVDT used to measure the position of the piston is shown in Figure A-3.

The phase-lock motion transducer and the pressure transducer are shown in Figure A-4. A detailed discussion of the phase-lock transducer is given in Appendix C. The pressure transducer was mounted at the end of a .250 tube and positioned axially with the carriage on the tank. The transducer using two active strain gages on a .196 inch diaphragm was connected through a shielded cable to form one half of a Wheatstone bridge. In order to eliminate noise an amplifier for the pressure transducer was constructed to provide approximately 1000:1 gain, and mounted as near the transducer as possible. An RF filter on the output from the amplifier provided the necessary final reduction in noise to produce a signal with a low background noise. In the final calibration this background noise was estimated

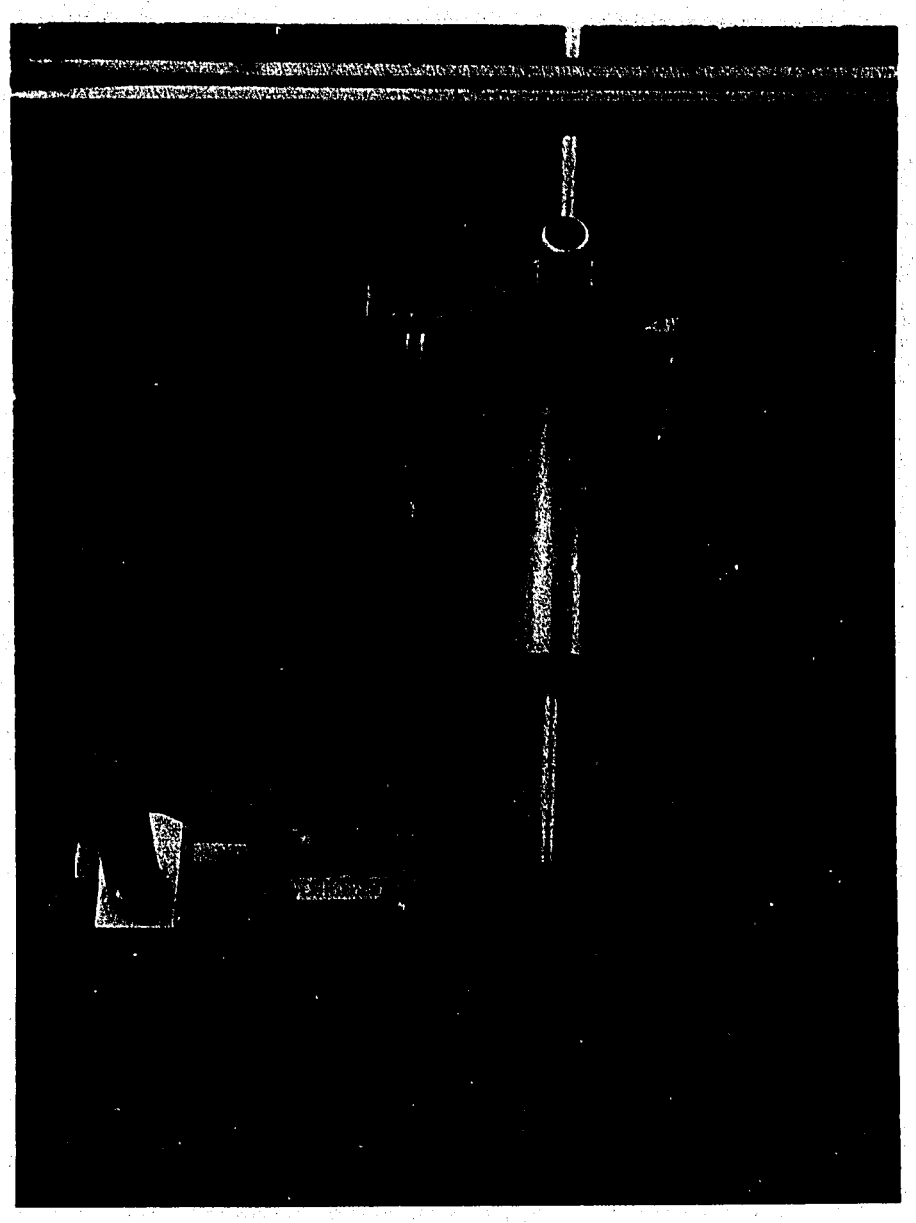

Figure A-4

PRESSURE AND MOTION TRANSDUCERS

to be .0008 psi.

Experimental Procedure

The experimental procedure was developed to produce short pulses (10 millisecond rise time) of controlled amplitude, and to investigate their propagation along a fluid-filled tube with nonuniform wall properties. In order to investigate the propagation of a single wave using only a single displacement transducer, and a single pressure transducer it was necessary to send 600 to 1000 identical single pulses along the tube each time repositioning the transducers to a different location.

The shape of the pressure pulse is shown in Figure 4-3 of Chapter 4. The contour of approximately a single sine wave was achieved by driving the piston through a half sine wave and allowing the inertia of the returning fluid and the reflection from the piston face to generate the remaining half of the pulse. The piston was constrained to move only in a half sine wave by mounting a nylon block at the rear of the shaker body to prevent the armature from traveling past the zero position of the returned stroke. The pulse was directed with the Wavetek 112 signal generator which, besides inputting the half sine pulse to the amplifier of the shaker, also started the sweep on the oscilloscope to begin recording data from the pressure and displacement transducers.

The procedure for making an experimental run started with mounting a tube in the tank. The tube was mounted

between the two tube holders with the clamping collars over the outside of the tube. The tube holders had previously been aligned both with the tank and the transducer carriage to within the tolerance of the scales, .010 inch. The electronics of the displacement transducer, even though of solid state construction, was noted to drift in calibration. It was left on for several days at a time to insure as much stability as possible. The amplifier for the shaker, the oscilloscope, and the amplifier for the pressure transducer were turned on the evening before the experiment to provide a greater than 6 hours of warmup. This was greater than necessary for the oscilloscope, but it was observed that the amplifiers for the shaker and the pressure transducer needed four hours or more to come to a stabilized condition. Since the pressure transducer was used throughout the experiment to check uniformity of the output pulse from the shaker, a uniform thermal drift in either unit would not have been detectable in relation to a constant baseline.

After turning on the various electronic devices, the pressure transducer was positioned in the center of the tube with the diaphragm of the transducer within .010 inch of the terminal tube-tube holder interface. This was the position used to monitor the amplitude of the pulse throughout the portion of the experiment when radial displacement information was recorded. The tube was pressurized with a static head of

water from an overhead tank to 37 inches of water by attaching the filling hose to the port in the pressure transducer positioner which had been drilled and fitted with a port to the interior of the tube. The crystal holder for the displacement transducer was mounted on the vertical shaft of one of the carriage trucks on the positioner, and aligned perpendicular to the tube axis. This concluded setting up the equipment the evening before an experimental run was to be begun. The motion of the water in the tank damped out, and all equipment was stabilized by the next morning.

The recording of the data consisted of initiating the pulse with the signal generator and recording the radial wall motion and centerline pressure along the axis of the tube. The radial wall motion was recorded first, with the pressure transducer at the terminal end of the tube used to maintain a uniform pulse amplitude throughout the duration of the experiment. The radial wall motion was recorded by sequentially moving the displacement transducer along the axis of the tube for each pulse wave which was initiated. Once the entire axis of the tube at one circumferential setting had been completed, the tube holders were rotated and the experiment repeated, recording data at the same axial position for the new angular orientation. Nonaxisymmetric tubes were rotated in 22.5° intervals and axisymmetric tubes were rotated in 45° intervals.

After the radial displacement had been recorded, the pressure transducer was advanced along the axis of the tube positioning it at the same axial positions where the radial deformation data had been recorded.

After the completion of recording the pressure and displacement data the calibration of the transducers was verified. The pressure transducer was calibrated by moving it over a one foot elevation in the tank of water using a machinist's scale as a reference. The displacement transducer was calibrated statically by removing the stop from the back of the shaker body, and attaching a micrometer stock. This calibration was performed at the distance and oscillator frequency used in the experiment that had just been concluded. The normal position for the displacement transducer crystal holder was .400 inches, and the operating frequency was normally 4.80Mhz. After concluding the calibration, all units with the exception of the transmitter and receiver for the phase-lock motion transducer were turned off. As a general rule this would conclude work starting at 6:00 am and ending sometime after 3:00 am the following day.

The general problems that prevented the rapid recording of the data were involved in the motion of the water bath, hence moving the tube of low rigidity suppored only at its ends, and in the problem of getting the displacement transducer to follow the motion of the tube wall with a

clean signal as determined by the output on the oscilloscope screen. These two problems were not unrelated. The motion of the tube due to water sloshing may be greater than .200 inch which is large enough for the transducer to "break lock" and either lock at another frequency, or to simply shift to its upper frequency limit and not follow any motion whatsoever. Also it was necessary to continuously work with the locking procedure to achieve a clean and locked signal once the tube had reduced its motion to an acceptable value of .003 inch or less. The reduced motion was not only necessary for effective operation of the phase-lock transducer, but more specifically, to achieve a stable baseline from which to determine the height of the pulse. The slow tube motion of .003 inch amplitude and a period of one second or more was accepted as stable for determining the height of the 10 millisecond pulse. The .003 inch amplitude of vibration was a worse case condition, and generally it was possible to have the tube motion held to within less than .001 inch. The variability noted in the data from the radial wall motion emphasized the need to keep the remaining variables minimized in order that measurement artifacts would not add to the already random nature of the information.

APPENDIX B

WATER BATH CORRECTION

The presence of the water bath surrounding the fluid-filled tube was necessary to provide low loss medium to propagate the ultrasound beam from the phase-lock transducer, and to provide a near neutral density environment for the fluid-filled tube. Without the external water bath, the thin-walled tube would have sagged and prevented performing the experiment with a horizontal tube. The water bath modified the propagation of the wave by introducing an additional mass surrounding the tube. In order to determine the effects on the propagation constant, the magnitude of radiant sound waves and viscous drag were evaluated. The radiated wave was calculated and experimentally measured, while the viscous drag was calculated.

Radiated sound waves from vibrating tubes was considered by both Junger(68) and Greenspon(48,48,49). Junger(68) predicted that sound radiation will not take place unless the rise times of the pulses were at least two orders of magnitude smaller than those used in this experiment, i.e., rise times less than .1 millisecond. Greenspon(49), using a different method of solution, predicted the existence of a compressional wave at slightly

greater than twice (2.10) that of Junger. Simultaneous pressure measurements from inside and outside the tube were obtained. The pressure transducer was inside the tube as near the piston as was practical (1/2 inch) to avoid destroying the transducer diaphragm from over excursion of the piston, and the transducer outside the tube was mounted next to the tube wall with a gap of less than .030" between the diaphragm and the tube wall. This gap was exceedingly small with a .125" diameter transducer but represented a worst case situation. The pressure ratio across the tube wall (P_o/P_i) in this case was less than 10^{-4}. From the two literature sources and the experiment it was concluded that the pulse wave generated a negligible compressional wave in the water bath, and hence the external pressure could be neglected.

The consideration given to viscous damping from the water bath was determined by approximating the viscous drag from the Navier-Stokes equation. The viscous effects are described by the relation

$$-2\mu\left(\frac{\partial u}{\partial r} - \frac{u}{r}\right)$$

For an incompressible fluid surrounding an axisymmetric tube moving radially with a velocity U_r, the velocity gradient at the wall is

$$\frac{\partial u}{\partial r} = -\frac{u}{r}$$

The viscous drag from the water bath will be

$$f_r < -4\mu\frac{u}{r}$$

For a radial displacement of .010 inch in .010 second

$$u = \frac{.010}{.010} = 1 \text{ inch/second}$$

The viscous force at the wall is:

$$f_r < 1.11 \times 10^{-6} \text{ psi.}$$

The viscous drag is negligible in comparison to the centerline tube pressure of the order of .10 psi.

The alteration in the propagation velocity was predicted by both Junger(68) and Greenspon(49) to be an inductive effect from the added mass of the water surrounding the tube. Womersley(149) used this same approach in accounting for the added mass of the tissue surrounding the pulsating artery. Whatever method is used, the effect is to increase the mass in the expression for the wave speed; hence, producing a slower wave speed. This represented as:

$$c = \sqrt{\frac{Eh}{2\alpha\rho R}}$$

Experimental data predicts that the value for α should be 1.75 for the case of a fluid-filled tube in a water bath with a propagating wave of .010 seconds rise time. The

dilational wave velocity was not observed to be affected by this correction as it is essentially axial motion of material in the wall with negligible fluid motion. This is contrasted to large fluid motion. This is contrasted to large fluid motion associated with the radial deformation of the pulse wave.

APPENDIX C

PHASE-LOCK MOTION TRANSDUCER

The motion of the tube wall was measured with the use of a phase-lock ultrasound transducer. This prototype device was developed at the University of Washington Bio-engineering Department for use in transcutaneously and nontraumatically measuring the motion of biological structures. The potential of measurement of arterial wall motion or the motion structures of the heart such as valve leaflets were presented as potentially valuable sources of diagnostic information.

The phase-lock is based upon a new type of ultrasonic circuitry. Two ultrasonic crystals are used in the transducer, one for transmission and the other for receiving the reflecting sound beam. The received sound beam is composed of both a leakage signal from the transmitting crystal, and a returned signal from the reflecting interface.

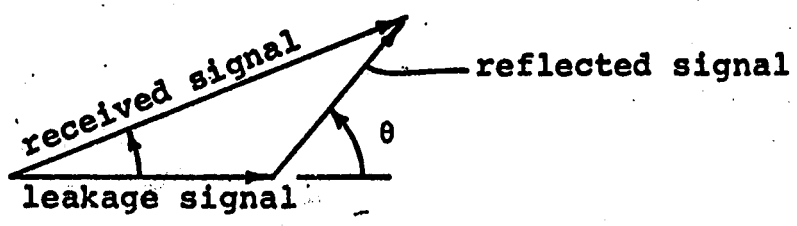

Figure C-1 Composition of returned signal

The reflected wave is represented as:

$$a = A \cos (\omega t - \theta)$$

where

$$\therefore \theta = 2\omega x/c$$

x = distance from transducer to reflecting surface

c = propagation speed of sound wave

The phase angle can be changed by alterations in either the frequency ω or the distance x . What, in fact, happens with the phase lock circuitry, is that the phase angle remains constant by changing the frequency of the oscillator as the distance x is changed.

The diagram of the phase-lock circuit is shown in Figure C-2.

The signal which is received is passed through a limiter to produce a signal of the same magnitude of the transmitted signal, and then goes to a phase detector where it is compared with the transmitted signal. Because the leakage is larger than the reflected signal, and of a capacitive nature, the received signal is essentially 90° out of phase with the transmitted signal. The phase detector is designed to produce a signal that is proportional to the amount that the phase difference between the transmitted and received wave differ in phase from 90°.

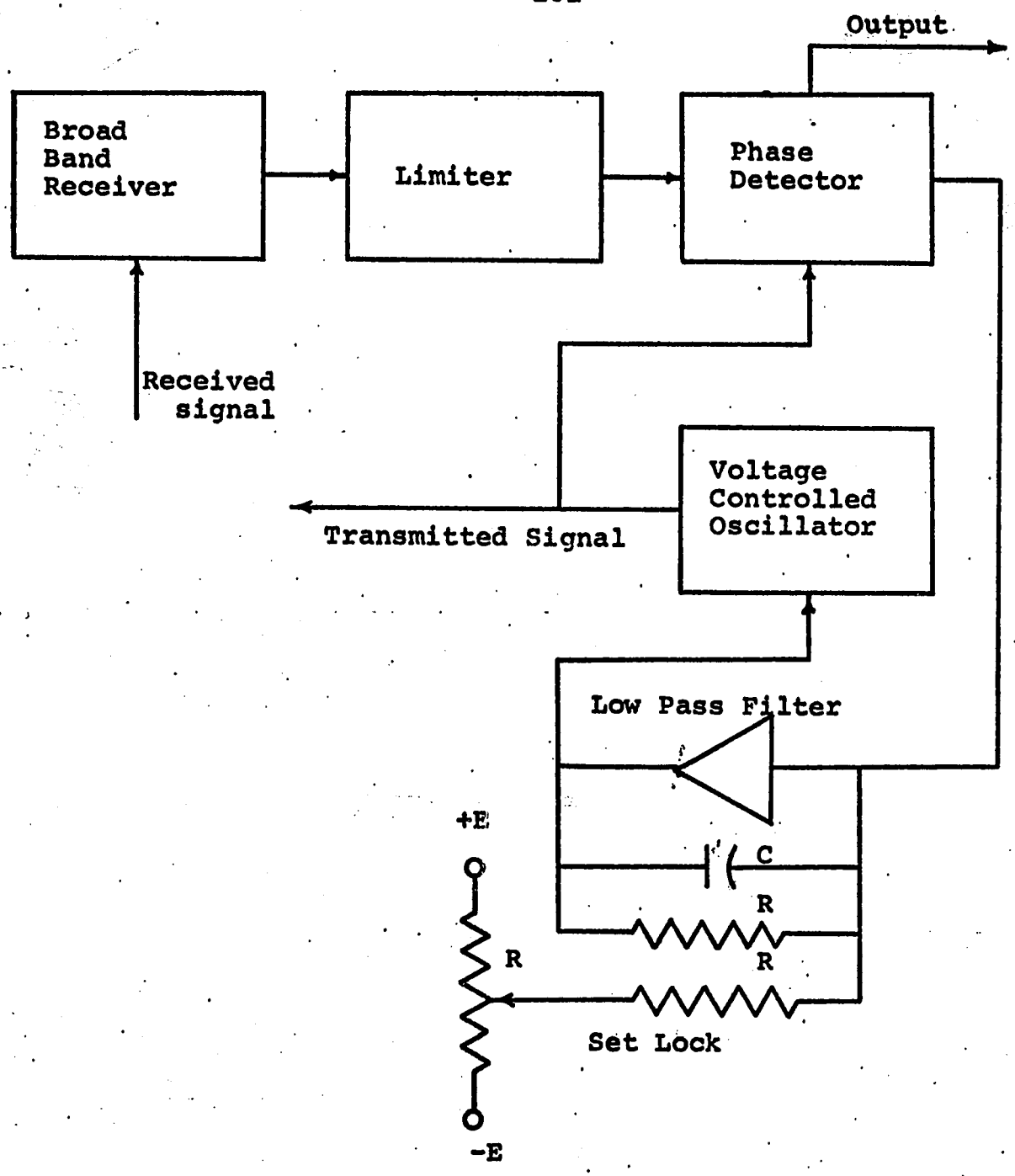

Figure C-2 Schematic circuit of phase-lock ultrasound transducer

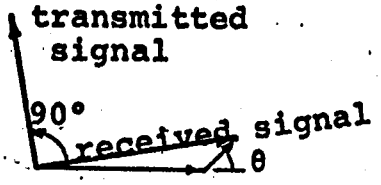

Figure C-3 Composition of transmitted and returned signals

This error signal is used to control the voltage-controlled-oscillator in the transmitter; hence, the frequency of the transmitter is controlled to keep the phase angle of the returned signal a constant value. The output signal from the phase detector is used to indicate the position of the reflecting surface.

Figures A-1 and A-4 in Appendix A show the components in the constructed form. The circuitry consisted of separate transmitter and receiver units with the transmitting and receiving crystals mounted in a lucite fixture which could be positioned exterior to the tube. The output signal was displayed on a storage oscilloscope.

The calibration of the phase-lock transducer was performed by using the face of the piston as the reflecting surface. Both static and dynamic results could be obtained in this manner. The static calibration was obtained by moving the armature of the shaker with a micrometer mounted to the shaker body. Figure C-4 shows the static calibration of the transducer. The spacing used in the experiment was .400 inches as this was the point where the sound beams from the two crystals were focused. The sensitivity of the unit, accounting for the inherent instrument noise, was such that motion less than .0005 inch could be accurately measured.

Figure C-5 shows the dynamic calibration of the phase-lock transducer at .400 inch spacing from the piston face,

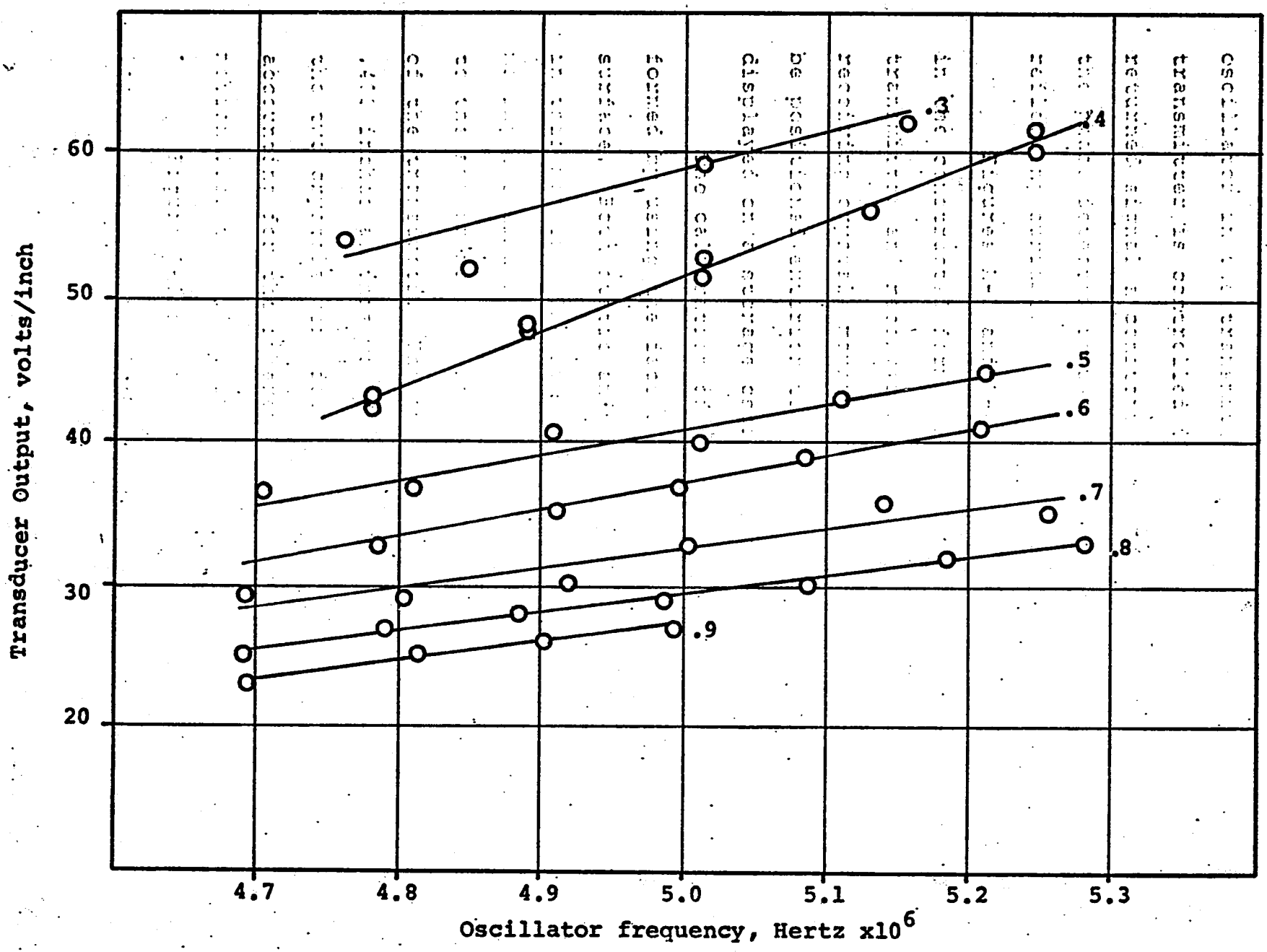

FIGURE C-4 PHASE-LOCK STATIC CALIBRATION. CURVES INDICATE TRANSDUCER TO INTERFACE DISTANCE IN INCHES

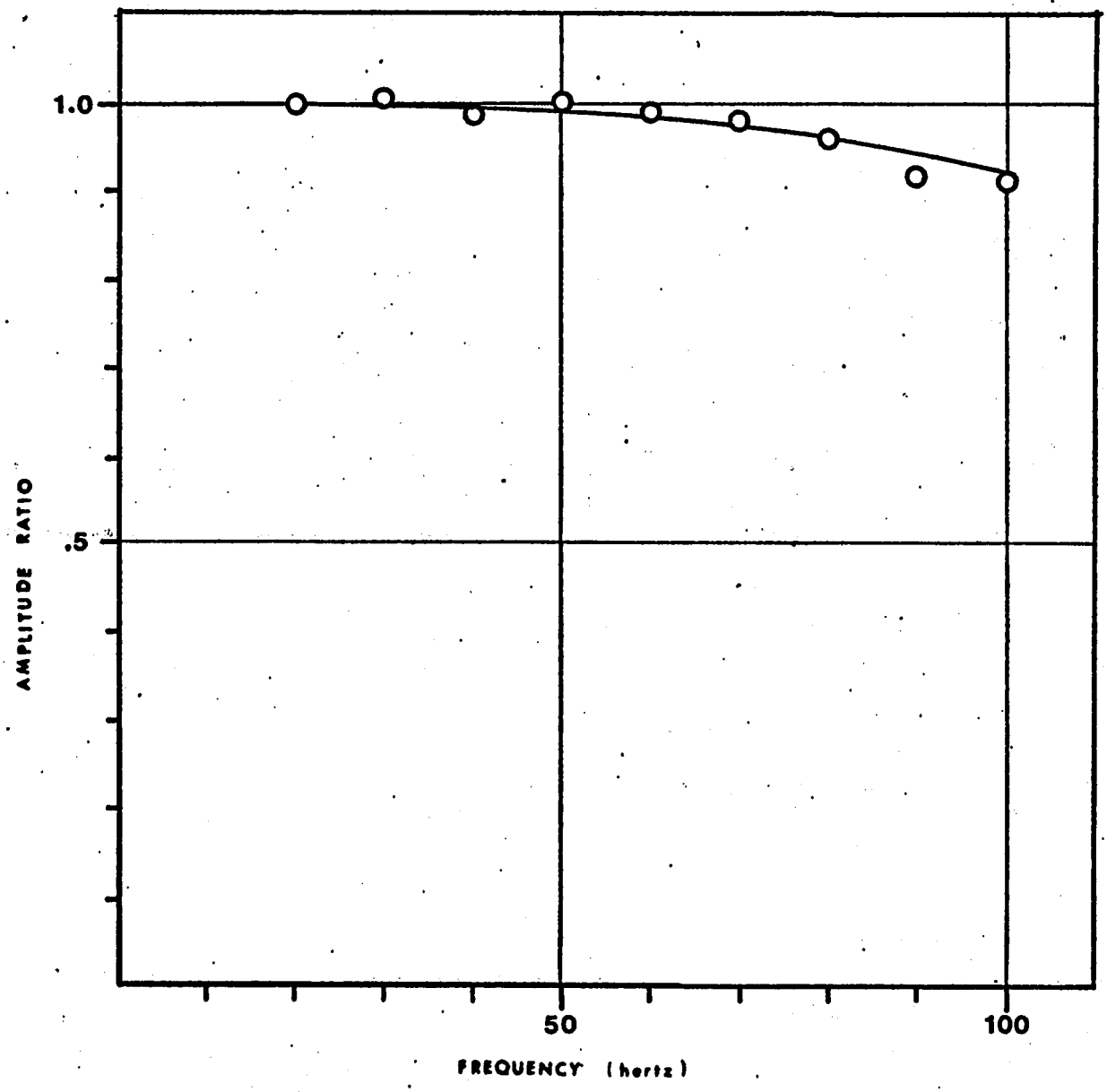

FIGURE C-5 DYNAMIC CALIBRATION OF PHASE-LOCK TRANSDUCER

and operating at 4.8 megahertz. The output from the phase track is compared with that from the LVDT, at frequencies up to 100 hertz. The response of the unit was within the range where no correction was made to the output to account for dynamic errors in terms of phase shift or attenuation.

Operation of the phase-lock transducer is highly dependent upon operating in the range of the focus of the sound beams. When the spacing is greater or less than the focus length of .400 inches the beam is difficult to lock on to an operating frequency, and the output displayed on the oscilloscope was not the stable and realitively clean signal achieved at the focused spacing. The choice of the operating frequency was determined from two sources, 1) the operating characteristics of the crystals were not adequate below 4.7 megahertz, and 2) the signal was cleaner and easier to achieve lock at 4.8 to 5.1 megahertz. Hence, 4.8 megahertz was normally chosen as an operating frequency. A check on two experiments were 4.8 megahertz was the nominal frequency showed that the average frequency was 4.805 megahertz with a standard deviation of .021 megahertz.

APPENDIX D

PROPAGATION PARAMETERS OF NONUNIFORM TUBES.

The development of a linearized relation for the reflection coefficient can be obtained from a transmission line analogy. The Fluid mass is represented by the inductance and the elasticity of the vessel wall by the capacitance. In terms of the electrical analog, the relations for momentum and continuity are:

$$-\frac{\partial E}{\partial x} = L(x)\frac{\partial I}{\partial t}$$

$$-\frac{\partial I}{\partial x} = C_p(x)\frac{\partial E}{\partial t} \qquad (1)$$

The characteristic impedance is:

$$Z(x) = \frac{L(x)}{C_p(x)} \qquad (2)$$

The nominal wave velocity is:

$$a(x) = [L(x)C_p(x)]^{-\frac{1}{2}} \qquad (3)$$

The analogies for inductance and capacitance are:

$$L(x) = \rho_f \qquad (4)$$

$$C_p(x) = \frac{1}{A}\frac{\partial A}{\partial p} \qquad (5)$$

The development of (5) inparts the vessel wall properties into the continuity equation by using a hoop stress model for the wall. The development of (5) can be used to show the origin of the Elastic Modulus Ratio used to identify the effective change in properties of a hardened section of a tube. For the uniform tube:

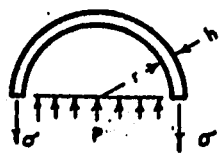

$$d\sigma = \frac{rdp}{h} \qquad (6)$$

the strain is:

$$\varepsilon = \frac{d\sigma}{E_o} = \frac{rdp}{E_o h} \tag{7}$$

In terms of a uniform displacement:

$$\varepsilon = \frac{dr}{r} \tag{8}$$

The change in area is:

$$dA = 2\pi r\, dr \tag{9}$$

Equate (7) and (9) to get the capacitance:

$$C_{p_o} = \frac{1}{A}\frac{dA}{\Delta P} = \frac{2r}{E_o h} \tag{10}$$

For an elastic modulus changing about the circumference of the tube (E= E(θ)), 7 becomes:

$$\varepsilon(\theta) = \frac{rdp}{h}\frac{1}{E(\theta)} \tag{11}$$

The change in circumference is:

$$\Delta Circ = \int_o^{2\pi} \Delta Circ = \int_o^{2\pi} \frac{rdp}{E(\theta)h}\, rd\theta \tag{12}$$

For a small change in circumference:

$$\Delta Circ = 2\pi dr \tag{13}$$

Equating (12) and (13):

$$dr = \frac{1}{2\pi}\,\frac{r^2\Delta P}{h}\int_o^{2\pi}\frac{d\theta}{E(\theta)} \tag{14}$$

From (9):

$$dA = \frac{r^3 dP}{h}\int_o^{2\pi}\frac{d\Theta}{E(\Theta)} \tag{15}$$

The expression for capacitance is:

$$C_p = \frac{r}{\pi h}\int_o^{2\pi}\frac{d\Theta}{E(\Theta)} \tag{16}$$

In terms of the original capacitance:

$$C_p = C_{p_o}\frac{E_o}{2\pi}\int_o^{2\pi}\frac{d\theta}{E(\theta)} \tag{17}$$

The expressions for wave speed are:

Uniform tube:

$$C_o = \sqrt{\frac{E_o h}{2r\rho_f}} \tag{18}$$

$$C = \frac{C_o}{\left[\frac{E_o}{2\pi}\int_o^{2\pi} \frac{d\theta}{E(\theta)}\right]^{\frac{1}{2}}} \tag{19}$$

The effect of the axial length of the hardened section will be investigated in terms of the changed impedance. The effect of the altered section will depend on the section length to pulse length ratio. From a tube shown below, the pulse amplitude will be of the corresponding form:

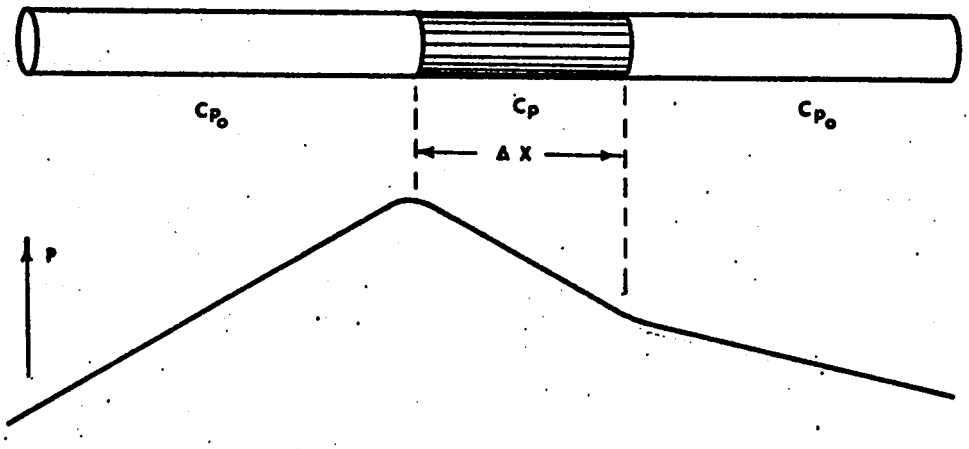

Figure D-1 Pressure versus Axial Position

The capacitance is taken to be that of the rising portion of the pulse wave. The effect of the hardened section will be determined by the wave speed of the section where the effective tube length is that which is seen from the proximal edge of the section. The capacitance will be the proportional sum of the two sections.

for

$$\frac{\Delta x}{c} < \Delta t$$

$$C_p = \frac{1}{\Delta t_r}\int_o^{\Delta tr} cp(x)\ \frac{dx}{c} = \frac{1}{\Delta t_r}\left[\int_o^{\Delta x/a_1} cp_1 \frac{dx}{c} + \int_{\Delta x/a_1}^{\Delta tr} cp_o \frac{dx}{c}\right]$$

$$= cp_1 \frac{\Delta x}{c\Delta t_r} + cp_o\left(1 - \frac{\Delta x}{c\Delta t_r}\right) \qquad (20)$$

$$\frac{\Delta x}{c} \geq \Delta t$$

$$C_p = C_{p_1} \qquad (21)$$

Inserting the values for cp_o and cp_1 and rearranging:

$$C_p = C_{p_o}\left[\left(\frac{E_o}{2\pi}\int_o^{2\pi}\frac{d\theta}{E(\theta)} - 1\right)\frac{\Delta x}{C_o\Delta t_r}\sqrt{\frac{E_o}{2\pi}\int_o^{2\pi}\frac{d\theta}{E(\theta)}} + 1\right] \qquad (22)$$

Making the following definitions:

$$E^* = \sqrt{\frac{E_o}{2\pi}\int_o^{2\pi}\frac{d\theta}{E(\theta)}} \qquad (23)$$

$$\zeta = (E^{*3} - E^*)\frac{\Delta x}{C_o\Delta t_r} \qquad (24)$$

Substitute (23) and (24) into (22):

$$C_p = C_{p_o}(1+\zeta) \qquad (25)$$

The reflection coefficient is defined:

$$C_{ref} = \frac{A_4}{A_1} = \frac{Z - Z_o}{Z + Z_o} \qquad (26)$$

Substitute (2) into (26)

$$C_{ref} = \frac{\sqrt{L/Cp} - \sqrt{L_o/Cp_o}}{\sqrt{L/Cp} + \sqrt{L_o/Cp_o}} \qquad (27)$$

Substitute (25) into (27) and note $L=L_o$:

$$C_{ref} = \frac{1-\sqrt{\zeta+1}}{1+\sqrt{\zeta+1}} \tag{28}$$

In terms of ζ we have:

$$\zeta = \left(\frac{1-C_{ref}}{1+C_{ref}}\right)^2 - 1 \tag{29}$$

Equate (24) and (29) and rearrange

$$E^{*3} - E^* + \left[1 - \left(\frac{1-C_{ref}}{1+C_{ref}}\right)^2\right] \frac{C_o \Delta t_r}{\Delta x} = 0 \tag{30}$$

Define:

$$RA = \left(\frac{1-C_{ref}}{1+C_{ref}}\right) \tag{31}$$

$$XS = \frac{C_o \Delta t_r}{\Delta x} \tag{32}$$

Substitute (31) and (32) into (30):

$$E^{*3} - E^* = (1-RA^2)\ XS = 0$$

This is a cubic equation in E*. The solution to a cube equation of this form is as follows:

For the equation:

$$y^3 + py + g = 0$$

The roots are:

$$y_1 = A+B$$

$$y_{2,3} = -\frac{A+B}{2} \pm i\frac{A-B}{2}\ 3$$

The specific values for A and B are:

$$A = \sqrt[3]{-\frac{g}{2} + \sqrt{Q}}$$

$$B = \sqrt[3]{-\frac{g}{2} + \sqrt{Q}}$$

$$Q = \left(\frac{p}{3}\right)^3 + \left(\frac{g}{2}\right)^2$$

The values from (33) are:

$$P = -1$$

$$g = (1-RA^2)XS$$

$$A = \left[\left(\frac{RA^2-1}{2}\right)XS - \sqrt{-\frac{1}{27} + \left[\left(\frac{RA^2-1}{2}\right)XS\right]^2}\ \right]^{\frac{1}{3}}$$

$$B = \left[\left(\frac{RA^2-1}{2}\right)XS - \sqrt{-\frac{1}{27} + \left[\left(\frac{RA^2-1}{2}\right)XS\right]^2}\ \right]^{\frac{1}{3}}$$

The solution for (33) is:

$$E^* = \left[\left(\frac{RA^2-1}{2}\right)XS + \sqrt{\frac{1}{27} + \left[\left(\frac{RA^2-1}{2}\right)XS\right]^2}\ \right]^{\frac{1}{3}} + \left[\left(\frac{RA^2-1}{2}\right)XS - \sqrt{-\frac{1}{27}\left[\left(\frac{RA^2-1}{2}\right)XS\right]^2}\ \right]^{\frac{1}{3}} \qquad (34)$$

After replacing the respective values we arrive at an expression for evaluating the Elastic Modulus Ratio from experimentally determined values.

$$\frac{E_o}{2\pi}\int_o^{2\pi}\frac{d\theta}{E(\theta)} = \left\{\left[\left(\frac{\left(\frac{1-C_{ref}}{1+C_{ref}}\right)^2-1}{2}\right)\frac{C_o\Delta t_r}{\Delta x} + \sqrt{\left[\left(\frac{\left(\frac{1-C_{ref}}{1+C_{ref}}\right)^2-1}{2}\right)\frac{C_o\Delta t_r}{\Delta x}\right]^2 - \frac{1}{27}}\ \right]^{\frac{1}{3}} + \left[\left(\frac{\left(\frac{1-C_{ref}}{1+C_{ref}}\right)^2-1}{2}\right)\frac{C_o\Delta t_r}{\Delta x} - \sqrt{\left[\left(\frac{\left(\frac{1-C_{ref}}{1+C_{ref}}\right)^2-1}{2}\right)\frac{C_o\Delta t_r}{\Delta x}\right]^2 - \frac{1}{27}}\ \right]^{\frac{1}{3}}\right\}^2 \qquad (35)$$

APPENDIX E

MECHANICAL PROPERTIES OF RUBBER TUBES

The dynamic mechanical properties of the rubber used in fabricating the tubes was determined to be a critical aspect of the interpretation of the results. A carefully conducted experimental technique was performed utilizing the equipment designed and assembled by Dr. C. Daly, Dr. J. D. Chalupnik, and Mr. James Danberg. Rubber, a long chain polymer exhibits viscoelastic behavior at the loading rates imposed in the experiment of which the viscous element contributes 5 to 10% of the total absolute value of the effective modulus.

The determination of the mechanical response of rubber has been explained with the use of Gaussian statistics on the polymer matrix. This has resulted in a formulation of the mechanical response with only one independent constant in addition to assuming rubber to be incompressible. The single constant representation has only been adequate for small deformations. In order to explain the mechanical behavior of rubber experiencing extension ratios greater than 125% up to as much as 600% it has been necessary to use a phenomonological approach which involves a power series expansion of the response function. The Mooney

formulation depicting the response of rubber is dependent on two independent constants and has been shown to be adequate for the description of moderate to large deformations. However, the strains encountered in this study were less than .02 with the result being that the single constant representation was adequate.

The dynamic behavior of rubber has been described by many various combinations of springs and dashpots, the Maxwell and the Voigt models being the most commonly used forms. These have been extended to combinations of these elements, and further to the representations utilizing distribution functions for relaxation times. At the present time this amounts to a convenient means of representing experimental data, having little relation to the network behavior of the deformation. The commonly used representation of rubber is the Voigt model incorporating a dynamic modulus of the form:

$$G^* = G_1 + iG_2$$

The experimental determination of the dynamic elastic has utilized the Voigt model as a representation of the response of the rubber. The samples which were evaluated were cut to the same form and mounted in the visture as shown in Figure E-1. The lower fixture attached to the load cell and the upper fisture attached to an electromagnetic shaker which was used to generate the dynamic

load. An optical tracker was used to monitor the motion of the upper fixture by following a target on the armature of electromagnetic shaker. The output from the load cell was displayed on the vertical trace of a dual sweep oscilloscope and the output from the optical tracker was displayed on the horizontal axis of the oscilloscope.

The data was taken with a cyclic loading of the rubber at 25 Hertz. This was selected as the comparable frequency to the 10 millisecond rise time experienced in the single pulses which propagated along the fluid-filled tubes of the experimental portion of the study. The results which are presented in Figure E-2 use the magnitude of the modulus at the loading rate to produce the effective elastic modulus for the material at the rate of loading used in the experimental portion of the study. Figure E-2 shows the effective modulus that was experimentally determined from this procedure.

The experimental equipment was not capable of experimentally accurately resolving the viscous component of the modulus for the 20 durometer rubbers. This quantity was obtained from extrapolated data from Payne and Scott(107) upon a suggestion made by Klip in his Thesis(70).

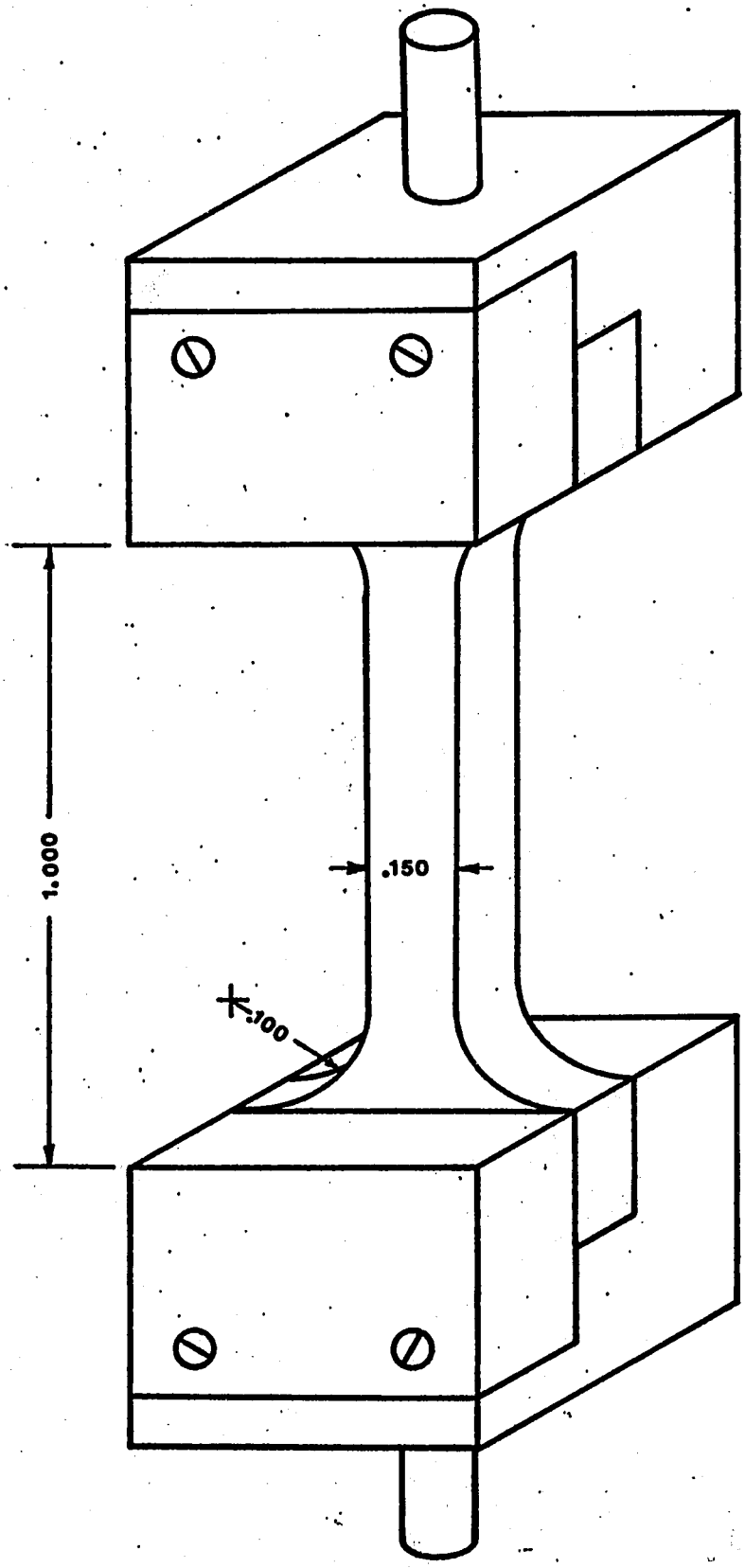

FIGURE E-1 RUBBER SPECIMEN TEST FIXTURE

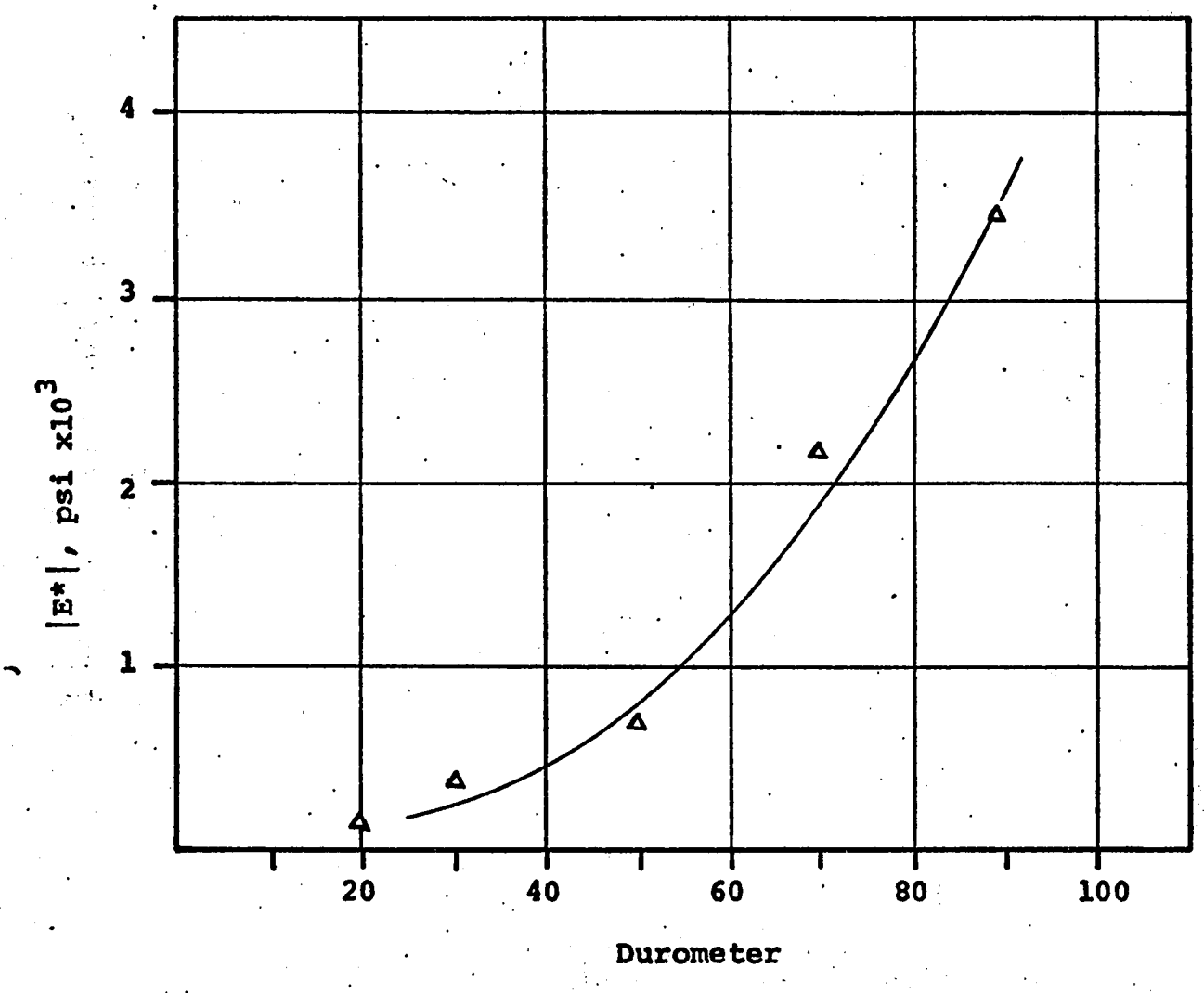

FIGURE E-2 MAGNITUDE OF ELASTIC MODULUS FOR RUBBER

APPENDIX F

REDUCED EXPERIMENTAL DATA

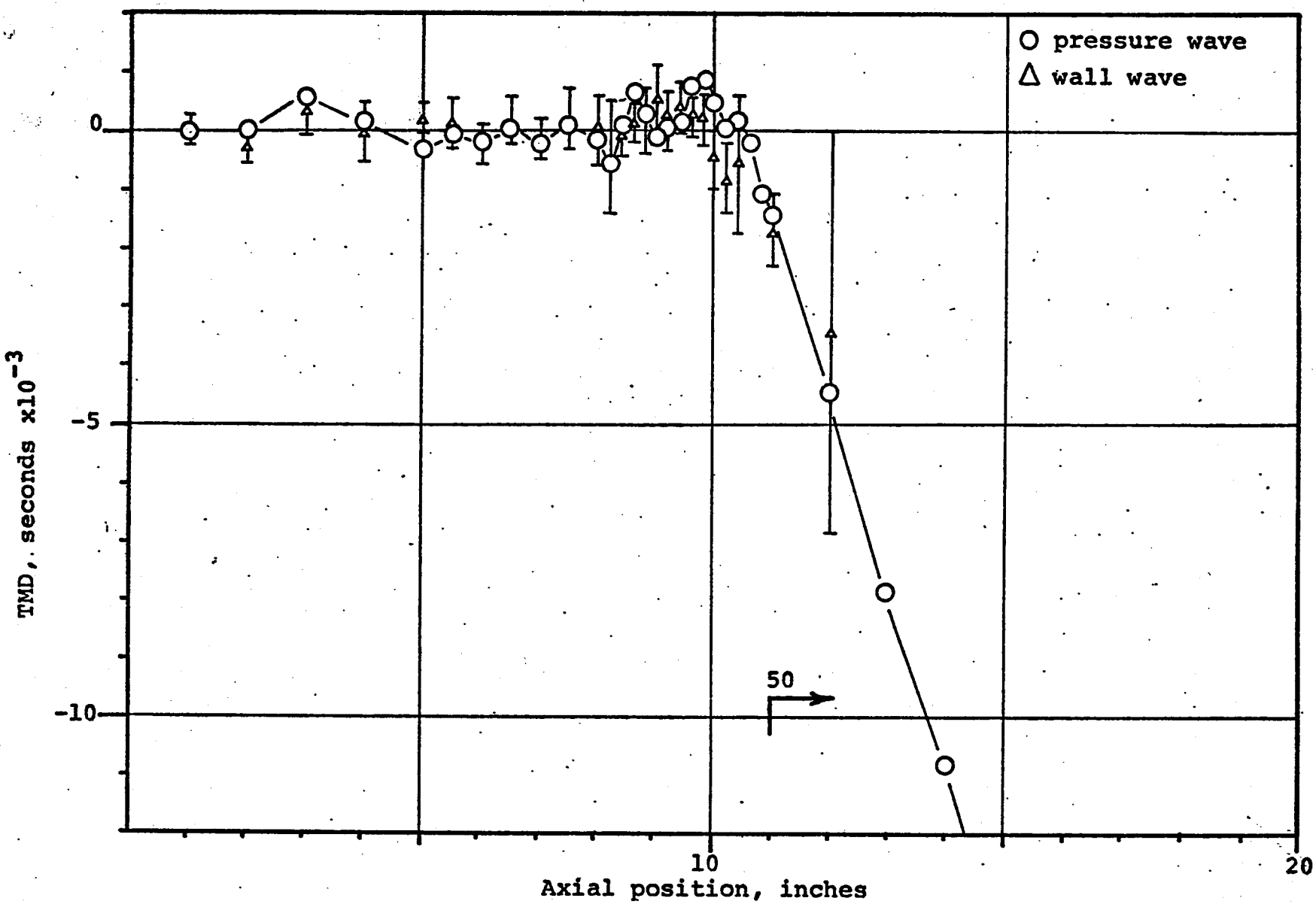

FIGURE F-1 TMD VERSUS AXIAL POSITION FOR SINGLE INTERFACE 20-50 TUBE. DATA INDICATES MEAN VALUE AND ONE STANDARD DEVIATION FOR WALL WAVE.

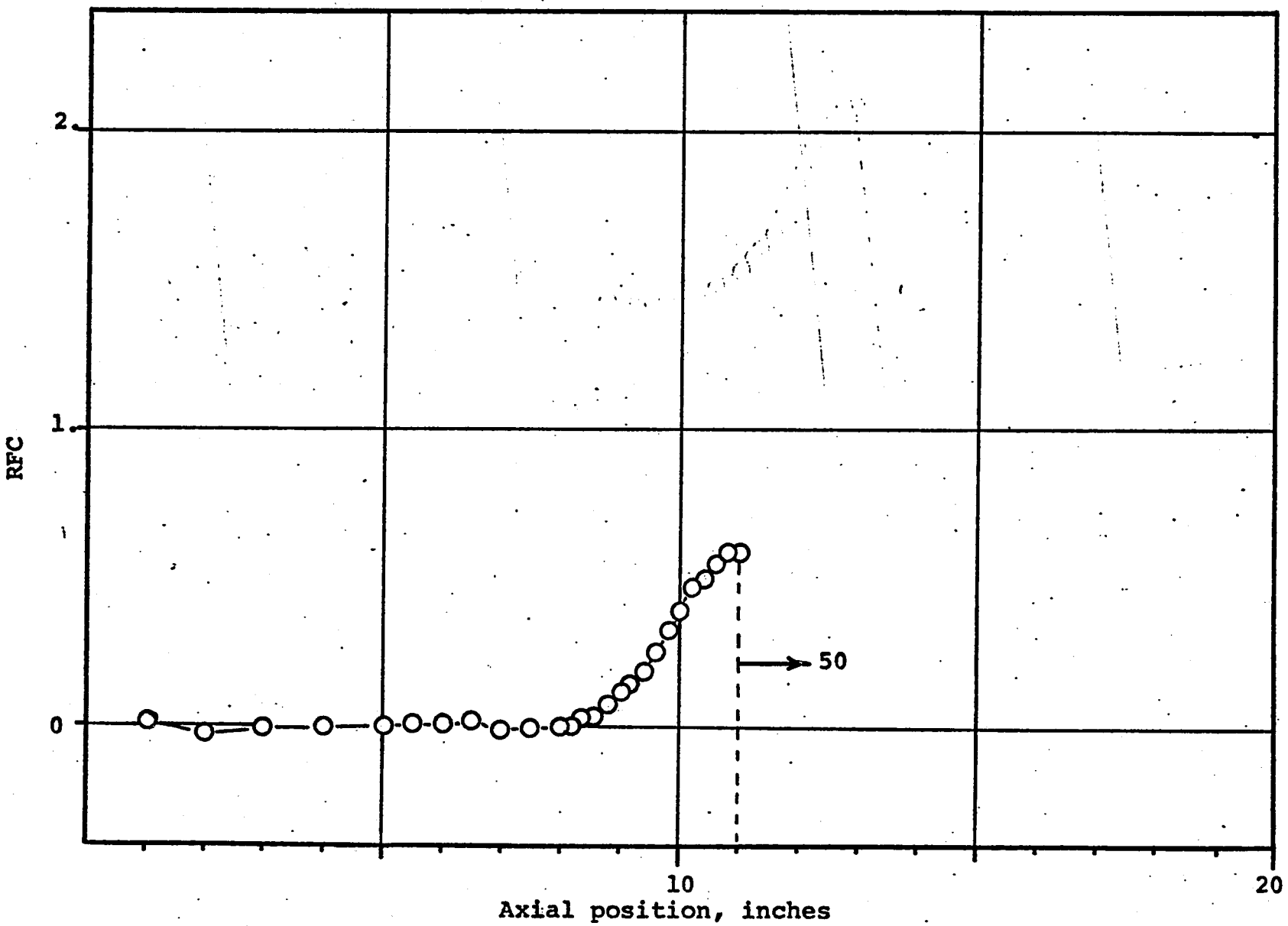

FIGURE F-2 RFC VERSUS AXIAL POSITION FOR SINGLE INTERFACE 20-50 TUBE.

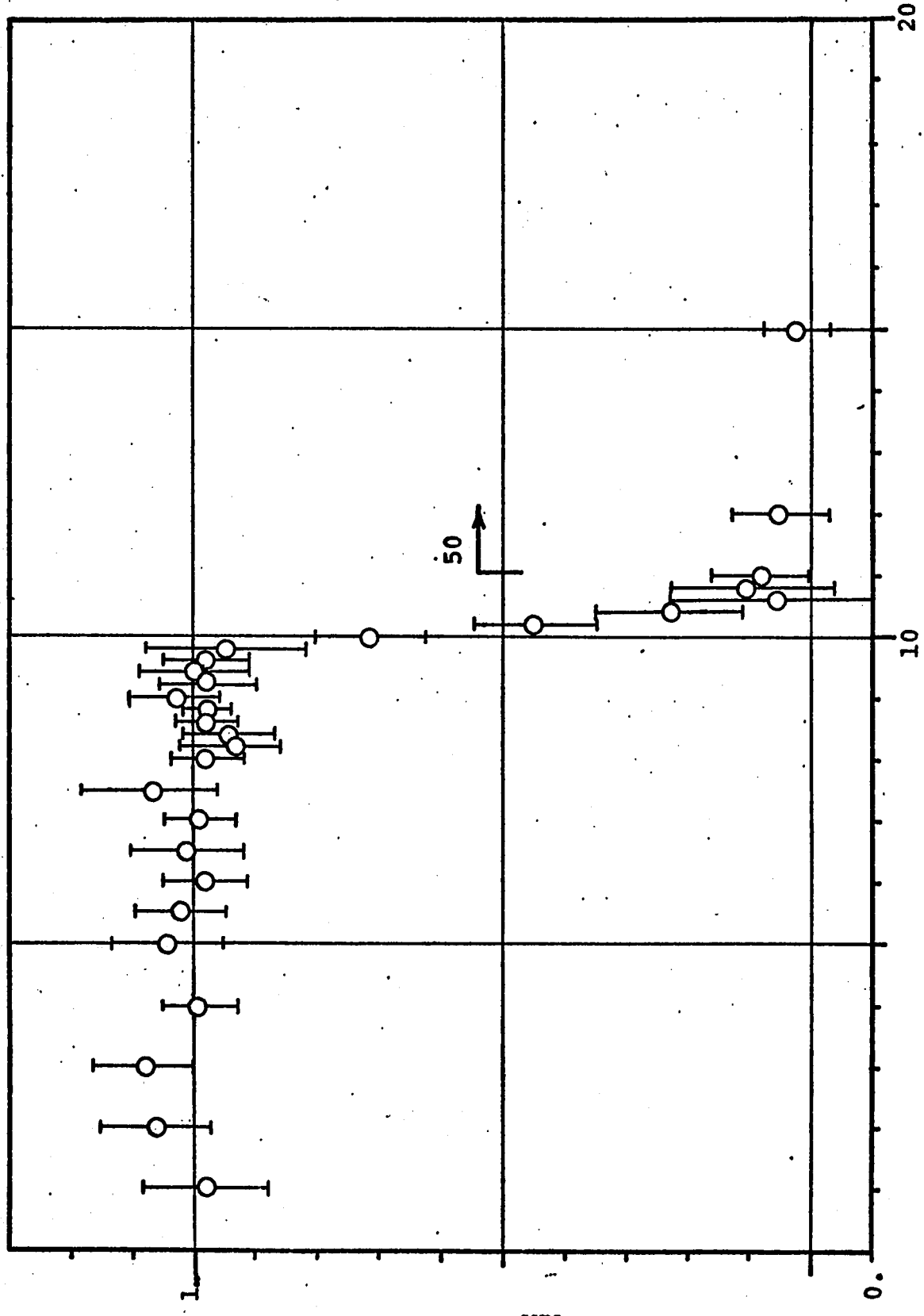

FIGURE F-3 RHP VERSUS AXIAL POSITION FOR SINGLE INTERFACE 20-50 TUBE. DATA INDICATES MEAN VALUES AND ONE STANDARD DEVIATION.

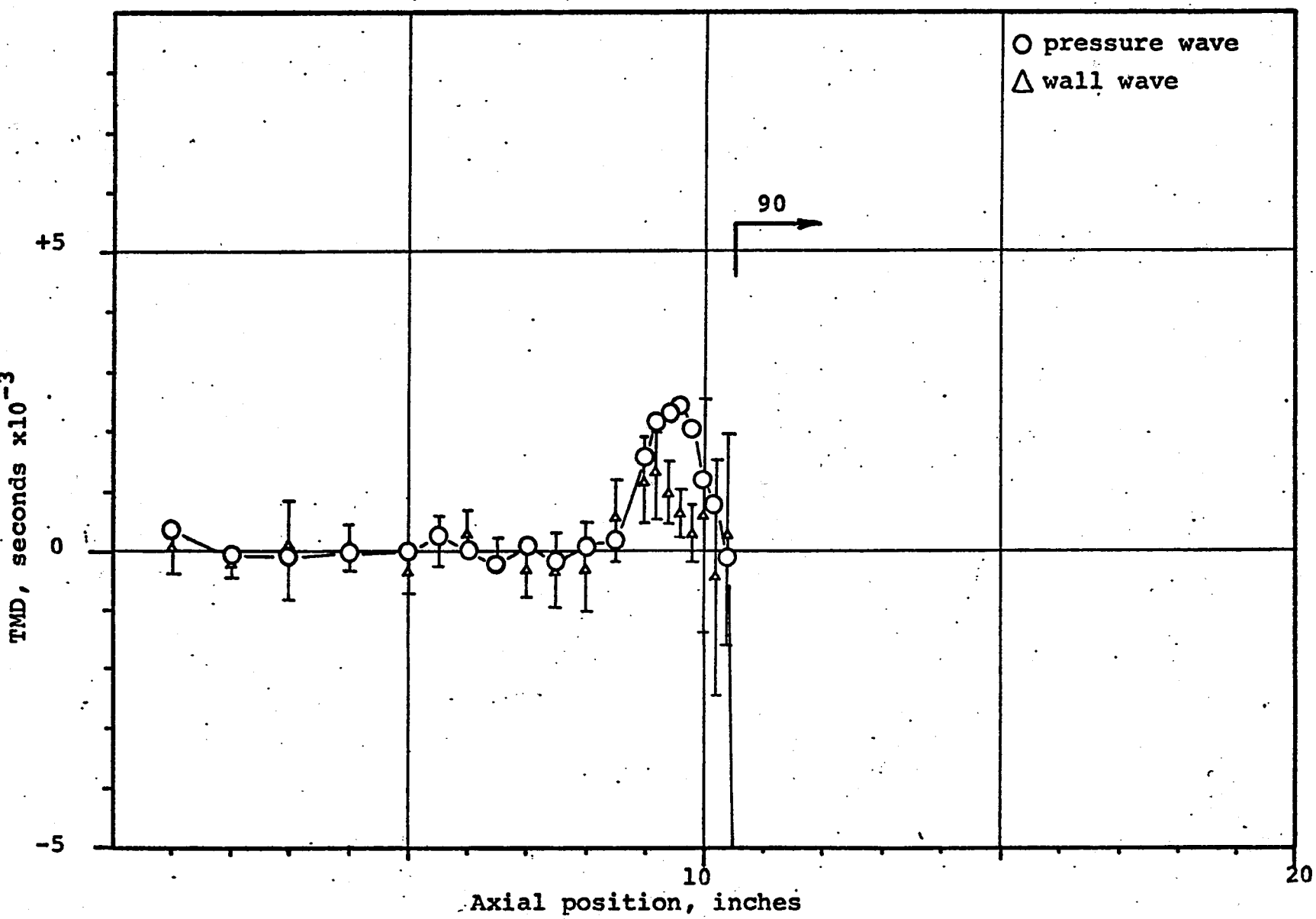

FIGURE F-4 TMD VERSUS AXIAL POSITION FOR SINGLE INTERFACE 20-90 TUBE. DATA INDICATES MEAN VALUE AND ONE STANDARD DEVIATION FOR WALL WAVE.

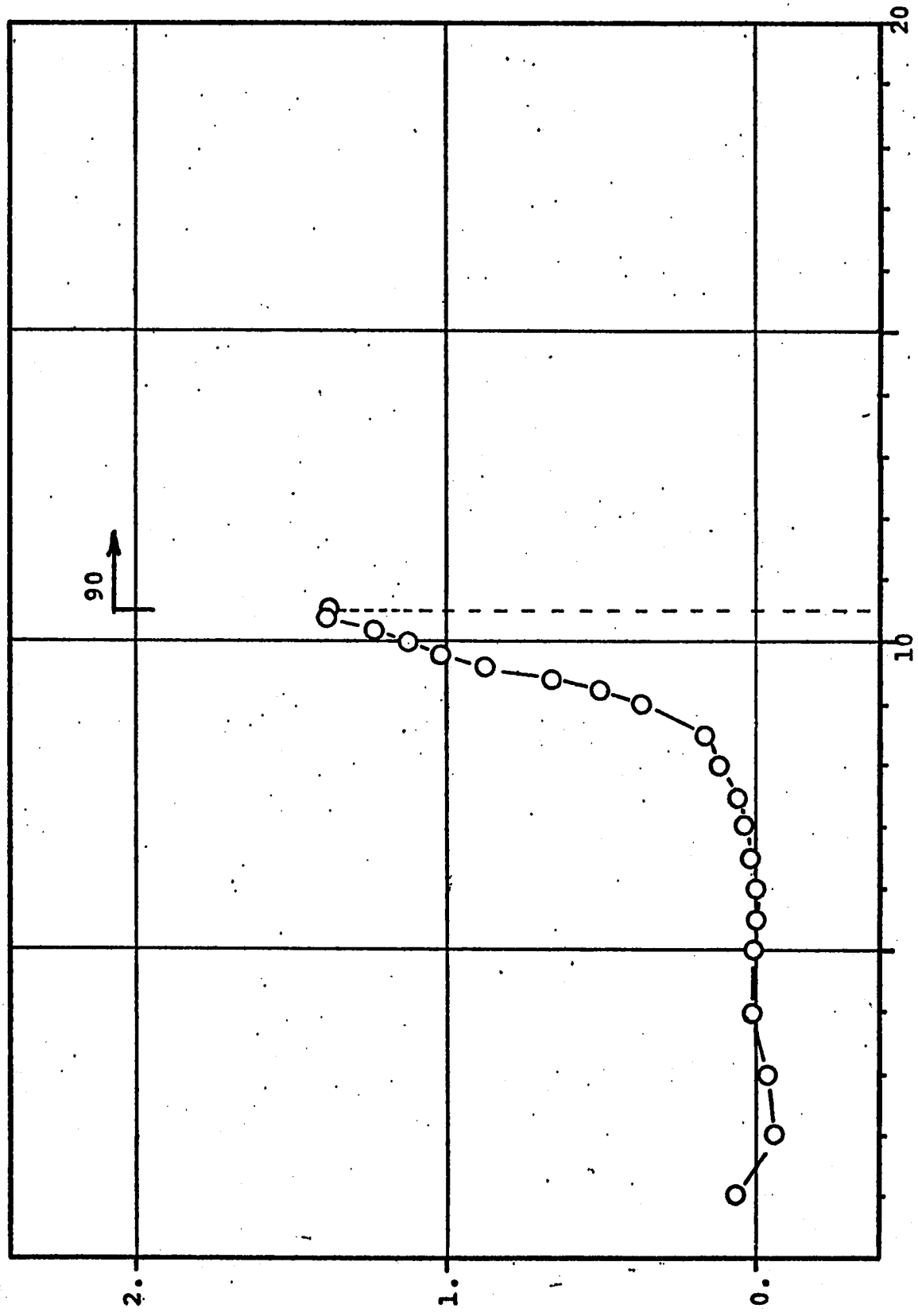

FIGURE F-5 RFC VERSUS AXIAL POSITION FOR SINGLE INTERFACE 20-90 TUBE

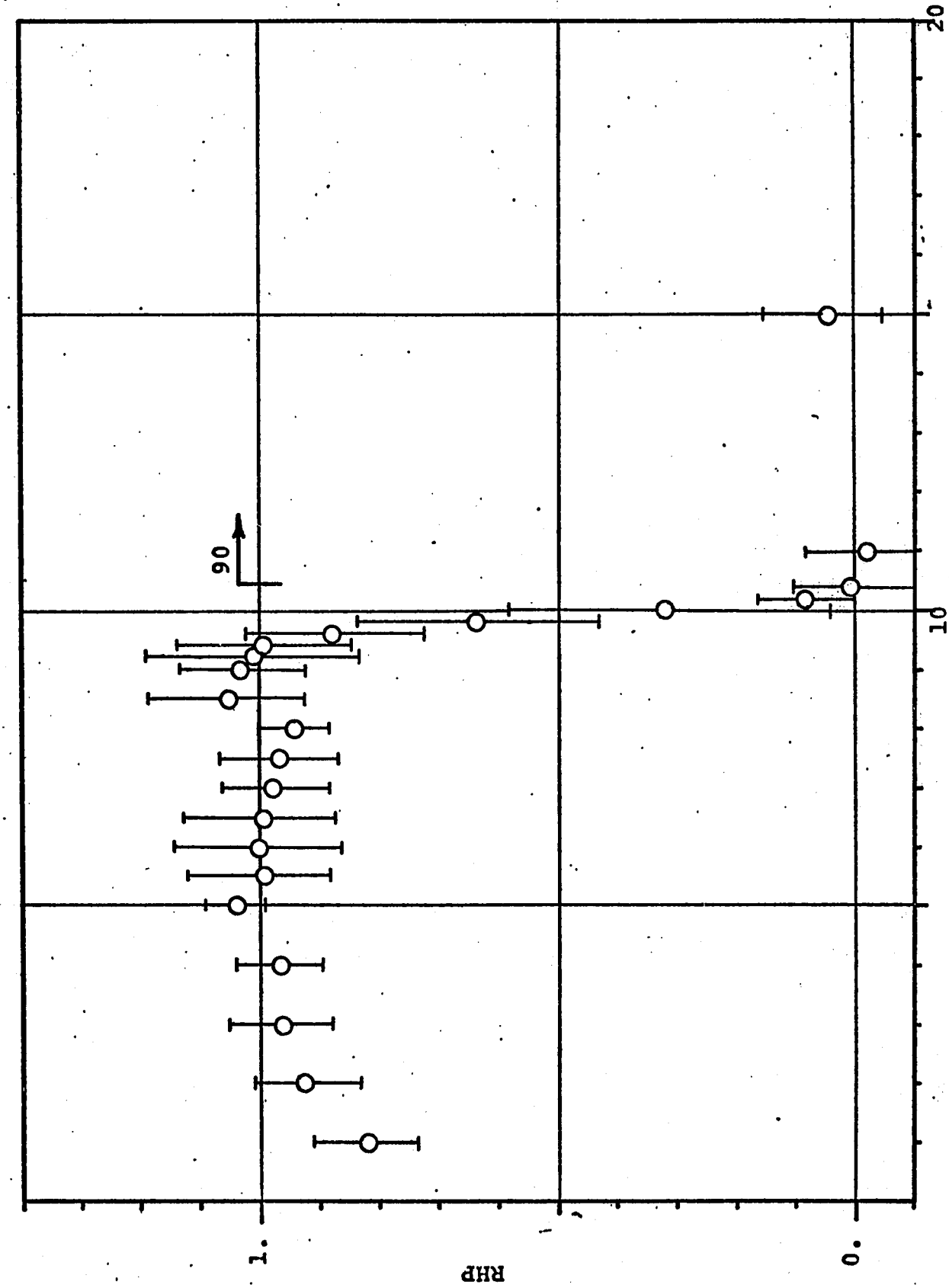

FIGURE F-6 RHP VERSUS AXIAL POSITION FOR SINGLE INTERFACE 20-90 TUBE. DATA INDICATES MEAN VALUE AND ONE STANDARD DEVIATION.

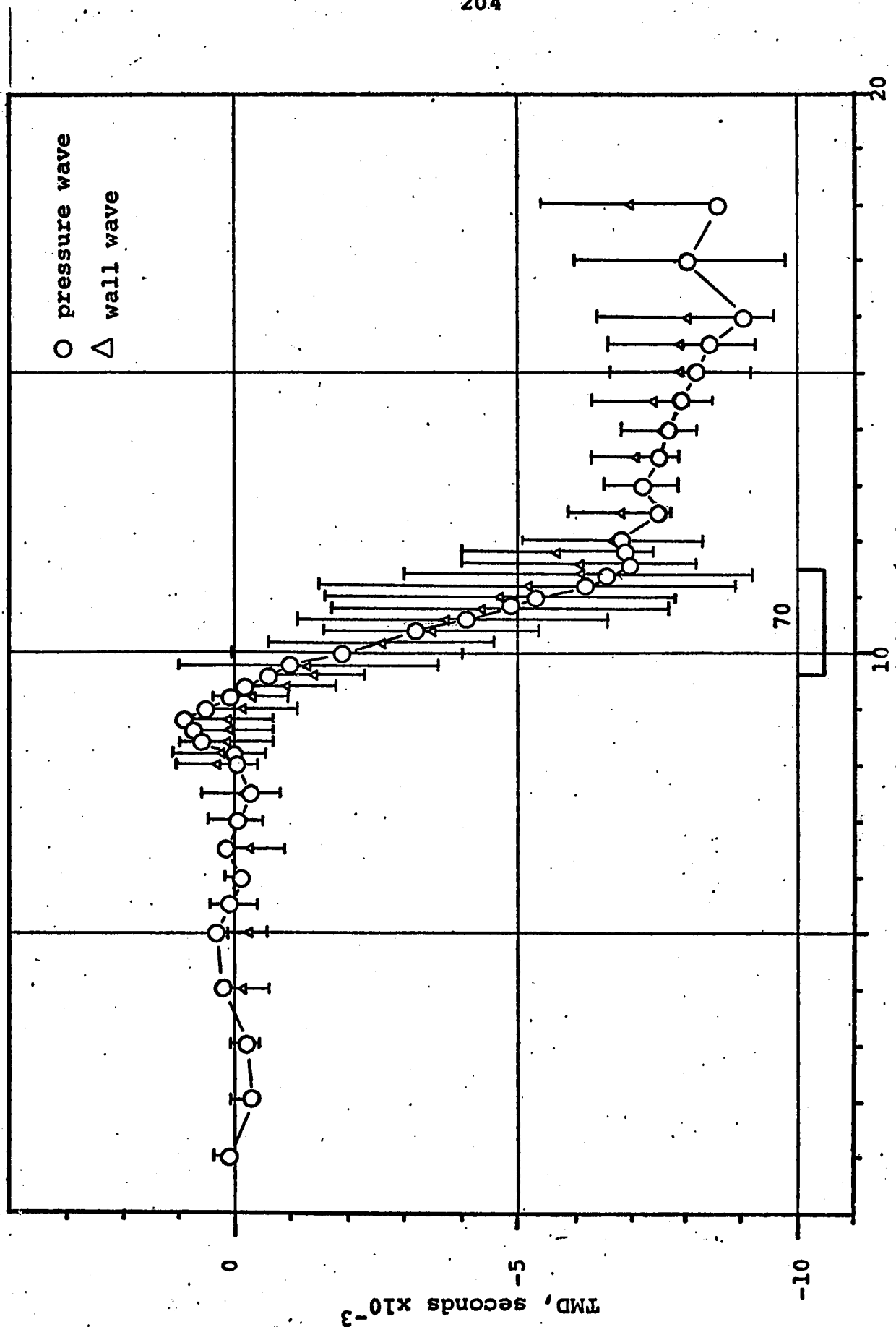

FIGURE F-7 TMD VERSUS AXIAL POSITION FOR 70 DUROMETER AXISYMMETRIC FINITE-LENGTH SECTION. DATA INDICATES MEAN VALUE AND ONE STANDARD DEVIATION FOR WALL WAVE.

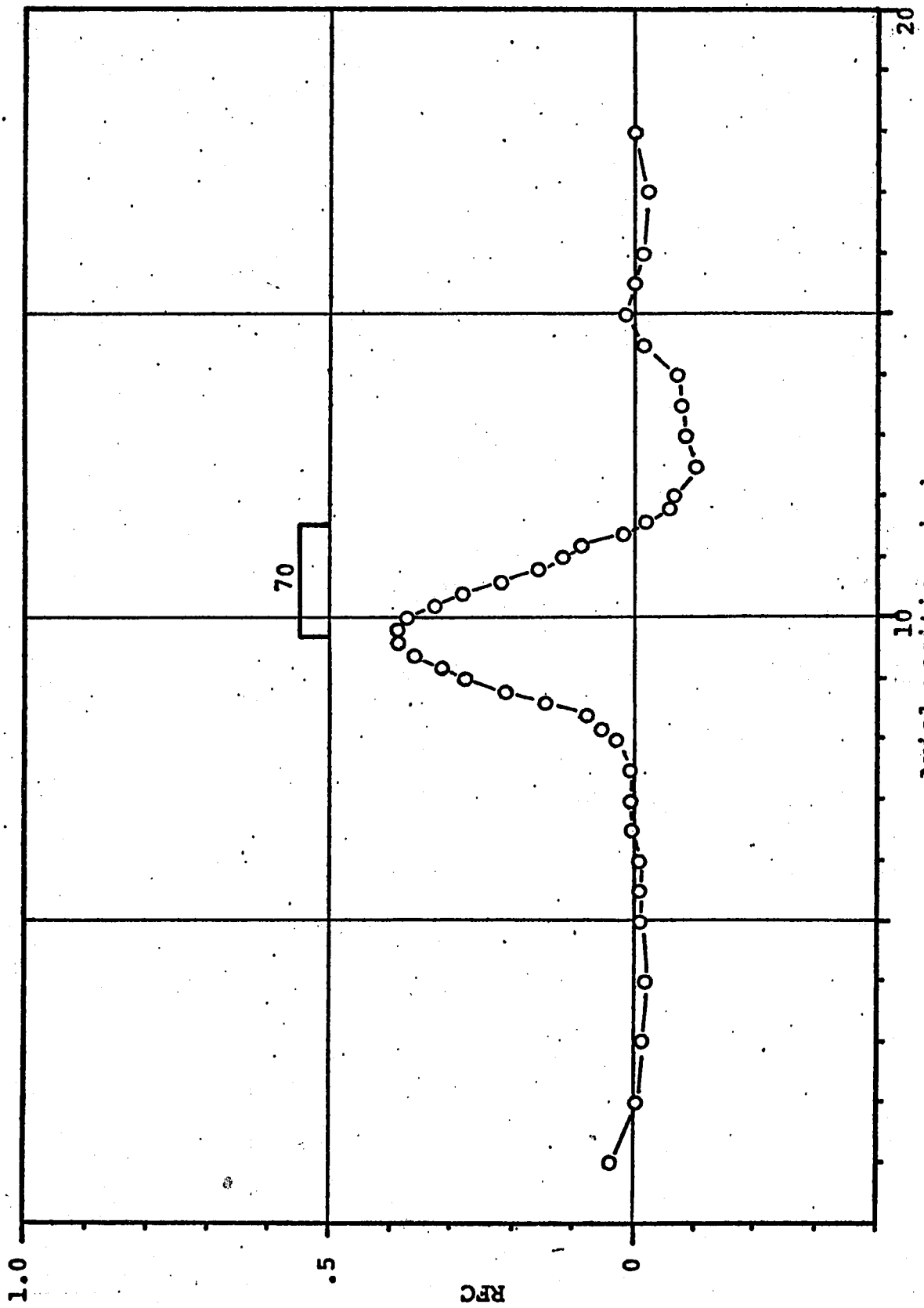

FIGURE F-8 RFC VERSUS AXIAL POSITION FOR 70 DUROMETER AXISYMMETRIC FINITE-LENGTH SECTION

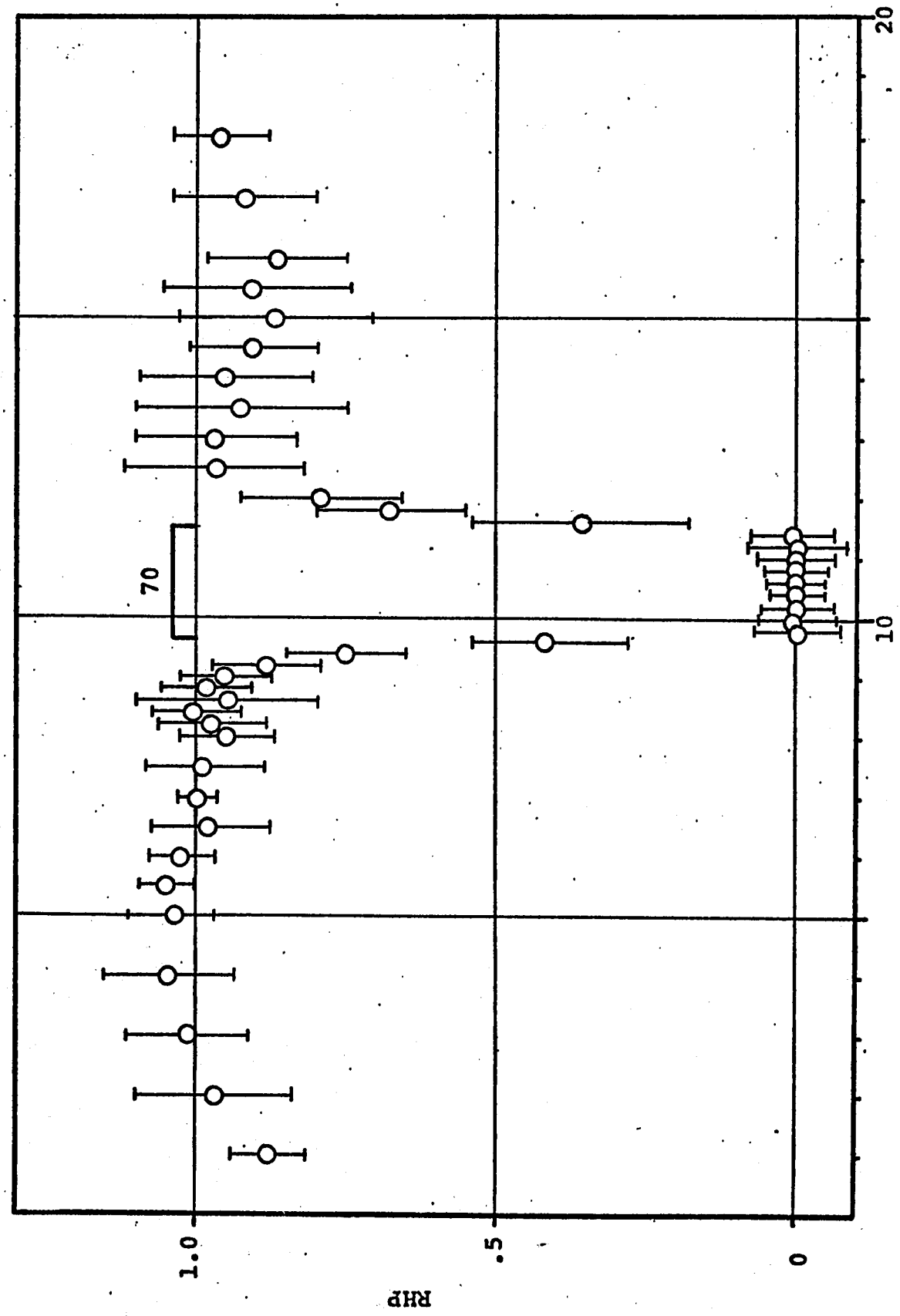

FIGURE F-9 RHP VERSUS AXIAL POSITION FOR 70 DUROMETER FINITE-LENGTH AXISYMMETRIC SEGMENT. DATA INDICATES MEAN VALUE AND ONE STANDARD DEVIATION

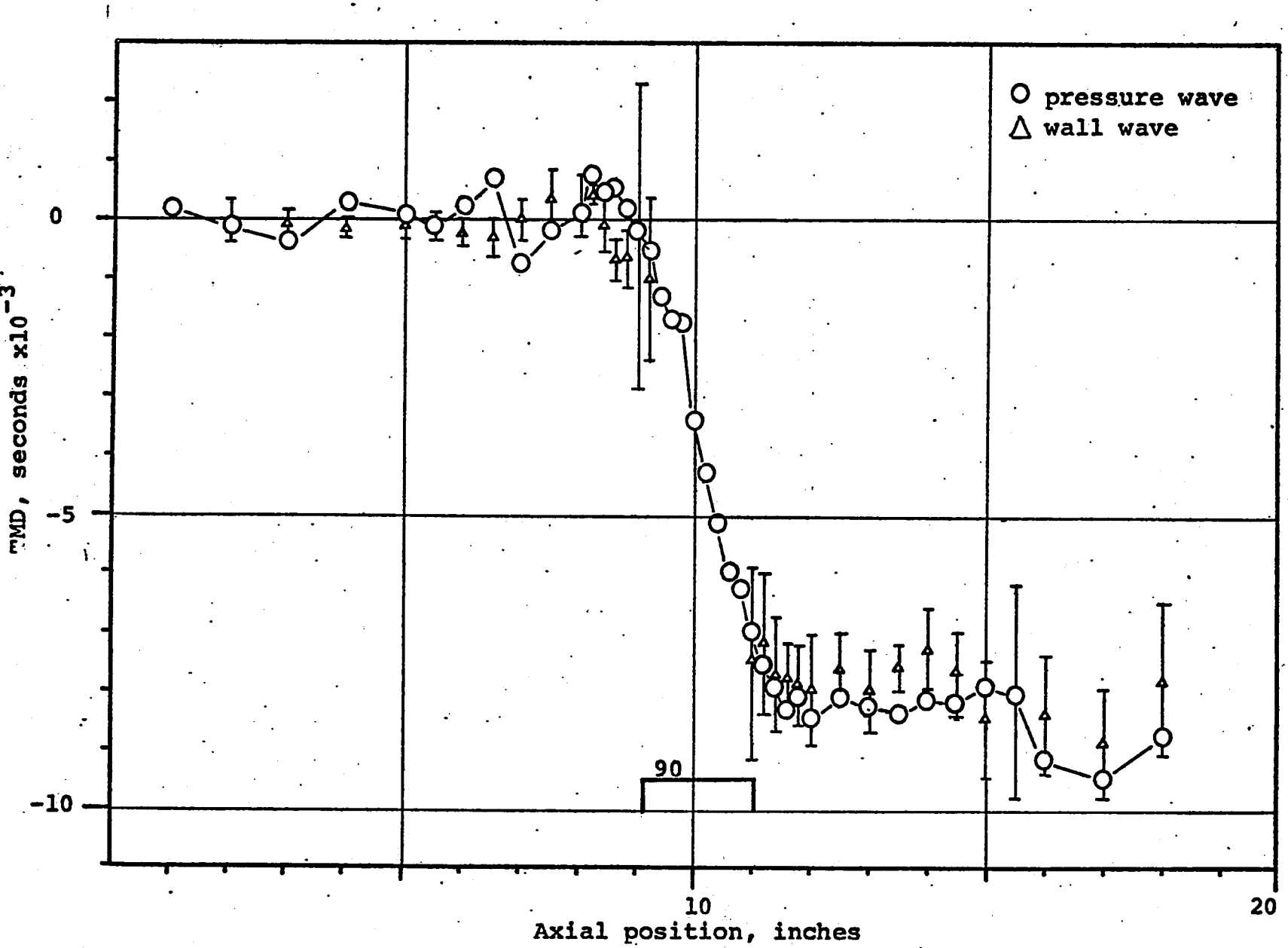

FIGURE F-10 TMD VERSUS AXIAL POSITION FOR 90 DUROMETER AXISYMMETRIC FINITE-LENGTH SECTION. DATA INDICATES MEAN VALUE AND ONE STANDARD DEVIATION FOR WALL WAVE

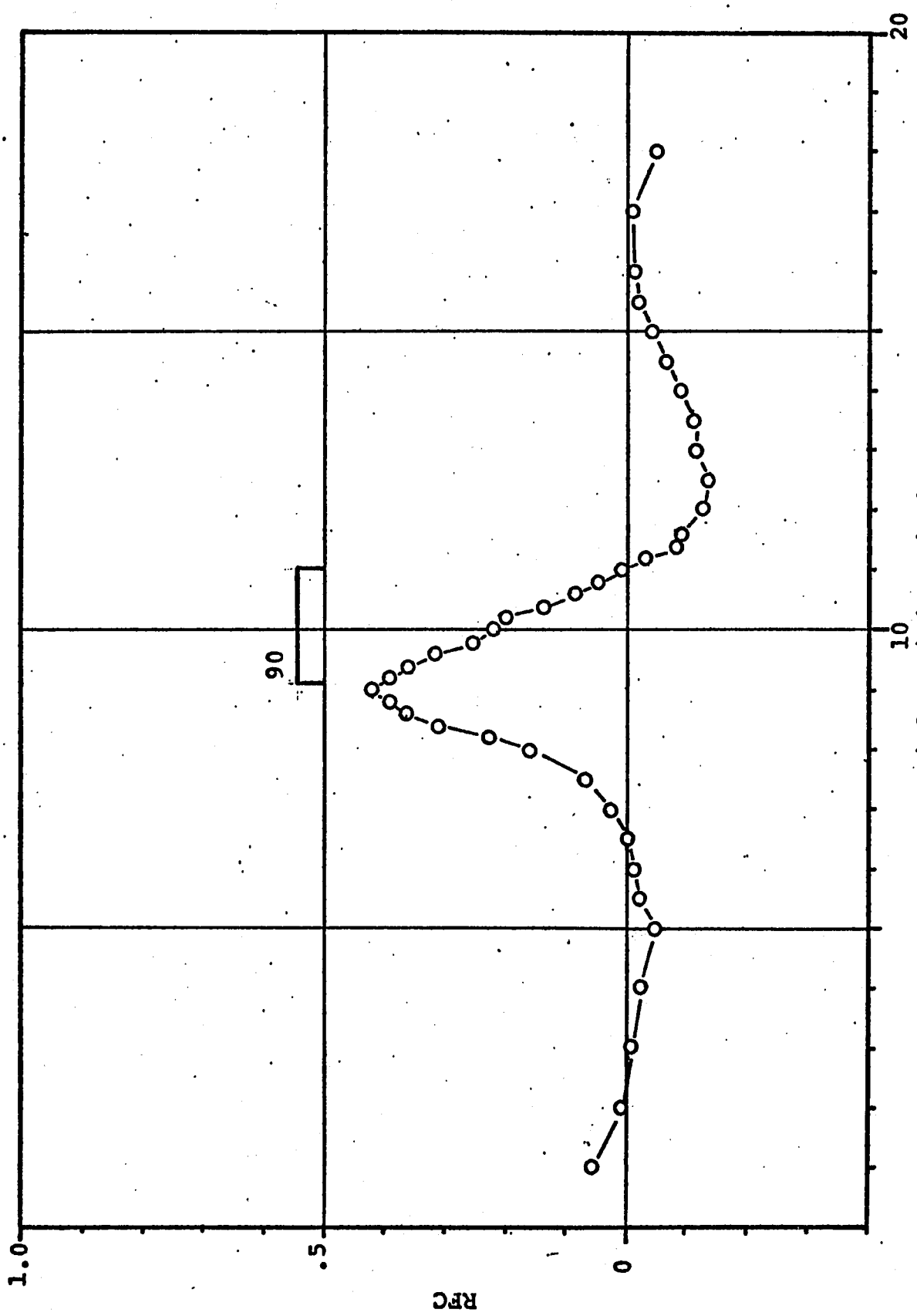

FIGURE F-11 TMD VERSUS AXIAL POSITION FOR 90 DUROMETER AXISYMMETRIC FINITE-LENGTH SECTION

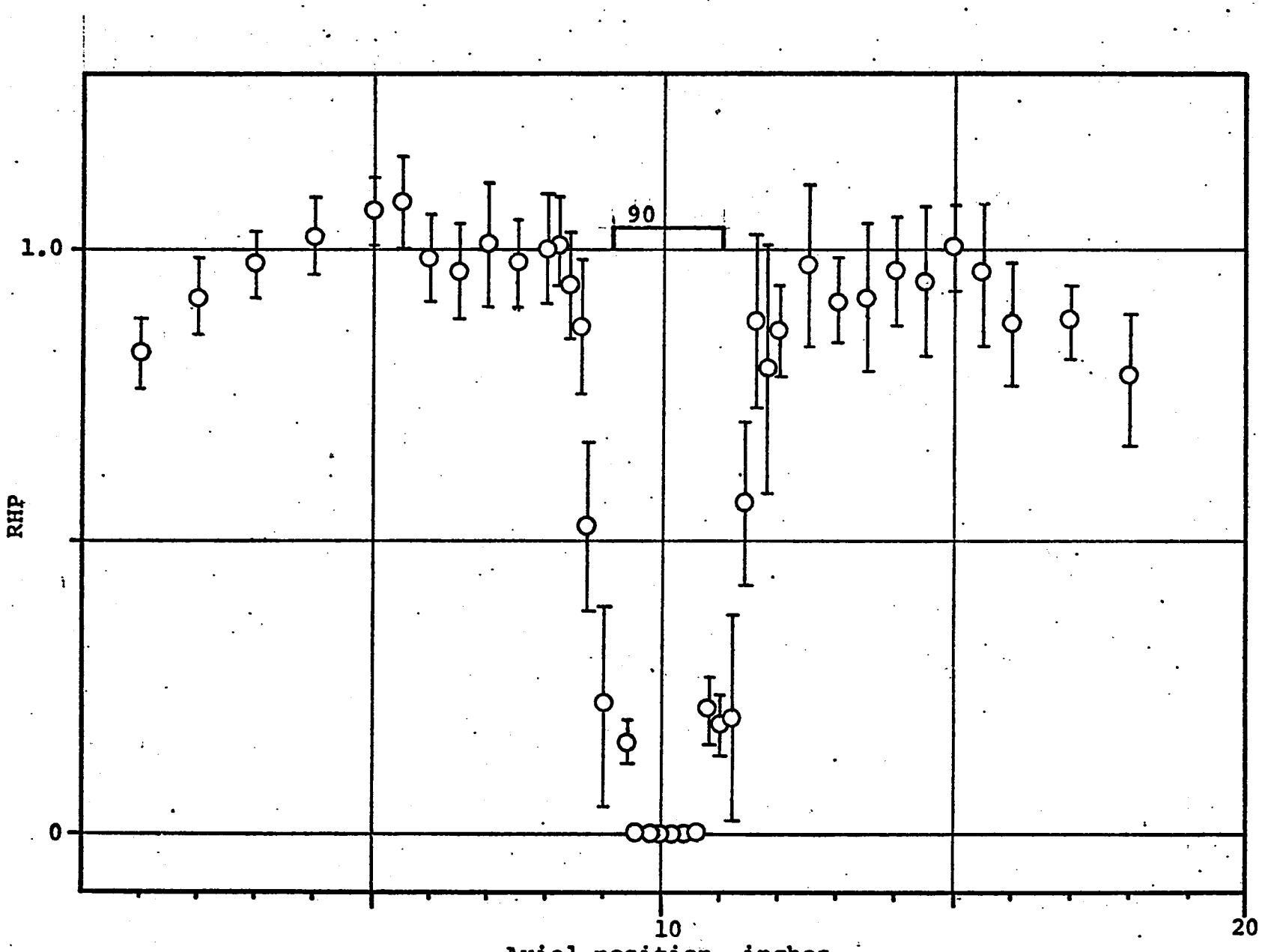

FIGURE F-12 RHP VERSUS AXIAL POSITION FOR 90 DUROMETER AXISYMMETRIC FINITE-LENGTH SECTION. DATA INDICATES MEAN VALUE AND ONE STANDARD DEVIATION

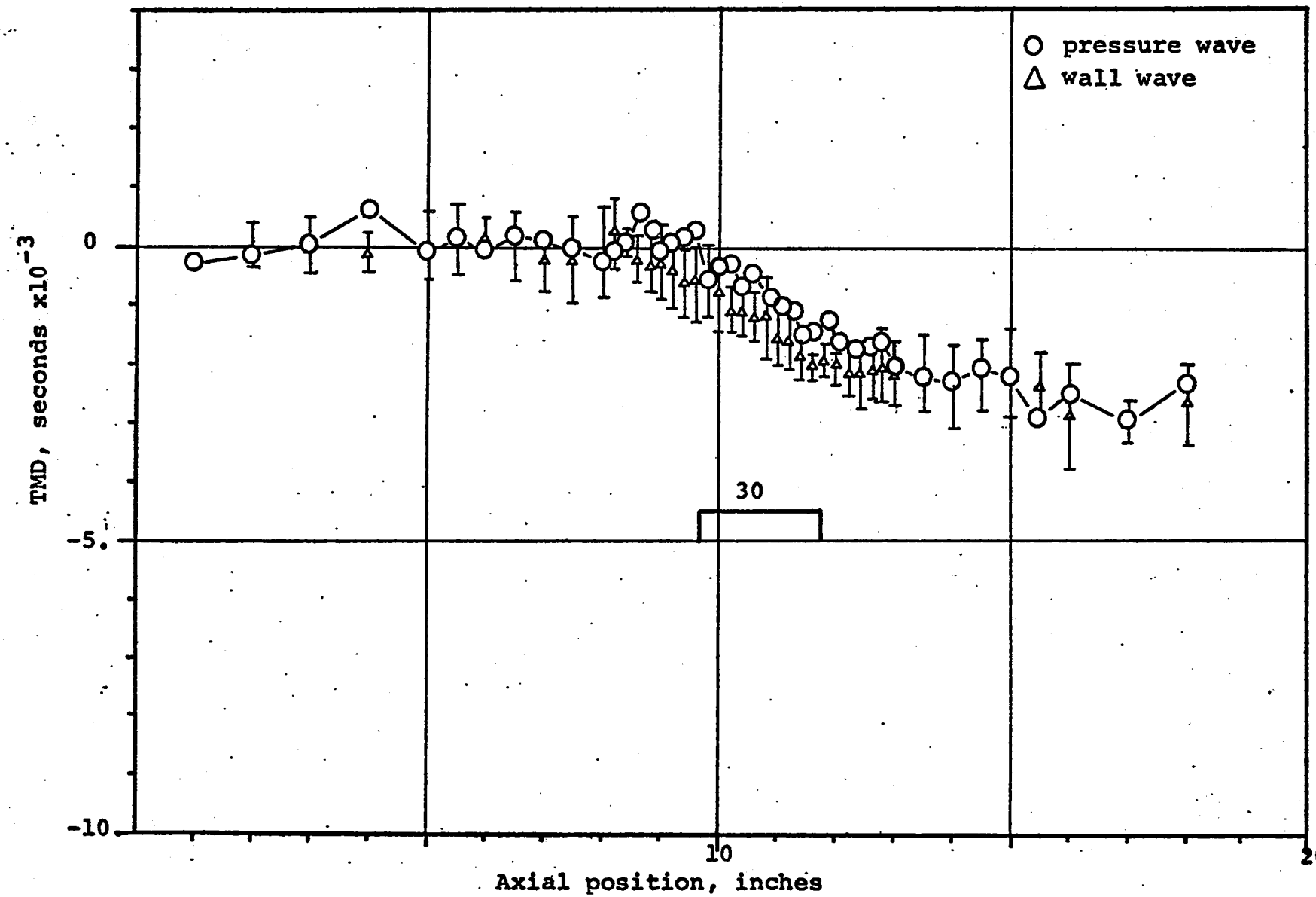

FIGURE F-13 TMD VERSUS AXIAL POSITION FOR 30 DUROMETER 120° SECTION. DATA INDICATES MEAN VALUE AND ONE STANDARD DEVIATION FOR WALL WAVE.

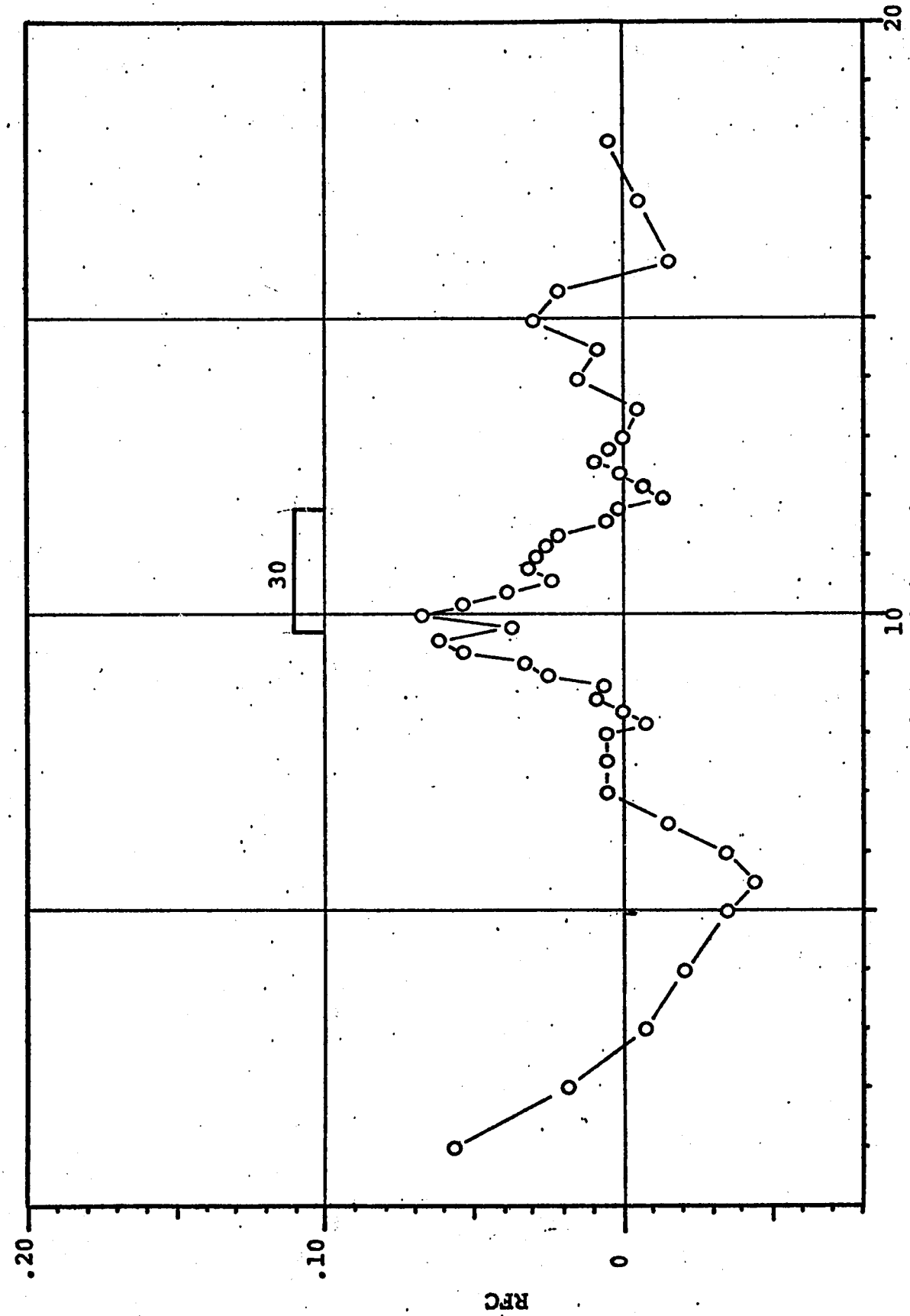

FIGURE F-14 RFC VERSUS AXIAL POSITION FOR 30 DUROMETER 120° SECTION

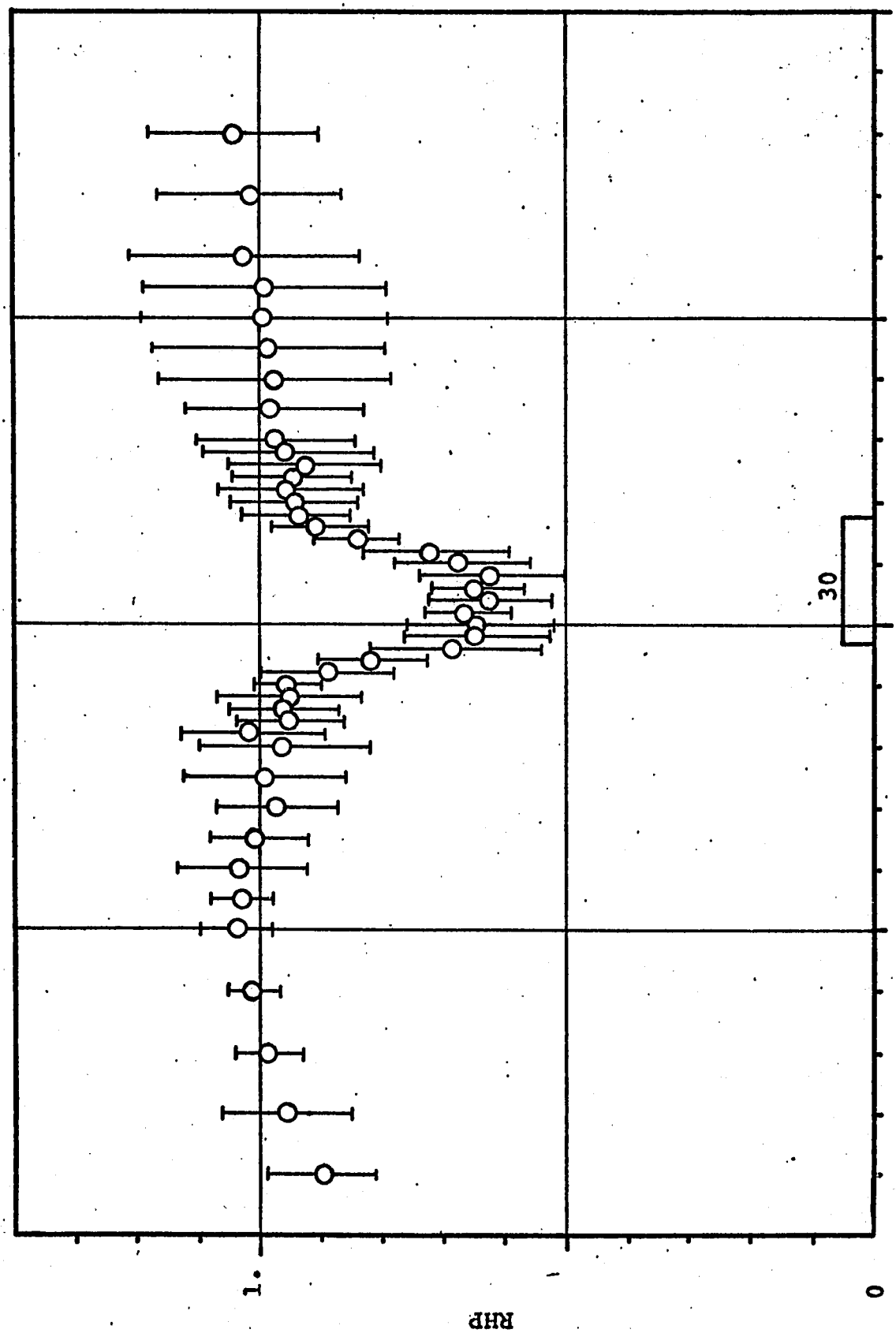

FIGURE F-15 RHP VERSUS AXIAL POSITION FOR 30 DUROMETER, 120° SECTION. DATA INDICATES MEAN VALUE AND ONE STANDARD DEVIATION

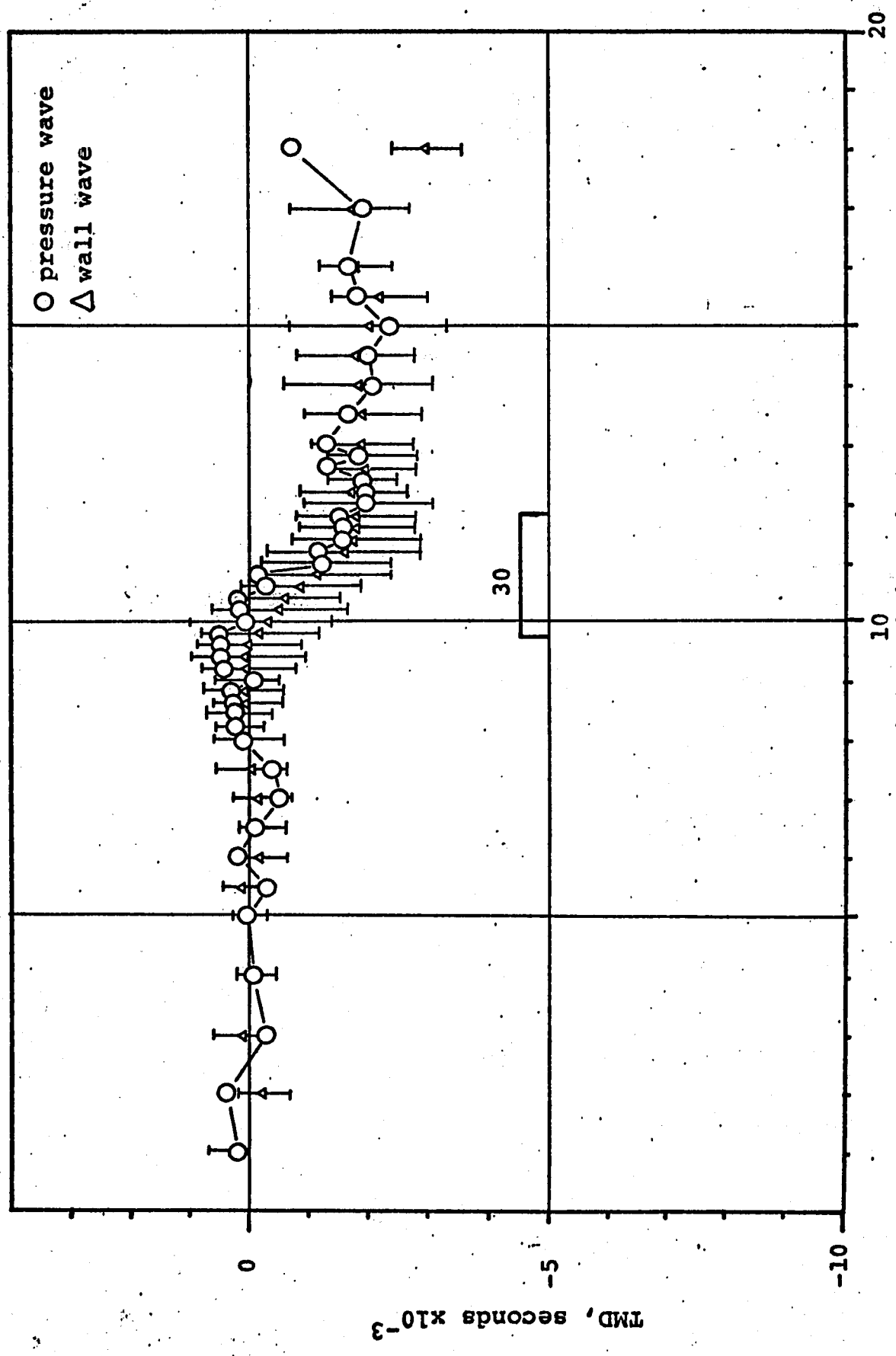

FIGURE F-16 TMD VERSUS AXIAL POSITION FOR 30 DUROMETER 180° SECTION. DATA INDICATES MEAN VALUE AND ONE STANDARD DEVIATION FOR WALL WAVE.

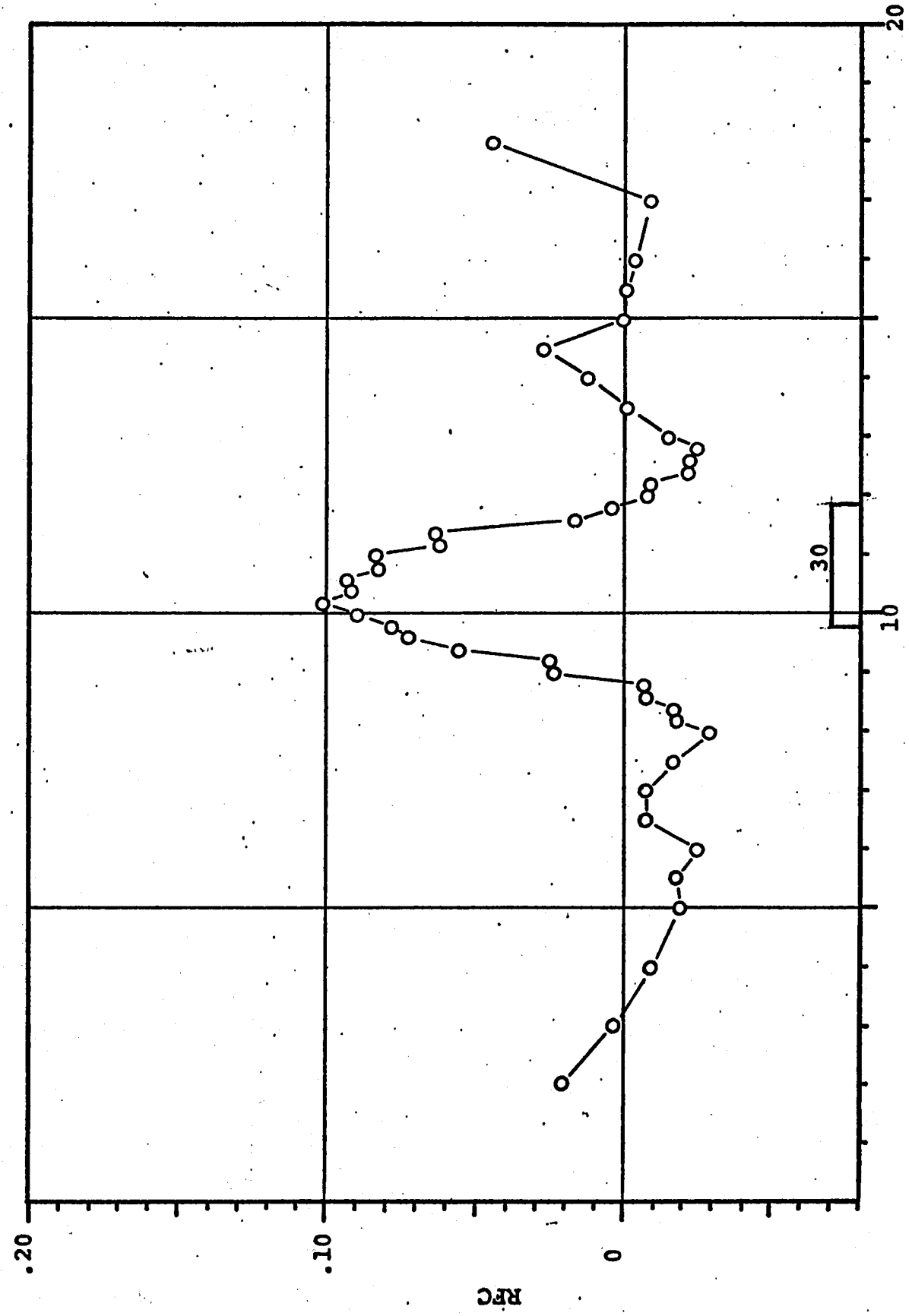

FIGURE F-17 RFC VERSUS AXIAL POSITION FOR 30 DUROMETER 180° SECTION

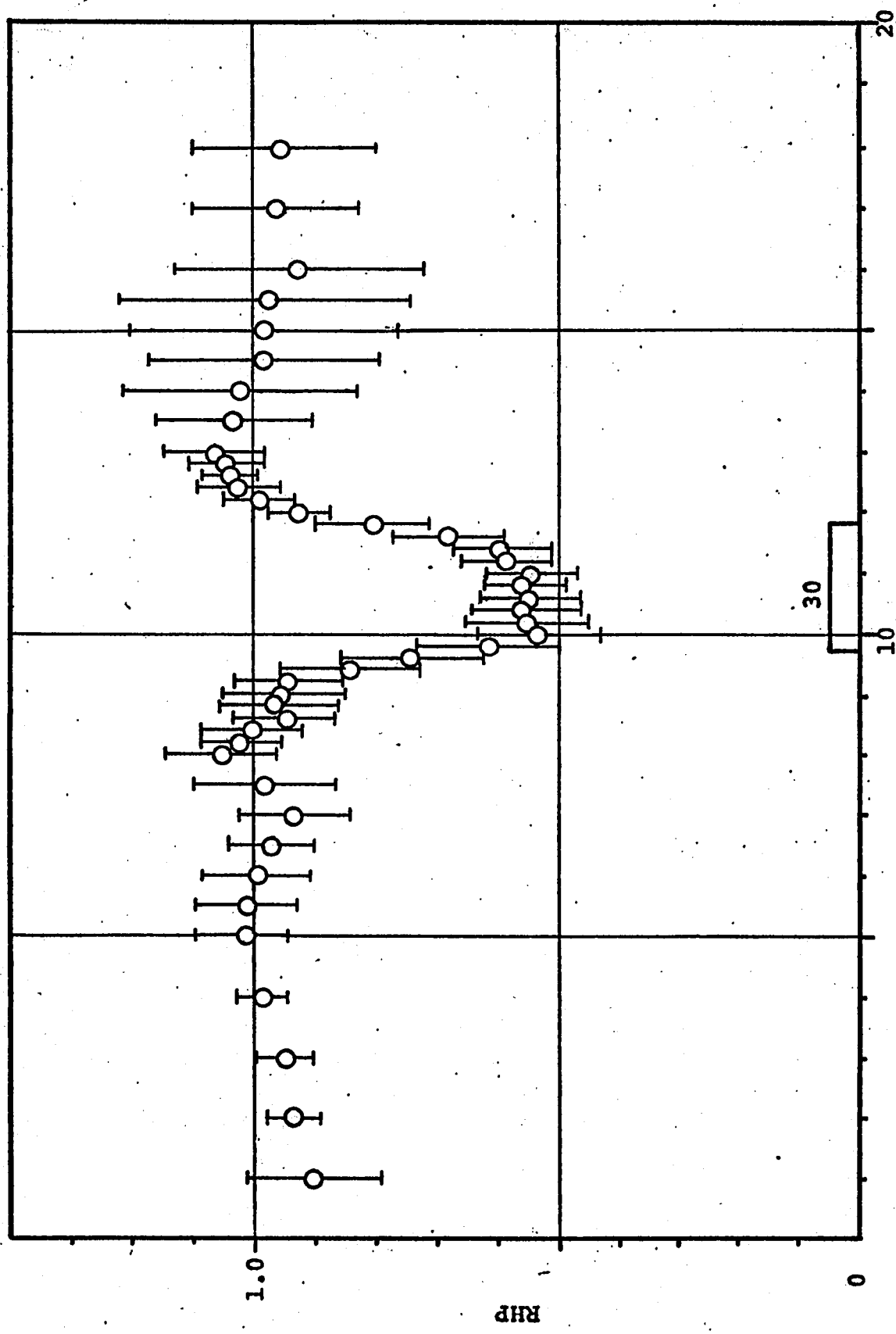

FIGURE F-18 RHP VERSUS AXIAL POSITION FOR 30 DUROMETER 180° SECTION. DATA INDICATES MEAN VALUE AND ONE STANDARD DEVIATION

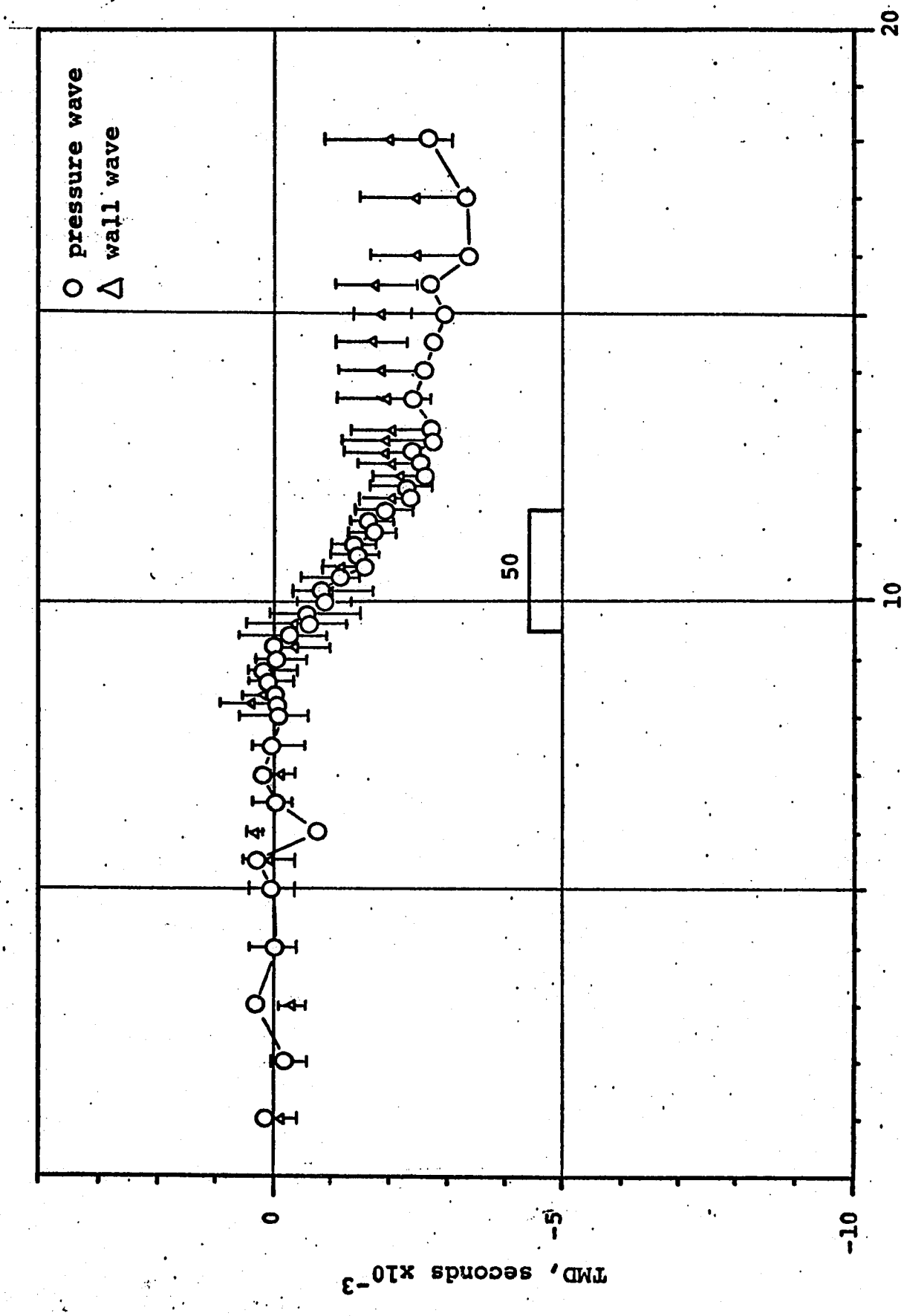

FIGURE F-19 TMD VERSUS AXIAL POSITION FOR 50 DUROMETER 120° SECTION. DATA INDICATES MEAN VALUE AND ONE STANDARD DEVIATION FOR WALL WAVES.

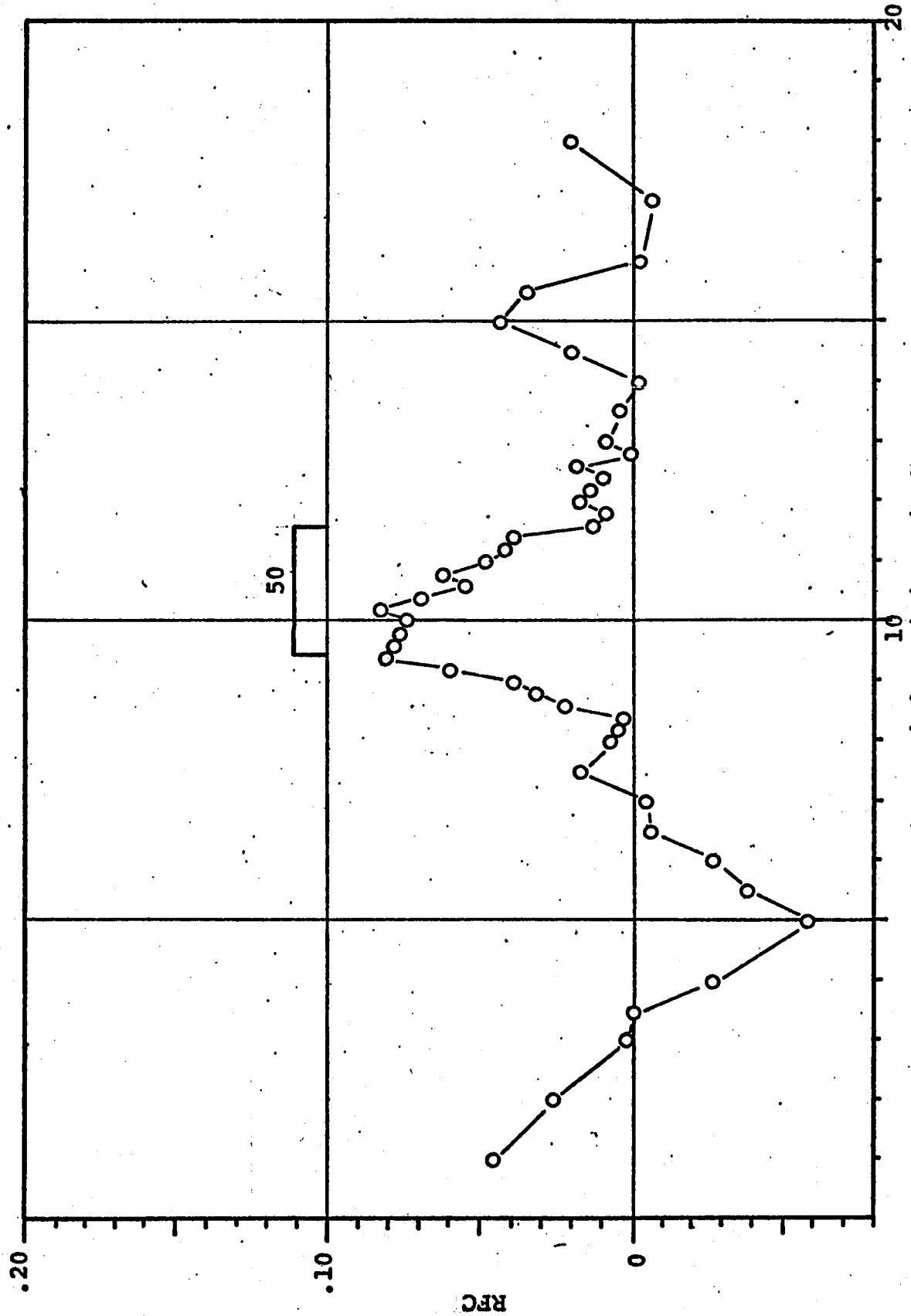

FIGURE F-20 RFC VERSUS AXIAL POSITION FOR 50 DUROMETER 120° SECTION

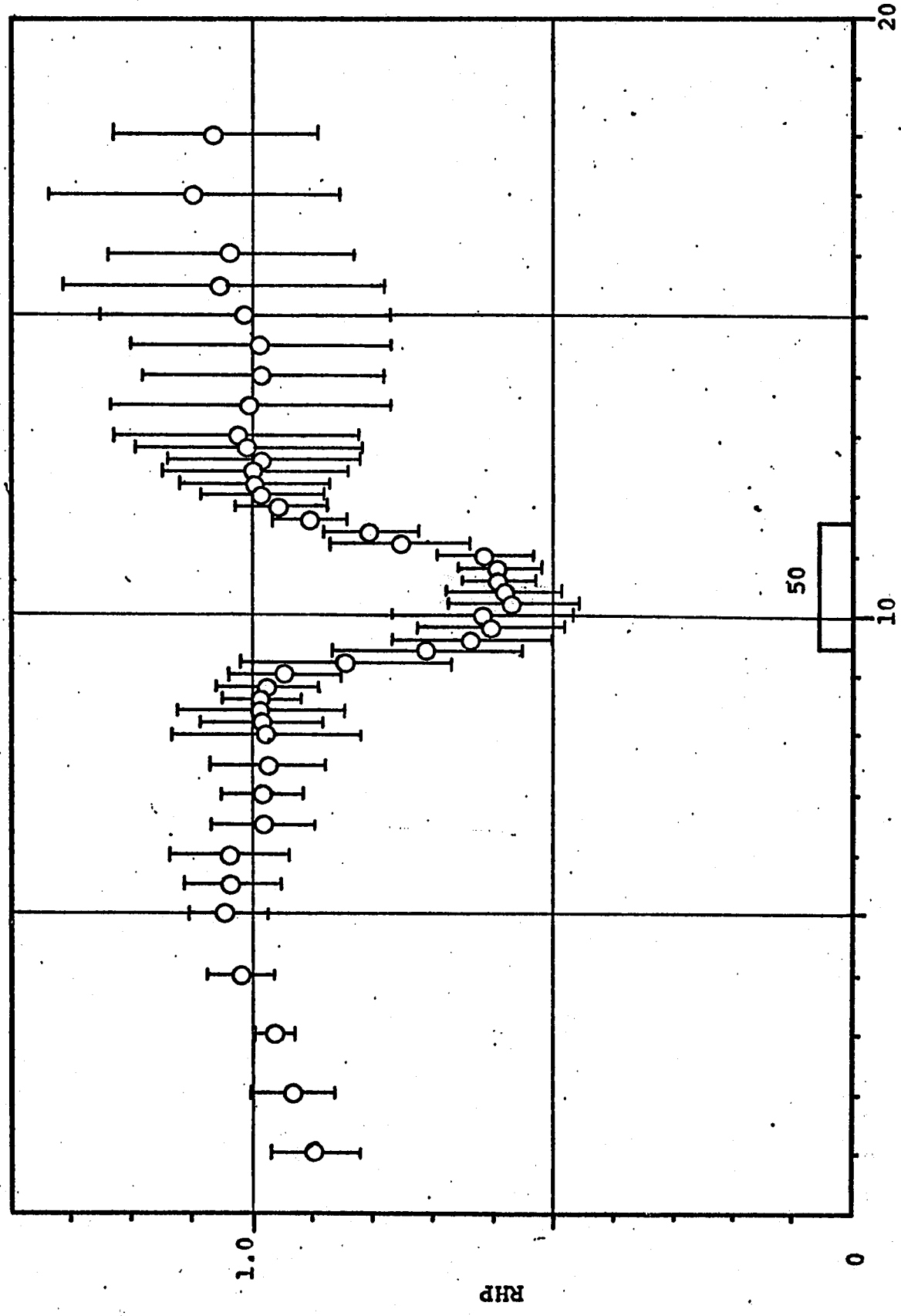

FIGURE F-21 RHP VERSUS AXIAL POSITION FOR 50 DUROMETER 120° SECTION. DATA INDICATES MEAN VALUE AND ONE STANDARD DEVIATION

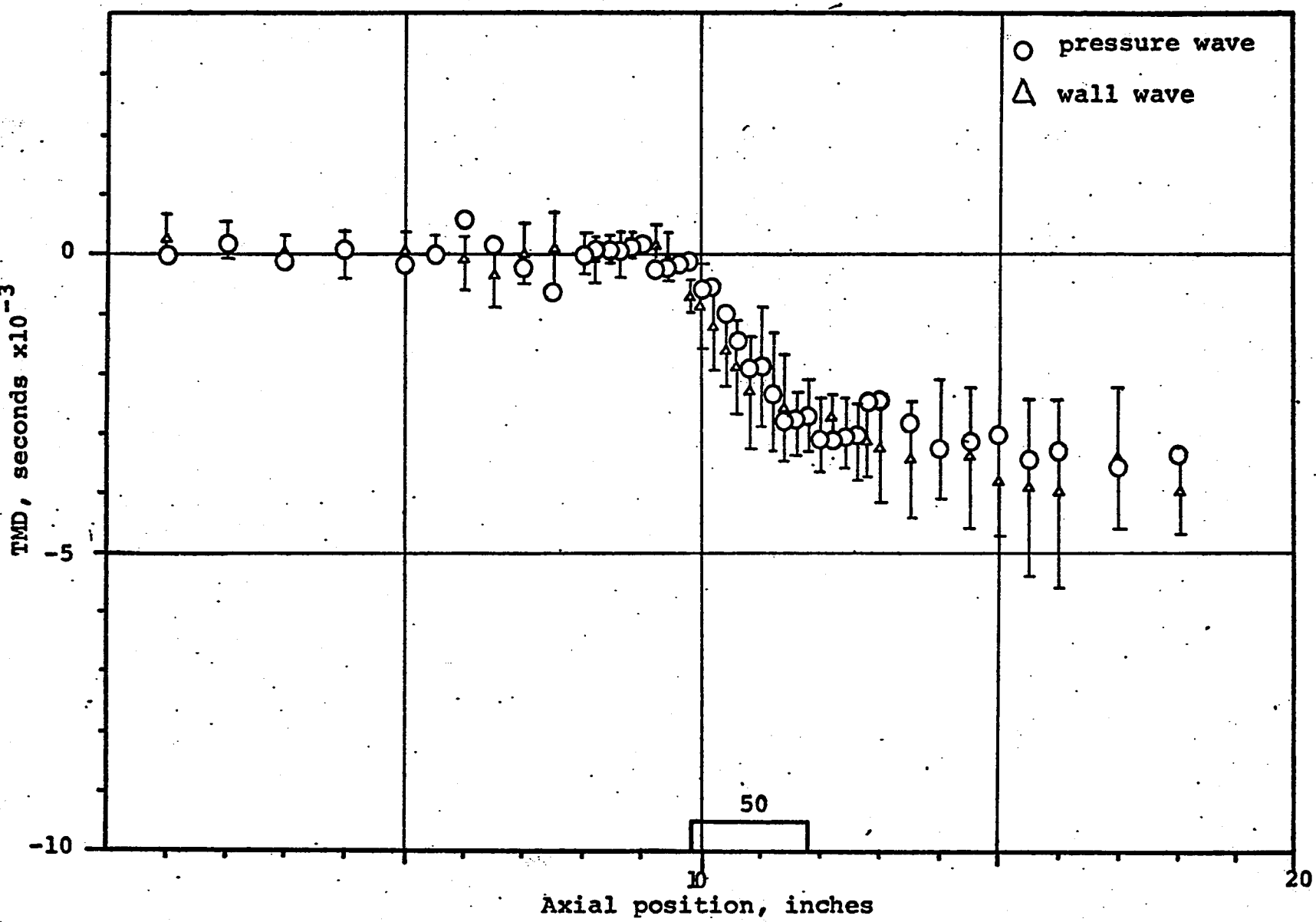

FIGURE F-22 TMD VERSUS AXIAL POSITION FOR 50 DUROMETER 180° SECTION. DATA INDICATES MEAN VALUE AND ONE STANDARD DEVIATION FOR WALL WAVE

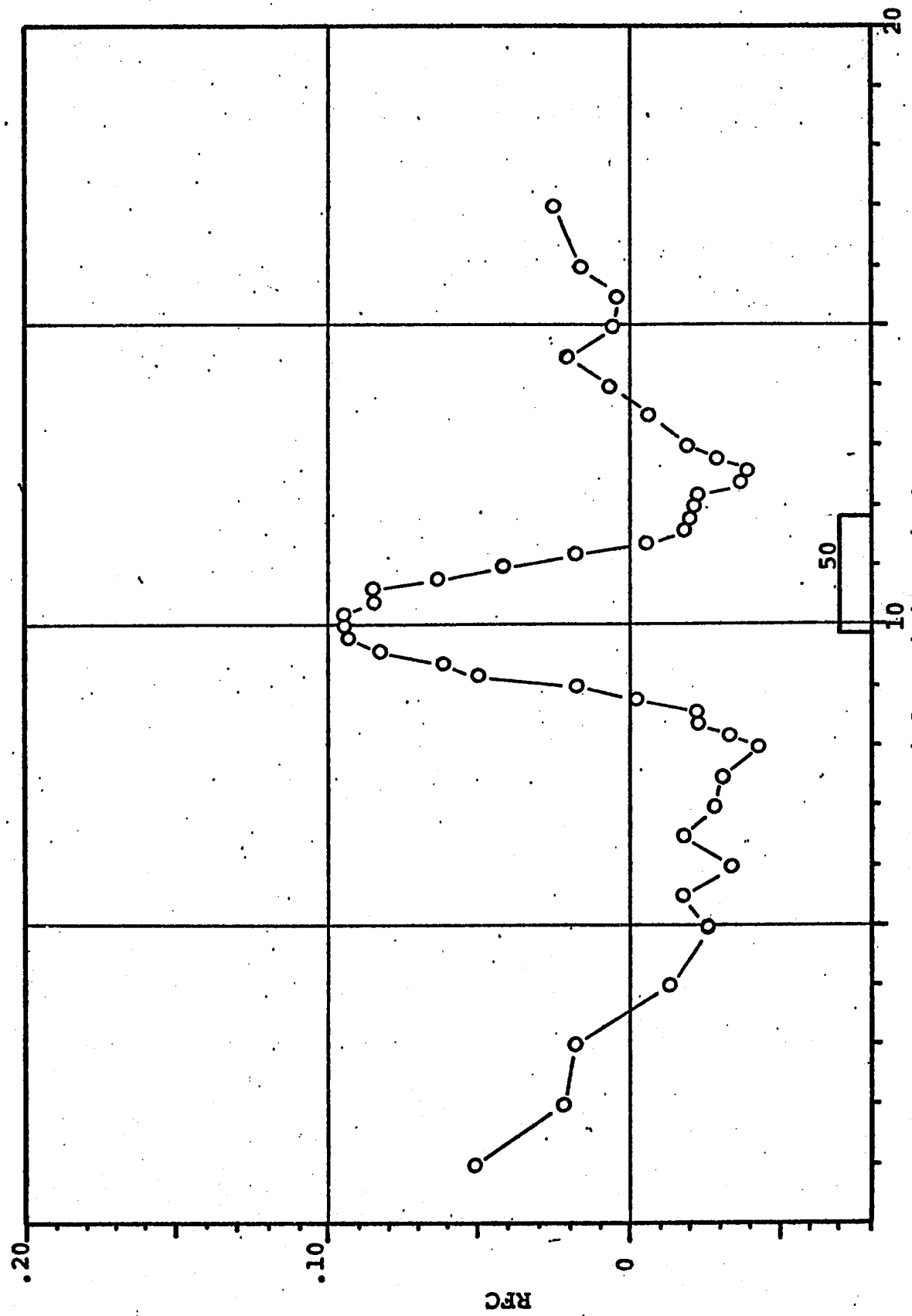

FIGURE F-23 RFC VERSUS AXIAL POSITION FOR A 50 DUROMETER 180° SECTION

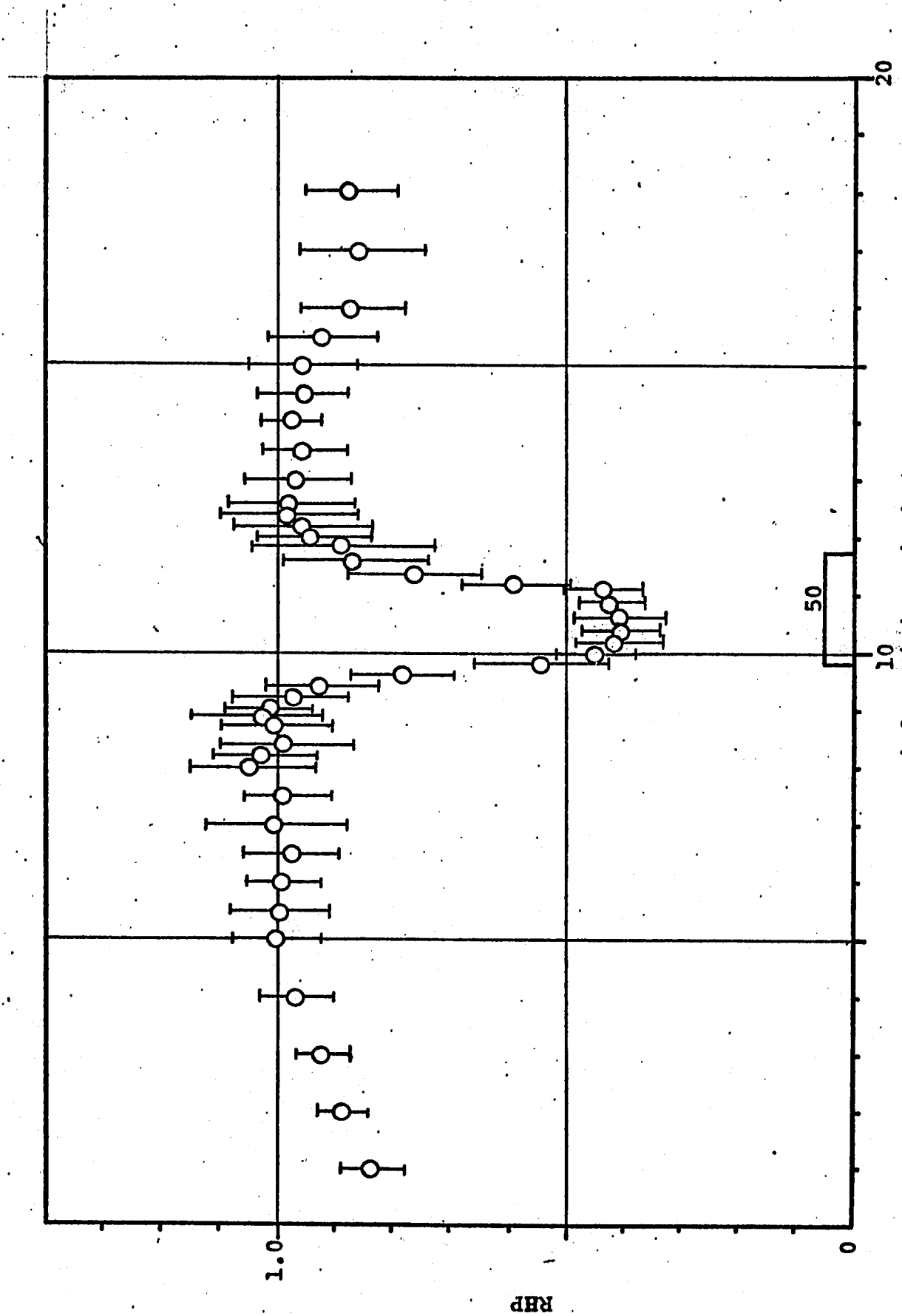

FIGURE F-24 RHP VERSUS AXIAL POSITION FOR 50 DUROMETER 180° SECTION. DATA INDICATES MEAN VALUE AND ONE STANDARD DEVIATION

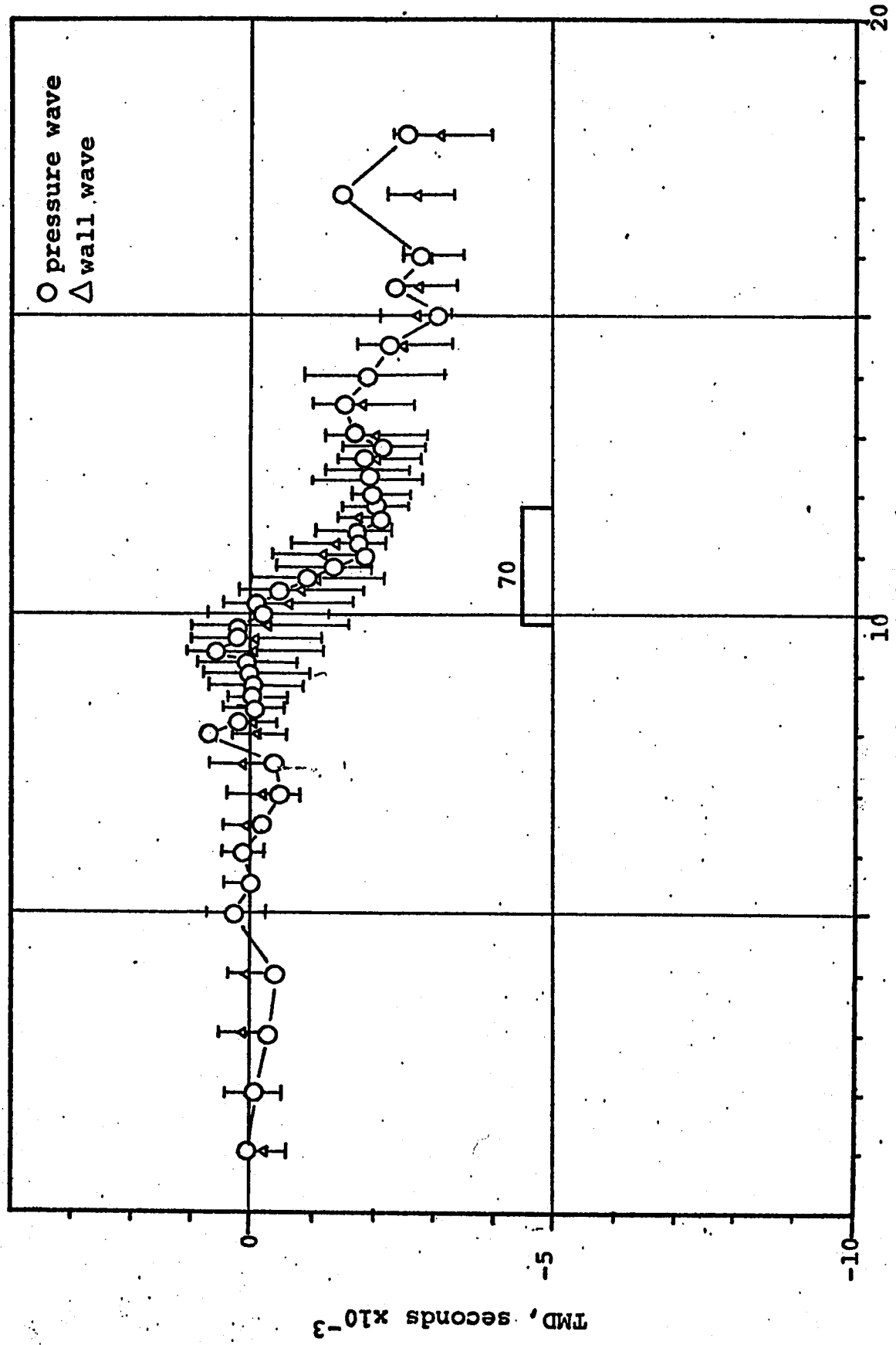

FIGURE F-25 TMD VERSUS AXIAL POSITION FOR 70 DUROMETER 120° SECTION. DATA INDICATES MEAN VALUE AND ONE STANDARD DEVIATION FOR WALL WAVE.

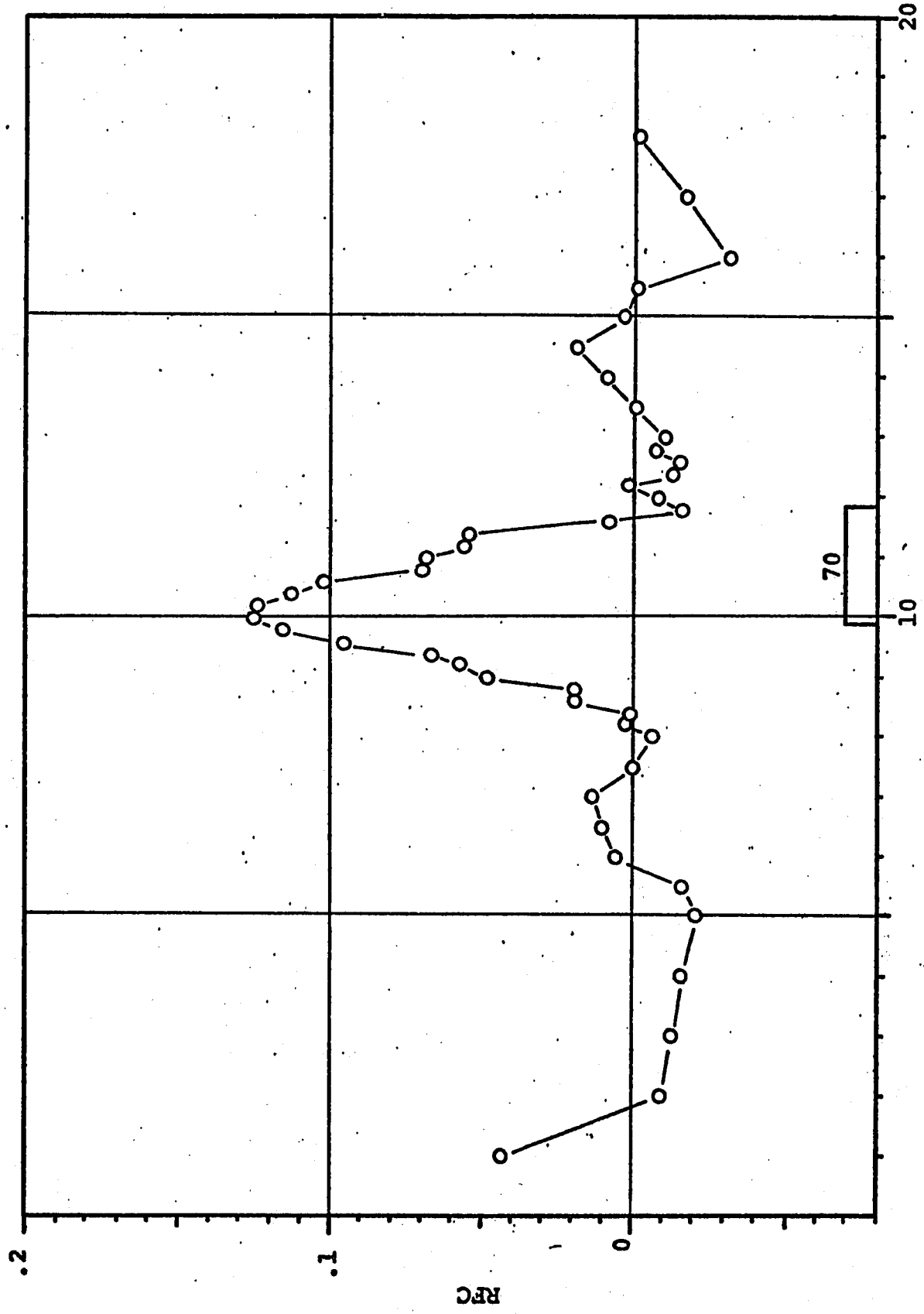

FIGURE F-26 RFC VERSUS AXIAL POSITION FOR 70 DUROMETER 120° SECTION

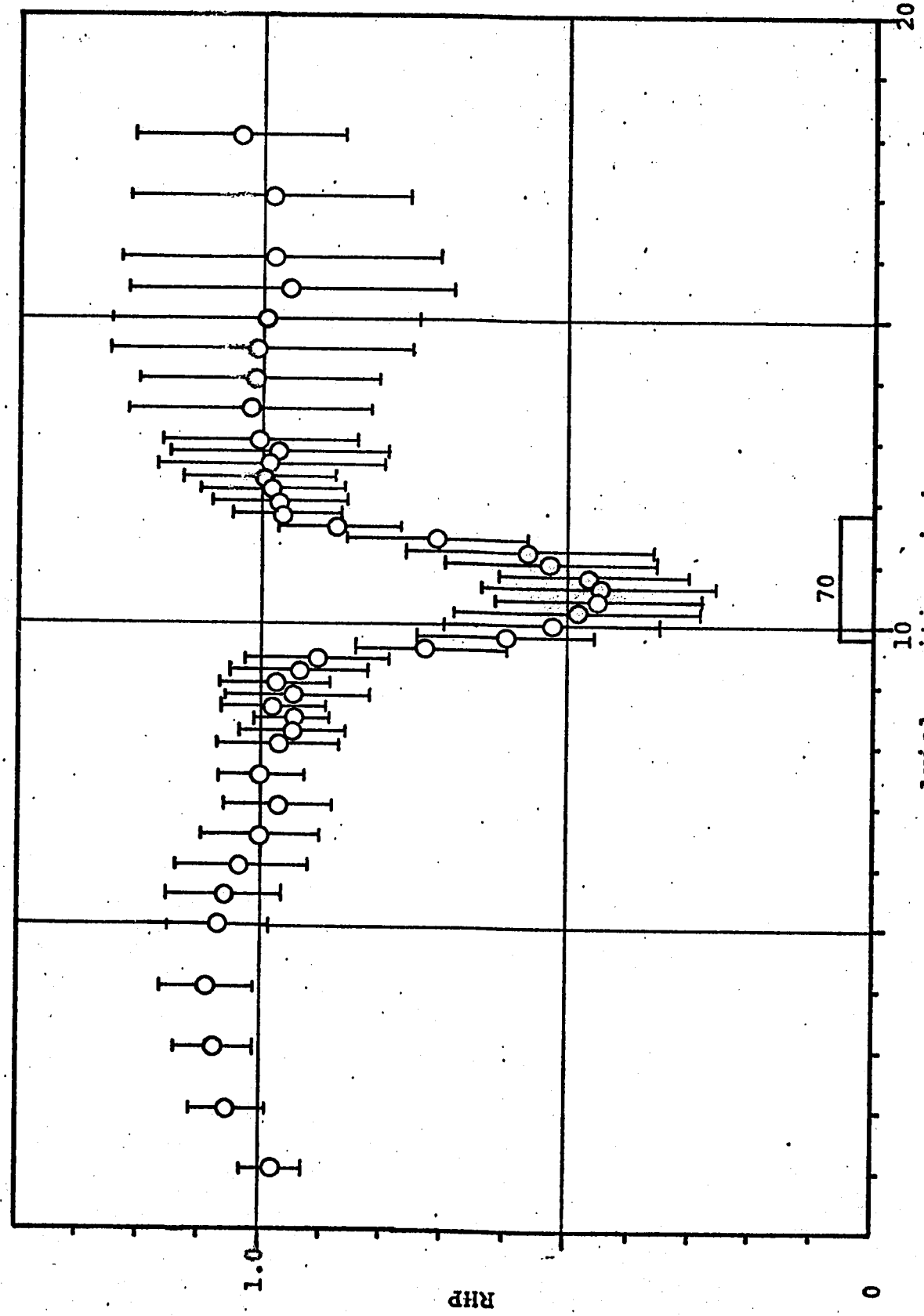

FIGURE F-27 RHP VERSUS AXIAL POSITION FOR 70 DUROMETER 120° SECTION. DATA INDICATES MEAN VALUE AND ONE STANDARD DEVIATION.

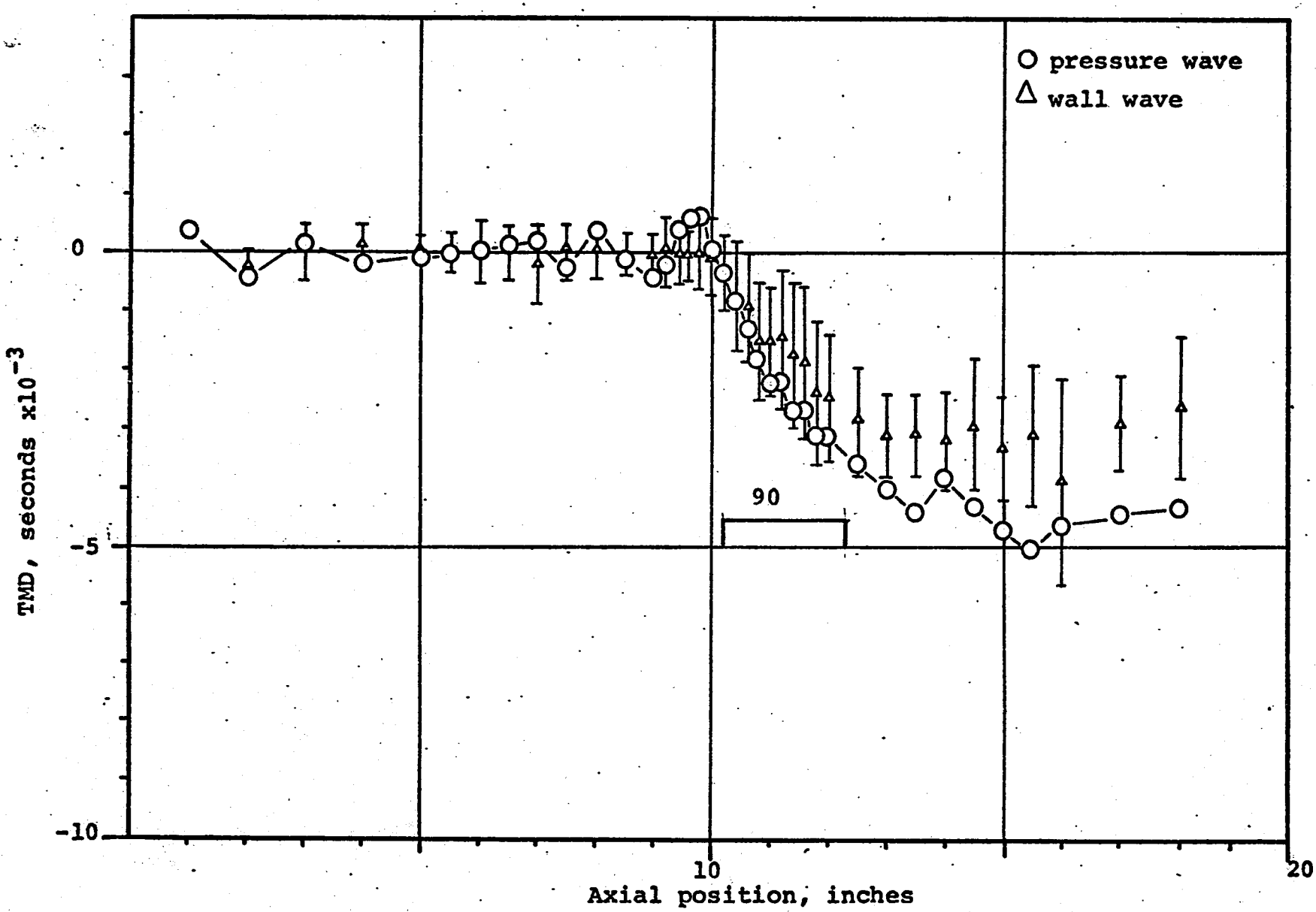

FIGURE F-28 TMD VERSUS AXIAL POSITION FOR 90 DUROMETER 120° SECTION. DATA INDICATES MEAN VALUE AND ONE STANDARD DEVIATION FOR WALL WAVE.

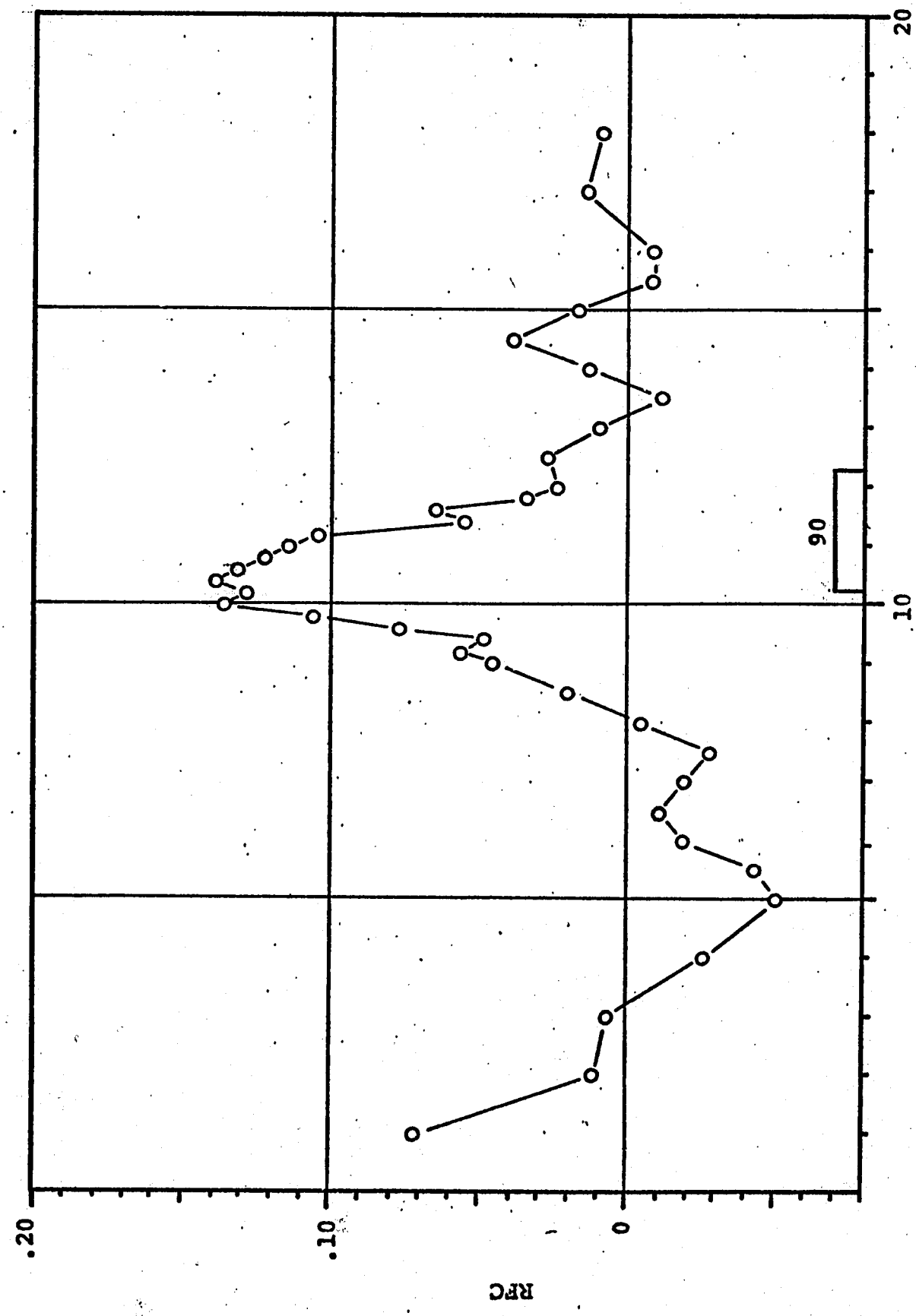

FIGURE F-29 RFC VERSUS AXIAL POSITION FOR 90 DUROMETER 120° SECTION

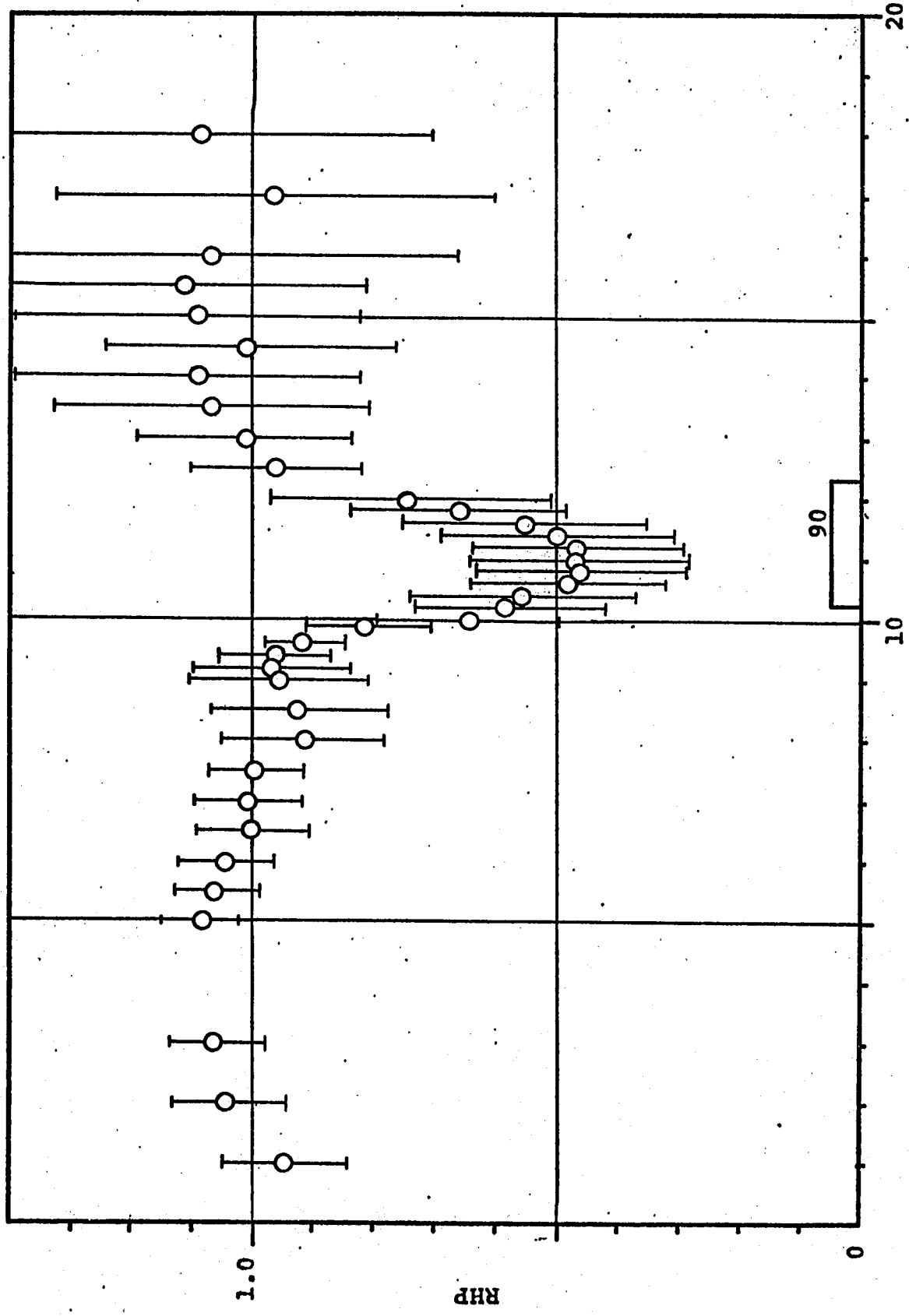

FIGURE F-30 RHP VERSUS AXIAL POSITION FOR 90 DUROMETER 120° SECTION. DATA INDICATES MEAN VALUE AND ONE STANDARD DEVIATION

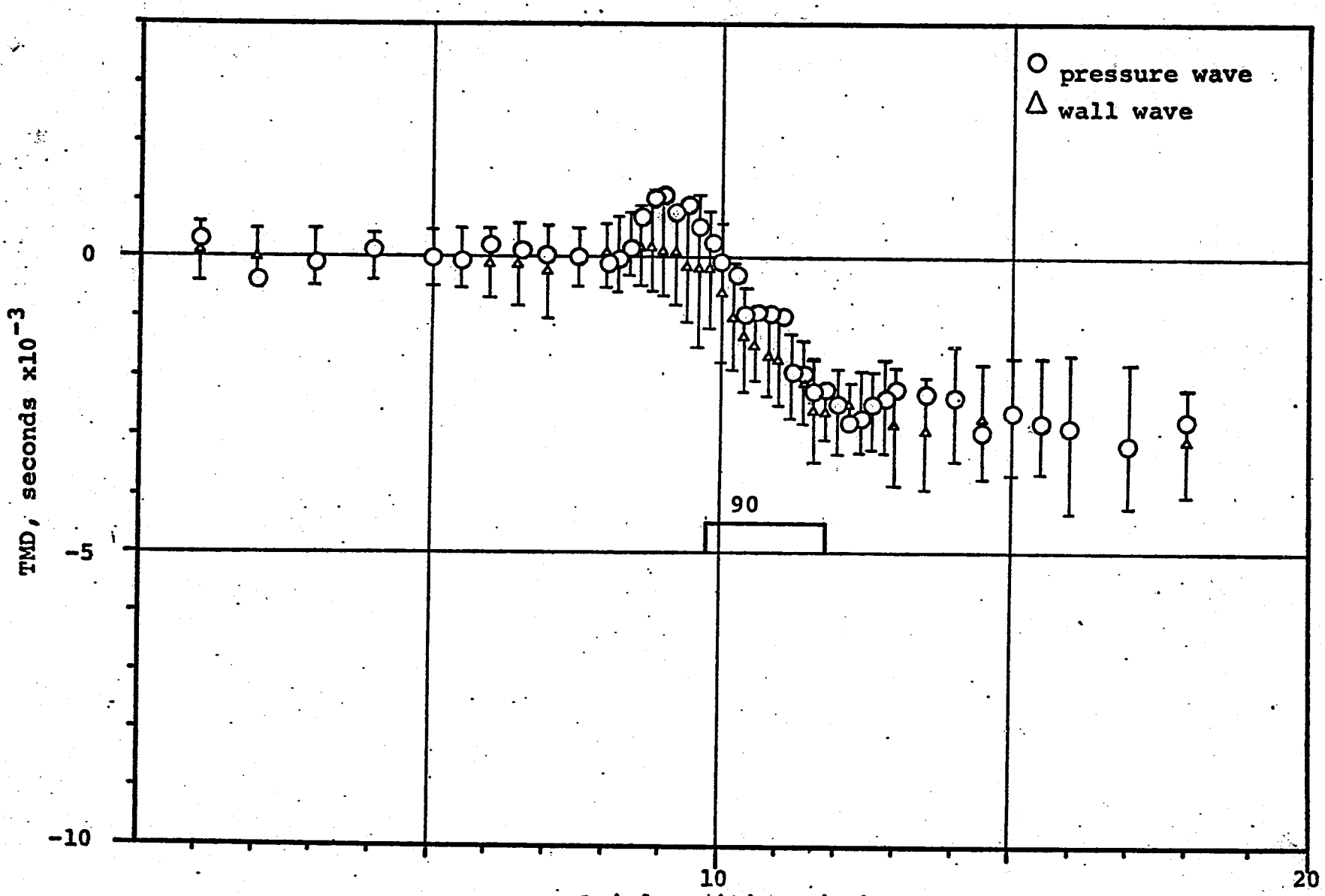

FIGURE F-31 TMD VERSUS AXIAL POSITION FOR 90 DUROMETER 180° SECTION. DATA INDICATES MEAN VALUE AND ONE STANDARD DEVIATION FOR WALL WAVE

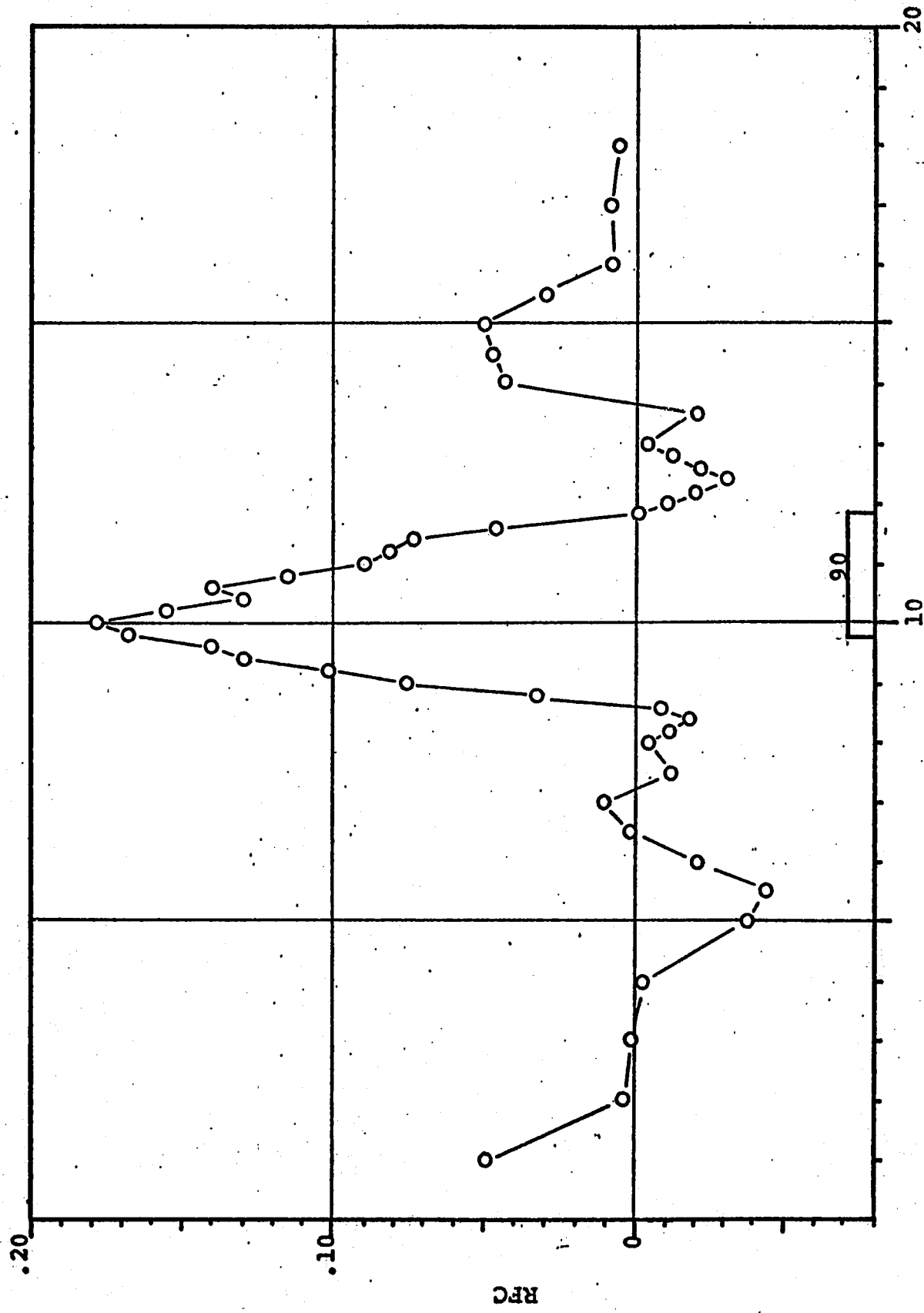

FIGURE F-32 RFC VERSUS AXIAL POSITION FOR 90 DUROMETER 180° SECTION

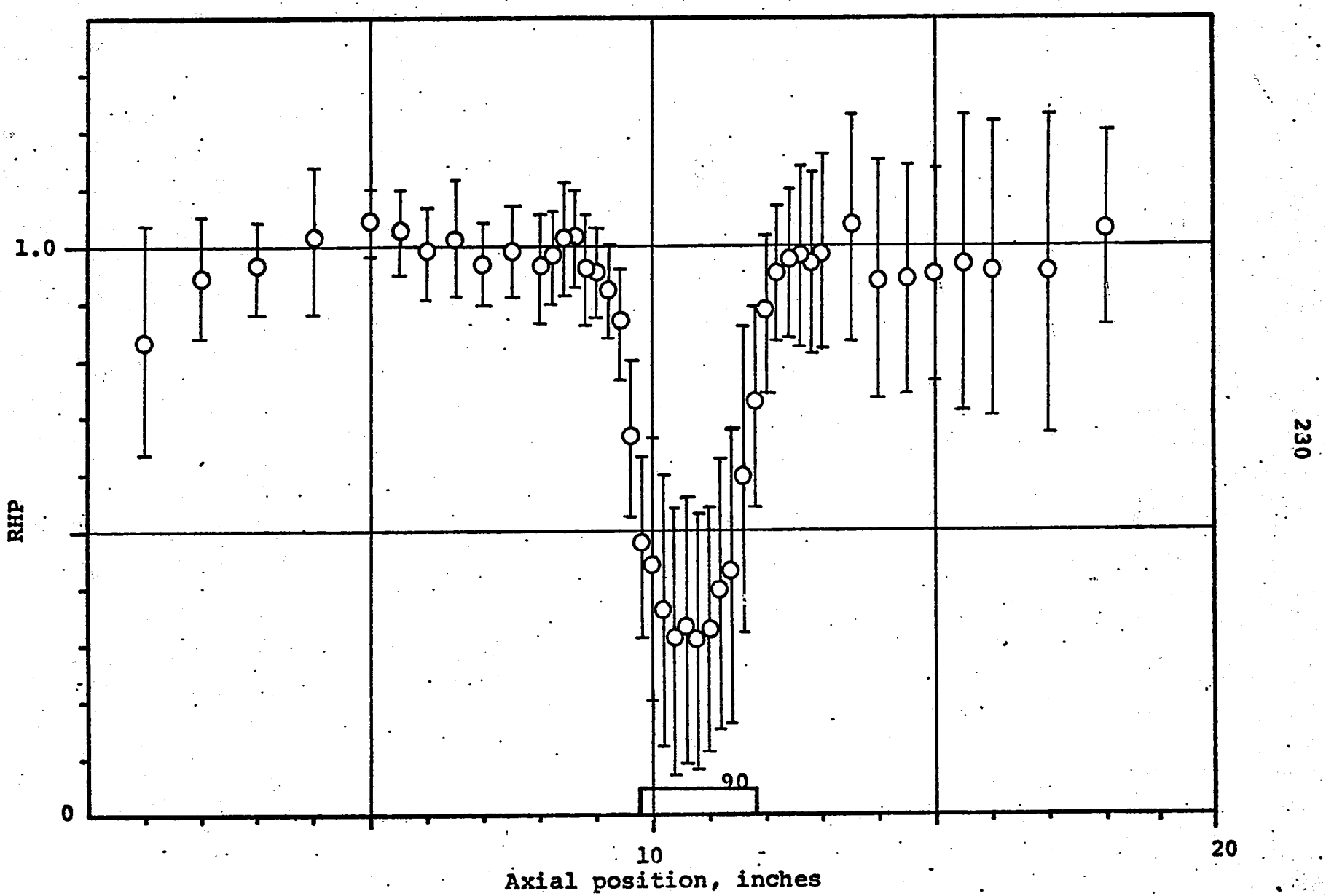

FIGURE F-33 RHP VERSUS AXIAL POSITION FOR 90 DUROMETER 180° SECTION. DATA INDICATES MEAN VALUE AND ONE STANDARD DEVIATION